

2022

Exploring The Effects Of Microplastics On Marine Biota

Meredith Evans Seeley

William & Mary - Virginia Institute of Marine Science, mmevans11@gmail.com

Follow this and additional works at: <https://scholarworks.wm.edu/etd>



Part of the [Water Resource Management Commons](#)

Recommended Citation

Seeley, Meredith Evans, "Exploring The Effects Of Microplastics On Marine Biota" (2022). *Dissertations, Theses, and Masters Projects*. William & Mary. Paper 1673277632.

<https://dx.doi.org/10.25773/v5-f1h0-9127>

This Dissertation is brought to you for free and open access by the Theses, Dissertations, & Master Projects at W&M ScholarWorks. It has been accepted for inclusion in Dissertations, Theses, and Masters Projects by an authorized administrator of W&M ScholarWorks. For more information, please contact scholarworks@wm.edu.

Exploring the Effects of Microplastics on Marine Biota

A Dissertation

Presented to

The Faculty of the School of Marine Science

The College of William & Mary

In Partial Fulfillment

of the Requirements for the Degree of

Doctor of Philosophy

by

Meredith Evans Seeley

January 2022

APPROVAL PAGE

This dissertation is submitted in partial fulfillment of
the requirements for the degree of
Doctor of Philosophy

Meredith Evans Seeley

Approved by the Committee, October 2021

Robert C. Hale, Ph.D.
Committee Chair / Advisor

Bongkeun Song, Ph.D.

Wolfgang K. Vogelbein, Ph.D.

Andrew R. Wargo, Ph.D.

Patty Zwollo, Ph.D.

Zhanfei Liu, Ph.D.
The University of Texas Marine Science Institute
Port Aransas, TX, USA

TABLE OF CONTENTS

ACKNOWLEDGEMENTS	IV
ABSTRACT.....	VI
INTRODUCTION	2
UV-WEATHERING OF PLASTICS	4
THE CHARACTERISTICS OF MICROPLASTICS	5
PLASTICS AND BIOTA	8
<i>Microbial communities.....</i>	8
<i>Aquaculture Salmonid Species.....</i>	10
<i>Microplastics in tissues and the immune response</i>	12
STRUCTURE OF THE DISSERTATION	13
REFERENCES	15
CHAPTER 1: MICROPLASTICS AFFECT SEDIMENTARY MICROBIAL COMMUNITIES AND NITROGEN CYCLING.....	28
INTRODUCTION	29
MATERIALS AND METHODS	32
<i>Experimental plastics</i>	32
<i>Sediment microcosm incubation.....</i>	33
<i>DNA extraction and 16S rRNA gene analysis.....</i>	35
<i>Quantitative PCR of targeted genes.....</i>	36
<i>Rate measurements of denitrification and anammox.....</i>	37
<i>Sediment and water column nutrients</i>	37
<i>Statistical Analyses.....</i>	37
RESULTS	38
<i>Microbial community structure.....</i>	38
<i>Nitrification and denitrification</i>	44
DISCUSSION	48
CONCLUSIONS.....	55
REFERENCES	56
CHAPTER 2: MICROPLASTICS EXACERBATE VIRUS-MEDIATED MORTALITY IN FISH . 61	
INTRODUCTION	62
MATERIALS AND METHODS	64
<i>Particle Preparation</i>	64
<i>Experimental Design and Procedures.....</i>	65
<i>Statistical Analyses.....</i>	70
RESULTS AND DISCUSSION	72
<i>Viral-mediated fish mortality</i>	72
<i>IHNV Shedding and Body Burden.....</i>	76
<i>Histopathology</i>	79
<i>Immune Response.....</i>	82
CONCLUSIONS.....	86
REFERENCES	90
CHAPTER 3: THE INFLUENCE OF NYLON MICROPLASTIC SHAPE AND TIME OF EXPOSURE ON VIRUS-MEDIATED MORTALITY IN FISH.....	98
INTRODUCTION	99
MATERIALS AND METHODS	101
<i>Particles</i>	101
<i>Experimental Animals and Husbandry</i>	101

<i>Experimental Design and Procedures</i>	102
<i>Statistical Analyses</i>	104
RESULTS AND DISCUSSION	106
<i>Mortality</i>	106
<i>Viral Shedding</i>	110
<i>Effects of microplastics independently versus as a co-stressor</i>	113
CONCLUSIONS.....	114
REFERENCES	117
CHAPTER 4: DOES UV-WEATHERING OF MICROPLASTICS AND A NATURALLY OCCURRING MICROPARTICLE ALTER VIRUS-RELATED MORTALITY IN FISH?.....	120
INTRODUCTION	121
MATERIALS AND METHODS	123
<i>Particle Preparation</i>	123
<i>Experimental Animals and Husbandry</i>	125
<i>Experimental Design and Procedures</i>	125
<i>Statistical Analyses</i>	127
RESULTS AND DISCUSSION	129
<i>Mortality</i>	129
<i>Viral Shedding</i>	135
CONCLUSIONS.....	136
REFERENCES	139
CONCLUSIONS	143
APPENDICES	147
CHAPTER 1 SUPPLEMENTARY INFORMATION.....	148
CHAPTER 2 SUPPLEMENTARY INFORMATION.....	182
CHAPTER 3 SUPPLEMENTARY INFORMATION.....	210
CHAPTER 4 SUPPLEMENTARY INFORMATION.....	217

ACKNOWLEDGEMENTS

This dissertation is the result of collaboration from a large group of people, who have taught and helped me more than I could put into writing. First, I would like to thank the Freeman family for making this research possible. Without their foresight and pioneering energy to fight plastic pollution, particularly Peggy Freeman, the funding would not have been available for me to peruse this research as a Ph.D. student. Beyond that, they have become lifelong friends who I admire greatly.

I would like to thank my advisor and committee for their dedication to my education and this work. When I was looking for a Ph.D. program to study microplastic pollution, Rob Hale was the first to enthusiastically agree that I could build an entire dissertation around this ‘new’ pollutant. Since, I’ve learned so much from him on the nature of pollution and how to approach science, and I’m eternally grateful for the opportunities he’s given me. Bongkeun (BK) Song is perhaps the most enthusiastic and inspiring scientist I’ve had the pleasure of working with. Not only do I appreciate his diligence in helping me accomplish research in the lab, but I also appreciate his mentorship and guidance outside of the laboratory. I appreciate the support in all things fishy from Wolfgang Vogelbein, who encouraged me to apply for opportunities and reach to the point where disciplines intersect – ‘where the magic happens’. I am grateful to Patty Zwollo for her patient support in allowing me to dabble in the immunological consequences of plastic pollution, and pushing me to be a better scientist. I’m also eternally grateful that she gave me the opportunity to see the extent of plastic pollution in remote Alaska firsthand, and will remember her company and that trip forever. The final chapters of my dissertation truly would not have been possible without Andrew Wargo. I thank him for his enthusiasm when I asked if he’d be interested in writing a long-shot proposal, and all his support in making the science possible. Also, for that homemade lasagna delivery during a pandemic quarantine...my husband and I still talk about it. Finally, but not least, I’m eternally grateful to Zhanfei Liu. When I first met Zhanfei I was unsure of my path and place in science. Zhanfei has been a true mentor throughout, not just my Master’s program with him, but through my Ph.D. and all the big life events along the way. I can say that my efforts in this dissertation would not have been possible without the foundation I built under his guidance at UTMSI.

To the science team that made it all possible. The Hale lab: Drew, Mark, Matt, Ellen, Kelley and Ashley – you’ve all helped me countless times in everything from finding the right tool to troubleshooting the strangest issues, thank you. I would not be in the same place without Ashley’s comradery and support, and officially dub her ‘best lab mate ever’. The Wargo lab: Barb, Gaelan, Hannah, Malina, Aman, and Anna – thank you for adopting me like one of your own and spending *countless* hours grinding through work in the hottest and coldest of temperatures. Most importantly, thank you for helping me do it with a smile and a belly full of potluck lunch. Your family-like approach to lab work will forever be a goal I strive toward. The Song lab: Stephanie, Michelle, Miguel, Sam and more – thank you for allowing me to work with you, and your extreme patience when I had no idea what I was doing. I learned so much from each of you and had a great time along the way (despite the conference bed bugs...). Thank you to Melanie Kolacy for

painstakingly teaching me the ins and outs of paraffin histology. And to countless others who've provided scientific inspiration and support along the way, including Hamish Small, Virginia Worrell, Lidia Epp, Mike Unger and more.

Thank you to the VIMS administration and community for immeasurable support. Thanks to the academic studies staff, Linda, Jen, Cathy and John, for your diligent advocacy for graduate students' work and health. Your open doors and patience made my experience as a graduate student easier in the best ways. Thank you to Carol Birch for being a patient purchasing wizard. Thanks to the advancement and outreach teams, Sally, Candice, and others, for keeping me involved with education. I've loved and grown from every opportunity and am inspired by the work they do to reach the communities for whom our science matters. To the green team members, past and present, for being such an inspiration to make change in our own backyard. To John Graves and Jon Allen for your support and wisdom in my first experiences with undergraduate education. Thank you to the entire VIMS community. VIMS is truly a special place to do research, but it has also been a wonderful place to grow and learn from everyone around me – scientists, staff, and friends alike. Your warm smiles and friendships are the things that mattered most.

To my family and friends, how can I thank you enough? To my parents, for encouraging me to follow my passion for marine science and never questioning my career choice (even when it meant coming home muddy with leaches). Thank you for being there and cheering along every step of my education. To my grandparents, papa and nana – your toasts to education at family events did not fall on deaf ears, papa, and both of your reminders that I could do whatever I set my mind to continue to mean the world. To my brothers for supporting me in your own unique ways, but especially to Hampton and Bub for reminding me that it could always be worse... I could be getting a Ph.D. in history. To my Texas and Okla-homies – your enduring friendships (even when I fall off the map, or into the lab, for days at a time) has made life so much more fun. Thanks for being there when it mattered, and for all the laughs along the way.

Thank you to my amazing husband, Matt. During my Ph.D. we moved across the country, lived in two states, got married, traveled to new countries, bought our first place, and owned at least four cars. And now, as I'm finishing this degree, we are both preparing to start new jobs, move across the world, and become parents for the first time. Through all the mayhem and challenges we've faced over the past four and a half years, you never let me lose sight of my goals and have truly supported me every step of the way. I don't know where I would be without all the meals you've cooked, draft documents you've read, times you've listened to me when I was frustrated, or times you were just the best friend I could ever ask for. In my book, you've earned an honorary Ph.D. for sure. And thanks to pumpkin, our daughter on the way, for all the kicks of encouragement in the home stretch.

ABSTRACT

There is mounting evidence that microplastics are a persistent and increasing hazard for aquatic organisms. The effects of microplastics on organisms and ecosystems are complex, however, and may be linked to a wide variety of particle characteristics including size, shape, polymer, additive chemistry, and degree of weathering. Assessing risk is complicated by the fact that many known effects of microplastics are sublethal, and that plastics have been postulated to interact with other stressors, such as pathogens. The work presented here expands our understanding of these complex effects.

First, the impacts of microplastics on sedimentary microbial ecosystems and biogeochemical carbon and nitrogen cycles were investigated. A microcosm experiment using salt marsh sediment amended with polyethylene (PE), polyvinyl chloride (PVC), polyurethane foam (PUF) or polylactic acid (PLA) microplastics was conducted. We found that the presence of microplastics altered sediment microbial community composition and nitrogen cycling processes. Compared to control sediments without microplastics, PUF- and PLA-treated sediments promoted nitrification and denitrification, while PVC inhibited both processes. These results indicate that nitrogen cycling processes in sediments can be significantly affected by different microplastics, which may serve as organic carbon substrates for microbial communities.

Second, we probed the virus-related mortality of a commercially important salmonid species under chronic exposure to nylon microfibers, polystyrene microplastics, and natural marsh grass microparticles. Mortality increased when fish were co-exposed to pathogen and microparticle, particularly nylon microfibers. This correlated with host viral load and mild gill inflammation. As such, we speculated that chronic exposure microplastics may create opportunities for pathogens to bypass defenses and colonize hosts via sensitive tissues. To investigate if this was enhanced by the physical properties of plastic microfibers, we assessed differences in mortality following chronic exposure to nylon microfibers and powder, finding that fibers had a greater effect than powdered counterparts. The importance of the timing of microplastic exposure was also confirmed by completing viral/microplastics co-exposures where microplastics were dosed before, after, or before and after viral introduction. Indeed, virulence was most enhanced when fish were exposed to microplastics pre-virus or chronically, significantly more so than post-virus only. Finally, we tested whether UV-weathering changed the effect of natural and plastic microparticles on disease-related mortality. We observed changes in the virulence effects of microparticles following UV-weathering, but the pattern of that change was inconsistent and merits further research.

Considering their ubiquity and increasing concentrations globally, further research on the effects of microplastics is warranted. Particularly, the work here demonstrates that microplastics may influence entire communities and inorganic nutrient cycling systems, classifying microplastics as a potential planetary boundary threat. Further, we illustrate that even when microplastics alone may not have substantial effects on a fish population, when combined with disease they may amplify pathogen-related mortality significantly. More research on the interplay between microplastics and infectious disease is recommended, particularly as it may inform researchers on the risks of microplastics to human health.

Exploring the Effects of Microplastics on Marine Biota

Introduction

Plastics have revolutionized everyday life, from the cars we drive, to the clothes we wear, and the food we buy. Although use of plastic from natural polymers dates back to early societies, the advent of inexpensive, petroleum-based plastics circa 1950 modernized and greatly expanded their use (1, 2). Particularly, single-use plastics have become commonplace. Waste management streams are now inundated with single-use plastic trash. In wealthy societies, the majority of plastic waste is retained within mechanisms such as landfilling. Lesser amounts are recycled or incinerated. In other societies, existing infrastructure can only manage a smaller portion (3, 4). As such, a fraction of plastic waste ‘leaks’ from waste management streams into the natural environment. The capacity to reduce this leakage is complicated by global infrastructure and politics. Plastic pollution is projected to increase dramatically over the coming decades as global population increases, even if intense management efforts were implemented (5, 6). Ironically, although many plastics are intended to be used by consumers for only a short period of time (due to their low cost and convenience), plastics are particularly resistant to chemical and physical degradation and persist in the natural environment for decades or more (7). Plastic pollution is, therefore, a persistent and increasing environmental contaminant.

The major focus of plastic pollution research to date has been within aquatic ecosystems, particularly the world’s oceans. Although plastic derives from (and can also pollute) terrestrial environments, it reaches large water bodies via precipitation, dry atmospheric deposition, storm and wastewater systems, streams, and rivers (3, 8, 9). The earliest published scientific documentation of floating plastic debris was reported in the Sargasso Sea in 1972 (10). Soon after, plastic debris was reported across all oceans and

coastal systems, particularly in the North Pacific Gyre which has been popularized as the *Great Pacific Garbage Patch* (11, 12). Today, estimates show that approximately 80,000 tons of plastic are floating in this gyre alone (13), while a cumulative 9.5 million metric tons enter the oceans annually (6). The fate of plastics within aquatic systems is complex and dictated by a variety of physical weathering processes and biological interactions.

UV-weathering of plastics

While in the aquatic environment, plastics will encounter a variety of natural weathering processes. Although they are designed to be physically and chemically resistant to degradation, plastic debris will fragment into smaller pieces over time. The signs of weathering can be both visually and chemically apparent on the surface of plastic debris (14). Weathering caused by light in the ultraviolet (UV) spectrum is particularly relevant and impactful on plastic properties.

UV light exists between wavelengths 200-400 nm, which is both shorter and carries more energy than the visible light spectrum. The energy imparted by UV light can alter chemical bonds, leading to photodegradation. Within the UV spectrum, UVA (315-400) is most dominant on the earth's surface (15). When UV light reaches plastics it is either reflected or absorbed. Absorption depends upon the presence of chromophores. Many plastics are chromophore-rich, including aromatic rings, double bonds, additives, trace metals from processing, sorbed environmental pollutants, or other impurities (15, 16). As such, most plastic can absorb some light in the UV range, albeit with differences between polymers and formulations, discussed later (17-19). The absorbed portion of light will often lead to removal of a hydrogen atom, generating a radical, which is

unstable and can react with other nearby chemical entities (16). These reactions may both degrade the polymer chemically and photophysically alter the polymer (14, 15, 20).

The most common UV-weathering reaction for polluted plastics in the aquatic environment is likely photooxidation. Oxygen is usually abundant where sunlight is and is reactive with the formed radicals. Indeed, oxygen uptake can be directly observed in plastic experimentally (21). In photooxidation pathways, oxygen is involved in radical propagation and the termination step may result in an oxidized hydrocarbon. During propagation, autooxidation may occur, creating additional oxygenated byproducts. Oxidized hydrocarbons, if separated from the polymer matrix, may be more bioavailable in the aquatic environment, akin to photooxidation following an oil spill (22, 23). Photooxidation also catalyzes the formation of smaller plastics. Oxygen is able to penetrate the amorphous (i.e., less chemically organized) areas of a plastic better than the crystalline ones, and the physical and chemical effects of photooxidation concentrate in these amorphous regions (24, 25). These weakened areas on the surface of the plastic may fracture, allowing small pieces to separate from the surface of the larger particle. The degree of UV-weathering will vary depending upon the complex additive/polymer complex of a specific plastic, and cannot be generalized by plastic type (see additive discussion below). As such, UV-weathering and photooxidation are integral processes modifying the physiochemical properties and fate of plastics in the aquatic environment.

The characteristics of microplastics

Plastics less than or equal to 5 mm in the longest axis are called microplastics (26). In general, there is considered to be an inverse relationship between plastic particle size and number of particles in the environment, so microplastic pollution is more

abundant than larger plastic debris (2). Microplastics that derive from the breakdown of larger plastics (e.g., from photooxidation) are most common, and termed secondary microplastics. Primary microplastics (i.e., plastics that were ≤ 5 mm in size from point of production) are also released to the environment; examples include microbeads from personal care products, nurdles (i.e., pre-production plastic pellets), and microfibers from textiles (27–29).

Microplastics, due in part to their small size, present challenges for field and laboratory science. In order to survey microplastic abundance in the environment, researchers require appropriate sampling, purification and identification methods, the latter often employ microscopic techniques (30–32). There is evidence (e.g., particle counts at different sizes from environmental surveys) that microplastics with diameters <300 μm are the most abundant in the marine environment (33, 34). However, most field surveys have targeted larger plastics (35). This is in part an artifact of common sampling net mesh size (in the case of commonly sampled surface waters), but also due to difficulties handling and identifying small microplastics. Microfibers are thought to be particularly underestimated due to their narrow widths, allowing them to escape many commonly used sample collection, pre-treatment and analysis processes (27, 36). As such, although research has clearly demonstrated the ubiquitous nature of microplastic pollution, the totality of its abundance is largely obscured by its difficulty as an analyte.

An additional consideration in microplastic studies involves plastic composition itself. A major classification of plastics is polymer type. Polymers constitute the main structure of a plastic (24), and determine how microplastics are named (e.g., polyvinyl chloride polymer, or PVC) or classified for recycling. Yet, plastics may contain

substantial amounts of a range of chemical additives, as well as fillers (e.g., calcium carbonate and carbon black). These property-modifying chemicals are added by the manufacturer to optimize plastics for specific purposes (37, 38). Additives include colorants (i.e., dyes), plasticizers for added flexibility (e.g., phthalates) and flame retardants. Antioxidant and UV-stabilizing additives are also common, and greatly affect aforementioned photooxidation pathways for the plastic particle, yet the impact of photooxidation on additive constituents themselves is not well understood (19, 39). Additives are a substantial aspect of particle chemistry and can be present in excess of 50% of plastic by weight (i.e., the molecular ‘majority’ of a plastic may not be the polymer itself; 37, 40). Additive composition is often considered a ‘trade secret’ by manufacturers and thus unknown to customers, recyclers, and the environmental community. Additive presence can complicate polymer identification, particularly for spectroscopic techniques (41, 42). In addition, some plastic additives are highly toxic and (although manufacturers sometimes establish that additives remain in the polymer matrix during *intended* use, e.g., microwave food containers) their ability to leach from plastic matrices in the environment over time and potentially affect surrounding biota has been demonstrated (43–45).

Polymer and additive chemistry are just two of many facets of a microplastics characteristics, however. Microplastics exist as a complex continuum of sizes, shapes, densities, colors, and concentrations in the environment (29). Resolving and characterizing microplastic pollution, therefore, is exceedingly complex, as is addressing how microplastics interact with biota and ecosystems.

Plastics and biota

Aquatic biota encounter plastic debris worldwide, across all trophic levels, from micro- (e.g., plankton) to mega-fauna (e.g., seabirds and marine mammals; 46–56). A widely documented pathway for harm from large debris is plastic ingestion and entanglement (51, 52, 54, 57, 58). The damage caused by these interactions can be obvious (even just visually), and often results in organismal mortality. Yet, the majority of plastic debris consists of small microplastics, for which it can be more challenging to elucidate the interactions between the particle and living species. Numerous researchers have highlighted the nuances and complexity of microplastic toxicity to aquatic organisms (59–61). At the same time, this research is paramount for crafting effective resource management efforts in the face of persistent and increasing microplastic pollution (62), and will build a foundation upon which to understand risk to humans from microplastics (63, 64).

Microbial communities

A growing body of work has been dedicated to characterizing the ‘plastisphere’, or the microbial community that colonizes floating plastic debris (65). The plastisphere forms an organic layer on the surface of plastics, or a biofilm, akin to biofilms that exist on a variety of materials in aquatic environments (e.g., shells, boat hulls, cement pilings, wooden piers). This biofilm is important in dictating the fate of plastics in the ocean (66, 67). Biofilms are composed of dynamic microbial communities (65). They affect microplastic agglomeration patterns (68, 69), the density of microplastics (70), and organic or inorganic contaminant sorption to plastics surfaces (71, 72).

The composition of microbial communities within the plastisphere is of great interest. According to sequencing studies, microbial eukaryotic taxa have often been shown to dominate plastic biofilms (65). These communities are notably different from the surrounding water, however, and can differ between solid substrate types from the same location (e.g., plastic, wood, glass) or between polymer types (73–77). Local ecology may play a larger role in shaping the plastisphere than the location where the microplastic originates from, which highlights that colonization is dynamic over time (78). At the same time, some cosmopolitan species are routinely found on the surface of plastics from different locations, although, no species has been documented to only exist on plastics to this point and the distinction between plastisphere generalists versus specialists has not been delineated (65). It has also been conjectured that the plastics may act as a sterile vector for disease agents, such as *Vibrio spp.* (66, 73, 77, 79–85). The potential for pathogen-colonized microplastics to spread and incite disease, however, is largely unexplored. Similarly, many species of hydrocarbon degrading bacteria have been found in sequencing analysis of plastic biofilms, yet their importance in the environmental degradation of plastics is undetermined and likely dependent upon the chemical properties of the plastic type (65).

The vast majority of research on the plastisphere has focused on plastics floating in water even though plastics are also abundant in aquatic sediments, in which rich microbial communities thrive (86). The ability for biofilms to form on the surface of sedimented plastics has been demonstrated. A 2016 investigation explored the surface colonization of plastic bags (polyethylene or a “biodegradable” polyester/corn starch composite) in organic-rich marine sediments. They documented rapid bacterial

colonization of the polymer surfaces from sediment microbes but did not characterize the community composition (87). In a study characterizing biofilm communities on sedimented polyethylene microplastics, microbial communities differed depending upon the sediment type in which microplastics were incubated – silt, fine or medium sand (88). Further, research comparing biofilm formation on sedimented polyethylene terephthalate microplastics, bioplastics and ceramic pieces found that the bioplastic community was least similar to either of the other substrates (89). These studies illustrate that the complexities of the plastisphere on floating microplastics are also true of microplastics in sediments. As plastics in sediments can physically disrupt a variety of sediment parameters (e.g., depth of oxidation), more research is needed to investigate how microplastics may affect entire sediment microbial communities (86, 90, 91).

Aquaculture Salmonid Species

Salmonid species (including wild salmon, trout, char, whitefish, and grayling) constitute important recreational and commercial fisheries in the United States, valued at \$258 million in 2016 (92). Unfortunately, many populations are now endangered or threatened. To supplement wild stocks, there is extensive aquaculture for many of these species. Of the salmonids, there is a growing rainbow/steelhead trout (*Oncorhynchus mykiss*) aquaculture industry, valued at \$691 million dollars in the Americas and \$1.3 billion worldwide, in 2016 (92). Considering their financial and resource value, and historical importance in tribal subsistence fishing, these are heavily managed by State, Federal, and Tribal agencies. *O. mykiss* populations are supported by an extensive hatchery program, where fish are spawned and reared until one to two years of age, and then released for completion of their normal marine to freshwater life cycle (93, 94).

Aquaculture production of *O. mykiss* can occur by raising fish in freshwater raceways (i.e., elongated flow-through tanks), in net-pens through their entire life (typically beginning with freshwater and possibly moving to marine) with harvesting at one to two years of age, or in hatcheries where fish are reared until one to two years of age and released to the wild.

The diverse natural, hatchery, and aquaculture management of trout present numerous opportunities for contact with plastic debris. In the U.S., adult fish residing in the marine environment will be exposed to microplastics present in the northeastern Pacific Ocean (95–97). Fish also spend considerable time during migration in near shore environments, which exhibit elevated concentrations of debris (96). This is a crucial period, as fish are particularly prone to disease during their acclimation from salt and freshwater (i.e., smoltification) (98, 99). *O. mykiss* may also be exposed to plastic debris in their natal rivers and estuaries (100, 101). In aquaculture, *O. mykiss* are held within plastic fiber nets (most commonly polypropylene, polyethylene and nylon) and tanks in high densities (during which time fish are prone to disease transfer). Fish are in close contact with these nets, floats and any microplastics in the water column. It is probable that small microplastics <50 µm are abundant in these environments (34, 102). As such, *O. mykiss* are likely exposed to microplastics across their entire life cycle, presenting an important issue for federal, state, private and tribal resource managers, and stakeholders.

Along with anthropogenic stressors such as microplastics, *O. mykiss* and other salmonids are heavily impacted by infectious hematopoietic necrosis virus (IHNV) (103, 104). IHNV has been extensively studied over the past several decades (99, 103, 105–119). IHNV is a negative-sense single stranded virus in the family *Rhabdoviridae*,

endemic to salmonid fishes from California to Alaska but occurring globally. It causes necrosis of the kidney and spleen (99). IHNV is spread horizontally through water via host urine, feces, milt, mucous and other fluids (99, 104, 110, 120–122). The virus can be extremely virulent (causing up to 100% mortality) and has major impacts on wild, hatchery, and aquaculture *O. mykiss* populations, as well as other salmonid species. Historical literature suggests that co-exposure of IHNV with other stressors may increase disease in exposed hosts (111, 112, 119, 123, 124). Yet, there has been little to no research exploring how microparticles in general, and microplastics in particular, impact the infectivity and severity of IHNV in salmonids. Fisheries managers would be well served by a better understanding of how the rapid increase of microplastics in the environments used for salmonid habitat and aquaculture may impact IHNV-mediated disease.

Microplastics in tissues and the immune response

There is increasing evidence that particles in the size range from sub-micron to 20 μm may enter the tissues of diverse marine animals. Studies have shown that microplastics accumulate in the tissues of invertebrates such as copepods (125) and fiddler crabs (126). Investigation of several finfishes showed that microplastics accumulate in the gills, alimentary tract, liver and muscle (127–132) with distribution among organs differing depending on particle size, but generally increasing over time in the order: alimentary tract > gills > liver/brain (133, 134). This research suggests that small microplastic particles (or nanoplastics, $\leq 1 \mu\text{m}$) may gain entry into the vascular system and be transported to diverse internal tissues, including blood filtering (e.g., liver) and immune organs (spleen, head kidney).

Few studies, however, have investigated the effects of microplastics on specific immune cells in teleosts (135, 136). In one study, juvenile zebra fish were exposed to polystyrene nanoparticles (0.7 µm) and their immune responses monitored using transcriptomics (136). The authors reported activation of immune pathways (e.g., complement) and interaction with phagocytic cells. In another study, head kidney leukocytes exhibited little response when exposed to polyethylene and polyvinylchloride microplastics 40 – 150 µm in diameter, several times larger than the average immune cell (135). Smaller polystyrene microplastics, however, have been shown to decrease monocyte proliferation (137) or dysregulate cytokine production in fish gills (138). Recently, the *in vitro* humoral immune response to irregularly shaped and beaded polystyrene microplastics was investigated. The authors observed that developing B cell populations were reduced following microplastic exposure of primary trout kidney cell cultures (139). In general, immune response seems to vary widely between types of plastics used, exposure assay types and the immune gene targets. Research to explore these relationships is needed. Considering the similarities between teleost fish and human immune systems, fish-based studies may provide insights into impacts on human health.

Structure of the dissertation

This dissertation aims to enhance our understanding of how plastics interact with and impact marine biota. The first chapter investigates how microplastics may alter the microbial community composition and structure of aquatic sediments, using a microcosm experiment and next generation sequencing. This work was published in *Nature Communications* (140). An article for young scientific audiences was also subsequently published (141). Chapters 2-4 investigate the relationship between microplastics and a

viral (IHNV) mediated disease in a salmonid fish species. This work was funded in 2019 by the National Oceanic and Atmospheric Administration Marine Debris Program office. The second chapter uses an *in vivo* rainbow trout system to address population mortality following co-exposure to microplastics (or a natural microparticle) and IHNV, with additional histopathological, gene expression and immunological work in an effort to elucidate the mechanism behind observed effects. The third chapter addresses how microparticle shape or dosage timing affects disease-related mortality trends observed in the second chapter. The fourth investigates how UV-weathering affects the toxicity of microparticles used in the second chapter. These works have been written in publication format and, as such, are written in the first-person plural as opposed to singular.

References

1. R. C. Hale, M. E. Seeley, B. E. Cuker, in *Diet for a Sustainable Ecosystem* (Springer, Cham), *Estuaries of the World*, pp. 325–348.
2. R. C. Hale, M. E. Seeley, M. J. La Guardia, L. Mai, E. Y. Zeng, A Global Perspective on Microplastics. *J. Geophys. Res. Oceans.* **125** (2020), doi:10.1029/2018JC014719.
3. J. R. Jambeck, R. Geyer, C. Wilcox, T. R. Siegler, M. Perryman, A. Andrady, R. Narayan, K. L. Law, Plastic waste inputs from land into the ocean. *Science.* **347**, 768–771 (2015).
4. R. Geyer, J. R. Jambeck, K. L. Law, Production, use, and fate of all plastics ever made. *Sci. Adv.* **3**, e1700782 (2017).
5. S. B. Borrelle, J. Ringma, K. L. Law, C. C. Monnahan, L. Lebreton, A. McGivern, E. Murphy, J. Jambeck, G. H. Leonard, M. A. Hilleary, M. Eriksen, H. P. Possingham, H. De Frond, L. R. Gerber, B. Polidoro, A. Tahir, M. Bernard, N. Mallos, M. Barnes, C. M. Rochman, Predicted growth in plastic waste exceeds efforts to mitigate plastic pollution. *Science.* **369**, 1515–1518 (2020).
6. W. W. Y. Lau, Y. Shiran, R. M. Bailey, E. Cook, M. R. Stuchtey, J. Koskella, C. A. Velis, L. Godfrey, J. Boucher, M. B. Murphy, R. C. Thompson, E. Jankowska, A. Castillo Castillo, T. D. Pilditch, B. Dixon, L. Koerselman, E. Kosior, E. Favoino, J. Gutberlet, S. Baulch, M. E. Atreya, D. Fischer, K. K. He, M. M. Petit, U. R. Sumaila, E. Neil, M. V. Bernhofen, K. Lawrence, J. E. Palardy, Evaluating scenarios toward zero plastic pollution. *Science.* **369**, 1455–1461 (2020).
7. C. P. Ward, C. M. Reddy, Opinion: We need better data about the environmental persistence of plastic goods. *Proc. Natl. Acad. Sci.* **117**, 14618–14621 (2020).
8. L. C. M. Lebreton, J. van der Zwet, J.-W. Damsteeg, B. Slat, A. Andrady, J. Reisser, River plastic emissions to the world's oceans. *Nat. Commun.* **8**, 15611 (2017).
9. X. Lv, Q. Dong, Z. Zuo, Y. Liu, X. Huang, W.-M. Wu, Microplastics in a municipal wastewater treatment plant: Fate, dynamic distribution, removal efficiencies, and control strategies. *J. Clean. Prod.* **225**, 579–586 (2019).
10. E. J. Carpenter, K. L. Smith, Plastics on the Sargasso Sea Surface. *Sci. New Ser.* **175**, 1240–1241 (1972).
11. C. Moore, Across the Pacific Ocean, plastics, plastics, everywhere. *Nat. Hist.* **112** (2003).
12. J. Kaiser, The dirt on Ocean garbage patches. *Science.* **328**, 1506 (2010).

13. L. Lebreton, B. Slat, F. Ferrari, B. Sainte-Rose, J. Aitken, R. Marthouse, S. Hajbane, S. Cunsolo, A. Schwarz, A. Levivier, K. Noble, P. Debeljak, H. Maral, R. Schoeneich-Argent, R. Brambini, J. Reisser, Evidence that the Great Pacific Garbage Patch is rapidly accumulating plastic. *Sci. Rep.* **8**, 4666 (2018).
14. A. ter Halle, L. Ladirat, M. Martignac, A. F. Mingotaud, O. Boyron, E. Perez, To what extent are microplastics from the open ocean weathered? *Environ. Pollut.* **227**, 167–174 (2017).
15. L. W. McKeen, in *The effect of UV light and weather on plastics and elastomers* (Elsevier Inc., ed. 3, 2013), pp. 17–41.
16. E. Yousif, R. Haddad, Photodegradation and photostabilization of polymers, especially polystyrene: Review. *SpringerPlus.* **2**, 1–32 (2013).
17. S. P. Garaba, H. M. Dierssen, Hyperspectral ultraviolet to shortwave infrared characteristics of marine-harvested, washed-ashore and virgin plastics. *Earth Syst. Sci. Data.* **12**, 77–86 (2020).
18. R. Kumar, S. A. Ali, A. K. Mahur, H. S. Virk, F. Singh, S. A. Khan, D. K. Avasthi, R. Prasad, Study of optical band gap and carbonaceous clusters in swift heavy ion irradiated polymers with UV-Vis spectroscopy. *Nucl. Instrum. Methods Phys. Res. Sect. B Beam Interact. Mater. At.* **266**, 1788–1792 (2008).
19. A. N. Walsh, C. M. Reddy, S. F. Niles, A. M. McKenna, C. M. Hansel, C. P. Ward, *Environ. Sci. Technol.*, in press, doi:10.1021/acs.est.1c02272.
20. P. Gijssman, G. Meijers, G. Vitarelli, Comparison of the UV-degradation chemistry of polypropylene, polyethylene, polyamide 6 and polybutylene terephthalate. *Polym. Degrad. Stab.* **65**, 433–441 (1999).
21. P. Gijssman, G. Meijers, G. Vitarelli, Comparison of the UV-degradation chemistry of polypropylene, polyethylene, polyamide 6 and polybutylene terephthalate. *Polym. Degrad. Stab.* **65**, 433–441 (1999).
22. C. Aepli, C. A. Carmichael, R. K. Nelson, K. L. Lemkau, W. M. Graham, M. C. Redmond, D. L. Valentine, C. M. Reddy, Oil weathering after the Deepwater Horizon disaster led to the formation of oxygenated residues. *Environ. Sci. Technol.* **46**, 8799–807 (2012).
23. C. P. Ward, C. J. Armstrong, A. N. Walsh, J. H. Jackson, C. M. Reddy, Sunlight converts polystyrene to carbon dioxide and dissolved organic carbon. *Environ. Sci. Technol. Lett.* **6**, 669–674 (2019).
24. A. L. Andrady, The plastic in microplastics: A review. *Mar. Pollut. Bull.* **119**, 12–22 (2017).

25. R. Asmatulu, G. A. Mahmud, C. Hille, H. E. Misak, Effects of UV degradation on surface hydrophobicity, crack, and thickness of MWCNT-based nanocomposite coatings. *Prog. Org. Coat.* **72**, 553–561 (2011).
26. N. B. Hartmann, T. Hüffer, R. C. Thompson, M. Hassellöv, A. Verschoor, A. E. Daugaard, S. Rist, T. Karlsson, N. Brennholt, M. Cole, M. P. Herrling, M. C. Hess, N. P. Ivleva, A. L. Lusher, M. Wagner, Are we speaking the same language? Recommendations for a definition and categorization framework for plastic debris. *Environ. Sci. Technol.* **53**, 1039–1047 (2019).
27. S. N. Athey, L. M. Erdle, Are we underestimating anthropogenic microfiber pollution? A critical review of occurrence, methods, and reporting. *Environ. Toxicol. Chem.*, 1-16 (2021).
28. C. M. Rochman, S. M. Kross, J. B. Armstrong, M. T. Bogan, E. S. Darling, S. J. Green, A. R. Smyth, D. Veríssimo, Scientific evidence supports a ban on microbeads. *Environ. Sci. Technol.* **49**, 10759–10761 (2015).
29. C. M. Rochman, C. Brookson, J. Bikker, N. Djuric, A. Earn, K. Bucci, S. Athey, A. Huntington, H. McIlwraith, K. Munno, H. De Frond, A. Kolomijeca, L. Erdle, J. Grbic, M. Bayoumi, S. B. Borrelle, T. Wu, S. Santoro, L. M. Werbowski, X. Zhu, R. K. Giles, B. M. Hamilton, C. Thaysen, A. Kaura, N. Klasios, L. Ead, J. Kim, C. Sherlock, A. Ho, C. Hung, Rethinking microplastics as a diverse contaminant suite. *Environ. Toxicol. Chem.* **38**, 703–711 (2019).
30. C. M. Rochman, E. Hoh, B. T. Hentschel, S. Kaye, Long-Term field measurement of sorption of organic contaminants to five types of plastic pellets: Implications for plastic marine debris. *Environ. Sci. Technol.* **47**, 1646–1654 (2013).
31. S. Bejgarn, M. MacLeod, C. Bogdal, M. Breitholtz, Toxicity of leachate from weathering plastics: An exploratory screening study with *Nitocra spinipes*. *Chemosphere.* **132**, 114–119 (2015).
32. R. C. Hale, Analytical challenges associated with the determination of microplastics in the environment. *Anal Methods.* **9**, 1326–1327 (2017).
33. M. Eriksen, L. C. M. Lebreton, H. S. Carson, M. Thiel, C. J. Moore, J. C. Borerro, F. Galgani, P. G. Ryan, J. Reisser, Plastic pollution in the world's oceans: More than 5 trillion plastic pieces weighing over 250,000 tons afloat at sea. *PLoS ONE.* **9**, 1–15 (2014).
34. A. Cozar, F. Echevarria, J. I. Gonzalez-Gordillo, X. Irigoien, B. Ubeda, S. Hernandez-Leon, A. T. Palma, S. Navarro, J. Garcia-de-Lomas, A. Ruiz, M. L. Fernandez-de-Puelles, C. M. Duarte, Plastic debris in the open ocean. *Proc. Natl. Acad. Sci.* **111**, 10239–10244 (2014).

35. I. Paul-Pont, K. Tallec, C. Gonzalez-Fernandez, C. Lambert, D. Vincent, D. Mazurais, J.-L. Zambonino-Infante, G. Brotons, F. Lagarde, C. Fabioux, P. Soudant, A. Huvet, Constraints and priorities for conducting experimental exposures of marine organisms to microplastics. *Front. Mar. Sci.* **5**, 1–22 (2018).
36. G. Suaria, A. Achtypi, V. Perold, J. R. Lee, A. Pierucci, T. G. Bornman, S. Aliani, P. G. Ryan, Microfibers in oceanic surface waters: A global characterization. *Sci. Adv.* **6**, eaay8493 (2020).
37. L. Hermabessiere, A. Dehaut, I. Paul-Pont, C. Lacroix, R. Jezequel, P. Soudant, G. Duflos, Occurrence and effects of plastic additives on marine environments and organisms: A review. *Chemosphere.* **182**, 781–793 (2017).
38. M. Rani, W. J. Shim, G. M. Han, M. Jang, N. A. Al-Odaini, Y. K. Song, S. H. Hong, Qualitative analysis of additives in plastic marine debris and its new products. *Arch. Environ. Contam. Toxicol.* **69**, 352–366 (2015).
39. L. W. McKeen, in *the effect of uv light and weather on plastics and elastomers* (Elsevier, 2013; <https://linkinghub.elsevier.com/retrieve/pii/B9781455728510000013>), pp. 1–16.
40. J. N. Hahladakis, C. A. Velis, R. Weber, E. Iacovidou, P. Purnell, An overview of chemical additives present in plastics: Migration, release, fate and environmental impact during their use, disposal and recycling. *J. Hazard. Mater.* **344**, 179–199 (2018).
41. A. Ballesteros-Gómez, T. Jonkers, A. Covaci, J. de Boer, Screening of additives in plastics with high resolution time-of-flight mass spectrometry and different ionization sources: direct probe injection (DIP)-APCI, LC-APCI, and LC-ion booster ESI. *Anal. Bioanal. Chem.* **408**, 2945–2953 (2016).
42. J. M. Levermore, T. E. L. Smith, F. J. Kelly, S. L. Wright, Detection of microplastics in ambient particulate matter using raman spectral imaging and chemometric analysis. *Anal. Chem.* **92**, 8732–8740 (2020).
43. M. Capolupo, L. Sørensen, K. D. R. Jayasena, A. M. Booth, E. Fabbri, Chemical composition and ecotoxicity of plastic and car tire rubber leachates to aquatic organisms. *Water Res.* **169**, 115270 (2020).
44. L. Zimmermann, G. Dierkes, T. A. Ternes, C. Völker, M. Wagner, Benchmarking the in vitro toxicity and chemical composition of plastic consumer products. *Environ. Sci. Technol.* **53**, 11467–11477 (2019).
45. L. Zimmermann, A. Dombrowski, C. Völker, M. Wagner, Are bioplastics and plant-based materials safer than conventional plastics? In vitro toxicity and chemical composition. *Environ. Int.* **145**, 106066 (2020).

46. J. A. Van Franeker, K. L. Law, Seabirds, gyres and global trends in plastic pollution. *Environ. Pollut.* (2015), doi:10.1016/j.envpol.2015.02.034.
47. S. Avery-Gomm, J. F. Provencher, M. Liboiron, F. E. Poon, P. A. Smith, Plastic pollution in the Labrador Sea: An assessment using the seabird northern fulmar *Fulmarus glacialis* as a biological monitoring species. *Mar. Pollut. Bull.* **127**, 817–822 (2017).
48. C. Pedà, L. Caccamo, M. C. Fossi, F. Gai, F. Andaloro, L. Genovese, A. Perdichizzi, T. Romeo, G. Maricchiolo, Intestinal alterations in European sea bass *Dicentrarchus labrax* (Linnaeus, 1758) exposed to microplastics: Preliminary results. *Environ. Pollut.* **212**, 251–256 (2016).
49. C. Scopetani, A. Cincinelli, T. Martellini, E. Lombardini, A. Ciofini, A. Fortunati, V. Pasquali, S. Ciattini, A. Ugolini, Ingested microplastic as a two-way transporter for PBDEs in *Talitrus saltator*. *Environ. Res.* **167**, 411–417 (2018).
50. M. C. Fossi, M. Bains, C. Panti, M. Galli, B. Jiménez, J. Muñoz-Arnanz, L. Marsili, M. G. Finoia, D. Ramírez-Macías, Are whale sharks exposed to persistent organic pollutants and plastic pollution in the Gulf of California (Mexico)? First ecotoxicological investigation using skin biopsies. *Comp. Biochem. Physiol. Part - C Toxicol. Pharmacol.* **199**, 48–58 (2017).
51. A. L. Lusher, M. McHugh, R. C. Thompson, Occurrence of microplastics in the gastrointestinal tract of pelagic and demersal fish from the English Channel. *Mar. Pollut. Bull.* **67**, 94–99 (2013).
52. J. F. Provencher, J. C. Vermaire, S. Avery-Gomm, B. M. Braune, M. L. Mallory, Garbage in guano? Microplastic debris found in faecal precursors of seabirds known to ingest plastics. *Sci. Total Environ.* **644**, 1477–1484 (2018).
53. F. E. Possatto, M. Barletta, M. F. Costa, J. A. Ivar do Sul, D. V. Dantas, Plastic debris ingestion by marine catfish: An unexpected fisheries impact. *Mar. Pollut. Bull.* **62**, 1098–1102 (2011).
54. J. P. W. Desforges, M. Galbraith, P. S. Ross, Ingestion of microplastics by zooplankton in the Northeast Pacific Ocean. *Arch. Environ. Contam. Toxicol.* **69**, 320–330 (2015).
55. E. G. Karakolis, B. Nguyen, J. B. You, P. J. Graham, C. M. Rochman, D. Sinton, Digestible fluorescent coatings for cumulative quantification of microplastic ingestion. *Environ. Sci. Technol. Lett.* **5**, 62–67 (2018).
56. M. A. Browne, A. J. Underwood, M. G. Chapman, R. Williams, R. C. Thompson, J. A. Van Franeker, Linking effects of anthropogenic debris to ecological impacts. *Proc. R. Soc. B Biol. Sci.* **282** (2015), doi:10.1098/rspb.2014.2929.

57. M. R. Gregory, Environmental implications of plastic debris in marine settings--entanglement, ingestion, smothering, hangers-on, hitch-hiking and alien invasions. *Philos. Trans. R. Soc. Lond. B. Biol. Sci.* **364**, 2013–2025 (2009).
58. S. Chiba, H. Saito, R. Fletcher, T. Yogi, M. Kayo, S. Miyagi, M. Ogido, K. Fujikura, Human footprint in the abyss: 30 year records of deep-sea plastic debris. *Mar. Policy.* **96**, 204–212 (2018).
59. V. Fernández-Juárez, X. López-Alforja, A. Frank-Comas, P. Echeveste, A. Bennasar-Figueras, G. Ramis-Munar, R. M. Gomila, N. S. R. Agawin, “The good, the bad and the double-sword” effects of microplastics and their organic additives in marine bacteria. *Front. Microbiol.* **11**, 581118 (2021).
60. K. Bucci, M. Tulio, C. M. Rochman, What is known and unknown about the effects of plastic pollution: A meta-analysis and systematic review. *Ecol. Appl.* **30** (2020), doi:10.1002/eap.2044.
61. G. Everaert, M. De Rijcke, B. Lonneville, C. R. Janssen, T. Backhaus, J. Mees, E. van Sebille, A. A. Koelmans, A. I. Catarino, M. B. Vandegehuchte, Risks of floating microplastic in the global ocean. *Environ. Pollut.* **267**, 115499 (2020).
62. M. MacLeod, H. P. H. Arp, M. B. Tekman, A. Jahnke, The global threat from plastic pollution. *Science.* **373**, 61–65 (2021).
63. Campanale, Massarelli, Savino, Locaputo, Uricchio, A detailed review study on potential effects of microplastics and additives of concern on human health. *Int. J. Environ. Res. Public Health.* **17**, 1212 (2020).
64. J. C. Prata, J. P. da Costa, I. Lopes, A. C. Duarte, T. Rocha-Santos, Effects of microplastics on microalgae populations: A critical review. *Sci. Total Environ.* **665**, 400–405 (2019).
65. L. A. Amaral-Zettler, E. R. Zettler, T. J. Mincer, Ecology of the plastisphere. *Nat. Rev. Microbiol.* **18**, 139–151 (2020).
66. S. Oberbeckmann, M. G. J. Löder, M. Labrenz, Marine microplastic-associated biofilms - A review. *Environ. Chem.* **12**, 551–562 (2015).
67. L. Miao, P. Wang, J. Hou, Y. Yao, Z. Liu, S. Liu, T. Li, Distinct community structure and microbial functions of biofilms colonizing microplastics. *Sci. Total Environ.* **650**, 2395–2402 (2019).
68. S. Summers, T. Henry, T. Gutierrez, Agglomeration of nano- and microplastic particles in seawater by autochthonous and de novo-produced sources of exopolymeric substances. *Mar. Pollut. Bull.* **130**, 258–267 (2018).

69. C. D. Rummel, A. Jahnke, E. Gorokhova, D. Kühnel, M. Schmitt-Jansen, Impacts of biofilm formation on the fate and potential effects of microplastic in the aquatic environment. *Environ. Sci. Technol. Lett.* **4**, 258–267 (2017).
70. M. Kooi, E. H. van Nes, M. Scheffer, A. A. Koelmans, Ups and downs in the ocean: effects of biofouling on vertical transport of microplastics. *Environ. Sci. Technol.* **51**, 7963–7971 (2017).
71. G. Bhagwat, T. K. A. Tran, D. Lamb, K. Senathirajah, I. Grainge, W. O’Connor, A. Juhász, T. Palanisami, Biofilms enhance the adsorption of toxic contaminants on plastic microfibers under environmentally relevant conditions. *Environ. Sci. Technol.* **55**, 8877–8887 (2021).
72. J. Guan, K. Qi, J. Wang, W. Wang, Z. Wang, N. Lu, J. Qu, Microplastics as an emerging anthropogenic vector of trace metals in freshwater: Significance of biofilms and comparison with natural substrates. *Water Res.* **184**, 116205 (2020).
73. E. R. Zettler, T. J. Mincer, L. A. Amaral-Zettler, Life in the “plastisphere”: Microbial communities on plastic marine debris. *Environ. Sci. Technol.* **47**, 7137–7146 (2013).
74. D. Debroas, A. Mone, A. Ter Halle, Plastics in the North Atlantic garbage patch: A boat-microbe for hitchhikers and plastic degraders. *Sci. Total Environ.* **599–600**, 1222–1232 (2017).
75. J. Jacquin, J. Cheng, C. Odobel, C. Pandin, P. Conan, M. Pujo-Pay, V. Barbe, A.-L. Meistertzheim, J.-F. Ghiglione, Microbial ecotoxicology of marine plastic debris: A review on colonization and biodegradation by the “plastisphere.” *Front. Microbiol.* **10**, 1–16 (2019).
76. I. V. Kirstein, A. Wichels, E. Gullans, G. Krohne, G. Gerds, The Plastisphere – Uncovering tightly attached plastic “specific” microorganisms. *PLoS ONE*, 1–17 (2019).
77. S. Oberbeckmann, A. M. Osborn, M. B. Duhaime, Microbes on a bottle: Substrate, season and geography influence community composition of microbes colonizing marine plastic debris. *PLoS ONE.* **11**, 1–24 (2016).
78. L. A. Amaral-Zettler, E. R. Zettler, B. Slikas, G. D. Boyd, D. W. Melvin, C. E. Morrall, G. Proskurowski, T. J. Mincer, The biogeography of the Plastisphere: Implications for policy. *Front. Ecol. Environ.* **13**, 541–546 (2015).
79. D. Debroas, A. Mone, A. Ter Halle, Plastics in the North Atlantic garbage patch: A boat-microbe for hitchhikers and plastic degraders. *Sci. Total Environ.* **599–600**, 1222–1232 (2017).

80. I. V. Kirstein, S. Kirmizi, A. Wichels, A. Garin-Fernandez, R. Erler, M. Löder, G. Gerdts, Dangerous hitchhikers? Evidence for potentially pathogenic *Vibrio* spp. on microplastic particles. *Mar. Environ. Res.* **120**, 1–8 (2016).
81. C. Dussud, C. Hudec, M. George, P. Fabre, P. Higgs, S. Bruzard, A. M. Delort, B. Eyheraguibel, A. L. Meistertzheim, J. Jacquin, J. Cheng, N. Callac, C. Odobel, S. Rabouille, J. F. Ghiglione, Colonization of non-biodegradable and biodegradable plastics by marine microorganisms. *Front. Microbiol.* **9**, 1–13 (2018).
82. A. McCormick, T. J. Hoellein, S. A. Mason, J. Schlupe, J. J. Kelly, Microplastic is an abundant and distinct microbial habitat in an urban river. *Environ. Sci. Technol.* **48**, 11863–11871 (2014).
83. P. Jiang, S. Zhao, L. Zhu, D. Li, Microplastic-associated bacterial assemblages in the intertidal zone of the Yangtze Estuary. *Sci. Total Environ.* **624**, 48–54 (2018).
84. M. Ogonowski, A. Motiei, K. Ininbergs, E. Hell, Z. Gerdes, K. I. Udekwu, Z. Bacsik, E. Gorokhova, Evidence for selective bacterial community structuring on microplastics. *Environ. Microbiol.* **20**, 2796–2808 (2018).
85. M. K. Viršek, M. N. Lovšin, Š. Koren, A. Kržan, M. Peterlin, Microplastics as a vector for the transport of the bacterial fish pathogen species *Aeromonas salmonicida*. *Mar. Pollut. Bull.* **125**, 301–309 (2017).
86. L. Van Cauwenberghe, L. Devriese, F. Galgani, J. Robbens, C. R. Janssen, Microplastics in sediments: A review of techniques, occurrence and effects. *Mar. Environ. Res.* **111**, 5–17 (2015).
87. A. Nauendorf, S. Krause, N. K. Bigalke, E. V. Gorb, S. N. Gorb, M. Haeckel, M. Wahl, T. Treude, Microbial colonization and degradation of polyethylene and biodegradable plastic bags in temperate fine-grained organic-rich marine sediments. *Mar. Pollut. Bull.* **103**, 168–178 (2016).
88. J. P. Harrison, M. Schratzberger, M. Sapp, A. M. Osborn, Rapid bacterial colonization of low-density polyethylene microplastics in coastal sediment microcosms. *BMC Microbiol.* **14** (2014), doi:10.1186/s12866-014-0232-4.
89. L. J. Pinnell, J. W. Turner, Shotgun metagenomics reveals the benthic microbial community response to plastic and bioplastic in a coastal marine environment. *Front. Microbiol.* **10**, 1252 (2019).
90. H. S. Carson, S. L. Colbert, M. J. Kaylor, K. J. McDermid, Small plastic debris changes water movement and heat transfer through beach sediments. *Mar. Pollut. Bull.* **62**, 1708–1713 (2011).

91. P. T. Harris, The fate of microplastic in marine sedimentary environments: A review and synthesis. *Mar. Pollut. Bull.* **158**, 111398 (2020).
92. FAO, Global Capture Production. *Rome* (2018), (available at www.fao.org).
93. K. A. Naish, J. E. Taylor III, P. S. Levin, T. P. Quinn, J. R. Winton, D. Huppert, R. Hilborn, An evaluation of the effects of conservation and fishery enhancement hatcheries on wild populations of salmon. *Adv. Mar. Biol.* **53**, 61–194 (2007).
94. I. L. Withler, Variability in life history characteristics of steelhead trout (*Salmo gairdneri*) along the Pacific Coast of North America. *J. Fish. Res. Board Can.* **23**, 365–393 (1966).
95. M. C. Goldstein, A. J. Titmus, M. Ford, Scales of spatial heterogeneity of plastic marine debris in the northeast Pacific Ocean. *PLoS ONE.* **8** (2013), doi:10.1371/journal.pone.0080020.
96. M. J. Doyle, W. Watson, N. M. Bowlin, S. B. Sheavly, Plastic particles in coastal pelagic ecosystems of the Northeast Pacific Ocean. *Mar. Environ. Res.* **71**, 41–52 (2011).
97. K. L. Law, S. E. Morét-Ferguson, D. S. Goodwin, E. R. Zettler, E. Deforce, T. Kukulka, G. Proskurowski, Distribution of surface plastic debris in the eastern Pacific Ocean from an 11-year data set. *Environ. Sci. Technol.* **48**, 4732–4738 (2014).
98. K. A. Garver, A. A. M. Mahony, D. Stucchi, J. Richard, C. Van Woensel, M. Foreman, Estimation of parameters influencing waterborne transmission of infectious hematopoietic necrosis virus (IHNV) in atlantic salmon (*Salmo salar*). *PLoS ONE.* **8** (2013), doi:10.1371/journal.pone.0082296.
99. P. Dixon, R. Paley, R. Alegria-Moran, B. Oidtmann, Epidemiological characteristics of infectious hematopoietic necrosis virus (IHNV): A review. *Vet. Res.* **47**, 1–26 (2016).
100. G. Hofmans, The quantification of microplastics along a primary Puget Sound river A study from headwaters to estuary (2017).
101. L. C. M. Lebreton, J. van der Zwet, J.-W. Damsteeg, B. Slat, A. Andrady, J. Reisser, River plastic emissions to the world's oceans. *Nat. Commun.* **8**, 15611 (2017).
102. M. Chen, M. Jin, P. Tao, Z. Wang, W. Xie, X. Yu, K. Wang, Assessment of microplastics derived from mariculture in Xiangshan Bay, China. *Environ. Pollut.* **242**, 1146–1156 (2018).

103. G. Kurath, K. A. Garver, R. M. Troyer, E. J. Emmenegger, K. Einer-Jensen, E. D. Anderson, Phylogeography of infectious haematopoietic necrosis virus in North America. *J. Gen. Virol.* **84**, 803–814 (2003).
104. L. M. Bootland, J. C. Leong, Infectious haematopoietic necrosis virus, in *Atlantic* (1988), vol. 3, pp. 57–122.
105. M. M. D. Peñaranda, A. R. Wargo, G. Kurath, In vivo fitness correlates with host-specific virulence of infectious hematopoietic necrosis virus (IHNV) in sockeye salmon and rainbow trout. *Virology.* **417**, 312–319 (2011).
106. A. R. Wargo, K. A. Garver, G. Kurath, Virulence correlates with fitness in vivo for two M group genotypes of infectious hematopoietic necrosis virus (IHNV). *Virology.* **404**, 51–58 (2010).
107. S. E. Lapatra, Factors affecting pathogenicity of infectious hematopoietic necrosis virus (Ihnv) for salmonid fish. *J. Aquat. Anim. Health.* **10**, 121–131 (1998).
108. A. R. Wargo, G. Kurath, In vivo fitness associated with high virulence in a vertebrate virus is a complex trait regulated by host entry, replication, and shedding. *J. Virol.* **85**, 3959–3967 (2011).
109. A. R. Wargo, A. M. Kell, R. J. Scott, G. H. Thorgaard, G. Kurath, Analysis of host genetic diversity and viral entry as sources of between-host variation in viral load. *Virus Res.* **165**, 71–80 (2012).
110. A. R. Wargo, R. J. Scott, B. Kerr, G. Kurath, Replication and shedding kinetics of infectious hematopoietic necrosis virus in juvenile rainbow trout. *Virus Res.* **227**, 200–211 (2017).
111. K. J. Eder, H. R. Köhler, I. Werner, Pesticide and pathogen: Heat shock protein expression and acetylcholinesterase inhibition in juvenile Chinook salmon in response to multiple stressors. *Environ. Toxicol. Chem.* **26**, 1233–1242 (2007).
112. K. R. Springman, G. Kurath, J. J. Anderson, J. M. Emlen, Contaminants as viral cofactors: Assessing indirect population effects. *Aquat. Toxicol.* **71**, 13–23 (2005).
113. R. M. Troyer, K. A. Garver, J. C. Ranson, A. R. Wargo, G. Kurath, In vivo virus growth competition assays demonstrate equal fitness of fish rhabdovirus strains that co-circulate in aquaculture. *Virus Res.* **137**, 179–188 (2008).
114. E. D. Anderson, H. M. Engelking, E. J. Emmenegger, G. Kurath, Molecular epidemiology reveals emergence of a virulent infectious hematopoietic necrosis (IHN) virus strain in wild salmon and its transmission to hatchery fish. *J. Aquat. Anim. Health.* **12**, 85–99 (2000).

115. R. Breyta, A. Black, J. Kaufman, G. Kurath, Spatial and temporal heterogeneity of infectious hematopoietic necrosis virus in Pacific Northwest salmonids. *Infect. Genet. Evol.* **45**, 347–358 (2016).
116. R. Breyta, A. Jones, G. Kurath, Differential susceptibility in steelhead trout populations to an emergent MD strain of infectious hematopoietic necrosis virus. *Dis. Aquat. Organ.* **112**, 17–28 (2014).
117. R. Breyta, A. Jones, B. Stewart, R. Brunson, J. Thomas, J. Kerwin, J. Bertolini, S. Mumford, C. Patterson, G. Kurath, Emergence of MD type infectious hematopoietic necrosis virus in Washington State coastal steelhead trout. *Dis. Aquat. Organ.* **104**, 179–195 (2013).
118. R. Breyta, C. Samson, M. Blair, A. Black, G. Kurath, Successful mitigation of viral disease based on a delayed exposure rearing strategy at a large-scale steelhead trout conservation hatchery. *Aquaculture.* **450**, 213–224 (2016).
119. K. A. Garver, W. N. Batts, G. Kurath, Virulence comparisons of infectious hematopoietic necrosis virus U and M genogroups in sockeye salmon and rainbow trout. *J. Aquat. Anim. Health.* **18**, 232–243 (2006).
120. D. F. Amend, Detection and transmission of infectious hematopoietic necrosis virus in rainbow trout. *J. Wildl. Dis.* **11**, 471–8 (1975).
121. S. E. LaPatra, J. S. Rohovec, J. L. Fryer, Detection of infectious hematopoietic necrosis virus in fish mucus. *Fish Pathol.* **24**, 197–202 (1989).
122. D. Mulcahy, R. J. Pascho, C. K. Jenes, Detection of infectious haematopoietic necrosis virus in river water and demonstration of waterborne transmission. *J. Fish Dis.* **6**, 321–330 (1983).
123. F. M. Hetrick, M. D. Knittel, J. L. Fryer, Increased susceptibility of rainbow trout to infectious hematopoietic necrosis virus after exposure to copper. *Appl. Environ. Microbiol.* **37**, 198–201 (1979).
124. S. LaPatra, W. J. Groberg, J. S. ROHOVEC, J. L. Fryer, Size-related susceptibility of salmonids to two strains of infectious hematopoietic necrosis virus. *Trans. Am. Fish. Soc.* **119**, 25–30 (1990).
125. C. J. Moore, S. L. Moore, M. K. Leecaster, S. B. Weisberg, A comparison of plastic and plankton in the North Pacific Central Gyre. *Mar. Pollut. Bull.* **42**, 1297–1300 (2001).
126. D. Brennecke, E. C. Ferreira, T. M. M. Costa, D. Appel, B. A. P. da Gama, M. Lenz, Ingested microplastics (>100µm) are translocated to organs of the tropical fiddler crab *Uca rapax*. *Mar. Pollut. Bull.* **96**, 491–495 (2015).

127. C. G. Avio, S. Gorbi, F. Regoli, Experimental development of a new protocol for extraction and characterization of microplastics in fish tissues: First observations in commercial species from Adriatic Sea. *Mar. Environ. Res.* **111**, 18–26 (2015).
128. A. C. Greven, T. Merk, F. Karagöz, K. Mohr, M. Klapper, B. Jovanović, D. Palić, Polycarbonate and polystyrene nanoplastic particles act as stressors to the innate immune system of fathead minnow (*Pimephales promelas*). *Environ. Toxicol. Chem.* **35**, 3093–3100 (2016).
129. O. Güven, K. Gökdağ, B. Jovanović, A. E. Kıdeyş, Microplastic litter composition of the Turkish territorial waters of the Mediterranean Sea, and its occurrence in the gastrointestinal tract of fish. *Environ. Pollut.* **223**, 286–294 (2017).
130. B. Jovanović, Ingestion of microplastics by fish and its potential consequences from a physical perspective. *Integr. Environ. Assess. Manag.* **13**, 510–515 (2017).
131. J. S. Choi, Y. J. Jung, N. H. Hong, S. H. Hong, J. W. Park, Toxicological effects of irregularly shaped and spherical microplastics in a marine teleost, the sheepshead minnow (*Cyprinodon variegatus*). *Mar. Pollut. Bull.* **129**, 231–240 (2018).
132. L. Su, H. Deng, B. Li, Q. Chen, V. Pettigrove, C. Wu, H. Shi, The occurrence of microplastic in specific organs in commercially caught fishes from coast and estuary area of east China. *J. Hazard. Mater.* **365**, 716–724 (2019).
133. Y. Lu, Y. Zhang, Y. Deng, W. Jiang, Y. Zhao, J. Geng, L. Ding, H. Ren, Uptake and accumulation of polystyrene microplastics in zebrafish (*Danio rerio*) and toxic effects in liver. *Environ. Sci. Technol.* **50**, 4054–4060 (2016).
134. J. Ding, S. Zhang, R. M. Razanajatovo, H. Zou, W. Zhu, Accumulation, tissue distribution, and biochemical effects of polystyrene microplastics in the freshwater fish red tilapia (*Oreochromis niloticus*). *Environ. Pollut.* **238**, 1–9 (2018).
135. C. Espinosa, J. M. García Beltrán, M. A. Esteban, A. Cuesta, In vitro effects of virgin microplastics on fish head-kidney leucocyte activities. *Environ. Pollut.* **235**, 30–38 (2018).
136. W. J. Veneman, H. P. Spaink, N. R. Brun, T. Bosker, M. G. Vijver, Pathway analysis of systemic transcriptome responses to injected polystyrene particles in zebrafish larvae. *Aquat. Toxicol.* **190**, 112–120 (2017).
137. M. Hamed, H. A. M. Soliman, A. G. M. Osman, A. E.-D. H. Sayed, Assessment the effect of exposure to microplastics in Nile tilapia (*Oreochromis niloticus*) early juvenile: I. blood biomarkers. *Chemosphere.* **228**, 345–350 (2019).
138. C. Lu, P. W. Kania, K. Buchmann, Particle effects on fish gills: An immunogenetic approach for rainbow trout and zebrafish. *Aquaculture.* **484**, 98–104 (2018).

139. P. Zwollo, F. Quddos, C. Bagdassarian, M. E. Seeley, R. C. Hale, L. Abderhalden, Polystyrene microplastics reduce abundance of developing B cells in rainbow trout (*Oncorhynchus mykiss*) primary cultures. *Fish Shellfish Immunol.* **114**, 102–111 (2021).
140. M. E. Seeley, B. Song, R. Passie, R. C. Hale, Microplastics affect sedimentary microbial communities and nitrogen cycling. *Nat. Commun.* **11**, 2372 (2020).
141. Can Microplastic Pollution Change Important Aquatic Bacterial Communities? *Front. Young Minds*, (available at <https://kids.frontiersin.org/articles/10.3389/frym.2021.596923>).

**Chapter 1: Microplastics affect sedimentary microbial communities and
nitrogen cycling**

Introduction

The increasing amount of plastic debris in the marine environment is a global concern. Consequences of large debris on individual organisms can be obvious (e.g., entanglement or intestinal blockage of a sea turtle or whale)¹. Although microplastics (< 5 mm) and nanoplastics (< 1 μm)² are the most abundant forms of debris, elucidating their biological consequences is challenging and ecosystem-level impacts have not been well demonstrated³. Such ecosystem-scale effects could affect biogeochemical cycles and categorize microplastics as a planetary boundary threat^{3,4}. Further, most studies have focused on microplastics in surface waters. Although many plastics are buoyant, microplastics are still exported to sediments after biofouling or incorporation into marine snow or fecal pellets^{5,6}. In fact, an increasing number of studies have identified microplastics in freshwater, coastal and even deep sea sediments⁷. Hence, impacts on sedimentary communities and associated processes merit investigation. While the interaction between floating plastic debris and microbes (forming a biofilm) has been well documented⁸⁻¹⁰, to our knowledge only three studies to date have addressed biofilm formation on plastic in sediments. Nauendorf et al. (2016) studied the surface colonization of plastic bags (polyethylene or a biodegradable polyester/corn starch composite) in organic-rich marine sediments. They observed rapid bacterial colonization of the polymer surfaces, but did not characterize the community composition¹¹. Harrison et al. (2014) investigated the surface colonization of low-density polyethylene (5 x 5 x 1 mm) in estuarine sediments. Using 16S rRNA gene clone libraries, they found that bacterial composition differed between sediment types (fine sand, medium sand and silt) and that two genera (*Arcobacter* and *Colwellia*) comprised 84 – 93% of the total

sequences identified¹². The biofilm formation on large microplastics (3-4 mm in diameter) at the sediment-water interface was explored by Pinnell and Turner (2019) using shotgun metagenomics¹³. These authors found that compared to polyethylene terephthalate (PET), a bioplastic (polyhydroxyalkanoate, PHA) promoted growth of sulfate reducing bacteria, while the biofilm of PET was not significantly different from a ceramic pellet control. These studies illustrate the ability of biofilms to form on plastic surfaces in sediments. However, an unanswered question is whether the addition of microplastics (a presumably recalcitrant carbon (C) pool) alters overall microbial community composition and biogeochemical cycling processes in sediments.

The impact of microplastics on sediment microbial communities may be particularly important in coastal salt marshes. These systems receive a direct influx of microplastics from land runoff¹⁴, poor waste management¹⁵, storm drains and sewage overflows¹⁶, and wastewater treatment plant outfalls^{17,18}. Marsh vegetation and water circulation patterns promote the entrainment and deposition of suspended solids, organic matter (OM) and microplastics¹⁹. As such, coastal salt marshes are also extremely active zones of OM remineralization and biogeochemical cycling. Sediment microbial communities work in a depth-dependent cascade to remineralize OM. This digestion typically starts with degradation of the most labile OM within the thin, oxygenated layer and ends with fermentation of less labile OM in the anoxic zone. Of these microbially-mediated, catabolic processes, denitrification is particularly important in removing excess reactive nitrogen (N) in coastal systems. Denitrification occurs in the suboxic zone and utilizes nitrate (NO_3^-) and nitrite (NO_2^-) instead of O_2 as the terminal electron acceptor in the oxidation of OM. Denitrification is nearly as energy efficient as the oxygen

respiration pathway. It acts to remove N by converting NO_3^- and NO_2^- to gaseous N species, such as nitrous oxide (N_2O) and dinitrogen (N_2). An equally important reaction is nitrification, which occurs in the oxic layer, oxidizing ammonium (NH_4^+) to NO_2^- and then NO_3^- . Denitrification activity is limited by NO_3^- and NO_2^- supply from *in situ* nitrification or anthropogenic sources. In general, these two pathways are critical for both the removal of excess N in polluted environments, as well as regulating productivity in N limited ecosystems²⁰. The response of these inorganic N forms to microplastic pollution has only been addressed in two studies to our knowledge, neither of which evaluated the role of bacterial community composition in relation to nutrient fluxes^{21,22}.

In our study, we explored the effects of microplastics on the structure and function (specifically, nitrification and denitrification) of microbial communities in coastal salt marsh sediments. Three common, petroleum-based plastics were chosen for testing: polyethylene (PE), polyvinyl chloride (PVC) and polyurethane foam (PUF). In addition, one biopolymer (polylactic acid, PLA) was included to compare the effects of a so-called biodegradable polymer with those presumably recalcitrant to degradation. To evaluate the potential for these plastics to influence sediment communities in the short-term, microplastics of these four polymers were added to individual sediment microcosms and incubated for 16 days (Fig. 1). Changes in the composition and diversity of sediment microbial communities were assessed based on Miseq sequencing of 16S rRNA genes, while the functional genes in nitrification and denitrification were determined with quantitative polymerase chain reaction (qPCR). Dissolved inorganic N concentrations in the overlying water of sediments were measured to infer sedimentary N cycling processes. At the end of the incubation, a sediment slurry incubation experiment

with $^{15}\text{NO}_3^-$ tracer was conducted to measure potential denitrification rates. From these results, we demonstrate that sediment microbial communities differentially respond to the addition of microplastics, with significantly different structural and functional responses occurring between polymer types.

Materials and Methods

Experimental plastics

Consumer plastics were milled and sieved to a defined size range, 53 – 300 μm . PE was a recycled product of predominantly high-density PE obtained from Envision Plastics (Reidsville, NC). PVC used consisted of yellow pellets from Teknor Apex. The PUF was a flexible, yellow PUF donated from a gymnastics studio, similar to PUF used in furniture cushioning. The PLA pellets were from IC 3D Printers LLC and are commonly used in 3D printing. All plastics were embrittled and ground to a powder using a Retsch CryoMill. Resulting powders were individually sieved to 53 – 300 μm using a Retsch AS 200 air jet sieve. In previous studies, PUF, PVC and PE were analyzed for flame retardants. PVC was tested for phthalate additive content (see Supplementary Methods and Table S1.10). Previous analysis of the PVC used here revealed diethylhexyl phthalate (DEHP) at 8.61 mg g^{-1} . PUF used in this study contained both brominated and phosphate-based flame retardants (Table S1.15). This additive analysis is not comprehensive, however, and does not include PLA. Further, being a foundational study in the field, the plastics we selected were not intended to be representative of all environmental sediment microplastic pollution, but rather to embody a range of the characteristics that may be encountered.

Sediment microcosm incubation

Sediment was collected at low tide from the top 2 cm of an intertidal marsh, located along the York River estuary in Gloucester Point, VA in March 2018. Sediment was sandy, with low organic C content (Fig. S1.16). It was thoroughly homogenized and interstitial water and large debris removed. An aliquot was sampled and immediately frozen for initial community analysis (T_0). Approximately 300 g of wet sediment were added to acid washed and combusted 500 ml glass jars (sediment depth reached 3 cm). The experimental design included four microplastic (53-300 μm) treatments (PE, PUF, PVC, PLA) and a no plastic control (CON), with three replicates each ($n=15$; Fig. 1). Microplastics were added to obtain a concentration of 0.5% by weight of sediment, or 1.5 g of microplastics per microcosm (300 g sediment), and thoroughly homogenized with the sediment prior to adding water. Published field data on microplastic sediment concentrations are limited. Many studies that report microplastics in sediments do so on a particle count (not weight) basis, making comparison with our microcosms impractical. Reports generally underestimate actual burdens as they do not include small microplastics. Carson et al. (2011) reported the weight-based sediment concentration of microplastics to sediment for a Hawaiian beach to be 3.3%, six times higher than our experimental concentration⁴⁷. Another Hawaiian study reported concentrations closer to 0.12% plastic by weight (reported as 2 g L⁻¹ and converted using 1.7 g cm⁻³ for marine sediment density⁴⁸), five times lower than our experimental concentration⁴⁹. Based on these available studies, we believe our exposure concentrations are environmentally relevant.

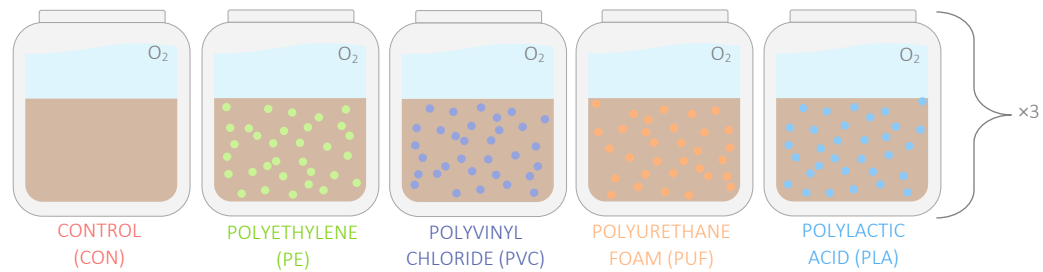


Fig. 1 Microcosm experimental design. All five treatments were repeated in triplicate and each microcosm was individually aerated to establish an oxygen gradient in the sediment.

Estuary water was collected adjacent to the sediment sampling location along the York River (salinity: 21) and filtered with a 38 μm pore size filter to remove particulate matter. Filtered water (50 mL) was added to each microcosm, mixed and sediments allowed to settle. All samples were carefully topped with an additional 200 mL of filtered seawater, so not to re-disturb the sediment. Microcosms were gently aerated to maintain oxygen in the overlying water and 24 hours were allowed to establish an oxic/anoxic gradient down the sediment prior to the start of incubation period. Microcosms were covered with aluminum foil to prevent evaporation and maintained at room temperature in the dark during incubation.

Sediment aliquots were collected at 7 and 16 days for microbial community analysis. Triplicate cores (depth: 1 cm; diameter: 0.5 cm) were randomly sampled at three locations within the jar. The three cores were homogenized, centrifuged and supernatant water removed by pipet. Sediment composites for each microcosm and sample date ($n = 30$) were stored in a $-60\text{ }^{\circ}\text{C}$ freezer for DNA extraction. Coincident with sediment sampling, 10 mL of overlying water were collected and immediately frozen for inorganic nutrient analysis.

DNA extraction and 16S rRNA gene analysis

A DNeasy® Powerlyzer® Powersoil® Kit (Qiagen) was used to extract DNA following the manufacture's instruction. Briefly, silica bead tubes were loaded with 0.5 g of sediment and extraction solution, using the bead beater to break cells and extract DNA. Microplastics were not removed from the sediments prior to DNA extraction. The supernatant in each tube was purified and prepared with a series of DNA cleaning solutions, and final DNA was eluted in 50 μL . Qbit fluorometric quantification (Thermo Scientific) was used to measure the extracted DNA, and each sample was diluted to 10 ng μL^{-1} . Diluted DNA (1 μL) was combined with 12.5 μL GoTaq mix, 9.5 μL nucleic acid free water and 1 μL each PCR primers (515F and 926R) to target the V4-5 regions of 16S rRNA genes⁵⁰. PCR was carried out with denaturation at 95°C for 3 minutes, 25 annealing cycles at 95°C for 30 seconds, 55°C for 30 seconds and 72°C for 30 seconds, followed by elongation at 72°C for 4 minutes. The PCR product was purified using an AMPure XP bead kit and the concentration calculated using Qbit fluorometric quantification. All PCR products were diluted to 0.2 ng μL^{-1} and 6 pM of this product was used for sequencing with the Illumina Miseq platform, following the manufacturer's instruction. All genes were normalized to the 16S qPCR concentration, to correct for nucleic acid concentration, further normalized to the initial community concentration (also normalized to 16S) and statistically evaluated, as described below.

The high quality sequences from the Illumina Miseq were processed using dada2 plugin for R Studio⁵¹. Briefly, forward and reverse sequences were trimmed to 200 and 250 base pairs and a maximum error number of 2 and 5 errors, respectively. Sequences were merged and aligned, and chimeras removed. The Silva reference database (version

132) was used to match the taxonomy information of sequences⁵². Code is provided in the Supplementary Code. RStudio packages (phyloseq, ggplot2 and vegan) were used for all graphical and statistical analyses (McMurdie and Holmes, 2013).

Quantitative PCR of targeted genes

Q-PCR assays of 16S rRNA, *amoA*, *nirS* and *nirK* genes were conducted using the QuantStudio 6 Flex (Thermo Scientific), as described by Lisa et al. (2015) and Semedo et al. (2018)^{24,53}. Standards were prepared through a serial dilution of M13 PCR products from plasmids carrying the target gene or fusion PCR products from environmental DNA and quantified using an Agilent 220 TapeStation System (Agilent Technologies). The primers used for qPCR of 16S rRNA genes were 515F and 926R⁵⁰. The primers *nirScd3aF* and *nirSR3cd* were used to generate 400 bp amplicons of bacterial *nirS* genes; *nirK* genes were detected using *nirKF1Ac* and *nirKR3Cu* primers⁵⁴; bacterial *amoA* genes were detected using *AmoA-1F* and *AmoA-2R*⁵³. The 12 μ L qPCR reactions for 16S, *nirS*, *nirK* and *amoA* quantification consisted of 6 μ L of SYBR green Go-Taq qPCR Master Mix (Promega), 0.03 μ L of CRX dye, 0.6 μ L of each primer (10 μ M), 0.12 μ L of bovine serum albumin (BSA), 8 ng of template DNA, and were adjusted to final volume with nuclease-free H₂O. The qPCR conditions can be found in reference publications for 16S²⁴, *nirS*, *nirK* and *amoA*⁵³. Amplification efficiencies were 69%, 76%, 74%, and 84%, for 16S rRNA, *nirS*, *nirK*, and *AmoA* genes, respectively. The R² value of the standard curves was 0.99 for the four genes. All reactions were performed in 384 well plates with three negative controls, which contained no template DNA, to exclude potential contamination. Reaction specificity was confirmed using gel electrophoresis in comparison with standards and monitored by analysis of dissociation

curves during quantitative amplification. Gene ratio of *amoA*, *nirS* and *nirK* genes in different treatments was calculated by dividing the gene copy numbers by bacterial 16S rRNA gene copy numbers.

Rate measurements of denitrification and anammox

Sediment slurry incubation experiments, with $^{15}\text{NO}_3^-$ as a tracer, were conducted after 17 days incubation time, with exetainer tubes for each treatment replicate (n=6 per treatment) following Lisa et al. (2015). Briefly, exetainer tubes with 2 g of homogenized sediment were helium-purged and dark-incubated overnight to remove residual NO_2^- and NO_3^- . Six replicates of exetainer tubes per sample were amended with 100 nmoles $^{15}\text{NO}_3^-$ and then incubated at room temperature in dark. Both anammox and denitrification activities were stopped by adding saturated zinc chloride (ZnCl) solution after 0, 1 and 2 hr of incubations. Time series production of $^{29}\text{N}_2$ and $^{30}\text{N}_2$ was measured on an isotope ratio mass spectrometer and used to calculate the rate of denitrification and Anammox following Song and Tobias (2011)⁵⁵.

Sediment and water column nutrients

Water samples from each collection date (including the initial water, n=31) were analyzed for NO_2^- , NO_3^- , NH_4^+ and PO_4^{3-} content using a Lachat QuickChem 8000 automated ion analyzer, per methods in Anderson et al. (2015)⁵⁶. In addition, total organic carbon and nitrogen content were analyzed by the Virginia Institute of Marine Science Analytical Service Center using an Exeter model 440CE CHN analyzer.

Statistical Analyses

Differences in rate, gene abundance or nutrient concentration between treatments were statistically compared using a one-way or two-way ANOVA ($\alpha < 0.05$) in

RStudio⁵⁷. Prior to analysis, the Shapiro-Wilks test for normality and Levene's test for homogeneity of the variance were conducted. A post-hoc Tukey test was used to determine which treatments were significantly different. A multivariate permutational ANOVA (PERMANOVA) was conducted using the `anodis` function (Vegan package, R studio) to evaluate significant effects of plastic, date, and the interaction of these on community dissimilarity. Results of all analyses may be found in Tables S1.1-S1.12.

Results

Microbial community structure

A total of 1,379,639 sequences were obtained after merging and filtering raw data of 16S reads, with an average of 44,504 sequences per sample. Bacterial 16S sequences were predominant in each sample with less than 2.21% of archaeal 16S sequences, which were excluded in further analyses. Bacterial diversity (alpha diversity measures) was highest in the biopolymer (PLA), lowest in PE-amended sediments and second lowest in the control treatment (Table 1; Fig. S1.1). Bacterial community diversity was compared among samples using a principal coordinate analysis (PCoA), which measures dissimilarity among communities based on beta diversity (Fig. 2). Using Bray-Curtis dissimilarity, the first two principal components explained 32.7% of community variance. Multivariate permutational ANOVA (PERMANOVA) was used to calculate significant differences between these community dissimilarities based upon plastic treatment ($p = 0.001$), day ($p = 0.001$) and the interaction between these ($p = 0.023$; Table S1.1). Sediment communities in the PVC treatment were distinctly different from the others. The initial community (sampled from the homogenized sediment upon experiment initiation) and the communities in control and PLA treatments clustered together in the

top left quadrant. The communities in control and PLA exhibited minimal changes over time. PE and PUF treatments exhibited the most variation in community composition over time, but were similar to each other. These two petroleum-based polymer treatments had distinctly different effects on communities from the third petroleum-based polymer treatment, PVC. The clear differences in bacterial communities between PVC treatment and other treatments were also observed in a cluster dendrogram (Fig. S1.2).

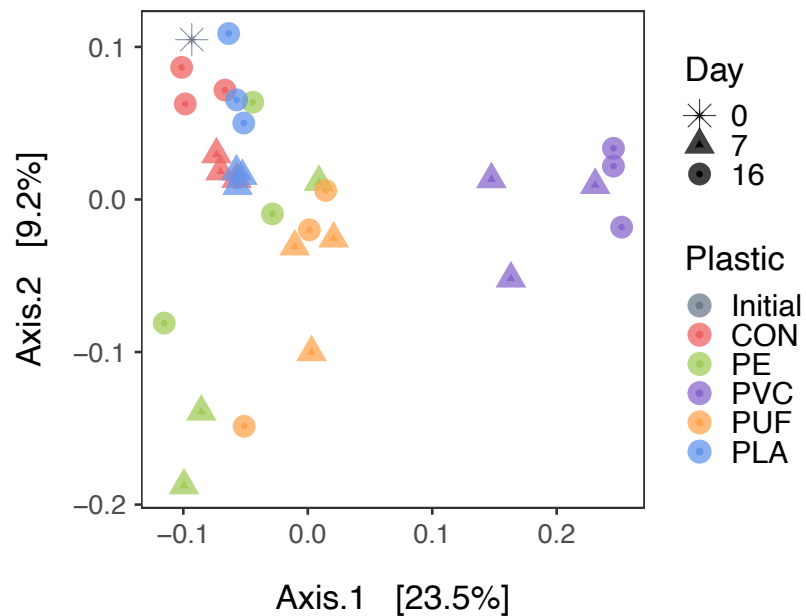


Fig. 2 Principal Coordinate Analysis of the sediment communities. Beta diversity was calculated using the Bray-Curtis dissimilarity index, and is plotted for all sample dates: initial (asterisk), 7 days (triangle) and 16 days (circle); and treatments: control (red; CON), PE (green), PVC (purple), PUF (orange) and PLA (blue). Significant effects of the plastic treatment ($p=0.001$), day ($p=0.001$) and interaction ($p=0.023$) were tested by PERMANOVA.

1

Table 1 Sediment community alpha diversity. Three diversity indices (Shannon, Chao and ACE) for bacterial communities within each sample day (0, 7 or 16) and treatment (n=3), except the initial where n = 1. Values are included plus or minus standard error.

	Initial	CON		PE		PVC		PUF		PLA	
	<i>0</i>	<i>7</i>	<i>16</i>	<i>7</i>	<i>16</i>	<i>7</i>	<i>16</i>	<i>7</i>	<i>16</i>	<i>7</i>	<i>16</i>
Shannon	5.68	5.8 ± 0.01	5.79 ± 0.05	5.55 ± 0.22	5.75 ± 0.13	5.73 ± 0.06	5.75 ± 0.02	5.89 ± 0.05	5.82 ± 0.17	5.85 ± 0.02	5.98 ± 0.03
Chao	634.92	666.48 ± 9.92	658.14 ± 32.09	511.43 ± 174.91	605.93 ± 103.29	724.42 ± 63.10	657.45 ± 32.42	705.15 ± 60.32	658.34 ± 130.66	668.62 ± 7.17	790.98 ± 15.97
ACE	625.72	660.16 ± 10.71	655.48 ± 32.67	510.54 ± 173.89	603.21 ± 101.5	721.73 ± 63.22	654.10 ± 32.08	701.10 ± 58.78	656.86 ± 130.62	667.15 ± 6.45	788.53 ± 16.92

2

All samples were dominated by species within phyla *Bacteriodes* and *Proteobacteria* (Fig. S1.3). Of the *Proteobacteria*, classes *Deltaproteobacteria* and *Gammaproteobacteria* dominated the communities (Fig. S1.4). There were significant differences in community composition between treatments, particularly at the family level. The relative abundance of families at > 1% in samples is illustrated in Fig. 3a (Fig. S1.5 illustrates relative abundance of each sample). Significant differences in the relative abundance of these families between each treatment and the control (determined from DeSeq analysis; $\alpha < 0.01$; Supplementary Fig.s 6-9) is illustrated in Fig. 3b. Several families showed a significantly higher relative abundance in the control than the PVC treatment community, including *Chromatiaceae*, *Ectothiorhodospiraceae*, *Lentimicrobiaceae*, *Magnetococcaceae*, *Pirellulaceae*, *Sedimenticolaceae*, *Thermoanaerobaculaceae*, and *Woeseiaceae*. Of these, *Chromatiaceae* and *Sedimenticolaceae* showed a significantly lower relative abundance in PVC-amended than all other treatments (Fig. S1.4). *Family_XII* was significantly more abundant in communities of all plastic treatments than the control community. *Izimaplasmataceae*, *Marinifilaceae*, and *Marinilabiliaceae* exhibited a significantly higher relative abundance in the PE, PUF and PVC treatments than the control, but not statistically more abundant than in the biopolymer (PLA) treatment. Several genera of *Desulfobacteraceae* and *Desulfobulbaceae* were significantly higher in the PVC-amended than the other treatments (Supplementary Fig.s 9-12), which is not reflected in Fig. 3b because, although most genera within *Desulfobacteraceae* and *Desulfobulbaceae* showed a significantly higher relative abundance in PVC than the other treatments (Fig. S1.9), at least one genera was also significantly lower which resulted in the exclusion of those

families from the heatmap. The most distinctly different treatment community, PVC, contained several families that showed a significantly higher relative abundance than all other treatment communities, including *Acholeplasmataceae*, *Anaerolineaceae*, *Family_XII*, *Izimaplasmataceae*, *Lachnospiraceae*, and *Marinilabiliaceae* (Fig. S1.13).

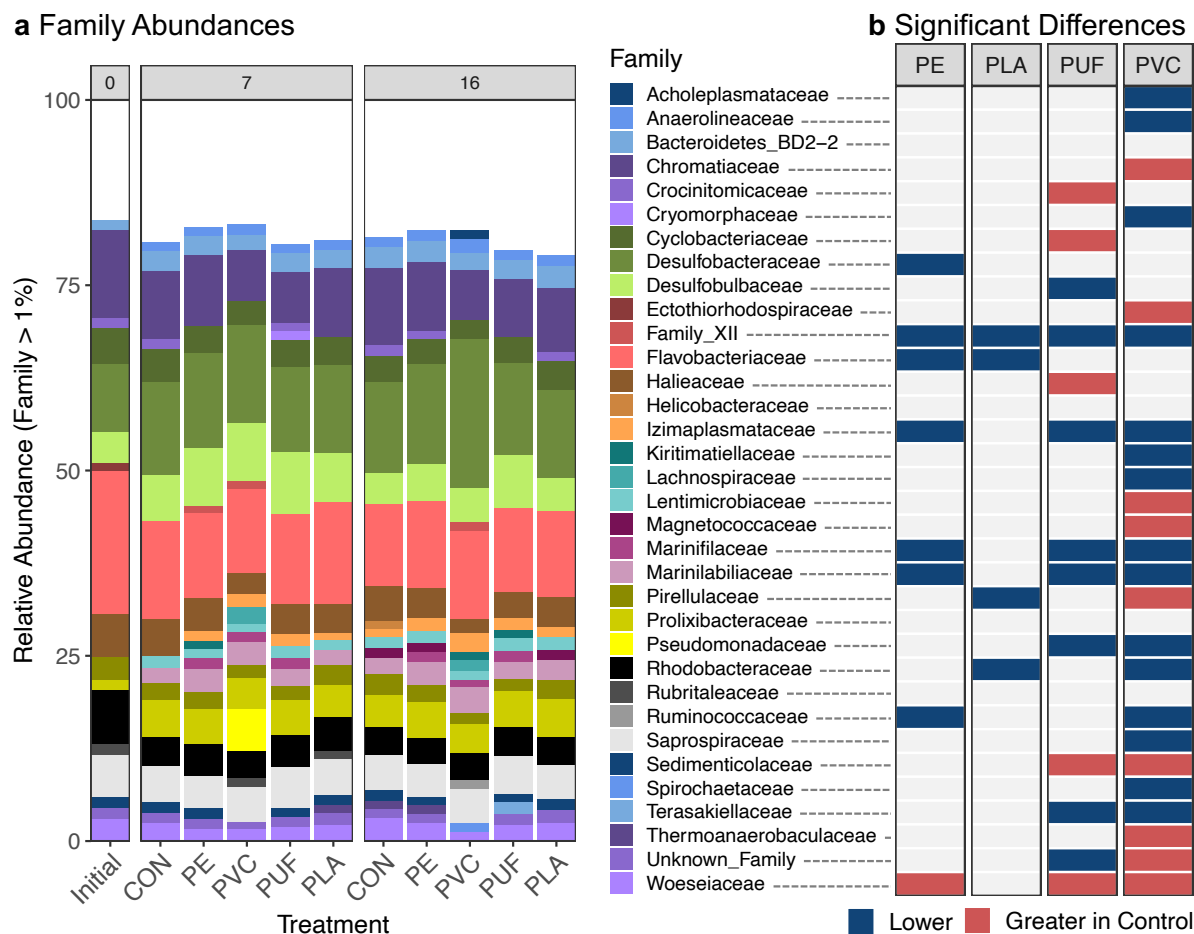


Fig. 3 Bacterial community composition and treatment effects. Comparison of taxonomic differences (family level) in bacterial communities with different microplastic treatments. Stacked bar plot of the relative abundance of families (greater than 1% abundance) for each plastic treatment (averaged for the three replicates, $n = 3$ per treatment) for each sediment collection date (0, 7 and 16 days), where CON is the control treatment (a). Families that are significantly different in relative abundance between treatments and controls (averaged across collection dates), determined using DeSeq ($\alpha = 0.01$). Panel b shows if each a family is significantly greater in one of the plastic treatments (blue) or the control (red).

Nitrification and denitrification

The concentrations of dissolved inorganic nitrogen forms (DIN), NO_3^- , NO_2^- and NH_4^+ , were measured in overlying water at each sampling point (Fig. 4). Concentrations of NO_3^- , NO_2^- and NH_4^+ in the starting water were low (0.072, 0.527, and 3.44 μM , respectively). In general, concentrations of NH_4^+ were three times greater than NO_3^- and NO_2^- across all treatments, and there were two times as much NO_2^- as NO_3^- . We observed greatest NO_2^- and NO_3^- in the 16-day PUF and PLA treatments, while NH_4^+ was lowest in these samples (Fig. 4). PE and control treatments had NO_3^- and NO_2^- in the water after 16 days, while PVC showed almost no detectable NO_3^- or NO_2^- at all time points. In contrast, NH_4^+ in the water was greatest in the PVC treatment after 16 days. In PE, PUF and PLA treatments, NH_4^+ was greater at 7 days than 16 days, opposite the PVC and control treatments. All statistical information can be found in Supplementary Tables 2-4. The PO_4^{3-} water concentrations were also measured and were greatest in the PVC treatments (Fig. S1.14, Table S1.5).

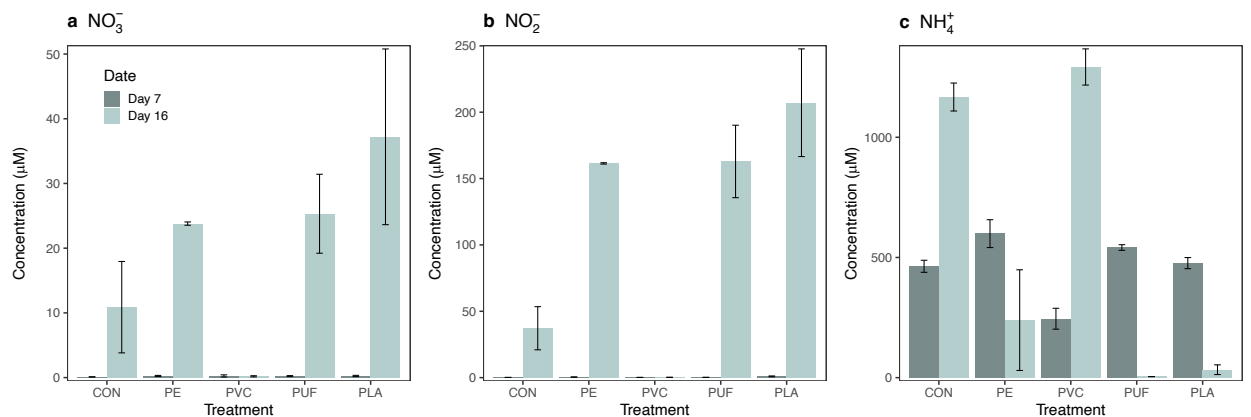


Fig. 4 Dissolved inorganic nitrogen concentrations in water. Concentrations (μM) of NO_3^- (a), NO_2^- (b) and NH_4^+ (c) are shown for each microplastic treatment and control microcosms after 7 and 16 days of incubation ($n = 3$ per treatment). Error bars are standard error and CON is the control treatment. Initial community ($n=1$) concentrations are 0.072, 0.527 and 3.44 μM for NO_3^- , NO_2^- and NH_4^+ , respectively. Statistical analyses can be found in Tables S1.2-S1.4.

The DIN concentrations can be used in conjunction with gene abundance to gain insights into nitrification and denitrification activities. Relative abundances of the genes involved in bacterial nitrification (*amoA*) and denitrification (*nirS* and *nirK*) were measured based on qPCR of the targeted genes relative to 16S rRNA gene abundance. Ammonia monooxygenase (encoded by the *amoA* gene) is a critical enzyme in nitrification, oxidizing ammonia (NH_3^+) to hydroxylamine (NH_2OH). The ratio of *amoA* to 16S in different treatments is plotted in Fig. 5. We specifically targeted ammonia-oxidizing bacteria (AOB), not ammonia-oxidizing archaea (AOA), as no AOA taxa were detected in 16S sequences of the samples. Bacterial *amoA* gene abundances increased from day 7 to day 16 for all treatments, suggesting enhanced nitrification potential with time. The highest *amoA* gene abundances were in PLA and PUF treatments after 16 days (compared to control after 16 days, two-way ANOVA p-value = 0.383 and 0.0093, respectively; see Table S1.6 for all treatment comparisons), portending the highest nitrification activities. This was corroborated by the high NO_3^- and NO_2^- and low NH_4^+ concentrations in these samples, which are the products and reactants of nitrification, respectively. In contrast, *amoA* gene abundance was lowest in PVC treatment, which corresponds with the accumulation of NH_4^+ over time, indicating nitrification inhibition in this treatment.

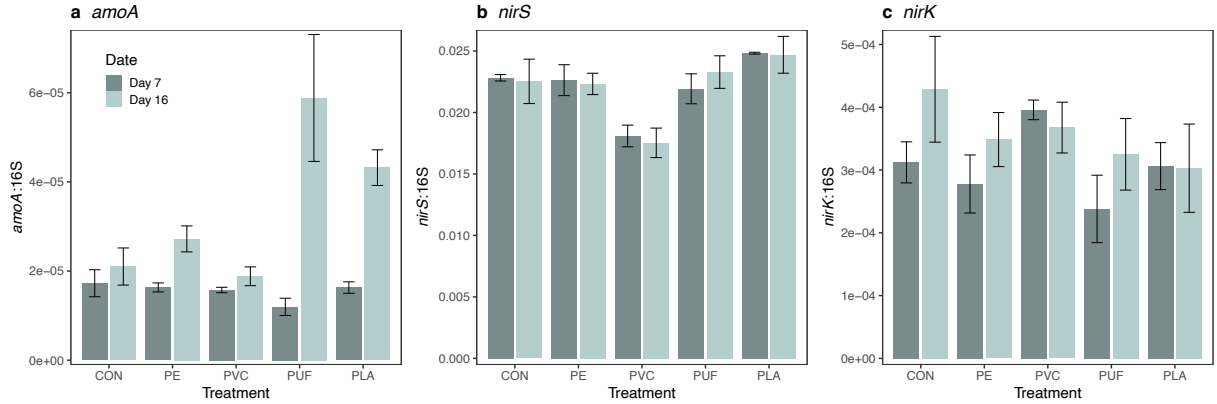


Fig. 5 Nitrification and denitrification gene abundances. The genes encoding ammonia monooxygenase (*amoA*, a) and nitrite reductase (*nirS*, a, and *nirK*, b) were quantified and normalized to 16S rRNA genes, presented here as the gene ratio. Error bars are standard error (n = 3 per treatment) and CON is the control treatment. Initial community ratios are 1.85e-5, 3.03e-2 and 3.25e-4 for *amoA*, *nirS* and *nirK*. Statistical analyses can be found in Tables S1.6-1.8.

A key enzyme in denitrification is nitrite reductase encoded by *nirS* and *nirK* genes. Denitrifiers carrying *nirS* genes are generally considered to be a complete denitrifier, converting NO_3^- and NO_2^- to dinitrogen (N_2); *nirK*-type denitrifiers are more likely to be incomplete denitrifiers, producing N_2O as an end product and contributing to greenhouse gas emission²³. The abundance of *nirS* and *nirK* genes (relative to bacterial 16S rRNA genes) showed very little variation over time within treatments (Fig. 5; Supplementary Tables 7-8). Control, PUF and PLA treatments had the highest *nirS* abundances, suggesting a higher denitrification activity than the PE and PVC treatments. PVC consistently exhibited the lowest *nirS* gene abundances, suggesting a lower denitrification activity. Conversely, the *nirK* abundance was relatively consistent across all treatments, but slightly higher in the control after 16 days.

The potential denitrification activity rate was measured at the end of the 16-day incubation. PVC had a lower potential denitrification rate (Fig. 6; Table S1.9) than any of

the other microplastic treatments, coincident with the lowest *nirS* gene abundances. Denitrification was potentially highest in PLA and PUF, tracking their higher *nirS* gene abundances. PUF and PLA treatments also had more substrate for denitrification (NO_3^- and NO_2^-). Interestingly, the control treatment had a significantly lower denitrification rate than PUF and PLA treatments, comparable to the PVC treatment. This deviates from the pattern of higher *nirS* and *nirK* gene abundances in the control than PVC treatment, but may be a product of relatively lower available NO_3^- and NO_2^- substrate compared to PUF and PLA. Potential rates of anaerobic ammonium oxidation (anammox) were also calculated in a subset of samples. Potential rates were highest in PLA and PUF, and lowest in PVC and the control (Fig. S1.15; Table S1.10), similar to denitrification. Sediment organic C and N contents were calculated at the end of the incubation (Fig. S1.16), as well as the C and N of the plastics themselves (Fig. S1.17), revealing that the control treatment was significantly lower in sediment organic C than all other treatments (Supplementary Tables 11-12). Further, the potential rates of denitrification and anammox were compared to total DIN, following Semedo and Song (2020), to estimate DIN removal capacity. This revealed that PVC and the control treatments had the lowest DIN removal capacity, while PLA and PUF had the highest (Fig. S1.18).²⁴

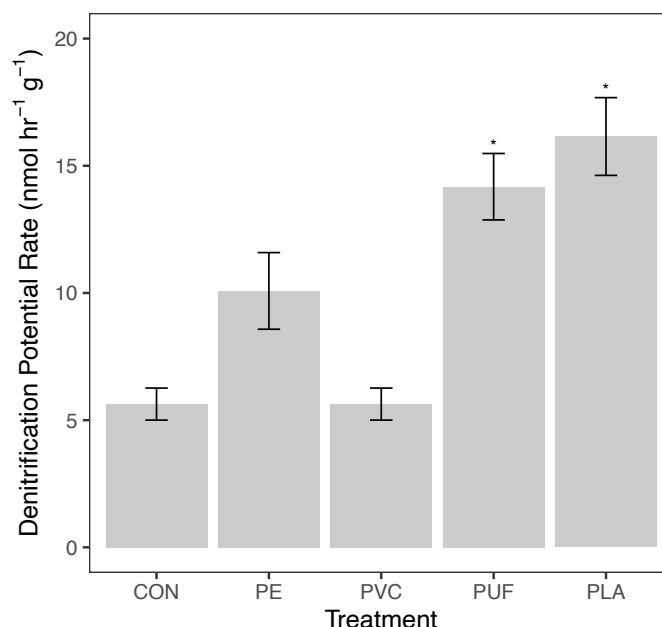


Fig. 6 Comparison of potential denitrification rates. Boxplot details potential rate for each treatment in $\text{nmol hr}^{-1} \text{g}^{-1}$, calculated after the end of the experiment (day 18). Error bars are the standard error ($n = 6$ per treatment) and asterix represent significant difference from the control ($p < 0.05$; Table S1.9).

Discussion

Our study demonstrates that microplastic contamination affects both composition and function of sediment microbial communities. We report changes in the sediment communities between the control and plastic treatments, as well as differences due to polymer type. These sediment communities encompass both the sediment in proximity to the microplastics, as well as the biofilms thereon. This unit is relevant as it reflects the overall impact of microplastic-contaminated sediments on the aquatic ecosystem. Further, attempts to physically separate the biological constituents of the microplastics and the sediment would disrupt these communities. The functional implications of these total sediment/biofilm changes were evaluated by monitoring DIN concentrations in the overlying water, as well as measuring relative abundance of nitrification and

denitrification genes and post-incubation estimates of denitrification rate.

Based on both alpha and beta diversity measures, the different plastic treatments resulted in significant differences in the overall sediment bacterial community diversities (Table 1, Fig. 2). In all alpha diversity indices, the biopolymer (PLA) treatment was the most diverse and PE the least diverse community (Table 1). Although the PCoA explained less than 50% of the variance among treatments, there were clear differences between PVC and the other petroleum-based polymer treatments. These differences are reflected in the significant differences between families present in those treatments (Fig. 3 and Fig. S1.13), motivated by the different polymer amendments. In contrast, the PLA treatment and the control were very similar. Although PE, PVC and PUF polymers are all synthesized from petroleum-derived hydrocarbons, their compositions, structures and physical properties (i.e., strength, density, crystallinity, etc.) differ²⁵. PE and PVC have C-C backbones, while PUF has a heteroatom in its main chain; further, PVC contains chlorine, while PUF contains N²⁶. In addition, polymers may be amended with chemical additives to modify their properties to meet market demands²⁷. Additive packages may be complex and often their compositions are withheld as confidential business information by the manufacturer. PE is the most abundant polymer in production and common in single-use containers²⁸. In terms of marine debris, it is frequently reported in surface waters and increasingly in sediments, likely after its inherent buoyancy is overcome by biofouling²⁹. PVC, on the other hand, is a high density polymer, commonly used in industrial applications and construction. Phthalates may be present in products that require flexibility²⁷. PUF is used in furniture, carpet underlayment and insulation, and therein often contains percent levels of flame retardant additives^{27,30}. Comparison of these

common fossil fuel-based polymers to PLA, a heteroatomic biopolymer, is also warranted³¹. Biopolymers have been promoted as a more environmentally compatible alternative and may become a greater proportion of the market, and thus, of marine debris in the future. Indeed, Nauendorf, et al. (2016) reported that even biopolymers exhibited little degradation in organic-rich marine sediments¹¹. In summary, all four treatment plastics evaluated here differ in physical and chemical characteristics, hence their selection for this study. These differences contributed to the different responses exhibited by the exposed bacterial communities.

We observed that microplastics generated from specific polymer types enhanced sedimentary nitrification and denitrification, while others inhibited these processes. In the case of PUF and PLA in particular, there was an increase in NO_3^- and NO_2^- concentrations, a decrease in NH_4^+ concentration (Fig. 4), as well as correspondingly elevated *amoA* gene abundances with time (Fig. 5), suggesting enhanced rates of nitrification relative to the control. Presumably, the enhanced nitrification in these treatments depended upon NH_4^+ substrate. This may have been available through active sediment OM remineralization. In fact, NH_4^+ increased with time in the control and PVC treatments. This suggests remineralization was active, but nitrification might not be operating at a rate sufficient to remove this excess NH_4^+ . Furthermore, in our microcosm experiment, nitrification and denitrification were coupled. Therefore, the increased NO_3^- and NO_2^- in PUF and PLA treatments may have facilitated the growth and activity of denitrifying communities, evidenced by higher *nirS* gene abundance (Fig. 5) and elevated potential denitrification rates (Fig. 6). For the same reasons, the PE treatments also appeared to slightly enhance nitrification and denitrification, although not significantly

so. Furthermore, some forms of polyurethane have been reported to be susceptible to microbial degradation³². PUF contains nitrogen in the polymer backbone, unlike the other polymers tested here²⁶. Theoretically, *in situ* degradation of PUF may have contributed to labile inorganic N for nitrification and coupled denitrification, and this possibility should be addressed in future studies.

In contrast, both nitrification and denitrification appeared to be inhibited in the PVC treatment. Not only were NO_3^- and NO_2^- concentrations in the overlying water extremely low, but the PVC treatment sediment also exhibited the lowest relative abundance of *nirS* gene and lowest potential rate of denitrification in the post-incubation sediment slurry experiment. Similar to the control, however, the PVC treatment had high concentrations of NH_4^+ which increased over time, likely due to sediment remineralization. Thus, nitrification was clearly limited in this system. Sulfide has been documented to inhibit nitrification in marine sediments³³. Most genera of *Desulfobacteraceae* and *Desulfobulbaceae* showed a significantly higher relative abundance in the PVC than the other treatments (Supplementary Fig.s 9-12). Members of the *Deltaproteobacteria* class had highest relative abundance in the PVC treatment after 16 days, which is characteristic of sulfate reduction. Sulfide production in the PVC treatment by these abundant sulfate-reducing bacteria may have inhibited nitrification, and thus denitrification³³. Pinnell and Turner (2019)¹³ observed significantly higher sulfate reducing microorganisms on the biofilm of a bioplastic (polyhydroxyalkanoate, PHA) formed at the sediment water interface, compared to PET plastic and a ceramic control. They suggested that this was attributable to the hydrocarbon degradation of PHA by sulfate reducers. Here, however, sulfate reducing bacteria were not observed in the

biopolymer treatment (PLA), decreasing the connection between sulfate reducing and hydrocarbon degradation. As such, the increase in sulfate-reducing bacteria in PVC remains unexplained. However, it may be a function of the plastic composition (e.g. a shared additive between tested PVC and Pinnell and Turner (2019) PHA) or a physical response of the sediment environment (e.g. increased hydrophobicity).

Insights into the mechanisms behind microplastic effects on the sediment microbiome and N cycling may be drawn from other studies. Cluzard et al. (2015) observed an increase in overlying water NH_4^+ concentration when sediments were amended with PE microbeads, similar to our PVC treatment²². These authors proposed that an increase in sediment porosity allowed for greater diffusion from the sediments. However, increasing porosity would also increase oxygen diffusion and thus nitrification, decreasing NH_4^+ . Indeed, our PVC treatment also exhibited high PO_4^{3-} concentrations in the overlying water (Fig. S1.14). This can be caused by decreased organic phosphorous burial and subsequent increased PO_4^{3-} in the overlying water in some anoxic systems, which would be characteristic of a less porous system³⁴. Cluzard et al. (2015) did not address community composition; thus, we cannot discern if sulfate-reducing bacteria, which could also have inhibited denitrification, were present in their samples. Another hypothesis is that the microplastics possessed antimicrobial properties, which may select for certain taxa (e.g. sulfate-reducers and gram-negative³⁵) and against others (e.g. nitrifiers³⁶)³⁷. Plasticizer-containing PVC products with antimicrobial properties are often used in the medical field³⁸. For example, Cluzard et al. (2015) used pre-rinsed PE microbeads derived from a skin cleansing personal care product, which likely originally contained antimicrobial additives. In contrast, the PE used in our experiment was a pre-

washed, composite of high- and low-density single-use, container-derived plastics. If microbial responses are indeed influenced by additive content and not polymer type alone, experimental and field research designs must consider both. We suggest future research to characterize additives, especially in controlled studies of organismal responses, so that their influence can be better assessed. If certain additives are found to inhibit coastal N cycling, their use in plastics could and should be controlled.

Compared to the plastic treatments, the control exhibited low denitrification activity following the incubation. This is contrary to denitrification genes (*nirS* and *nirK*), which were generally highest in the control treatment at 7 and 16 days. Over time, nitrification increased in the control (i.e., there was a slight increase in NO_3^- , NO_2^- and *amoA*), thus denitrification was not limited by NO_3^- and NO_2^- substrate. Yet, partial denitrification contributing to the NO_2^- pool could have occurred, in addition to nitrification, as evidenced by the considerably higher dissolved NO_2^- than NO_3^- . The amount of organic C in sediments was notably different between control and plastic treatments, the latter receiving supplemental OM in the form of C from the polymer amendments (Fig. S1.17). This suggests that the higher denitrification in plastic treatments, particularly PLA and PUF, may have been facilitated by the polymer OM itself. PLA and PUF are also the only heteroatomic polymers tested and more susceptible to hydrolytic cleavage, compared to the other plastics with solely C backbones²⁶. However, again, other researchers have suggested that biodegradation of plastics in sediments is low¹¹. Longer duration experiments should be performed to observe if bacteria can degrade plastic over time when faced with a labile sediment C limitation. Another factor for future consideration is pre-weathering of plastics, especially by photo-

oxidation. This may prime them to subsequent biodegradation²⁶.

Clearly, plastic amendments also affected C cycling in our sediment microcosms. In aquatic environments, the bulk of plastic degradation studies have been on water column-originating biofilms of plastics and have focused on the presence of known hydrocarbon degrading species⁹ or metabolic pathways⁸. In either case, the true capacity for bacterial plastic degradation and the responsible organisms are yet undetermined. Certain plastic degrading species have been suggested for PE^{10,39}, PUF^{10,39}, PVC³⁹ and PLA³⁹. Yet very few, if any, of these were found in our samples at greater than 0.1% abundance (Table S1.13). This is not surprising, however, as the above-cited studies are based on water column biofilm assemblages. In a study addressing sediment microbial degradation of PUF, Shah et al. (2008) reported the significant presence of *Pseudomonas spp*⁴⁰. We also observed these taxa in our PUF and PVC samples (Table S1.14), including *Pseudomonadales Pseudomonadaceae*, a previously reported petroleum hydrocarbon degrader in oil-polluted salt marshes⁴¹. Insight into novel, sediment-based, hydrocarbonclastic taxa may be inferred from operational taxonomic units (OTUs) that are significantly higher in plastic-amended treatments than the non-amended control. *Family_XII Fusibacter* was significantly higher in all treatments than in the control (Fig. 3). Families *Marinifilaceae* and *Marinilabiliaceae* were higher in all petroleum-based plastic treatments than the control and PLA treatments. No publications to our knowledge, however, suggest hydrocarbon degradation capacity of these organisms. Therefore, further research is needed. Nonetheless, the results from potential denitrification activity measurements suggest that plastics may be acting as an organic C source for sediment microbial communities (Fig. S1.16). Our microcosm design provided

no additional source of C substrate, which may have motivated sediment microorganisms to utilize microplastics as C for energy compared to natural systems.

Conclusions

Massive amounts of plastic enter and reside within riverine, estuarine and coastal sediments. Although it was once considered completely recalcitrant, we now know that plastic degrades to varying extents in the marine environment over time and that microbial communities may play a role in this^{9,25,42}. The leaching of chemicals from plastic alone has been shown to potentially contribute to the dissolved organic C pool in marine waters⁴³ and to the production of greenhouse gases, such as methane and ethylene⁴⁴. Recently, it was estimated that between 1.15 and 2.41 million tons of plastic enter the coastal zone and oceans from rivers annually, much of which eventually reaches sediments⁴⁵. These plastics once served a variety of consumer purposes; as such, they are extremely diverse in form and chemistry. Here, we have demonstrated that microplastics generated from four diverse polymers influenced marsh sediment microbiomes and biogeochemical cycling. Although the difference between biofilm communities and that of the surrounding sediment cannot be differentiated using our approach, the outcomes between our treatments robustly illustrate the influence microplastics may have on intact sediment ecosystems. This is foundational for future efforts to assess risks of microplastic pollution in diverse environments. Further, the work presented here demonstrates that microplastics are indeed capable of ecosystem-level effects, including alteration of biogeochemical cycles³. Thus, we should evaluate plastic debris as a potential planetary boundary threat^{3,4,46}.

References

1. Gregory, M. R. Environmental implications of plastic debris in marine settings--entanglement, ingestion, smothering, hangers-on, hitch-hiking and alien invasions. *Philos. Trans. R. Soc. B.* **364**, 2013–2025 (2009).
2. Hartmann, N. B. *et al.* Are we speaking the same language? Recommendations for a definition and categorization framework for plastic debris. *Environ. Sci. Technol.* **53**, 1039–1047 (2019).
3. Galloway, T. S., Cole, M. & Lewis, C. Interactions of microplastic debris throughout the marine ecosystem. *Nat. Ecol. Evol.* **1**, 1–8 (2017).
4. Villarrubia-Gómez, P., Cornell, S. E. & Fabres, J. Marine plastic pollution as a planetary boundary threat – The drifting piece in the sustainability puzzle. *Mar. Policy* **96**, 213–220 (2018).
5. Fazey, F. M. C. & Ryan, P. G. Biofouling on buoyant marine plastics: An experimental study into the effect of size on surface longevity. *Environ. Pollut.* **210**, 354–360 (2016).
6. Kooi, M., Van Nes, E. H., Scheffer, M. & Koelmans, A. A. Ups and downs in the ocean: Effects of biofouling on vertical transport of microplastics. *Environ. Sci. Technol.* **51**, 7963–7971 (2017).
7. Van Cauwenberghe, L., Devriese, L., Galgani, F., Robbins, J. & Janssen, C. R. Microplastics in sediments: A review of techniques, occurrence and effects. *Mar. Environ. Res.* **111**, 5–17 (2015).
8. Debroas, D., Mone, A. & Halle, A. T. Plastics in the North Atlantic garbage patch: A boat-microbe for hitchhikers and plastic degraders. *Sci. Total Environ.* **599–600**, 1222–1232 (2017).
9. Zettler, E. R., Mincer, T. J. & Amaral-Zettler, L. A. Life in the ‘plastisphere’: Microbial communities on plastic marine debris. *Environ. Sci. Technol.* **47**, 7137–7146 (2013).
10. Oberbeckmann, S., Löder, M. G. J. & Labrenz, M. Marine microplastic-associated biofilms - A review. *Environ. Chem.* **12**, 551–562 (2015).
11. Nauendorf, A. *et al.* Microbial colonization and degradation of polyethylene and biodegradable plastic bags in temperate fine-grained organic-rich marine sediments. *Mar. Pollut. Bull.* **103**, 168–178 (2016).
12. Harrison, J. P., Schratzberger, M., Sapp, M. & Osborn, A. M. Rapid bacterial colonization of low-density polyethylene microplastics in coastal sediment

- microcosms. *BMC Microbiol.* **14**, 2–15 (2014).
13. Pinnell, L. J. & Turner, J. W. Shotgun metagenomics reveals the benthic microbial community response to plastic and bioplastic in a coastal marine environment. *Front. Microbiol.* **10**, 1–13 (2019).
 14. Rochman, C. M. Microplastics research-from sink to source. *Science* **360**, 28–29 (2018).
 15. Jambeck, J. R. *et al.* Plastic waste inputs from land into ocean. *Science* **347**, 768–771 (2015).
 16. Dris, R., Gasperi, J. & Tassin, B. Sources and fate of microplastics in urban areas: A focus on Paris megacity. in *Freshwater Microplastics: Emerging Environmental Contaminants?* (eds. Wagner, M. & Lambert, S.) 69–83 (Springer International Publishing, 2018).
 17. Mintenig, S. M., Int-Veen, I., Löder, M. G. J., Primpke, S. & Gerdt, G. Identification of microplastic in effluents of waste water treatment plants using focal plane array-based micro-Fourier-transform infrared imaging. *Water Res.* **108**, 365–372 (2017).
 18. Raju, S. *et al.* Transport and fate of microplastics in wastewater treatment plants: implications to environmental health. *Rev. Environ. Sci. Biotechnol.* **17**, 637–653 (2018).
 19. Fagherazzi, S. *et al.* Fluxes of water, sediments, and biogeochemical compounds in salt marshes. *Ecol. Process.* **2**, 1–16 (2013).
 20. Ward, B. B. & Jensen, M. M. The microbial nitrogen cycle. *Front. Microbiol.* **5**, 1–2 (2014).
 21. Green, D. S., Boots, B., O’Connor, N. E. & Thompson, R. Microplastics affect the ecological functioning of an important biogenic habitat. *Environ. Sci. Technol.* **51**, 68–77 (2017).
 22. Cluzard, M., Kazmiruk, T. N., Kazmiruk, V. D. & Bendell, L. I. Intertidal concentrations of microplastics and their influence on ammonium cycling as related to the shellfish industry. *Arch. Environ. Contam. Toxicol.* **69**, 310–319 (2015).
 23. Helen, D., Kim, H., Tytgat, B. & Anne, W. Highly diverse *nirK* genes comprise two major clades that harbour ammonium-producing denitrifiers. *BMC Genomics* **17**, 1–13 (2016).
 24. Semedo, M., Song, B., Sparrer, T. & Phillips, R. L. Antibiotic effects on microbial

- communities responsible for denitrification and N₂O production in grassland soils. *Front. Microbiol.* **9**, 1–16 (2018).
25. Andrady, A. L. The plastic in microplastics: A review. *Mar. Pollut. Bull.* **119**, 12–22 (2016).
 26. Gewert, B., Plassmann, M. M. & MacLeod, M. Pathways for degradation of plastic polymers floating in the marine environment. *Environ. Sci. Process. Impacts* **17**, 1513–1521 (2015).
 27. Hermabessiere, L. *et al.* Occurrence and effects of plastic additives on marine environments and organisms: A review. *Chemosphere* **182**, 781–793 (2017).
 28. Geyer, R., Jambeck, J. R. & Law, K. L. Production, use, and fate of all plastics ever made. *Sci. Adv.* **3**, 25–29 (2017).
 29. Erni-Cassola, G., Zadjelovic, V., Gibson, M. I. & Christie-Oleza, J. A. Distribution of plastic polymer types in the marine environment; A meta-analysis. *J. Hazard. Mater.* **369**, 691–698 (2019).
 30. Hale, R. C., La Guardia, M. J., Harvey, E. & Matt Mainor, T. Potential role of fire retardant-treated polyurethane foam as a source of brominated diphenyl ethers to the US environment. *Chemosphere* **46**, 729–735 (2002).
 31. Lunt, J. Large-scale production, properties and commercial applications of polylactic acid polymers. *Polym. Degrad. Stab.* **59**, 145–152 (1998).
 32. Howard, G. T. Biodegradation of polyurethane: A review. *Int. Biodeterior. Biodegrad.* **49**, 245–252 (2002).
 33. Ward, B. B. Nitrification in marine systems. in *Nitrogen in the marine environment* (eds. Capone, D.G., Bronk, D.A., Mulholland, M.R. & Carpenter, E.J.) 199–261 (Academic Press, 2008).
 34. Lenton, T. M. & Watson, A. J. Regulation of nitrate, phosphate, and oxygen in the ocean. *Global Biogeochem. Cycles* **14**, 225–248 (2000).
 35. Córdova-Kreylos, A. L. & Scow, K. M. Effects of ciprofloxacin on salt marsh sediment microbial communities. *ISME J.* **1**, 585–595 (2007).
 36. Beddow, J. *et al.* Nanosilver inhibits nitrification and reduces ammonia-oxidising bacterial but not archaeal amoA gene abundance in estuarine sediments. *Environ. Microbiol.* **19**, 500–510 (2017).
 37. Barra Caracciolo, A., Topp, E. & Grenni, P. Pharmaceuticals in the environment: Biodegradation and effects on natural microbial communities. A review. *J. Pharm.*

- Biomed. Anal.* **106**, 25–36 (2015).
38. Choi, S. Y. *et al.* Dual functional ionic liquids as plasticisers and antimicrobial agents for medical polymers. *Green Chem.* **13**, 1527–1535 (2011).
 39. Pathak, V. M. & Navneet. Review on the current status of polymer degradation: a microbial approach. *Bioresour. Bioprocess.* **4**, 1–31 (2017).
 40. Shah, A. A., Hasan, F., Akhter, J. I., Hameed, A. & Ahmed, S. Degradation of polyurethane by novel bacterial consortium isolated from soil. *Ann. Microbiol.* **58**, 381–386 (2008).
 41. Beazley, M. J. *et al.* Microbial community analysis of a coastal salt marsh affected by the *Deepwater Horizon* oil spill. *PLoS One* **7**, 1–13 (2012).
 42. Da Costa, J. P. *et al.* Degradation of polyethylene microplastics in seawater: Insights into the environmental degradation of polymers. *J. Environ. Sci. Heal. Part A* **4529**, 1–10 (2018).
 43. Romera-Castillo, C., Pinto, M., Langer, T. M., Álvarez-Salgado, X. A. & Herndl, G. J. Dissolved organic carbon leaching from plastics stimulates microbial activity in the ocean. *Nat. Commun.* **9**, 1–7 (2018).
 44. Royer, S.-J., Ferrón, S., Wilson, S. T. & Kar, D. M. Production of methane and ethylene from plastic in the environment. *PLoS One* **13**, 1–13 (2018).
 45. Lebreton, L. C. M. *et al.* River plastic emissions to the world's oceans. *Nat. Commun.* **8**, 1–10 (2017).
 46. MacLeod, M. *et al.* Identifying chemicals that are planetary boundary threats. *Environ. Sci. Technol.* **48**, 11057–11063 (2014).
 47. Carson, H. S., Colbert, S. L., Kaylor, M. J. & McDermid, K. J. Small plastic debris changes water movement and heat transfer through beach sediments. *Mar. Pollut. Bull.* **62**, 1708–1713 (2011).
 48. Tenzer, R. & Gladkikh, V. Assessment of density variations of marine sediments with ocean and sediment depths. *Sci. World J.* **2014**, 1–9 (2014).
 49. McDermid, K. J. & McMullen, T. L. Quantitative analysis of small-plastic debris on beaches in the Hawaiian archipelago. *Mar. Pollut. Bull.* **48**, 790–794 (2004).
 50. Walters, W. *et al.* Improved bacterial 16S rRNA gene (V4 and V4-5) and fungal internal transcribed spacer marker gene primers for microbial community surveys. *mSystems* **1**, 1–10 (2016).

51. Callahan, B. J. *et al.* DADA2: High-resolution sample inference from Illumina amplicon data. *Nat. Methods* **13**, 581–583 (2016).
52. Yilmaz, P. *et al.* The SILVA and ‘all-species Living Tree Project (LTP)’ taxonomic frameworks. *Nucleic Acids Res.* **42**, D643–D648 (2014).
53. Lisa, J. A., Song, B., Tobias, C. R. & Hines, D. E. Genetic and biogeochemical investigation of sedimentary nitrogen cycling communities responding to tidal and seasonal dynamics in Cape Fear River Estuary. *Estuar. Coast. Shelf Sci.* **167**, A313–A323 (2015).
54. Throbäck, I. N., Enwall, K., Jarvis, Å. & Hallin, S. Reassessing PCR primers targeting *nirS*, *nirK* and *nosZ* genes for community surveys of denitrifying bacteria with DGGE. *FEMS Microbiol. Ecol.* **49**, 401–417 (2004).
55. Song, B. & Tobias, C. R. Chapter three - Molecular and stable isotope methods to detect and measure anaerobic ammonium oxidation (anammox) in aquatic ecosystems. in *Research on Nitrification and Related Processes, Part B* (eds. Klotz, M. G. & Stein, L. Y.) vol. 496, 63–89 (Academic Press, 2011).
56. Anderson, I. C. *et al.* Impacts of climate-related drivers on the benthic nutrient filter in a shallow photic estuary. *Estuaries and Coasts* **37**, 46–62 (2014).
57. Team, R. RStudio: Integrated Development for R. *RStudio, Inc., Boston, MA* <http://www.rstudio.com/>. (2015).

Chapter 2: Microplastics exacerbate virus-mediated mortality in fish

Introduction

Plastic production, use, and environmental release are increasing worldwide. Despite their chemical stability, plastics may weather and fragment into microplastics ($\leq 5\text{mm}$) over time. This has led to the accumulation of microplastics in aquatic, terrestrial, and atmospheric environments (1–5). While long presumed to be toxicologically inert, research suggests that microplastics may present health risks to living resources and humans (6–8). The oversimplification of microplastics as a single contaminant, however, ignores their toxicological complexity, as microplastics vary in size, shape, density, polymer chemistry, additive composition, and more (6, 9–14). Generally, research suggests that many effects of microplastics are sub-lethal (e.g., they can affect innate and adaptive animal defenses) and can derive from their physical parameters as well as chemical composition (4, 6, 7, 15). Additionally, the relative toxicities of naturally occurring polymer-based microparticles (any particle $\leq 5\text{mm}$, relative to petroleum-derived microplastics) are rarely investigated. Information on toxicology of microfibers is also sparse, despite their widespread environmental abundance (16–18). Despite these difficulties in pinpointing toxicological endpoints, research illustrates that microplastics are a relevant threat to aquatic resources, potentially in concert with other stressors (13, 19).

Infectious disease is a major threat to natural ecosystems. Pathogen fitness and virulence (i.e., infection-related morbidity and mortality) can be influenced by external environmental stressors, such as pollutants (20–25). Connections between microplastics and infectious disease have been postulated. For example, prevalence of plastic debris and disease in Asian Pacific corals were found to be correlated (26). Possible responsible

mechanisms include (but are not limited to): plastics act as a sterile vector for pathogens (27, 28); contact of plastic with hosts causes tissue damage and has deregulatory or pro-inflammatory effects on the immune system, decreasing host capacity to fight infection (7, 29–31); or coincident plastic and pathogen pollution (e.g., arising from local human populations), possibly in combination with additional stressor(s). Available research is limited and has not clarified these mechanisms (32, 33). Yet, considering the ubiquity of microplastic pollution, expanded research is warranted to protect valuable resources that are threatened by infectious disease outbreaks, such as fisheries and aquaculture species (34).

We probed the effect of microplastics on infectious disease-related mortality (i.e., virulence), and possible underlying histopathological and immunological mechanisms, using a well-studied aquatic virus and host, of commercial and conservation relevance. Rainbow trout (*Oncorhynchus mykiss*) were chronically exposed to microparticles in water at different concentrations (0, 0.1, 1.0 and 10 mg L⁻¹) over eight weeks (Fig. S2.1). Microparticles included a polystyrene microplastic (expanded polystyrene, ground and sieved to ~20 µm), nylon microfibers (10 x 500 µm flocking fibers), and a natural microparticle, ‘spartina’ (marsh grass, *Spartina alterniflora*, washed, ground, and sieved to ~20 µm; Fig. S2.2). Polymer types were selected for their likely association with fisheries activities (e.g., polystyrene buoys or containers, nylon nets or lines) and exist in environments encountered by these species (35–38). After four weeks, half of the fish were acutely exposed by immersion to a controlled dose of infectious hematopoietic necrosis virus (IHNV), a salmonid pathogen that causes significant losses to aquaculture and wild fisheries worldwide (39). For each treatment, three replicate tanks of 20 fish

were monitored for *in vivo* mortality and viral shedding. A fourth tank for each high particle concentration and controls (IHNV+ and -) was maintained for destructive sampling to analyze tissue viral load, histopathology, and immunological markers over time (Table S2.1; Fig. S2.3). We hypothesized that chronic exposure to polystyrene microplastics and nylon microfibers would increase IHNV virulence compared to fish co-exposed to the natural microparticle (derived from spartina, a widely distributed marsh grass) and virus, or virus alone, and that insights into the mechanism underlying virulence changes could be gained from viral load/shedding, histopathological and immunological analyses.

Materials and Methods

Particle Preparation

Expanded polystyrene foam, commonly used as building insulation, was purchased from a local houseware store. Foam was embrittled and ground in a Retsch CryoMill, sieved to $\leq 20 \mu\text{m}$ with a Retsch AS 200 air jet sieve and Gilson Performer III Sieve shaker (40). Dead *Spartina alterniflora* (marsh cordgrass) was collected from estuarine marshes near Yorktown, VA by cutting dead stems near the base. Grass was sorted in a fume hood, washed with deionized water, and dried in a muffle oven at 60°C . Sections were ground in a standard blender, then the Retsch CryoMill, and sieved as above. Undyed nylon 6'6 fibers were obtained from Claremont Flock, Inc. Fibers measured 0.8 denier (approximately $10 \mu\text{m}$) in diameter and 0.5 mm in length. Size ranges of the particles were measured using a Beckman-Coulter Laser Diffraction Particle Size Analyzer, which measures the longest diameter of a particle. Photo-flo (© Eastman Kodak Company) was added to the particle/water mix to increase dispersion and

decrease particle clumping. Particle size analysis confirmed the 500 x 10 μm measurement of nylon fibers provided by the manufacturer. The median diameter of polystyrene particles was 26.8 μm ; 25% of particles were less than 16.4 μm . The median diameter of spartina particles was 39.2 μm ; 25% of particles fell below 21.3 μm . Particle size analysis and microscopic images of particles are provided in Fig. S2.2. The data illustrated that spartina contained longer particles than polystyrene (a product of the plant cellular structure) which passed through the sieve via their shortest axis; this and any potential clumping may account for the overall greater size particles than polystyrene despite using the same sieving approach. The laser analyzed the nylon fibers at different orientations in the fluid. This likely accounts for the wide range of diameters measured. However, the abundance of measurements of 10 and 500 μm supported our expectation that these were the primary size axes of the nylon fibers (as provided by the manufacturer).

Experimental Design and Procedures

Rainbow trout (*Oncorhynchus mykiss*) eggs were obtained from the National Center for Cool and Cold Water Aquaculture in West Virginia (NCCCWA; within USDA's Agricultural Research Service). Trout were reared at the Virginia Institute of Marine Science (VIMS), according to guidelines from the Institutional Animal Care and Use Committee (IACUC-2020-06-24-14322-arwargo) and previously established protocols (41). Briefly, fish were maintained at 1-3% weight food, fed daily. Fish were initially held in a specific pathogen-free recirculating system supplied with UV-irradiated fresh well-water at 12°C until reaching the desired size for experiments.

For the experiment, fish were transferred to a flow-through tower rack tank system (Aquaneering) housed in a BSL-II aquatic animal laboratory at VIMS, supplied by UV-irradiated fresh well-water at 15°C. Room temperature was maintained at $15.8 \pm 0.4^\circ\text{C}$, water temperature at $15.0 \pm 0.2^\circ\text{C}$, dissolved oxygen at $100.1 \pm 0.5\%$ saturation, and lighting on a 12-hour diurnal cycle. Fish were housed in 6 L tanks (20 fish each) with one water line, two air stones, and fry screens, to facilitate particle circulation and oxygenation through the entire tank. Water flow rate was set to $300\text{-}350 \text{ mL min}^{-1}$. During the experiment, fish were fed 2.0% of their average body weight every four days, 1 hour after the start of a flush (below). Average fish weight was $5.2 \pm 0.4 \text{ g fish}^{-1}$ at the start of the experiment.

Fish received one of 20 possible treatments, outlined in Table S2.1 and Fig. S2.1. Each treatment contained triplicate tanks of 20 fish tracked for mortality and sampled for viral shedding. A fourth replicate was included for destructive tissue sampling in the high particle treatments and controls. Treatments and replicate tanks were randomly distributed throughout the tower rack system. For plastic exposure, fish were dosed with particles every other day, beginning on the first day of the experiment. In the first half of the experiment (weeks 1-4, prior to IHNV exposure) all tanks were held static for 24 hours during particle exposure. The flow was then resumed and tanks flushed for 24 hours to maintain water quality. Fish were switched to clean tanks after two weeks to remove buildup of feces debris and reduce ammonia levels (water ammonium maintained $\leq 5\text{-}8 \text{ ppm}$). In the second half of the experiment, the static period was reduced from 24 to ~ 10 hours, followed by a 38-hour flushing period rather than conducting tank changes to reduce risk of contamination of IHNV across tanks. In total, the experiment lasted 56

days with 28 particle dosing events. The experiment was monitored at the same time daily, recording temperature, dissolved oxygen, and the number of fish mortalities in each tank.

To reduce microplastic discharge to the local wastewater system, during the first hour of each tank flushing effluent was pumped through a series of in-line filters (75 μm , 20 μm , 5 μm and 1 μm), before passage through UV-irradiation (sufficient for virus inactivation) and eventual discharge to the municipal wastewater system.

Halfway through the experiment (day 28), fish were dosed with virus or a mock control. Experimental virus, IHNV (*Salmonid novirhabdovirus*) isolate C (genotypemG119M; GenBank accession number AF237984) was obtained from established laboratory stock (titer of 7.56×10^8 plaque forming units (PFU) mL^{-1}) diluted to 1.0×10^6 PFU mL^{-1} in Minimum Essential Media (MEM) with 10% fetal bovine serum (42). Fish were dosed with 5 mL of diluted IHNV stock in 995 mL water, to reach a final IHNV dose of 5.0×10^3 PFU mL^{-1} , in a 1-hr static immersion challenge, followed by resumption of water flow to the tanks (42). Non-virus (IHNV-) treatments were mock dosed with 5 mL of MEM with 10% fetal bovine serum.

To quantify viral shedding, water samples were collected on days 28, 30, 32, 34, 36, 38, 40, 42, 48, and 54, from triplicate survival analysis tanks. Each water sample was collected at the end of the static period just prior to flushing, such that virus had maximum and consistent time to accumulate in tanks. An 800 μL water sample was collected per tank and stored at -80°C prior to extraction and analysis. A 210 μL volume of sampled water then underwent RNA extraction and qPCR as detailed in Jones et al. 2020 (27).

Tissue samples were collected following virus exposure on day 31, 35, 42 and 56 (3, 7, 14, and 28 days post-virus respectively; Fig. S2.3). Five fish were euthanized via overdose of tricaine methanesulfonate (MS-222) from each tissue sampling tank (Table S2.1) on each dissection day. On day 56 some tissue sampling tanks had less than 5 survivors, so fish were collected from survival analysis tanks of the same treatment (number collected from another tank in no particle IHNV-: 3; no particle IHNV+: 3; spartina IHNV+: 2; polystyrene IHNV+: 4; nylon IHNV+: 5). Fish were observed for clinical signs of infection, weighed, and dissected following standard procedures to excise two gill arches (left side) and the anterior kidney (43). One gill arch and the anterior kidney were preserved separately in RNA later for viral load and immune marker analysis. A second gill arch was preserved in a buffered formalin fixative (Z-Fix, Anatech) for paraffin histology.

Routine methods of paraffin histology were used for the analysis of gill arches (43). Briefly, individual gill arches were washed, decalcified, dehydrated in a graded series of alcohols, cleared in xylene substitute, and embedded in paraffin wax. Tissue blocks were sectioned to 5 μm with a rotary microtome, stained with haematoxylin and eosin, and prepared slides were evaluated on an Olympus AX-70 photomicroscope, focusing analysis on the best-preserved section of gill tissue for each sample. A severity scale 0-3 was applied for semi-quantitative comparison between samples, where 0: no pathology observed, 1: mild (low-density mild focal inflammation, no necrosis), 2: moderate (moderate density inflammation involving ~10–25% area of tissue, moderate signs of early necrosis) and 3: severe (>25% area of tissue, recruitment of immune cells,

advanced necrotic region(s) and multiple areas of pyknosis, karyolysis, and/or karyorrhexis).

RNA extraction from gill arches and anterior kidneys proceeded following Zwollo et al. 2021 (29). Briefly, RNA was purified in RNazol RT and cDNA synthesized with iScript™ Reverse Transcriptase Supermix. Extracted RNA was normalized by concentration to 1 µg RNA (quantified by Nanodrop spectrophotometer) prior to cDNA synthesis, to account for different extraction efficiencies and RNA quality. Quantitative real time polymerase chain reaction (qPCR) was used to quantify IHNV N-gene with analytical standards (44), as well as immune markers membrane-bound immunoglobulin mu (memHCmu), secreted immunoglobulin mu (secHCmu), secreted immunoglobulin tau (secHCtau), interferon gamma (IFN γ), macrophage colony-stimulating factor receptor (MCSFR) and acidic ribosomal protein (ARP). Sequences and references in Table S2.4. In general, five fish were included per treatment; in certain cases, a sample was removed due to poor RNA quality, detailed in Table S2.3. All TaqMan probe sequences (N-gene, secHCtau) were run in a single replicate per fish, while SybrGreen probe sequences were ran in triplicate per fish. IHNV N-gene was expressed as the log-adjusted viral RNA copy number per µg extracted RNA (14). For all immune markers, the relative fold change (RFC) was calculated using critical threshold (Ct) values, normalized to the no particle IHNV- control on day 31, according to Livak and Schmittgen, 2001 $2^{-\Delta Ct}$ method (45). Tissues collected on day 56 (28 days post-IHNV exposure) were not analyzed for viral load or immune gene expression.

Statistical Analyses

All graphical and statistical analyses were completed in R and significance was inferred with $\alpha = 0.05$. For all data sets, every possible combination of fixed and random effects was modeled, and the best fit model determined using Akaike Information Criterion (AIC) and parsimony, with significance at $\Delta AIC \geq 2$.

Mortality analyses were visualized with Kaplan-Meier survival curves using package ‘survival’ (Fig.1) and differences between treatments determined with Cox proportional hazard models in R with the “coxph” function (46). The maximum model tested included fixed factors of virus presence/absence (2 levels: virus, mock; categorical), microparticle type (4 levels: no particle, polystyrene, nylon, spartina; categorical), concentration (4 levels: none, low, medium, high; categorical), a ‘treatment’ factor in which microparticle dose and type were combined (10 levels: no particle, low nylon, medium nylon, high nylon, low polystyrene, medium polystyrene, high polystyrene, low spartina, medium spartina and high spartina; categorical) and their interactions, and random factor of tank. A first analysis was conducted to investigate the main effect of virus. Because no mortality was observed in IHNV- treatments, a second analysis was conducted among IHNV+ fish only, to avoid issues related to non-proportional hazards (same fixed and random factors) and failed convergence of interactions between treatment/virus. This model was used to report significant differences between IHNV+ control (no particle) and all IHNV+ particle co-exposure treatments. The treatments that were significantly different did not vary between mortality analysis 1 and 2.

IHNV load in water was illustrated for all tanks treated with virus for high concentration only (Fig. 2A) and all concentrations in the supplement (Fig. S2.4). Tanks not treated with virus and day 28 (day 0 after virus exposure) were not included in statistical analyses, because virtually no fish had started shedding virus by day 28 and our goal was to determine how viral load differed after the point shedding began. Statistical analyses were conducted with a linear fixed effects model (R package ‘nlme’ version 3.1-152). The maximum model tested included fixed factors as above including treatment, microparticle, concentration, as well as day (continuous variable) and their interactions, and the random factor of tank. The best fitting model included treatment, day, and their interaction, as well as the random influence of tank.

The best fit linear models for IHNV load in gill and anterior kidney samples were determined using a linear model (R package ‘stats’ version 4.0.5), analyzing gill and anterior kidney separately. The maximum model included categorical factors of microparticle, collection day and their interactions. The best model for both anterior kidney and gill included the microparticle treatment and collection day; the model for anterior kidney included their interaction, while gill did not.

Gills pathological severity scale was illustrated including all fish sampled (n = 5), apart from four gills that were not successfully embedded for analysis (n = 4 for spartina IHNV- day 31, nylon IHNV- day 42, polystyrene IHNV+ day 56, no particle IHNV+ day 56 n = 4). The maximum linear model (R package ‘stats’ version 4.0.5) was tested including all categorical factors (microparticle, virus, and day) and their interactions. The best model was this maximum model, for which a three-way ANOVA was run (R package ‘stats’ version 4.0.5). Significant differences in three-way interactions between

treatments were analyzed with the post-hoc Tukey honest significant differences test (R package ‘stats’ version 4.0.5), with full comparisons provided in supplementary material and comparisons deemed biologically significant reported.

Genetic markers for immune response were evaluated (Table S2.3), and the results of IFN γ and secreted IgT in the gill tissue graphed and analyzed separately. The maximum linear model (R package ‘stats’ version 4.0.5) included all categorical factors of microparticle, virus, day and their interactions. The best linear model was fit to the data and included all factors but not any of their interactions. Although we looked at interactions and did not find them to improve the model, power to resolve them may have been limited; however, main effects are discussed and their relation to other patterns observed.

Prior to all the analyses, data were analyzed graphically (interquartile and variance plots) to validate normality and homogeneity of variance model assumptions. No outliers were found that justified removal of any data points from the data set. Complete output of statistical analyses and best fit models can be found in the supplementary materials. Results are typically presented with subscripts on test statistic denoting factor, residual degrees of freedom. P-values were rounded to the third decimal place and values less than 0.001 were shown as <0.001.

Results and Discussion

Viral-mediated fish mortality

Fish mortality was monitored daily (Fig. 1). There was no significant mortality (3 of 1560 fish dead) prior to IHNV exposure, regardless of microparticle exposure. The hazard of death increased significantly (354-fold) among fish exposed to virus compared

to those unexposed (Cox proportional hazard analysis, $X^2_{1,17.16} = 33.73$, p-value <0.001; Fig. 1). Because virtually no mortality was observed in virus negative treatments, we focused our further analysis on only virus exposed groups. Among the virus-exposed fish, there was a suggestive trend that all microparticles further increased mortality, however, the significance and magnitude of this effect depended on particle type and dosage. The greatest increase in mortality was observed in the high nylon fiber treatment (10 mg L⁻¹), reaching approximately 80%, compared to 20% for fish = without microparticles, increasing hazard of death by 6.4 times (Fig. 1A; $X^2_{1,15.71} = 11.10$, p-value < 0.001). The medium nylon fiber dose (1.0 mg L⁻¹) did not significantly increase the hazard of death, despite suggestive trends. Exposure to 1 mg L⁻¹ polystyrene micropastics and virus increased the hazard of death by 3.2 times ($X^2_{1,15.71} = 4.10$, p-value = 0.043). However, the 10 or 0.1 mg L⁻¹ polystyrene treatments did not have a significant effect, although there was a suggestive trend of elevated mortality. Mortality was not significantly enhanced by co-exposure to spartina microparticles at any concentration (Fig. 1C). The observed kinetics of mortality were consistent among treatments and with previous *in vivo* studies (47–49).

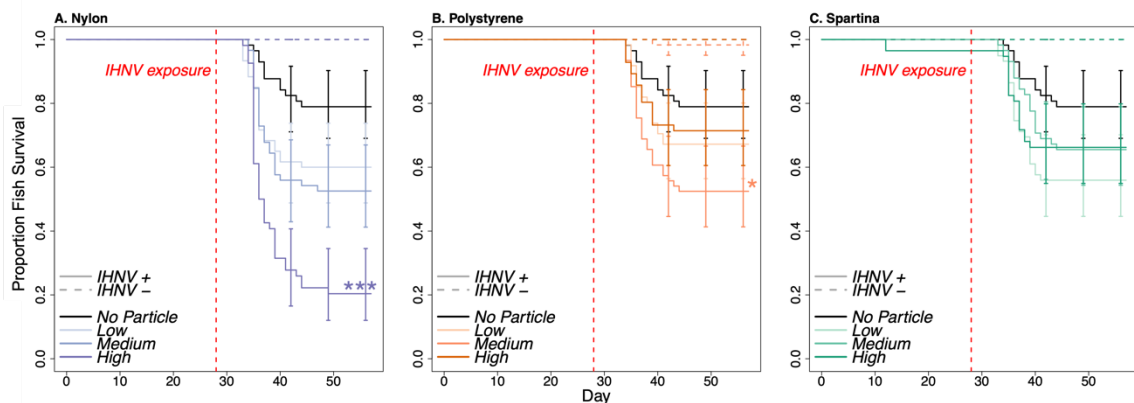


Fig. 1 Survival analysis of fish co-exposed to microparticles and virus. Mortality is illustrated as proportion of surviving fish over 56 days. IHNV exposure is indicated by

the vertical red line on day 28. Virus unexposed (IHNV-; dashed lines) treatments elicited little to no fish mortality, compared to virus exposed (IHNV+; solid lines). Fish not exposed to any microparticles are denoted with a black line, while microparticle exposures are denoted in blue (nylon, A), orange (polystyrene, B) and green (spartina, C). Color shade corresponds to low (0.1 mg L^{-1}), medium (1.0 mg L^{-1}) and high (10.0 mg L^{-1}) microparticle exposure concentrations. Significant differences in survival between IHNV+ no particle and particle treatments are denoted (Cox proportional hazard analysis, $p\text{-value} \leq 0.05$: *, ≤ 0.001 : ***). Most mortalities occurred between days 35 and 45 (7 and 17 days post IHNV exposure). Co-exposure to microparticles, especially nylon fibers, resulted in increased fish mortalities following co-exposure to IHNV.

We initially hypothesized that microplastics would increase IHNV virulence, while the natural microparticle (spartina) would have no effect – a product of particle chemistry (natural polymer v. synthetic polymers with chemical additives). Our results were consistent with this hypothesis as only microplastics (nylon microfibers and polystyrene microplastics) had a significant effect on virulence. Toxicity may derive from chemical constituents (50), or more simply that the higher crystallinity (and therefore, hardness) observed in synthetic polymers is important (51). The polystyrene used here was expanded polystyrene used for insulation and contained the hazardous brominated flame retardant hexabromocyclododecane (Table S2.2). Expanded polystyrene is also commonly found in buoys and floats, as well as single use containers and shipping packaging (38, 52, 53). The nylon microfibers were pure polymer, apart from TiO_2 as a delustrant additive (Table S2.2). Spartina was mostly lignocellulose polymer-based (54). Thus, the microparticle treatments with the most significant effect on IHNV virulence were similarly composed of petroleum-based polymers but did not have equally toxic constituent additives. Were the presence of toxic additives a driver of virulence changes, we would expect polystyrene to cause a greater effect than relatively additive-free nylon

microfibers. Rather, our findings suggest that, in this case, the physical properties of microplastics may have driven effects more than the chemical additive constituents.

The specific size and shape of nylon microfibers may also be important drivers of IHNV-induced mortality. Indeed, some recent studies propound that microfibers have distinct toxicological impacts (16, 55). Although it is often speculated that the smallest particles may have the greatest magnitude of effect due to cellular-level interactions, the polystyrene and spartina were similarly small but enhanced mortality less so than nylon microfibers (11, 56, 57). We calculated (using particle sizes and densities) that our mass-based exposures (high to low concentrations) equated to approximately 29,000 to 290 nylon microfibers and 2,400,000 to 24,000 polystyrene microplastics per liter. This underscores the relative potency of the nylon microfibers; that is, far fewer number of nylon microfibers caused a greater effect than more numerous polystyrene microplastics. By using a range of doses, we spanned possible environmental concentrations, which are typically stochastic and are generally greatly underestimated due to sampling and analytical biases (4).

Interestingly, virulence response to nylon microfibers followed a clear dose response, while polystyrene did not. Although dose generally correlates with toxicity, the absence of a dose response in polystyrene-exposed fish suggests other processes may contribute to the outcomes of viral disease. For example, smaller microparticles (polystyrene and spartina) may be more likely to aggregate in water at high doses, effectively decreasing the number of particles to which an organism is exposed. Microplastic agglomeration can be influenced by size, surface charge/chemistry, biofilm formation, microplastic concentration and salinity (58–60). As no mechanisms beyond

aeration were used to separate particles we cannot exclude this hypothesis, even though particles were visually observed to quickly disperse within tanks. In addition, the lack of a dose response could be a result of variation between tanks or individual fish within tanks, which was accounted for in our models by including tank as a random effect (model 1: $X^2_{13.93,17.16} = 34.33$, p-value = 0.002; model 2: $X^2_{13.52,15.71} = 33.82$, p-value = 0.002).

IHNV Shedding and Body Burden

Host viral entry, replication, and shedding are important factors in understanding virulence, viral fitness, and population level spread (i.e., transmission). Viral shedding in surrounding water was quantified at ten different time points following infection (Fig. 2A). Water samples collected from tanks provided a quantification of the total amount of virus shed by all fish in each tank over the previous 23 hours. Previous studies have shown fish to fish variation in shedding can be high, yet the kinetics of viral shed observed here are consistent with traditional single-fish systems (42, 61), and treatment differences were observed. As expected, viral load was not detectable immediately following virus dosing and flushing, but this was followed by a rapid increase in IHNV shedding, which peaked on day two to three post-infection and by a significant decrease in shedding through time (day effect, linear mixed effects model, $T_{1,229} = -4.9$, p-value < 0.001) as fish died (and were removed) or survived and cleared infection (42, 61, 62). The high nylon co-exposed fish shed significantly more than those exposed to virus alone ($T_{20} = 2.175$, p-value = 0.042), which was not true of the other microparticle co-exposures. This trend appeared to be driven by the peak amount of virus shed, which was greatest in the high nylon dose/virus co-exposure and lowest when exposed to virus

alone, as observed most clearly during the first week after IHNV challenge (Figs. 2A, S2.4, S2.5). The kinetics of shedding through time of any microparticle co-exposures were not determined to be significantly different from the IHNV+ control, despite inclusion of the day*treatment interaction improving the model fit.

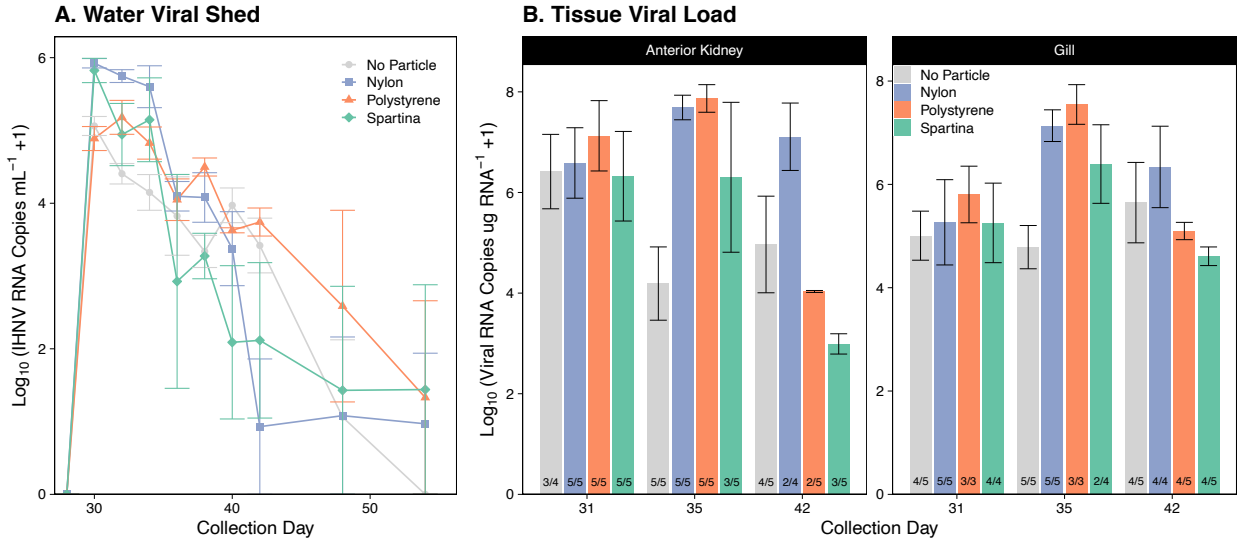


Fig. 2 Viral load in water and tissue samples over time. (A) Virus shed in water is illustrated for the high concentration of each treatment and no particle control (all treatment data provided in Fig. S2.4). Water was collected from each tank and points represent mean viral RNA copies μL^{-1} water of triplicate tanks per treatment (± 1 standard error of mean (SEM)). Viral shed was significantly influenced by collection day, decreasing through time (linear mixed effects model, $T_{229} = -4.9$, $p\text{-value} < 0.001$) and higher overall in nylon co-exposed fish than those exposed to virus alone ($T_{1,20} = 2.175$, $p\text{-value} = 0.042$), but not any other microparticle treatments. (B) IHNV loads in anterior kidney and gill tissues are presented for each collection day. Bars show mean viral RNA copies in one μg of RNA (± 1 SEM) for groups of fish terminally sampled on each day. Only fish with virus detected are included in the means; the number of virus positive (numerator) out of total fish sampled (denominator) are shown as ratio at base of bars. In the anterior kidney, viral load was significantly influenced by the interaction between microparticle and collection day ($F_{6,35} = 2.739$, $p\text{-value} = 0.027$). In gill tissues, viral load was significantly influenced by microparticle dose and day (linear mixed effects model, $F_{5,41} = 1.741$, $p\text{-value} = 0.032$).

Host viral body burden was also quantified in both the anterior kidney and gill at 31, 35 and 42 days (3, 7 and 14 days post-IHNV exposure, respectively; Fig. 2B). The

anterior kidney is a key site of IHNV replication and commonly analyzed to quantify IHNV body burden, while the gill is believed to be a primary point of IHNV host-entry and exit but rarely assayed to quantify body burdens (20, 63). Shortly following virus exposure (i.e., day 31), viral loads in the anterior kidney and gill of infected fish were similar between microparticle and non-particle treatments. In the anterior kidney, tissue burdens tissue burden was significantly higher in nylon and polystyrene co-exposed fish on day 35, compared to non-particle control (Fig 2. interaction day*particle, Tukey post-hoc test, p-values = 0.029 and 0.018, respectively). No other biologically significant differences were observed between particle types or days (chapter 2 statistical supplement). In the gills, nylon microfiber co-exposure had significantly higher viral loads compared to the no particle IHNV+ treatment, regardless of day (particle main effect, $T_{1,41} = 2.395$, p-value = 0.021). There was also more virus present in gills across all particle types compared to day 28 ($T_{1,41} = 2.284$, $P=0.028$). As hematopoietic tissue is a main organ target for IHNV replication with the most severe cytopathic effects, this supports the increased viral load in anterior kidney of fish that had were exposed to both microplastic and virus. These trends are the same when fish whose tissue viral loads were below quantitation (i.e., low or no infection) were included (Fig. S2.6). However, this later analysis could not distinguish between whether effects were driven by fewer fish being positive for virus, or harboring virus but at lower loads.

These data support the conclusion that host viral replication increased, and perhaps more importantly clearance rate decreased, when fish were co-exposed to virus and microplastics (especially nylon microfibers), leading to exacerbated disease and mortality. This also resulted in more viral shedding in the nylon co-exposure. Together,

this suggests that the increased mortality associated with exposure to microplastics was driven by higher viral loads for a longer period of time, rather than compromised tolerance for the same viral load. Again, co-exposed microparticle type was an important driver of these dynamics, with nylon having the most pronounced effect. These data agree with previous work that IHNV *in vivo* fitness and duration of infection can correlate with virulence (48, 49, 61, 62, 64), and demonstrates for the first time that both are influenced by the microparticle co-contaminants presented here. Further, the increase in shedding following nylon and viral co-exposure suggests that between-host transmission may also be increased by microplastic co-exposure. This has major epidemiological implications for the spread of disease and may be an important consideration in controlling disease in populations, such as aquaculture rainbow trout.

Histopathology

Gill tissues were examined from the same fish for which viral loads were quantified and five terminally sampled fish after 56 days. Each fish gill was rated on a severity scale from 0 to 3, where 3 was the highest degree of observed tissue response (e.g., respiratory epithelial tissue damage, inflammation, leukocyte invasion; Fig. 3A). In general, gills of fish exposed to IHNV exhibited severe pathology compared to the predominantly normal healthy gill architecture observed in virus-unexposed fish (Fig 3B), significantly so for no particle on days 42 and 56 (p-values = 0.024 and 0.017, respectively), nylon on days 35, 42 and 56 (p-values each <0.001) and polystyrene on day 35 (p-value < 0.001). This is consistent with the increased viral load burden and virulence in the microfiber co-exposure. In nylon and virus co-exposed fishes, pathological severity of IHNV infection was significantly higher in gills sampled on days 35, 42 and 56 than

day 31 (p-values all < 0.001), a sign of worsening infection with time. Likewise, severity of pathology increased significantly from day 31 to 35 for polystyrene co-exposed fish (p-value = 0.002). This rapid increase in severity of tissue pathology suggests that microplastics-exposed fish may already be in a pro-inflammatory state by the time virus challenge was initiated (day 28). There was a significant decrease in pathological severity over time from day 35 to 56 in polystyrene co-exposed fish (p-value = 0.030), which is consistent with viral load clearance. It is also possible that this pattern was driven by survivor-sampling bias (i.e., infection is less severe among the survivors collected at later time points because they are more resistant to infection), but if this was true we would expect this pattern to be most pronounced for nylon co-exposed fish (where mortality was highest), which it was not. It is worth noting that IHNV is known to also cause extensive necrosis of the hematopoietic tissues (e.g., head kidney, spleen) and this was observed in this study as well (data not shown). Histopathology following IHNV infection is rarely evaluated in gill tissue (20, 63, 66). The gills are an important site of host entry, however, and were found to have viral loads similar to hematopoietic tissue, suggesting either gill being an important site for entry and/or a systemic presence of virus in the host at that time (Fig. 2B). Further, respiration of microplastic-containing water likely led to gill inflammation and pathology. In this study, among virus-exposed fish, gill pathology was consistent with severity of infection, as illustrated by viral load and shedding.

A. Gill Histopathological Characteristics



B. Severity of Gill Histopathological Response

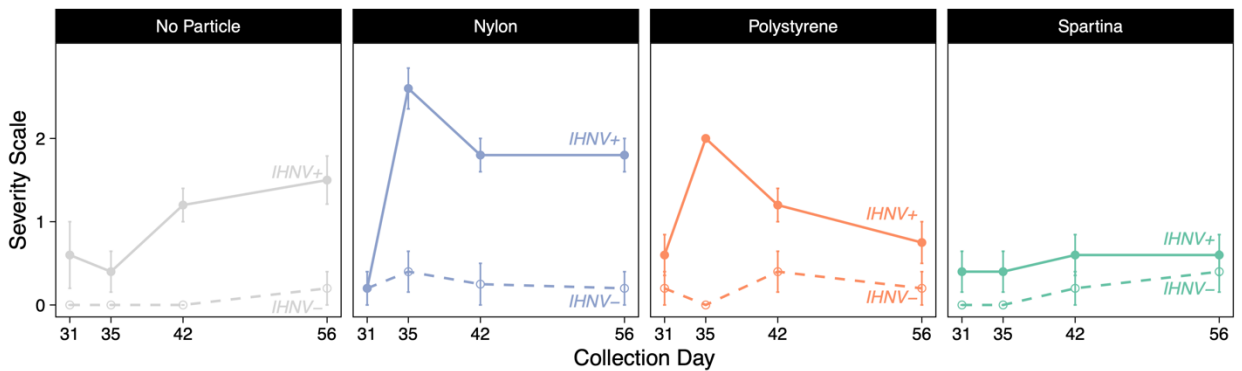


Fig. 3 Histopathological analyses of trout gill tissues. (A) Microscopic images of gill tissues at 40 times magnification (black bar: 20 μ m; Olympus AX-70 photomicroscope). Healthy tissue (severity: 0) are on the left and unhealthy tissue sections on the right (severity: 3). Healthy tissue exhibited normal primary gill filament and secondary lamellae cell structure (65), while fish with increased pathology exhibited significant damage to the gill tissue, including widespread respiratory epithelial cell hyperpigmentation (prominent areas circled), necrosis (bracketed region in right severity scale 3 image), and inflammation indicated by hypertrophy, hyperplasia and leukocytic infiltrates. (B) Pathological severity scale for each particle and virus treatments (IHNV+: solid lines; IHNV-: dashed lines), averaged for each treatment with \pm 1 SEM (n = 5). According to a three-way ANOVA, the severity of histological response was significantly affected by the interaction between microparticle, virus, and collection day ($F_{9,124} = 7.631$, p-value < 0.001).

Evaluation of gill tissues in fish not exposed to IHNV was also essential, as we anticipated observing evidence of tissue damage and subsequent inflammation if microplastics constituted a major irritant to vulnerable gill tissues. This was observed in isolated samples for microparticle exposed fish, with minor sites of focal inflammation, leukocytes infiltration and epithelial damage, recorded as a severity scale of 1 (Fig. 3B;

Fig. S2.7). However, these findings were not statistically significant. As such, we cannot state that increased gill pathology observed in microplastic and virus co-exposed fish was a result of microplastics directly, but that a mechanism related to microplastics increased viral load which amplified disease, and thus gill pathology. This mechanism may be related to the low-severity inflammatory response visually observed in fish exposed to microplastics with no virus exposure, and supports analysis of a pro-inflammatory host response in the gills following microplastic exposure. Moreover, we were unable to identify microplastic particles in histologic tissue sections. This could be due to the multiple rinse steps required for excised gill arch preparation and/or lack of substantial physical microparticle integration into the cellular matrix.

Immune Response

To further explore the state of gill inflammation and immune response as a cause of increased disease mortality, immune gene expression was evaluated. Several genes spanning the innate and adaptive branches of the immune system were measured in gill and anterior kidney of individual fish collected for viral load analysis. The relative fold change (RFC) in expression of these genes compared to the day 31 negative control (no particle, IHNV-) was analyzed following standard practices (45), illustrated for interferon gamma ($\text{IFN}\gamma$) and secreted immunoglobulin tau (IgT) in gill tissues (Fig. 4).

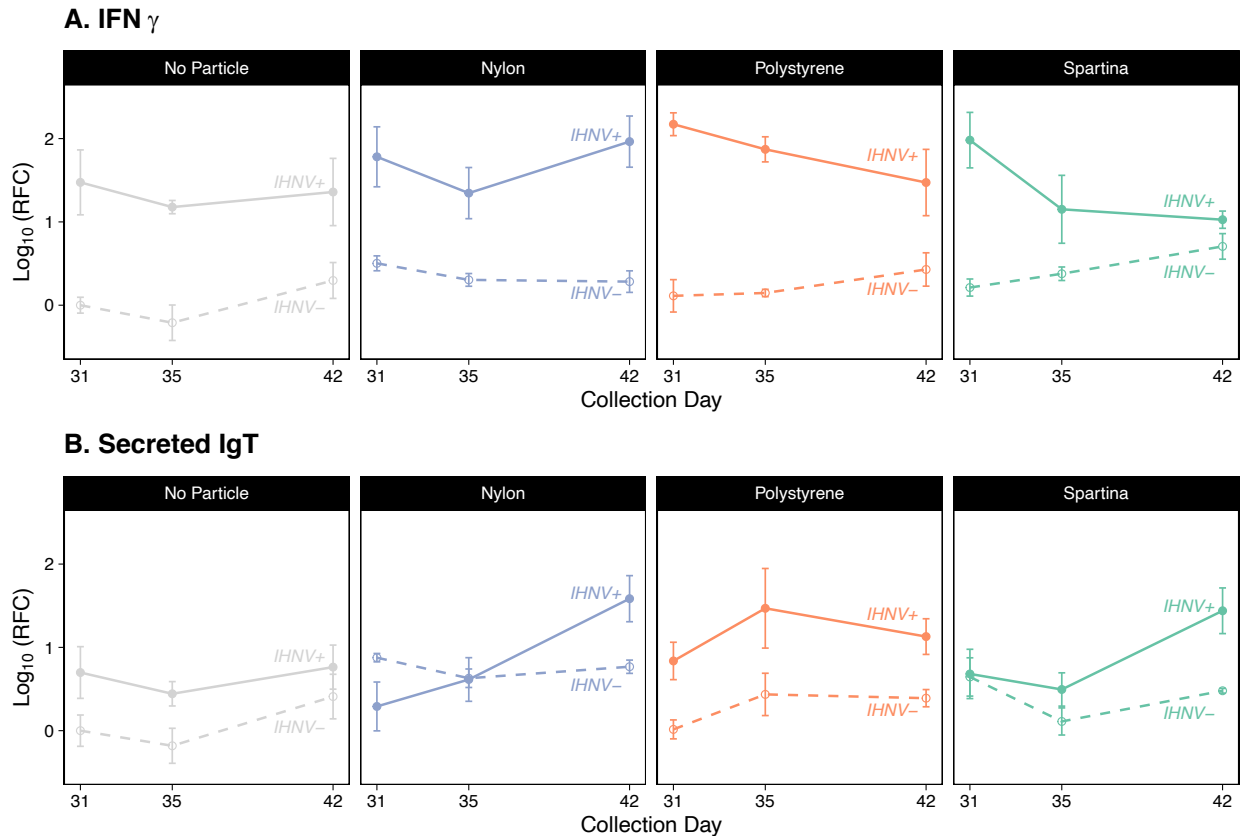


Fig. 4 Response of IFN γ (A) and secreted IgT (B) in gill tissue over time. The relative fold change (RFC; log₁₀-adjusted) compared to the control (no particle, IHNV-) on day 31 is plotted for each microparticle and virus treatment on each collection day, with +/- 1 SEM (n = 5, with exceptions: Table S2.3). For IFN γ , expression was significantly affected by microparticle, day and virus, but not their interactions (linear mixed effects model, $F_{6,97} = 26.26$, p-value <0.001). For secreted immunoglobulin tau (IgT), expression was also significantly affected by microparticle, day and virus, but not their interactions (linear mixed effects model, $F_{6,97} = 7.655$, p-value <0.001).

IFN γ is integral in early anti-viral activity and commonly analyzed as a marker of IHNV immune response (64, 67–69). IFN γ generally triggers pro-inflammatory responses through activation of monocytes and neutrophils (70). Previous work has evaluated IFN γ in hematopoietic tissues or whole-body homogenates of juvenile fish, even though gills may be an important site of IHNV entry into host organisms (20, 69). Our analysis of IFN γ in the anterior kidney was similar to that of the gill tissue, supporting the use of gill

tissue as a model for immune response to this virus (Table S2.3). These data demonstrated a marked increase in IFN γ when exposed to virus ($T_{1,97}=11.92$, p-value <0.001). This agrees with previous work demonstrating rapid IFN γ response in rainbow trout exposed to IHNV (68). Expression of IFN γ was also significantly higher in fish exposed to nylon microfibers ($T_{1,97} = 2.42$, p-value = 0.018) and polystyrene microplastics ($T_{1,97} = 2.20$, p-value = 0.03), regardless of virus exposure. This illustrates that there was IFN γ immune activation in response to nylon microfiber exposure, in presence or absence of virus (Fig. S2.8). This increased IFN γ expression was likely associated with the mild degree of inflammation observed histopathologically and suggests that microplastics increased the pro-inflammatory state of gills prior to virus exposure. It is likely, therefore, that they act as a mild physical irritant on the gill respiratory epithelium. To further evaluate innate host defenses, we measured expression of macrophage colony stimulating factor receptor (MCSFR) expression. MCSFR identifies macrophages/monocytes in teleost fishes, highly phagocytic cell types (71). No differences in MCSFR expression between treatment groups were observed (Table S2.3). Although professional phagocytes have been documented to engulf microplastics $\leq 10 \mu\text{m}$ *in vitro* (29, 72, 73), the number of polystyrene or spartina particles of this size encountering fish gills may have been too low to trigger a phagocytic response. Neutrophil marker myeloperoxidase (MPO) should be targeted for future work.

To investigate potential effects of microplastics and IHNV on the humoral immune response, we evaluated expression of secreted IgT. Secreted IgT is a key component of teleost fish mucosal antibody response, but has not been well-studied in response to infection with IHNV (69). Our results demonstrate that infection with IHNV

significantly increased secreted IgT expression compared to uninfected fish ($T_{1,97} = 4.56$, $p\text{-value} < 0.001$), indicating that there was a mucosal antibody response to IHNV in the gills. This response increased over time, as demonstrated by significantly increased expression from day 31 to 42 ($T_{1,97} = 3.01$, $p\text{-value} = 0.003$). Although it could not be discerned statistically, this pattern of initially low and increased expression through time appeared to be most pronounced in the nylon microfiber and IHNV co-exposed fish, suggesting a potential delay in secreted IgT response when fish faced this co-challenge. Secreted IgT expression was significantly higher among fish exposed to nylon, polystyrene or spartina microparticles ($T_{1,97} = 2.81, 2.36, 2.08$, and $p\text{-values} = 0.006, 0.02$ and 0.04 , respectively) than those not exposed to microparticles, regardless of IHNV exposure (Fig. S2.9). This suggests that the presence of microparticles increased the mucosal antibody response, but that this activation was not protective, as co-exposure to virus and microplastics is correlated with both increased viral load/shedding and mortality in our study. This agrees with other studies that have shown correlations between level of inflammation, pathogen load and disease expression (74).

Secreted and membrane-bound forms of the more systemic immunoglobulin Mu (IgM) were also analyzed to assess humoral immune response. *In vitro* work suggested that B-lymphoid development in the anterior kidney was suppressed by the presence of the polystyrene microplastics (29), which has been reported by others (75). However, we did not observe any change in expression of the membrane form of immunoglobulin mu between treatments in anterior kidney tissues (Table S2.3). The response was highly variable between sampling times, suggesting our analyses may not have had sufficient temporal resolution or power (limited sample size) to distinguish any relationship

between humoral immunity and microparticle exposure *in vivo*. Further, effects to B-lymphopoiesis would be most pronounced if microparticles translocated to the tissue of the anterior kidney, and histopathology showed no evidence of microplastic incorporation into tissues (although we cannot rule it out).

With the data gathered here, we conclude there was mild evidence of pro-inflammatory immune response caused by chronic exposure to microplastics, particularly nylon microfibers, in the gills. This may be correlated with the isolated instances of inflammation observed in gill histopathology. Therefore, the combination of tissue damage, associated inflammation and potentially associated tissue damage following microplastic exposure may be important in the underlying mechanism of increased viral load (leading to increased virulence) under microplastic and virus co-exposure scenarios.

Conclusions

Here, for the first time we demonstrate that exposure to microplastics can increase lethality of a serious infectious disease in an economically important fish species. This has global implications, exacerbated by the widespread distribution and increasing concentrations of microplastics. Overall, viral virulence and *in vivo* viral fitness increased when fish were co-exposed to IHNV and microparticles, particularly for nylon microfibers above 1 mg L⁻¹. This was associated with an increase in viral load and shedding among microplastic and virus co-exposed fish, which enhanced tissue damage to gills. Expression of select markers indicative of host defense mechanisms suggest that microplastic and IHNV co-exposed fish did not exhibit plastic-induced immunosuppression of the marker genes analyzed here; rather, there is evidence of a pro-inflammatory immune response among uninfected fish exposed to nylon microfibers.

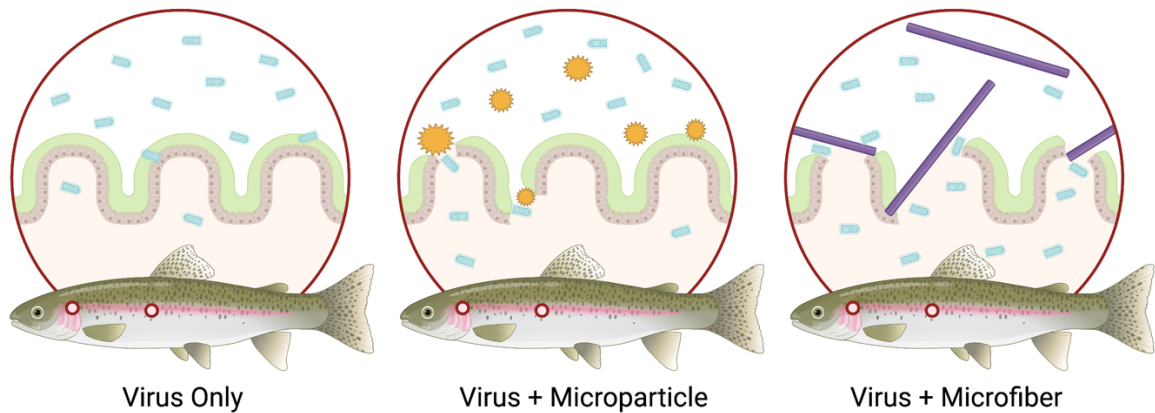


Fig. 5 Illustration of proposed mechanism of increased virulence. When exposed to virus alone (blue virions), mucosal and epithelial barriers of the gill and intestinal tract may successfully block some portion of the virus from entering the tissues. When exposed to microparticles and virus, the epithelial/mucosal barrier may incur mild physical damage to membranes causing inflammatory response. Damage is greater for microfibers, which are larger and may be more likely to become entrapped in and damage the outer membrane of delicate epithelia. This would facilitate greater viral entry and ultimately increased disease virulence. Image created with biorender.com and not to scale.

A mechanism that may explain these results is that microparticles increased virulence by enhancing physical viral entry, initially into host barrier epithelial cells (Fig. 5). Successful host colonization is the first step in establishing infection, to which fish present both physical and immunological defenses (62, 76, 77). Here, microparticles (including the nylon microfibers) likely contacted the gills when particles passed over respiratory surfaces and digestive tract when particles were ingested – both sites of IHNV host invasion (20, 63). The likelihood that a particle could damage associated epithelia may be a product of its size, shape and crystallinity. Synthetic polymers are often less flexible (more crystalline) than natural materials, which may make them more likely to damage sensitive tissues such as the mucosal and respiratory epithelia (51). Recent research has found that microplastics can cause significant intestinal damage, and that

longer plastic microfibers ($\leq 200 \mu\text{m}$) may be more damaging than shorter counterparts (78, 79). This may explain why smaller polystyrene microplastics (and, to a lesser degree, natural spartina microparticles) enhanced virulence, but less than nylon microfibers and without a clear dose response. Further, although microplastic biofilms have been proposed as a viral vector which could enhance exposure pathways (27, 28), our fish were exposed to IHNV in the absence of microparticles (plastic dosing occurred before and after viral exposure). Also, we observed that virus did not readily sorb to the surface of the particles in a separate *in vitro* study (Fig. S2.10). With the data gathered here, enhanced host colonization caused by physical interactions of the host with microparticles (particularly microfibers) seems probable (Fig. 5).

Our research is an important step towards a fuller understanding of the health consequences of microplastics on living systems. Here, we included a range of microparticle types (both plastic and natural; fiber and fragment). The proposed physical disruption of the mucosal and respiratory epithelial membranes by microplastics facilitating pathogen colonization of host merits further investigation. Duration of microparticle exposure prior to pathogen encounter should also be considered, as important relationships between particles and infectious disease may be overlooked in shorter experiments (32). Importantly, the characteristics of microplastics (i.e., size, shape, chemistry, crystallinity) responsible for eliciting detrimental effects should be further evaluated; including the question of whether microparticles of a larger size or microfibers of a natural material cause similar damage remains unanswered (16, 78). Nonetheless, our findings suggest that both microplastics and plastic microfibers are capable of increasing mortality in fish exposed to infectious disease agents, which has

implications across a range of host-pathogen systems. This includes humans, who are likely highly coincidentally exposed to microplastics and infectious agents in indoor environments (8). The latter has been dramatically illustrated in the case of the SARS-CoV-2 virus. Host and pathogen systems such as the one used here can serve as a model for the relationship between pathogen and microplastics in many systems, and interdisciplinary work regarding the mechanisms underlying these relationships should be a priority.

References

1. R. Geyer, J. R. Jambeck, K. L. Law, Production, use, and fate of all plastics ever made. *Sci. Adv.* **3**, e1700782 (2017).
2. J. R. Jambeck, R. Geyer, C. Wilcox, T. R. Siegler, M. Perryman, A. Andrady, R. Narayan, K. L. Law, Plastic waste inputs from land into the ocean. *Science*. **347**, 768–771 (2015).
3. S. B. Borrelle, J. Ringma, K. L. Law, C. C. Monnahan, L. Lebreton, A. McGivern, E. Murphy, J. Jambeck, G. H. Leonard, M. A. Hilleary, M. Eriksen, H. P. Possingham, H. De Frond, L. R. Gerber, B. Polidoro, A. Tahir, M. Bernard, N. Mallos, M. Barnes, C. M. Rochman, Predicted growth in plastic waste exceeds efforts to mitigate plastic pollution. *Science*. **369**, 1515–1518 (2020).
4. R. C. Hale, M. E. Seeley, M. J. La Guardia, L. Mai, E. Y. Zeng, A global perspective on microplastics. *J. Geophys. Res. Oceans*. **125** (2020), doi:10.1029/2018JC014719.
5. C. M. Rochman, Microplastics research—from sink to source. *Science*. **360**, 28–29 (2018).
6. K. Bucci, M. Tulio, C. M. Rochman, What is known and unknown about the effects of plastic pollution: A meta-analysis and systematic review. *Ecol. Appl.* **30** (2020), doi:10.1002/eap.2044.
7. M. D. Prokić, T. B. Radovanović, J. P. Gavrić, C. Faggio, Ecotoxicological effects of microplastics: Examination of biomarkers, current state and future perspectives. *TrAC Trends Anal. Chem.* **111**, 37–46 (2019).
8. J. C. Prata, J. P. da Costa, I. Lopes, A. C. Duarte, T. Rocha-Santos, Environmental exposure to microplastics: An overview on possible human health effects. *Sci. Total Environ.* **702**, 134455 (2020).
9. C. M. Rochman, C. Brookson, J. Bikker, N. Djuric, A. Earn, K. Bucci, S. Athey, A. Huntington, H. McIlwraith, K. Munno, H. De Frond, A. Kolomijeca, L. Erdle, J. Grbic, M. Bayoumi, S. B. Borrelle, T. Wu, S. Santoro, L. M. Werbowski, X. Zhu, R. K. Giles, B. M. Hamilton, C. Thaysen, A. Kaura, N. Klasios, L. Ead, J. Kim, C. Sherlock, A. Ho, C. Hung, Rethinking microplastics as a diverse contaminant suite. *Environ. Toxicol. Chem.* **38**, 703–711 (2019).
10. M. Kooi, A. A. Koelmans, Simplifying microplastic via continuous probability distributions for size, shape, and density. *Environ. Sci. Technol. Lett.* **6**, 551–557 (2019).

11. E. Besseling, P. Redondo-Hasselerharm, E. M. Foekema, A. A. Koelmans, Quantifying ecological risks of aquatic micro- and nanoplastic. *Crit. Rev. Environ. Sci. Technol.* **49**, 32–80 (2019).
12. V. N. de Ruijter, P. E. Redondo-Hasselerharm, T. Gouin, A. A. Koelmans, Quality criteria for microplastic effect studies in the context of risk assessment: a critical review. *Environ. Sci. Technol.* **54**, 11692–11705 (2020).
13. G. Everaert, M. De Rijcke, B. Lonneville, C. R. Janssen, T. Backhaus, J. Mees, E. van Sebille, A. A. Koelmans, A. I. Catarino, M. B. Vandegheuchte, Risks of floating microplastic in the global ocean. *Environ. Pollut.* **267**, 115499 (2020).
14. A. E. Rubin, A. K. Sarkar, I. Zucker, Questioning the suitability of available microplastics models for risk assessment – A critical review. *Sci. Total Environ.* **788**, 147670 (2021).
15. A. D. Gray, J. E. Weinstein, Size- and shape-dependent effects of microplastic particles on adult daggerblade grass shrimp (*Palaemonetes pugio*): Uptake and retention of microplastics in grass shrimp. *Environ. Toxicol. Chem.* **36**, 3074–3080 (2017).
16. S. N. Athey, L. M. Erdle, Are we underestimating anthropogenic microfiber pollution? A critical review of occurrence, methods, and reporting *Environ. Toxicol. Chem.*, 1-16 (2021).
17. A. Mateos-Cárdenas, J. O’Halloran, F. N. A. M. van Pelt, M. A. K. Jansen, Beyond plastic microbeads – Short-term feeding of cellulose and polyester microfibers to the freshwater amphipod *Gammarus duebeni*. *Sci. Total Environ.* **753**, 141859 (2021).
18. T. Stanton, M. Johnson, P. Nathanail, W. MacNaughtan, R. L. Gomes, Freshwater and airborne textile fibre populations are dominated by ‘natural’, not microplastic, fibres. *Sci. Total Environ.* **666**, 377–389 (2019).
19. M. MacLeod, H. P. H. Arp, M. B. Tekman, A. Jahnke, The global threat from plastic pollution. *Science.* **373**, 61–65 (2021).
20. P. Dixon, R. Paley, R. Alegria-Moran, B. Oidtmann, Epidemiological characteristics of infectious hematopoietic necrosis virus (IHNV): a review. *Vet. Res.* **47**, 63 (2016).
21. A. R. Wargo, G. Kurath, Viral fitness: definitions, measurement, and current insights. *Curr. Opin. Virol.* **2**, 538–545 (2012).
22. S. E. Lapatra, Factors affecting pathogenicity of infectious hematopoietic necrosis virus (IHNV) for salmonid fish, 11.

23. K. R. Springman, G. Kurath, J. J. Anderson, J. M. Emlen, Contaminants as viral cofactors: assessing indirect population effects. *Aquat. Toxicol.* **71**, 13–23 (2005).
24. K. J. Eder, H. Köhler, I. Werner, Pesticide and pathogen: Heat shock protein expression and acetylcholinesterase inhibition in juvenile Chinook salmon in response to multiple stressors. *Environ. Toxicol. Chem.* **26**, 1233–1242 (2007).
25. F. M. Hetrick, M. D. Knittel, J. L. Fryer', Increased susceptibility of rainbow trout to infectious hematopoietic necrosis virus after exposure to copper. **37**, 4 (1979).
26. J. B. Lamb, B. L. Willis, E. A. Fiorenza, C. S. Couch, R. Howard, D. N. Rader, J. D. True, L. A. Kelly, A. Ahmad, J. Jompa, C. D. Harvell, Plastic waste associated with disease on coral reefs. *Science.* **359**, 460–462 (2018).
27. L. A. Amaral-Zettler, E. R. Zettler, T. J. Mincer, Ecology of the plastisphere. *Nat. Rev. Microbiol.* **18**, 139–151 (2020).
28. C. D. Rummel, A. Jahnke, E. Gorokhova, D. Kühnel, M. Schmitt-Jansen, Impacts of biofilm formation on the fate and potential effects of microplastic in the aquatic environment. *Environ. Sci. Technol. Lett.* **4**, 258–267 (2017).
29. P. Zwollo, F. Quddos, C. Bagdassarian, M. E. Seeley, R. C. Hale, L. Abderhalden, Polystyrene microplastics reduce abundance of developing B cells in rainbow trout (*Oncorhynchus mykiss*) primary cultures. *Fish Shellfish Immunol.* **114**, 102–111 (2021).
30. M. Hamed, H. A. M. Soliman, A. G. M. Osman, A. E.-D. H. Sayed, Assessment the effect of exposure to microplastics in Nile Tilapia (*Oreochromis niloticus*) early juvenile: I. blood biomarkers. *Chemosphere.* **228**, 345–350 (2019).
31. C. Lu, P. W. Kania, K. Buchmann, Particle effects on fish gills: An immunogenetic approach for rainbow trout and zebrafish. *Aquaculture.* **484**, 98–104 (2018).
32. R. R. Leads, K. G. Burnett, J. E. Weinstein, The effect of microplastic ingestion on survival of the grass shrimp *Palaemonetes pugio* (holthuis, 1949) challenged with *Vibrio campbellii*. *Environ. Toxicol. Chem.* **38**, 2233–2242 (2019).
33. A. L. Laverty, S. Primpke, C. Lorenz, G. Gerds, F. C. Dobbs, Bacterial biofilms colonizing plastics in estuarine waters, with an emphasis on *Vibrio* spp. and their antibacterial resistance. *PLOS ONE.* **15**, e0237704 (2020).
34. S. Jennings, G. D. Stentiford, A. M. Leocadio, K. R. Jeffery, J. D. Metcalfe, I. Katsiadaki, N. A. Auchterlonie, S. C. Mangi, J. K. Pinnegar, T. Ellis, E. J. Peeler, T. Luisetti, C. Baker-Austin, M. Brown, T. L. Catchpole, F. J. Clyne, S. R. Dye, N. J. Edmonds, K. Hyder, J. Lee, D. N. Lees, O. C. Morgan, C. M. O'Brien, B. Oidtmann, P. E. Posen, A. R. Santos, N. G. H. Taylor, A. D. Turner, B. L. Townhill, D. W.

- Verner-Jeffreys, Aquatic food security: insights into challenges and solutions from an analysis of interactions between fisheries, aquaculture, food safety, human health, fish and human welfare, economy and environment. *Fish Fish.* **17**, 893–938 (2016).
35. M. J. Doyle, W. Watson, N. M. Bowlin, S. B. Sheavly, Plastic particles in coastal pelagic ecosystems of the Northeast Pacific ocean. *Mar. Environ. Res.* **71**, 41–52 (2011).
 36. A. P. W. Barrows, S. E. Cathey, C. W. Petersen, Marine environment microfiber contamination: Global patterns and the diversity of microparticle origins. *Environ. Pollut.* **237**, 275–284 (2018).
 37. G. Suaria, A. Achtypi, V. Perold, J. R. Lee, A. Pierucci, T. G. Bornman, S. Aliani, P. G. Ryan, Microfibers in oceanic surface waters: A global characterization. *Sci. Adv.* **6**, eaay8493 (2020).
 38. M. Jang, W. J. Shim, G. M. Han, M. Rani, Y. K. Song, S. H. Hong, Widespread detection of a brominated flame retardant, hexabromocyclododecane, in expanded polystyrene marine debris and microplastics from South Korea and the Asia-Pacific coastal region. *Environ. Pollut.* **231**, 785–794 (2017).
 39. L. Bootland, J.-A. Leong, in *Fish diseases and disorders* (2011), vol. 3, pp. 66–109.
 40. M. E. Seeley, B. Song, R. Passie, R. C. Hale, Microplastics affect sedimentary microbial communities and nitrogen cycling. *Nat. Commun.* **11**, 2372 (2020).
 41. J. L. Everson, D. R. Jones, A. K. Taylor, B. J. Rutan, T. D. Leeds, K. E. Langwig, A. R. Wargo, G. D. Wiens, Aquaculture reuse water, genetic line, and vaccination affect rainbow trout (*oncorhynchus mykiss*) disease susceptibility and infection dynamics. *Front. Immunol.* **12**, 3894 (2021).
 42. D. R. Jones, B. J. Rutan, A. R. Wargo, Impact of vaccination and pathogen exposure dosage on shedding kinetics of infectious hematopoietic necrosis virus (IHNV) in rainbow trout, 14.
 43. D. Gauthier, A. Haines, W. Vogelbein, Elevated temperature inhibits *Mycobacterium shottsii* infection and *Mycobacterium pseudoshottsii* disease in striped bass *Morone saxatilis*. *Dis. Aquat. Organ.* **144**, 159–174 (2021).
 44. M. Purcell, R. Thompson, K. Garver, L. Hawley, W. Batts, L. Sprague, C. Sampson, J. Winton, Universal reverse-transcriptase real-time PCR for infectious hematopoietic necrosis virus (IHNV). *Dis. Aquat. Organ.* **106**, 103–115 (2013).
 45. K. J. Livak, T. D. Schmittgen, Analysis of relative gene expression data using real-time quantitative PCR and the $2^{-\Delta\Delta CT}$ method. *Methods.* **25**, 402–408 (2001).

46. T. Therneau, *A package for survival analysis in S, version 2.38*. (2015; Available: <https://CRAN.R-project.org/package=survival>).
47. D. G. McKenney, G. Kurath, A. R. Wargo, Characterization of infectious dose and lethal dose of two strains of infectious hematopoietic necrosis virus (IHNV). *Virus Res.* **214**, 80–89 (2016).
48. A. R. Wargo, K. A. Garver, G. Kurath, Virulence correlates with fitness in vivo for two M group genotypes of infectious hematopoietic necrosis virus (IHNV). *Virology.* **404**, 51–58 (2010).
49. Ma. M. D. Peñaranda, A. R. Wargo, G. Kurath, In vivo fitness correlates with host-specific virulence of infectious hematopoietic necrosis virus (IHNV) in sockeye salmon and rainbow trout. *Virology.* **417**, 312–319 (2011).
50. L. Zimmermann, G. Dierkes, T. A. Ternes, C. Völker, M. Wagner, Benchmarking the in vitro toxicity and chemical composition of plastic consumer products. *Environ. Sci. Technol.* **53**, 11467–11477 (2019).
51. A. L. Andrady, The plastic in microplastics: A review. *Mar. Pollut. Bull.* **119**, 12–22 (2017).
52. P. O. Darnerud, Toxic effects of brominated flame retardants in man and in wildlife. *Environ. Int.* **29**, 841–853 (2003).
53. H. Sh, Expanded polystyrene (eps) buoy as a possible source of hexabromocyclododecanes (hbcds) in the marine environment. *Organohalogen Compd.* **75**, 5 (2013).
54. R. Hodson, R. Christian, A. Maccubbin, Lignocellulose and lignin in the salt marsh grass *Spartina alterniflora*: initial concentrations and short-term, post-depositional changes in detrital matter (1984), doi:10.1007/BF00397619.
55. R. P. Singh, S. Mishra, A. P. Das, Synthetic microfibers: Pollution toxicity and remediation. *Chemosphere.* **257**, 127199 (2020).
56. T. Kögel, Ø. BJORØY, B. Toto, A. M. Bienfait, M. Sanden, Micro- and nanoplastic toxicity on aquatic life: Determining factors. *Sci. Total Environ.* **709**, 136050 (2020).
57. L. Wang, W.-M. Wu, N. S. Bolan, D. C. W. Tsang, Y. Li, M. Qin, D. Hou, Environmental fate, toxicity and risk management strategies of nanoplastics in the environment: Current status and future perspectives. *J. Hazard. Mater.* **401**, 123415 (2021).

58. H. J. Shupe, K. M. Boenisch, B. J. Harper, S. M. Brander, S. L. Harper, Effect of nanoplastic type and surface chemistry on particle agglomeration over a salinity gradient. *Environ. Toxicol. Chem.* **40**, 1820–1826 (2021).
59. S. Summers, T. Henry, T. Gutierrez, Agglomeration of nano- and microplastic particles in seawater by autochthonous and de novo-produced sources of exopolymeric substances. *Mar. Pollut. Bull.* **130**, 258–267 (2018).
60. F. Lagarde, O. Olivier, M. Zanella, P. Daniel, S. Hiard, A. Caruso, Microplastic interactions with freshwater microalgae: Hetero-aggregation and changes in plastic density appear strongly dependent on polymer type. *Environ. Pollut.* **215**, 331–339 (2016).
61. A. R. Wargo, R. J. Scott, B. Kerr, G. Kurath, Replication and shedding kinetics of infectious hematopoietic necrosis virus in juvenile rainbow trout. *Virus Res.* **227**, 200–211 (2017).
62. A. R. Wargo, G. Kurath, In vivo fitness associated with high virulence in a vertebrate virus is a complex trait regulated by host entry, replication, and shedding. *J. Virol.* **85**, 3959–3967 (2011).
63. B. S. Drolet, J. S. Rohovec, J. C. Leong, The route of entry and progression of infectious haematopoietic necrosis virus in *Oncorhynchus mykiss* (Walbaum): a sequential immunohistochemical study. *J. Fish Dis.* **17**, 337–344 (1994).
64. M. M. D. Penaranda, M. K. Purcell, G. Kurath, Differential virulence mechanisms of infectious hematopoietic necrosis virus in rainbow trout (*Oncorhynchus mykiss*) include host entry and virus replication kinetics. *J. Gen. Virol.* **90**, 2172–2182 (2009).
65. J. Zhang, Yin and yang interplay of IFN-gamma in inflammation and autoimmune disease. *J. Clin. Invest.* **117**, 871–873 (2007).
66. D. F. Amend, W. T. Yasutake, R. W. Mead, A hematopoietic virus disease of rainbow trout and sockeye salmon. *Trans. Am. Fish. Soc.* **98**, 796–804 (1969).
67. M. K. Purcell, G. Kurath, K. A. Garver, R. P. Herwig, J. R. Winton, Quantitative expression profiling of immune response genes in rainbow trout following infectious haematopoietic necrosis virus (IHNV) infection or DNA vaccination. *Fish Shellfish Immunol.* **17**, 447–462 (2004).
68. M. K. Purcell, S. E. LaPatra, J. C. Woodson, G. Kurath, J. R. Winton, Early viral replication and induced or constitutive immunity in rainbow trout families with differential resistance to Infectious hematopoietic necrosis virus (IHNV). *Fish Shellfish Immunol.* **28**, 98–105 (2010).

69. M. K. Purcell, K. J. Laing, J. R. Winton, Immunity to fish rhabdoviruses. *Viruses*. **4**, 140–166 (2012).
70. J. Zou, C. Secombes, The function of fish cytokines. *Biology*. **5**, 23 (2016).
71. F. Takizawa, S. Magadan, D. Parra, Z. Xu, T. Korytář, P. Boudinot, J. O. Sunyer, Novel teleost cd4-bearing cell populations provide insights into the evolutionary origins and primordial roles of cd4⁺ lymphocytes and cd4⁺ macrophages. *J. Immunol.* **196**, 4522–4535 (2016).
72. J. A. Champion, A. Walker, S. Mitragotri, Role of particle size in phagocytosis of polymeric microspheres. *Pharm. Res.* **25**, 1815–1821 (2008).
73. A.-C. Greven, T. Merk, F. Karagöz, K. Mohr, M. Klapper, B. Jovanović, D. Palić, Polycarbonate and polystyrene nanoplastic particles act as stressors to the innate immune system of fathead minnow (*Pimephales promelas*): Nanoplastics' effect on the immune system of fish. *Environ. Toxicol. Chem.* **35**, 3093–3100 (2016).
74. F. Quddos, P. Zwollo, A BCWD-Resistant line of rainbow trout is less sensitive to cortisol implant-induced changes in IgM response as compared to a susceptible (control) line. *Developmental & Comparative Immunology*. **116**, 103921 (2021).
75. H. Yang, Polystyrene microplastics decrease F-53B bioaccumulation but induce inflammatory stress in larval zebrafish, 8 (2020).
76. A. R. Wargo, A. M. Kell, R. J. Scott, G. H. Thorgaard, G. Kurath, Analysis of host genetic diversity and viral entry as sources of between-host variation in viral load. *Virus Res.* **165**, 71–80 (2012).
77. I. Salinas, The mucosal immune system of teleost fish. *Biology*. **4**, 525–539 (2015).
78. Y. Zhao, R. Qiao, S. Zhang, G. Wang, Metabolomic profiling reveals the intestinal toxicity of different length of microplastic fibers on zebrafish (*Danio rerio*). *J. Hazard. Mater.* **403**, 123663 (2021).
79. Y. Jin, J. Xia, Z. Pan, J. Yang, W. Wang, Z. Fu, Polystyrene microplastics induce microbiota dysbiosis and inflammation in the gut of adult zebrafish. *Environ. Pollut.* **235**, 322–329 (2018).
80. W. N. Batts, J. R. Winton, Enhanced detection of infectious hematopoietic necrosis virus and other fish viruses by pretreatment of cell monolayers with polyethylene glycol, 7.
81. K. Martins, B. Applegate, B. Hagedorn, J. Kennish, P. Zwollo, Di(2-ethylhexyl) phthalate inhibits B cell proliferation and reduces the abundance of IgM-secreting

- cells in cultured immune tissues of the rainbow trout. *Fish Shellfish Immunol.* **44**, 332–341 (2015).
82. P. Zwollo, J. C. Ray, M. Sestito, E. Kiernan, G. D. Wiens, S. Kaattari, B. StJacques, L. Epp, B cell signatures of BCWD-resistant and susceptible lines of rainbow trout: A shift towards more EBF-expressing progenitors and fewer mature B cells in resistant animals. *Dev. Comp. Immunol.* **48**, 1–12 (2015).
83. R. Krishnan, S. S. N. Qadiri, J.-O. Kim, J.-O. Kim, M.-J. Oh, Validation of housekeeping genes as candidate internal references for quantitative expression studies in healthy and nervous necrosis virus-infected seven-band grouper (*Hyporthodus septemfasciatus*). *Fisheries and Aquatic Sciences.* **22**, 28 (2019).

Chapter 3: The influence of nylon microplastic shape and time of exposure on virus-mediated mortality in fish

Introduction

Production and use of plastic products, particularly single-use plastics, have steadily increased since 1950 (1). Accordingly, plastic waste that has escaped waste management streams has polluted the natural environment and become a persistent global environmental contaminant of concern (2). Microplastic (≤ 5 mm) pollution mostly arises from the abrasion and weathering of larger plastic products and debris in the environment (3, 4). Microplastic ubiquity within all natural environments (particularly aquatic), has motivated research on their effects on biota, from microbes to large marine mammals (5). Over time, these studies have illustrated that assessing potential risk caused by microplastics can be complex (2, 6, 7). Not only does this risk vary between the organism or system investigated (5), but also varies between microplastic types. Microplastics are extremely diverse, existing in a continuum of sizes, shapes, colors, densities, polymer makeups and additive chemistries (8). In addition, some effects of microplastics have been found to be sub-lethal in nature, making it challenging to discern their ultimate risk to ecosystems or organisms, including humans (9–12).

Recently, limited research has highlighted the potential of plastic debris as a co-stressor with other hazards, including infectious disease. Once in the environment, microplastics may become colonized by microbes, including pathogens, suggesting that microplastics may act as a sterile vector for disease (13, 14). In addition, microplastics can cause a host of sub-lethal responses, including stress or immune responses, which may affect an organism's ability to mount a response to infectious agents (4, 15). In the marine environment it was recently reported that abundance of plastic correlated with the prevalence of disease on Indo-Pacific coral reefs (16). Our previous work found that co-

exposure to microplastics increased virulence of the common fish virus, infectious hematopoietic necrosis virus (IHNV; chapter 2). This effort suggested that nylon microplastic fibers caused the largest increase in virulence (defined here as disease-caused population mortality), greater than spheroid polystyrene microplastics or natural marsh grass microparticles. The question of why this occurred merited investigation. We speculated that the fibroid shape was more damaging to delicate tissues than spheroidal microplastics. Further, we speculated that the period of chronic exposure to microfibers preceding virus introduction was most important, creating the opportunity for enhanced viral fitness in a way that microplastic exposure coincident with or following viral exposure would not. So, our question was would the same virulence trends we observed under chronic exposure be observed if: 1) fibers were only provided prior to or following viral exposure; or 2) nylon were in a spheroid versus fibrous form?

Here, we use the same well-characterized disease and host system to further elucidate the mechanisms behind virulence changes following exposure to nylon microfibers. Rainbow trout (*Oncorhynchus mykiss*) were held for eight weeks, and half of the fish were exposed to a controlled dose of IHNV after four weeks. Across both virally-exposed and unexposed groups, fish were exposed to nylon microfibers either chronically, pre-virus or post-virus, or nylon powder chronically. Mortality was monitored daily to assess virulence changes over time. Water samples were also collected to quantify viral shedding, a proxy for host body burden and transmission. We hypothesized that if the mechanism of increased virulence observed in Chapter 2 was specific to the shape of nylon fibers and caused by tissue damage prior to viral-exposure, virulence and viral shed observed in chronic and pre-virus nylon microfiber-exposed fish

would be significantly higher than among fish exposed to nylon microfiber post-virus only or nylon powder.

Materials and Methods

Particles

Undyed nylon 6'6 fibers were provided by Claremont Flock, Inc. (Leominster, MA). The manufacturer reported fibers to be 0.8 denier (approximately 10 μm in diameter) and 500 μm in length. These sizes were confirmed using a Beckman-Coulter Laser Diffraction Particle Size Analyzer. The fibers were reported to not contain additives aside from a TiO_2 delustrant. Nylon powder (polyamide 6) was purchased from Goodfellow (Coraopolis, PA, "Polyamide – Nylon 6 – Powder"). Particles were spheroidal, with particle diameter ranging from 5-50 μm and mean particle size of 15-20 μm . The manufacturer reported that properties are similar to nylon 6'6 such that they are interchangeable, but nylon 6'6 in powder form was not available. Manufacturer also reported that the product is free of chemical additives. Prior to dosing, particles were prepared in pre-weighed foil sachets using a hooded scale.

Experimental Animals and Husbandry

Juvenile rainbow trout (*Oncorhynchus mykiss*) were obtained as fry (~0.5 g) from the National Center for Cool and Cold Water Aquaculture in West Virginia (NCCCWA; within USDA's Agricultural Research Service). Trout were reared at the Virginia Institute of Marine Science (VIMS), according to guidelines from the Institutional Animal Care and Use Committee (IACUC-2020-06-24-14322-arwargo) and previously established protocols (17). Briefly, fish were maintained at 1-3% weight food, fed daily. Fish were

initially held in a pathogen-free recirculating system supplied with UV-irradiated fresh well-water at 12°C until reaching the desired size for experiments.

For the experiment, fish were transferred to a flow-through tower rack tank system (Aquaneering) housed in a BSL-II aquatic animal laboratory at VIMS, supplied by UV-irradiated fresh well-water at 15°C. Average fish weight was 1.9 ± 0.2 g fish⁻¹ at the start of the experiment. Room temperature was maintained at 15 °C, water temperature at 15 °C, dissolved oxygen at approximately 100% saturation, and lighting on a 12-hour diurnal cycle. Fish were housed in 6 L tanks (20 fish each) with one water line, two air stones, and fry screens, to facilitate particle movement and oxygenation through entire tank. Water flow rate was set to 300-350 mL min⁻¹. During the experiment, fish were fed 2.0% of their average body weight every four days, 1 hour after the start of a flush (below).

Experimental Design and Procedures

Fish received one of 10 possible treatments, outlined in Table 1. Each treatment contained quadruplicate tanks of 20 fish tracked for mortality and sampled for viral shedding (Fig. S3.1). Tanks were randomly distributed throughout the tower rack system for each treatment to minimize placement effects. For plastic exposure, fish were dosed with particles every other day, beginning on the first day of the experiment. Particles were dosed at concentration of 10 mg L⁻¹ by opening pre-weighed foil sachets and submerging the contents in the tank so that all particles were added to the water. All tanks were held static for 24 hours during particle exposure. The flow was then resumed and tanks flushed for 24 hours, which was necessary in order to maintain water quality. To reduce microplastic discharge to the local wastewater system, during the first hour of

each tank flushing effluent was pumped through a series of in-line filters (75 µm, 20 µm, 5 µm and 1 µm) before passing through UV-irradiation (sufficient for virus inactivation) and eventual discharge to the institutional municipal wastewater stream. In total, the experiment lasted 56 days with 28 particle dosing events for all chronically microplastic dosed treatments (i.e., nylon fibers chronic, nylon powder chronic). For the pre- and post-virus treatment, fish were also exposed to nylon fibers only in the first or last four weeks respectively, resulting in 14 particle dosing events. The experiment was monitored at the same time daily, recording temperature, dissolved oxygen, and the number of fish mortalities in each tank.

Table 1 Experimental treatments included a combination of particle types, dosing times and virus exposure scenarios. All treatments were performed in quadruplicate tanks of 20 fish each.

Microparticle	Dosing Time	Virus
None	None	IHNV+
None	None	IHNV-
Nylon Fibers	Chronic (weeks 1-8)	IHNV+
Nylon Fibers	Chronic (weeks 1-8)	IHNV-
Nylon Fibers	Pre-virus (weeks 1-4)	IHNV+
Nylon Fibers	Pre-virus (weeks 1-4)	IHNV-
Nylon Fibers	Post-virus (weeks 5-8)	IHNV+
Nylon Fibers	Post-virus (weeks 5-8)	IHNV-
Nylon Powder	Chronic (weeks 1-8)	IHNV+
Nylon Powder	Chronic (weeks 1-8)	IHNV-

Midway in the experiment (day 28) fish were dosed with virus or a mock control. Experimental virus, IHNV (*Salmonid novirhabdovirus*) isolate C (genotypemG119M; GenBank accession number AF237984) was obtained from established laboratory stock (titer of 7.56×10^8 plaque forming units (PFU) mL⁻¹) diluted to 8.0×10^5 PFU mL⁻¹ in Minimum Essential Media (MEM) with 10% fetal bovine serum (18). Fish were dosed

with 5 mL of diluted IHNV stock in 995 mL water, to reach a final IHNV dose of 4.0×10^3 PFU mL⁻¹, in a 1-hr static immersion challenge, followed by resumed water flow to tanks (18). Non-virus (IHNV-) treatments were mock dosed with 5 mL of MEM in 10% fetal bovine serum.

To quantify viral shedding, water samples were collected on days 29, 31, 33, 35, 37, 39, 41, 43, 47, and 55, from all tanks. Each water sample was collected at the end of the static period just prior to flushing, such that virus had maximum and consistent time to distribute within tanks (approximately 23 hours). An 800 µL water sample was collected per tank and stored at -80°C prior to extraction and analysis. Extraction and qPCR procedures are detailed in Jones et al. 2020 (27). Briefly, RNA was extracted from 210 µL of water using a Tecan Freedom EVO 100 liquid handling robot. RNA extract was converted to cDNA using oligo (dT) random primers (Promega). Diluted cDNA (1:2) was quantified with forward and reverse primers IHNV N-gene 796F (5'-AGAGCCAAGGCACTGTGCG-3') and 875R (5'-TTCTTTGCGGCT TGGTTGA-3') with TaqMan probe IHNV N-gene 818MGB. An 8-step, 10-fold dilution series of DNA plasmid standard APC was included on each plate in triplicate for quantification (27).

Statistical Analyses

All graphical and statistical analyses were completed in R Studio and significance was inferred with $\alpha = 0.05$. Mortality analyses were illustrated with Kaplan-Meier survival curves using package 'survival'. Statistically significant differences between treatments were determined with Cox proportional hazard models in R with the "coxph" function (package "survival"). All possible combinations of fixed and random effects were modeled, and best fit minimal models selected based on rules of parsimony and

delta Akaike Information Criterion (AIC) ≥ 2 . Possible fixed effects include treatment (five options: chronic nylon fibers, pre-virus exposure nylon fibers, post-virus exposure nylon fibers, nylon powder, no microplastic) and virus (IHN+ or IHNV-), while tank was a possible random effect. The best model included treatment and virus, but a model including their interaction failed to converge. Inclusion of the random effect tank did not improve fit, so it was dropped from the model. This model was used to report the overall significance of virus exposure on mortality. However, because mortality levels in virus negative tanks were low, a second model using the same factors was generated among IHNV+ fish only, to determine how survival differed between particle treatments when fish were exposed to virus.

For the analysis of viral shedding over time among IHNV+ tanks only, all possible combinations of factors (same as for survival analysis with the addition of day as a continuous factor) in linear mixed effects models were considered (lme function in R package ‘lmer’) and the models compared. The model of best fit was again determined by lowest AIC. The chosen model included treatment and day as fixed effects, and collection tank as a random effect. For analysis of peak viral shed, the data did not pass a homogeneity of variance test and therefore, could not be analyzed via traditional one-way analysis of variance (ANOVA). As such, a Welch’s ANOVA analysis using the same factors was completed, which does not require homogeneity of variance between treatments. For all statistical analyses, full model output can be found in the supplementary information. As with previous chapters, test statistics are provided with degrees of freedom (factor,residual) as subscripts.

Results and Discussion

Mortality

Fish mortality as a product of microplastic and/or virus exposure was monitored daily (Fig. 1). Significantly more fish died when exposed to virus than not, increasing the hazard of death by 3.7 times ($Z_{1,755} = 9.17$, $p\text{-value} < 0.001$). Among only the fish exposed to virus, chronic exposure to nylon fibers significantly increased the hazard of death by 1.6 times compared to no particle exposure ($Z_{1,387} = 9.17$, $p\text{-value} = 0.033$). Exposure to nylon fibers only during the pre-virus or post-virus period did not significantly increase the hazard of death in either case compared to no particle exposure ($p\text{-values} = 0.092$ and 0.077 respectively), despite a suggestive trend for the pre-virus treatment. Exposure to nylon powder also did not significantly change the hazard of death compared to no particle co-exposure ($p\text{-value} = 0.661$). There were no significant differences between treatments among fish not exposed to IHNV.

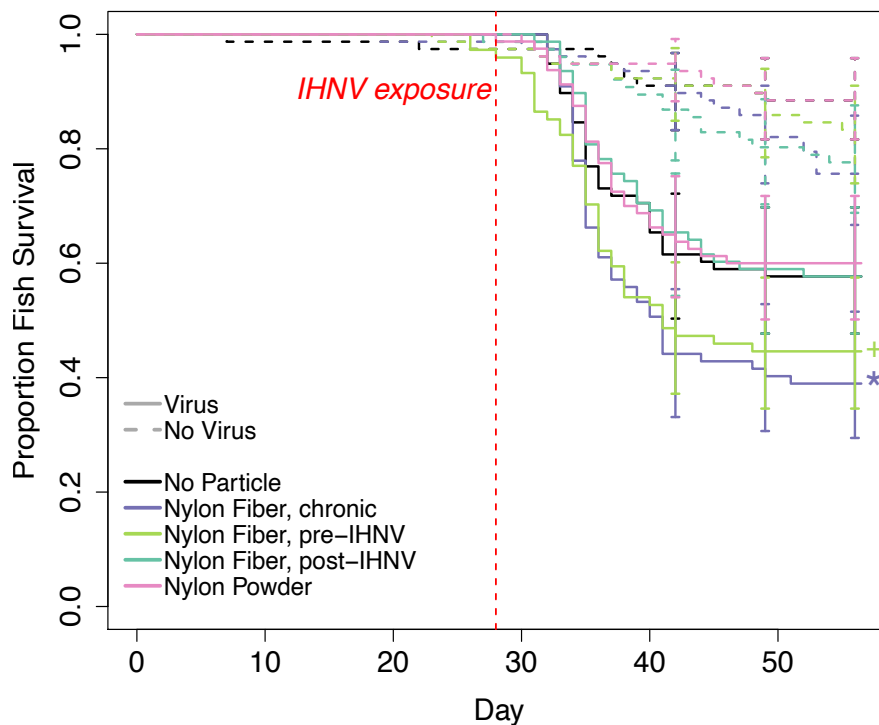


Fig. 1 Fish mortality over time, modeled for different nylon and virus co-exposure scenarios. Mortality was illustrated as proportion of surviving fish over 56 days, with IHNV exposure on day 28 (denoted with red vertical dashed line). Fish exposed to IHNV are denoted with solid lines, while those not exposed to virus are shown with dashed lines. Microplastic treatments included nylon fibers dosed chronically (purple), pre-IHNV only (green) and post-IHNV only (blue), nylon powder dosed chronically (pink), and no particles dosed (control, black). Using cox proportional hazards analysis, mortality was significantly affected by the particle treatment ($X_2 = 11.85$, $Df = 4$, $p = 1.85e-2$) and the presence of virus ($X_2 = 96.97$, $Df = 1$, $p < 00.1$). Significance of differences in survival between IHNV+ control and other virus-exposed treatments is denoted on graph (p -value ≤ 0.05 : *).

Not surprisingly, these data demonstrated that exposure to IHNV was significant in predicting mortality among juvenile rainbow trout. When fish were also exposed to nylon microfibers (i.e., chronic microfiber treatments), the chance of death was more than twice as high as when they were exposed to virus alone. This agrees with our previous results that microfiber exposure over the course of the entire experiment increased rainbow trout mortality among IHNV-exposed populations (Chapter 2). That work did

not investigate the timing of that microfiber exposure, however. Here, exposure to nylon microfibers post-virus only did not significantly increase the hazard of death; this treatment led to similar mortality as to exposure to IHNV-alone (Fig. 1). As such, we conclude that exposure to nylon fibers prior to viral introduction is a key aspect of the mechanism behind microfibers increasing virulence. In particular, nylon microfibers may create greater opportunity for infection upon initial virus exposure, possibly via the proposed epithelial damage model postulated in chapter 2.

Continuous exposure to nylon fibers (both before and after virus exposure) was slightly more impactful on virulence than exposure to nylon fibers pre-virus alone. If nylon microfibers were only important in creating opportunity for initial host infection, we would expect the virulence among these two treatments to be equal. Rather, this suggests that initial infection, as well as continued exposure or transmission between hosts, may influence population mortality. In our experiment, fish were also exposed to microplastic from day 28 to 56. As a result of this, fish that were not initially infected might become infected as infected individuals within their tank shed virus. If they continue to be exposed to nylon microfibers, we speculate that the odds of this between-host transmission increases because the opportunity for epithelial or immune damage (facilitating host viral entry) has remained constant. In fact, previous work illustrated that viral body burden was higher among fish exposed to nylon microfibers and that they shed more virus than fish only exposed to virus, suggesting they have greater capacity to transmit virus to other fish in the tank (chapter 2). In the period of time following initial infection, if fish did not continue to be exposed to nylon fibers, they would have an opportunity to recover from fiber exposure (e.g., delicate mucosal epithelium may heal

within 24-48 hr, or immune response may recover). This period of healing could decrease the likelihood that a fish would contract infection from host-to-host transmission. As such, although the exposure to nylon microfibers before introduction of virus appears to be most important in determining virulence outcomes in this host-pathogen system, the exposure to nylon fibers following initial viral introduction may also be a factor by increasing the likelihood of viral transmission within the population. However, the amount of IHNV transmission between fish in tanks is unknown, and previous studies indicate the majority of transmission occurs during the initial inoculation of tanks with virus, as such, this warrants further exploration (18).

Shape of the nylon microplastics was also observed to be a factor in virulence. Chapter 2 discussion postulated that the size and shape of the fiber created greater opportunity for mucosal epithelium damage (and thus, host viral colonization), as they were large and rigid (i.e., crystalline) enough to irritate or mildly damage fish epithelia (e.g., skin, gill, intestinal mucosa) and trigger host response. Conversely, smaller and more spheroidal particles (such as the polystyrene microplastics used previously) might pass over these epithelia without irritating or damaging epithelia, similar to natural particulates or food. By presenting fish with both nylon microfibers and spheroidal nylon powder, we can determine if size/shape was indeed the driving factor, or if particle chemistry was an important factor (i.e., nylon is more damaging than polystyrene). Indeed, these results illustrate that chronic exposure to spheroidal nylon microplastics did not affect virulence to the same extent exposure to fibrous microplastics did. This indicates that plastic microfibers, increasingly being reported in the environment, may

pose hazards that some microparticles do not, as suggested by other recent works (19–22).

A caveat to this conclusion is that the chemistry composition of the nylon powder and fibers used here is similar but not identical. Thus, we cannot say with complete certainty that the differences in virulence were not derived from those small chemical inconsistencies. That said, we suspect that leaching of additive compounds from these microplastics was not as relevant in this exposure scenario as in other toxicity models, demonstrating the importance of particle chemistry in toxicity, as our particles were refreshed every 24 hours and not allowed to leach in the water over a longer time (23–25). Further, most published studies have suggested that the additive not the polymer chemistry is involved (23). It is noteworthy that the manufacturers of the plastics used here reported the materials contained relatively benign additives. This nonetheless underscores the challenges associated with microplastic work. For example, limited microplastic reference materials of similar compositions, but different physical parameters, are available. This highlights the need for greater availability of standard reference materials for microplastics identification and toxicity work.

Viral Shedding

Shedding kinetics of IHNV has been shown to correlate with virulence in previous work with juvenile rainbow trout populations (26, 27). Viral shedding can also be used as a proxy for viral body burden and is important in determining the likelihood of host-to-host transmission within a population (28). We collected water samples to analyze viral shedding at ten time points following introduction of IHNV, modeled for all IHNV-exposed tanks (Fig. 2). Viral shedding rapidly increased following infection and,

for all treatments, peaked three days following infection (day 31). Following this peak shedding period, viral shed significantly decreased through time ($t_{1,179} = 13.98$, $p\text{-value} \leq 0.001$) to undetectable levels by day 47 (19 days post-infection), by which time infected fish that died as a result of virus had been removed from the tank and remaining fish had stopped shedding.

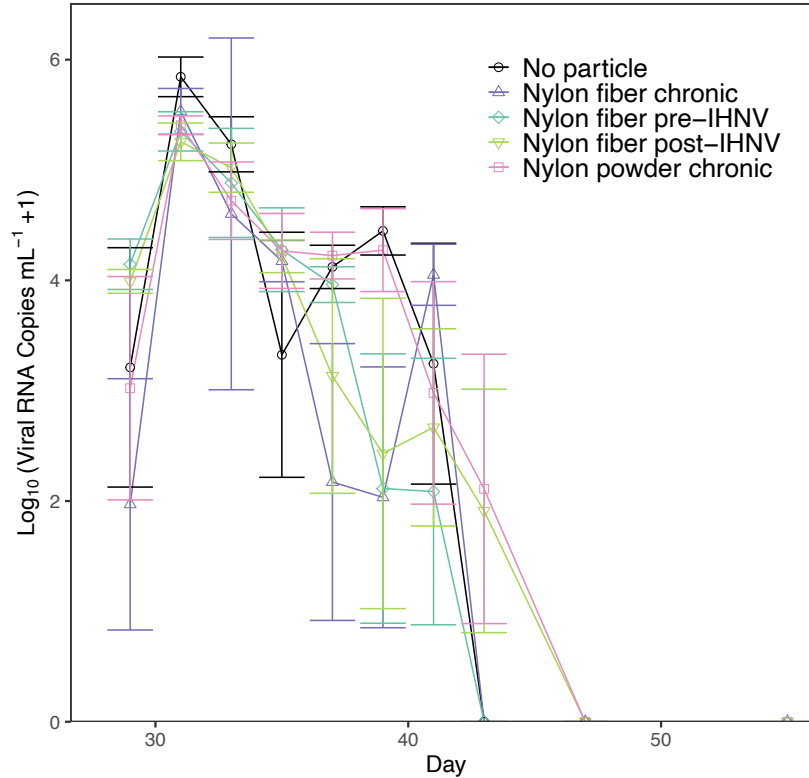


Fig. 2 Viral shed in water illustrated over time. Water was collected on 10 days from quadruplicate tanks per treatment (± 1 standard error of mean (SEM)). Tanks not exposed to IHNV are excluded from analysis, and no virus was detected in those tanks. Viral shed was significantly influenced by the collection day (linear mixed effects model, $t = 13.98$, $DF = 179$, $p\text{-value} \leq 0.001$) but not any of the particle treatments.

The observed pattern of viral shedding was not significantly different when fish were exposed to different nylon treatments (particle shape or timing of exposure). This is contrary to work demonstrating that IHNV shedding correlates with virulence, which would lead us to expect significantly different shedding in the chronic nylon fiber and

pre-IHNV nylon fiber treatments (18, 26, 29). This may be due to the fact that, unlike previous viral shedding models which address shed from one fish in an individual tank, we measured total shed from multiple fish in a group tank, possibly making the shedding kinetics less synchronous between fish.. As fish exposed to nylon fibers chronically or pre-virus exposure died faster than other IHNV-exposed fish (Fig. 1), there were fewer fish remaining in those tanks post-infection, meaning fewer infected fish actively shedding virus. Indeed, this leads to the hypothesis that the average viral body burden among fish exposed to IHNV and nylon fibers chronically or pre-virus only may have been higher than those under other IHNV+ exposure scenarios, in order for the total tank shedding to be approximately equal. This supports the conclusion from chapter 2 that increased virulence associated with certain microplastic treatments may be a product of increased viral entry into host but would benefit from future analyses of shedding adjusted for the number of surviving hosts.

The amount of virus in the water at peak shedding may also be useful for understanding virulence. Fig. 3 illustrates the average concentrations of virus shed at the time of peak shedding for all nylon exposure treatments. The highest shed was in tanks where fish were chronically exposed to nylon fibers in addition to virus, although not statistically significant. This correlates with the observed virulence trends, for which these fish had significantly higher mortality than all other virus-exposed fish. Although the number of surviving fish may explain differences in the kinetics of viral shed over time (Fig. 2), at the time of peak shedding (day 31) population mortality was just beginning to increase, so we would expect fewer differences in the number of fish per tank affecting peak viral shed. Rather, the lack of statistical significance may be

explained by the variance and asynchrony in shedding dynamics among tanks, which is particularly high for tanks exposed chronically to nylon fibers and IHNV (the total amount of virus shed for each tank was also found not to be significantly different between treatments, Fig. S3.2).

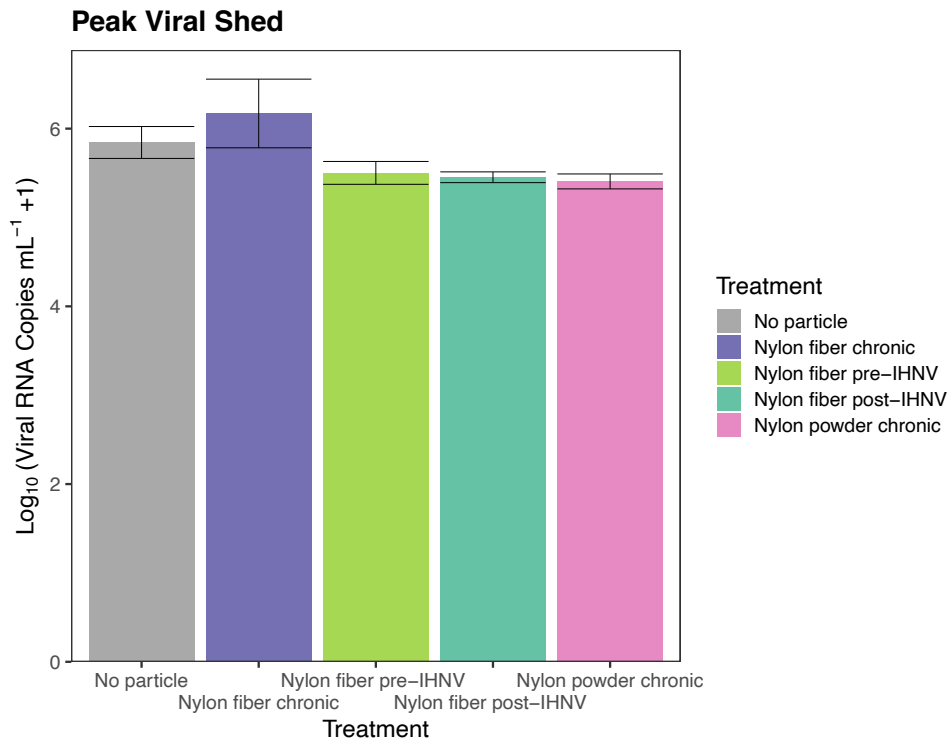


Fig. 3 Peak amount of viral shed for each treatment (highest amount on any one day per tank). Mean of the peak amount of viral shed (log-adjusted viral RNA copies mL⁻¹) was calculated for quadruplicate tanks (+/- 1 SEM). The treatment had no significant influence on peak viral shed (Welch's ANOVA analysis; $F_{4,7.1} = 2.55$, Df = 4, p-value = $8.24e-2$).

Effects of microplastics independently versus as a co-stressor

The work presented here is novel in that it demonstrates that microplastics may serve as an important co-stressor in association with ongoing infectious disease. When only fish not exposed to virus (IHNV-) were analyzed, mortality was not significantly affected by the particle treatment (Cox proportional hazards model, $X^2_{4,388} = 7.24$, p =

0.123). This is visually evident in the mortality analyses, as there was no difference between microplastic treatments and the no particle control among uninfected fish (Fig. 1; IHNV-, dashed lines). As a result, the data suggest that (at the concentrations used here) when fish were chronically exposed to nylon microfibers or nylon powder over four or eight weeks in the absence of IHNV challenge, their survival was not significantly affected. The majority of published research investigating the effects of microplastics on biota has been performed with microplastic(s) as the sole stressor (5, 10). In experiments where dose responses are investigated, results often demonstrate that high concentrations are necessary to elicit observable effects. In fact, a common criticism of microplastics effects studies is that the exposure concentration is not environmentally relevant (5, 30). This has led some to suggest that the effects of microplastics may be exaggerated (31). Caveats include that reported environmental levels are likely underestimated due to inadequate sampling and analysis methods and that environmental releases of plastic debris are rapidly increasing.

Conclusions

The work presented here follows up on research demonstrating that microplastics (particularly nylon microfibers) cause higher mortality among fish co-exposed to a pathogenic virus than when that population is exposed to virus alone (chapter 2). In that study, a mechanism of effect was proposed by which the particles damaged the surface of vulnerable teleost respiratory and mucosal epithelia, creating a pro-inflammatory response or allowing more virus to enter a host, ultimately leading to higher virulence within that population. In this scenario, we demonstrate that the timing of exposure is important, as the microplastics appear to require time to damage the host tissues prior to

pathogen introduction. Here, we investigated the differences in population mortality when fish were exposed to nylon fibers continuously, before, or after pathogen introduction. Additionally, the nylon microfibers were postulated to elicit a greater effect due to their size and shape (i.e., larger than polystyrene microplastics used in Chapter 2). Differences between these treatments could also have resulted from different particle chemistries. As such, we also investigated the mortality differences between populations exposed to nylon microfibers and powdered nylon microplastics.

We observed that virulence significantly increased when fish were co-exposed to nylon microfibers chronically, but not when exposure to nylon microfibers commenced post-virus or when nylon powder was chronically dosed. This supports the hypothesis that exposure to microplastic prior to pathogen introduction is critical, creating an opportunity for increased pathogen within-host fitness; IHNV fitness directly correlates with virulence in salmonids (27). This may explain why Leads et al. (2019) did not report enhanced infection when a bacterial pathogen was co-exposed with microplastics, as in that work the period of exposure to microplastics prior to exposure to pathogen was relatively short (32).

Further, it is often suggested that smaller sized microplastics (including nanoplastics) may have a greater effect than larger ones, due to their ability to cross epithelial membranes, enter the internal environment, and cause stress responses (33, 34). Here, it is postulated that organisms may incur damage as a result of interactions with larger particles, which may abrade skin, gills and other mucosae, block digestive tracts or cause entrapment (4). Recent published research supports the proposition that microfibers may be more damaging than spheroidal particles, and that longer fibers ($\geq 200 \mu\text{m}$) may

be more damaging than smaller counterparts in certain situations (19, 20). Future work should consider the impact of synthetic microfibers compared to semi-synthetic (e.g., rayon) and natural polymer microfibers (e.g., cellulose), as these fibers are extremely abundant in the natural environment from textile pollution and natural sources (21, 35). Nonetheless, the work we presented here highlights the importance of understanding the interactions of microplastics and other stressors, and the roles exposure timing and particle size and shape play. Co-stressor models should be considered for future work on microplastics in order to understand the scope of the threat microplastics pose to living systems, including humans, more fully.

References

1. R. Geyer, J. R. Jambeck, K. L. Law, Production, use, and fate of all plastics ever made. *Sci. Adv.* **3**, e1700782 (2017).
2. M. MacLeod, H. P. H. Arp, M. B. Tekman, A. Jahnke, The global threat from plastic pollution. *Science*. **373**, 61–65 (2021).
3. C. M. Rochman, Microplastics research—from sink to source. *Science*. **360**, 28–29 (2018).
4. R. C. Hale, M. E. Seeley, M. J. La Guardia, L. Mai, E. Y. Zeng, A global perspective on microplastics. *J. Geophys. Res. Oceans*. **125** (2020), doi:10.1029/2018JC014719.
5. K. Bucci, M. Tulio, C. M. Rochman, What is known and unknown about the effects of plastic pollution: A meta-analysis and systematic review. *Ecol. Appl.* **30** (2020), doi:10.1002/eap.2044.
6. J. Ha, M.-K. Yeo, The environmental effects of microplastics on aquatic ecosystems. *Mol. Cell. Toxicol.* **14**, 353–359 (2018).
7. G. Everaert, M. De Rijcke, B. Lonneville, C. R. Janssen, T. Backhaus, J. Mees, E. van Sebille, A. A. Koelmans, A. I. Catarino, M. B. Vandegehuchte, Risks of floating microplastic in the global ocean. *Environ. Pollut.* **267**, 115499 (2020).
8. C. M. Rochman, C. Brookson, J. Bikker, N. Djuric, A. Earn, K. Bucci, S. Athey, A. Huntington, H. McIlwraith, K. Munno, H. De Frond, A. Kolomijeca, L. Erdle, J. Grbic, M. Bayoumi, S. B. Borrelle, T. Wu, S. Santoro, L. M. Werbowski, X. Zhu, R. K. Giles, B. M. Hamilton, C. Thaysen, A. Kaura, N. Klasios, L. Ead, J. Kim, C. Sherlock, A. Ho, C. Hung, Rethinking microplastics as a diverse contaminant suite. *Environ. Toxicol. Chem.* **38**, 703–711 (2019).
9. H. P. H. Arp, D. Kühnel, C. Rummel, M. MacLeod, A. Potthoff, S. Reichelt, E. Rojo-Nieto, M. Schmitt-Jansen, J. Sonnenberg, E. Toorman, A. Jahnke, Weathering plastics as a planetary boundary threat: Exposure, fate, and hazards. *Environ. Sci. Technol.* **55**, 7246–7255 (2021).
10. M. D. Prokić, T. B. Radovanović, J. P. Gavrić, C. Faggio, Ecotoxicological effects of microplastics: Examination of biomarkers, current state and future perspectives. *TrAC Trends Anal. Chem.* **111**, 37–46 (2019).
11. Campanale, Massarelli, Savino, Locaputo, Uricchio, A detailed review study on potential effects of microplastics and additives of concern on human health. *Int. J. Environ. Res. Public Health*. **17**, 1212 (2020).
12. J. C. Prata, J. P. da Costa, I. Lopes, A. C. Duarte, T. Rocha-Santos, Environmental exposure to microplastics: An overview on possible human health effects. *Sci. Total Environ.* **702**, 134455 (2020).

13. E. R. Zettler, T. J. Mincer, L. A. Amaral-Zettler, Life in the “Plastisphere”: Microbial communities on plastic marine debris. *Environ. Sci. Technol.* **47**, 7137–7146 (2013).
14. C. D. Rummel, A. Jahnke, E. Gorokhova, D. Kühnel, M. Schmitt-Jansen, Impacts of biofilm formation on the fate and potential effects of microplastic in the aquatic environment. *Environ. Sci. Technol. Lett.* **4**, 258–267 (2017).
15. P. Zwollo, F. Quddos, C. Bagdassarian, M. E. Seeley, R. C. Hale, L. Abderhalden, Polystyrene microplastics reduce abundance of developing B cells in rainbow trout (*Oncorhynchus mykiss*) primary cultures. *Fish Shellfish Immunol.* **114**, 102–111 (2021).
16. J. B. Lamb, B. L. Willis, E. A. Fiorenza, C. S. Couch, R. Howard, D. N. Rader, J. D. True, L. A. Kelly, A. Ahmad, J. Jompa, C. D. Harvell, Plastic waste associated with disease on coral reefs. *Science.* **359**, 460–462 (2018).
17. J. L. Everson, D. R. Jones, A. K. Taylor, B. J. Rutan, T. D. Leeds, K. E. Langwig, A. R. Wargo, G. D. Wiens, Aquaculture reuse water, genetic line, and vaccination affect rainbow trout (*Oncorhynchus mykiss*) disease susceptibility and infection dynamics. *Front. Immunol.* **12**, 3894 (2021).
18. D. R. Jones, B. J. Rutan, A. R. Wargo, Impact of vaccination and pathogen exposure dosage on shedding kinetics of infectious hematopoietic necrosis virus (IHNV) in rainbow trout, 14 (2020).
19. R. P. Singh, S. Mishra, A. P. Das, Synthetic microfibers: Pollution toxicity and remediation. *Chemosphere.* **257**, 127199 (2020).
20. Y. Zhao, R. Qiao, S. Zhang, G. Wang, Metabolomic profiling reveals the intestinal toxicity of different length of microplastic fibers on zebrafish (*Danio rerio*). *J. Hazard. Mater.* **403**, 123663 (2021).
21. L. Kim, S. A. Kim, T. H. Kim, J. Kim, Y.-J. An, Synthetic and natural microfibers induce gut damage in the brine shrimp *Artemia franciscana*. *Aquat. Toxicol.* **232**, 105748 (2021).
22. A. Mateos-Cárdenas, J. O’Halloran, F. N. A. M. van Pelt, M. A. K. Jansen, Beyond plastic microbeads – Short-term feeding of cellulose and polyester microfibers to the freshwater amphipod *Gammarus duebeni*. *Sci. Total Environ.* **753**, 141859 (2021).
23. L. Zimmermann, G. Dierkes, T. A. Ternes, C. Völker, M. Wagner, Benchmarking the in vitro toxicity and chemical composition of plastic consumer products. *Environ. Sci. Technol.* **53**, 11467–11477 (2019).
24. B. Carney Almroth, J. Cartine, C. Jönander, M. Karlsson, J. Langlois, M. Lindström, J. Lundin, N. Melander, A. Pesqueda, I. Rahmqvist, J. Renaux, J. Roos, F. Spilsbury, J. Svalin, H. Vestlund, L. Zhao, N. Asker, G. Ašmonaitė, L. Birgersson, T. Boloori,

- F. Book, T. Lammel, J. Sturve, Assessing the effects of textile leachates in fish using multiple testing methods: From gene expression to behavior. *Ecotoxicol. Environ. Saf.* **207**, 111523 (2021).
25. M. Jang, W. J. Shim, G. M. Han, Y. Cho, Y. Moon, S. H. Hong, Relative importance of aqueous leachate versus particle ingestion as uptake routes for microplastic additives (hexabromocyclododecane) to mussels. *Environ. Pollut.* **270**, 116272 (2021).
 26. A. R. Wargo, K. A. Garver, G. Kurath, Virulence correlates with fitness in vivo for two M group genotypes of Infectious hematopoietic necrosis virus (IHNV). *Virology.* **404**, 51–58 (2010).
 27. Ma. M. D. Peñaranda, A. R. Wargo, G. Kurath, In vivo fitness correlates with host-specific virulence of Infectious hematopoietic necrosis virus (IHNV) in sockeye salmon and rainbow trout. *Virology.* **417**, 312–319 (2011).
 28. A. R. Wargo, G. Kurath, Viral fitness: definitions, measurement, and current insights. *Curr. Opin. Virol.* **2**, 538–545 (2012).
 29. A. R. Wargo, G. Kurath, In vivo fitness associated with high virulence in a vertebrate virus is a complex trait regulated by host entry, replication, and shedding. *J. Virol.* **85**, 3959–3967 (2011).
 30. I. Paul-Pont, K. Tallec, C. Gonzalez-Fernandez, C. Lambert, D. Vincent, D. Mazurais, J.-L. Zambonino-Infante, G. Brotons, F. Lagarde, C. Fabioux, P. Soudant, A. Huvet, Constraints and priorities for conducting experimental exposures of marine organisms to microplastics. *Front. Mar. Sci.* **5**, 252 (2018).
 31. G. A. Burton, Stressor exposures determine risk: So, why do fellow scientists continue to focus on superficial microplastics risk? *Environ. Sci. Technol.* **51**, 13515–13516 (2017).
 32. R. R. Leads, K. G. Burnett, J. E. Weinstein, The effect of microplastic ingestion on survival of the grass shrimp *Palaemonetes pugio* (holthuis, 1949) challenged with *Vibrio campbellii*. *Environ. Toxicol. Chem.* **38**, 2233–2242 (2019).
 33. E. Besseling, P. Redondo-Hasselerharm, E. M. Foekema, A. A. Koelmans, Quantifying ecological risks of aquatic micro- and nanoplastic. *Crit. Rev. Environ. Sci. Technol.* **49**, 32–80 (2019).
 34. H. Jacob, M. Besson, P. W. Swarzenski, D. Lecchini, M. Metian, Effects of virgin micro- and nanoplastics on fish: trends, meta-analysis, and perspectives. *Environ. Sci. Technol.* **54**, 4733–4745 (2020).
 35. S. N. Athey, L. M. Erdle, Are we underestimating anthropogenic microfiber pollution? A critical review of occurrence, methods, and reporting *Environ. Toxicol. Chem.*, 1-16 (2021).

Chapter 4: Does UV-weathering of microplastics and a naturally occurring microparticle alter virus-related mortality in fish?

Introduction

Plastic pollution has been a persistent environmental problem since the large-scale production of inexpensive plastics began circa 1950 (1–3). Although plastic debris likely pollute every compartment, from deep ocean trenches to indoor air, a major focus of plastic pollution research has been on marine debris, as plastic debris is likely to be transported with rain and inland water bodies to the oceans (4, 5). Debris is likely to accumulate in quiescent zones, such as sediments, the open ocean gyres, or along shorelines and within coastal freshwater environments, such as estuaries (6). Within these environments, plastics will be exposed to a variety of natural weathering processes, including ultraviolet (UV) light. Despite their resistance to degradation, UV-weathering has been shown to dramatically impact the surface properties of most plastics and is thought to be a primary mechanism whereby larger plastic particles are embrittled and ultimately fragmented to smaller debris and microplastics (2, 7, 8). Microplastics (≤ 5 mm) are increasingly abundant in environmental studies and elucidating the role of UV-weathering is critical in understanding their ultimate fate and effects.

UV light is defined as that between wavelengths 200-400 nm, of which UVA (315-400) is most dominant on the earth's surface. When UV light reaches plastics, is it either reflected or absorbed by chromophores, which can include aromatic rings, double bonds, additives, trace metals from processing, sorbed environmental pollutants, or other impurities (9, 10). As such, most plastic can absorb some light in the UV range, albeit with differences between polymers and additive formulations (11–13). The absorbed light may lead to photodegradation through a variety of pathways. Photooxidation is a common pathway in the marine environment, where surface waters are periodically

illuminated and oxygen rich (14–16). Photooxidation can lead to a variety of outcomes, most notably the surface of the plastic may become embrittled as amorphous areas between crystalline bond organizations are oxidized and become less stable (15–18). Indeed, these regions on a plastics surface may encourage fragmentation over time into smaller particles or eventually dissolved organic matter (2, 13, 19). This affects the surface charge or polarity of a particle as well, altering its likelihood to form agglomerations, physical fate in water, interactions with biota, and more (8, 20, 21).

Vulnerability to UV-weathering is just one aspect of a microplastic's many physical and chemical characteristics. Microplastics vary considerably in degree of weathering, size, shape, polymer/co-polymer composition, additive chemistry, density and more (22). The effects that microplastics of different characteristics have on living organisms is a rapidly growing area of research (22, 23). Research suggests that toxicological outcomes differ depending upon the type of plastic or organism assayed and may be lethal or sub-lethal in nature. Recent research has illustrated that microplastics may be an important consideration in the spread or contraction of infectious disease, as microplastics may act as a sterile vector for pathogens and have been correlated with disease incidence on coral reefs (24–27). In previous work, we found that the virulence (i.e., disease-related mortality) of a common salmonid rhabdovirus increased when fish were co-exposed to microplastics (Chapter 2).

Here, we investigate the influence of UV-weathered microparticles (≤ 5 mm diameter) on the virulence of infectious hematopoietic necrosis virus (IHNV) in rainbow trout (*Oncorhynchus mykiss*). This is a commercially important wild and aquaculture species that suffers mortality in global populations from IHNV, leading to substantial

financial losses (28, 29). As such, this pathogen and host system has been well-studied, but the influence of UV-weathered microplastic as a co-stressor on IHNV virulence has not been previously explored. Here, nylon microfibers (10 x 500 μm flocking fibers), polystyrene microplastics (expanded polystyrene, ground and sieved to $\sim 20 \mu\text{m}$) and a natural microparticle, ‘spartina’ (marsh grass, *Spartina alterniflora*, washed, ground, and sieved to $\sim 20 \mu\text{m}$) were artificially UV-weathered to an equivalent of six months in average Florida sunlight. Particles were chronically exposed to fish via immersion at different concentrations (0, 0.1, 1.0 and 10 mg L^{-1}) over eight weeks. Half of the fish were exposed to a controlled dose of IHNV by immersion once, half-way through the eight-week experiment. Each treatment (microparticle type/concentration and viral exposure) was replicated in quadruplicate tanks of 20 fish each. Fish were monitored for mortality daily, and water samples were collected at ten time points post-IHNV exposure to assess the amount of viral shed. We hypothesized that the UV-weathering of microparticles would increase their hydrophilicity and surface complexity, meaning UV-weathered particles would be more likely to encounter fish and cause tissue damage, increasing disease virulence relative to their unweathered counterparts (as found in our previous work; see Chapter 2).

Materials and Methods

Particle Preparation

Unweathered nylon, polystyrene and spartina were obtained and prepared according to methods outlined in Chapter 2. Briefly, expanded polystyrene foam sheet, commonly used as insulation, was purchased from a local houseware store. Foam was cryogenically embrittled and ground in a Retsch CryoMill, sieved to $\leq 20 \mu\text{m}$ with a

Retsch AS 200 air jet sieve and Gilson Performer III Sieve shaker (30). The median diameter of polystyrene particles was 26.8 μm and 25% of particles fell below 16.4 μm . Undyed nylon 6'6 fibers were provided by Claremont Flock, Inc. (Leominster, MA, USA). The manufacturer reported fibers to be 0.8 denier (approximately 10 μm) in diameter and 500 μm in length. Particle size analysis using a Beckman-Coulter Laser Diffraction Particle Size Analyzer confirmed the 500 x 10 μm measurement of nylon fibers. The fibers were reported to not contain additives aside from a TiO_2 delustrant. Dead *Spartina alterniflora* (marsh cordgrass) was collected from estuarine marshes near Yorktown, VA by cutting stems near the base. Grass was sorted in a fume hood, washed with deionized water, and dried overnight in a muffle oven at 60°C. Sections were ground in a standard blender, then treated in the Retsch CryoMill, and sieved as above. The median diameter of spartina particles was 39.2 μm ; 25% of particles were below 21.3 μm . The ground and sieved spartina-derived fragments contained more elongated particles (a product of the plant cellular structure) than the spheroidal polystyrene fragments. Some of the spartina fragments passed through the sieve on their shortest axis; this and any potential clumping may account for the overall greater size particles than polystyrene despite using the same sieving approach.

Particles were weathered using in a Q-SUN XE-1 xenon test chamber (Q-lab Westlake, OH, USA). This instrument mimics the spectrum of natural sunlight with xenon arc lamps and a daylight-BB filter. No other weathering features (e.g., salt spray, humidity, etc.) were included. Samples were contained in individual glass chambers, covered with quartz lids to prevent material loss, and placed inside the weathering chamber. Samples were irradiated under the maximum setting (0.68 W m^{-2} @ 340 nm)

for 500 hours, reaching a total of 140 mJ m⁻² total UV. This is considered equivalent to approximately six months of exposure to Florida sunlight (31).

Experimental Animals and Husbandry

Juvenile rainbow trout (*Oncorhynchus mykiss*) were obtained from the National Center for Cool and Cold Water Aquaculture in West Virginia (NCCCWA; within USDA's Agricultural Research Service) and reared at VIMS as discussed in chapter 3. Trout were reared at the Virginia Institute of Marine Science (VIMS), according to guidelines from the Institutional Animal Care and Use Committee (IACUC-2020-06-24-14322-arwargo) and previously established protocols (32). For the experiment, fish were transferred to a flow-through tower rack tank system (Aquaneering) housed in a BSL-II aquatic animal laboratory at VIMS, with room, water and husbandry parameters as described in chapter 3.

Experimental Design and Procedures

Fish received one of 22 possible treatments, outlined in Table 1. Each treatment was completed with quadruplicate tanks of 20 fish each, monitored for mortality and water sampled for viral shedding. Tanks were randomly distributed for each treatment to minimize placement effects. For microplastic exposure, fish were dosed with particles every other day, beginning on the first day of the experiment. Particles were dosed by opening pre-weighed foil sachets and submerging the contents in the tank, ensuring all particles were added to the water. Tank water was held static for 24 hours during particle exposure. The flow was then resumed, and tanks flushed for 24 hours to maintain water quality. To reduce microplastic discharge to the local wastewater system, during the first hour of each tank flushing effluent was pumped through a series of in-line filters (75 µm,

20 µm, 5 µm and 1 µm) before passing through UV-irradiation (sufficient for virus inactivation) and eventual discharge to the institutional municipal wastewater stream. In total, the experiment lasted 56 days with 28 particle dosing events. The experiment was monitored at the same time daily, recording temperature, dissolved oxygen, and the number of fish mortalities in each tank.

Table 1 Experimental treatments included a combination of particle types, dosing concentrations and virus exposures. All treatments were completed in quadruplicate tanks of 20 fish each.

Microparticle	Dose	Virus
No Particle	None	IHNV+
No Particle	None	IHNV-
UV-weathered Nylon Microfibers	10 mg L ⁻¹	IHNV+
UV-weathered Nylon Microfibers	10 mg L ⁻¹	IHNV-
UV-weathered Nylon Microfibers	1 mg L ⁻¹	IHNV+
UV-weathered Nylon Microfibers	1 mg L ⁻¹	IHNV-
UV-weathered Nylon Microfibers	0.1 mg L ⁻¹	IHNV+
UV-weathered Nylon Microfibers	0.1 mg L ⁻¹	IHNV-
Unweathered Nylon Microfibers	10 mg L ⁻¹	IHNV+
Unweathered Nylon Microfibers	10 mg L ⁻¹	IHNV-
UV-weathered Polystyrene Microplastics	10 mg L ⁻¹	IHNV+
UV-weathered Polystyrene Microplastics	10 mg L ⁻¹	IHNV-
UV-weathered Polystyrene Microplastics	1 mg L ⁻¹	IHNV+
UV-weathered Polystyrene Microplastics	1 mg L ⁻¹	IHNV-
UV-weathered Polystyrene Microplastics	0.1 mg L ⁻¹	IHNV+
UV-weathered Polystyrene Microplastics	0.1 mg L ⁻¹	IHNV-
UV-weathered Spartina Microparticles	10 mg L ⁻¹	IHNV+
UV-weathered Spartina Microparticles	10 mg L ⁻¹	IHNV-
UV-weathered Spartina Microparticles	1 mg L ⁻¹	IHNV+
UV-weathered Spartina Microparticles	1 mg L ⁻¹	IHNV-
UV-weathered Spartina Microparticles	0.1 mg L ⁻¹	IHNV+
UV-weathered Spartina Microparticles	0.1 mg L ⁻¹	IHNV-

Halfway through the experiment (day 28), fish were dosed with virus or a mock control. Experimental virus, IHNV (*Salmonid novirhabdovirus*) isolate C

(genotype mG119M; GenBank accession number AF237984) at a dose of 4.0×10^3 PFU mL⁻¹, as discussed in chapter 3.

To quantify viral shedding, water samples were collected on days 29, 31, 33, 35, 37, 39, 41, 43, 47, and 55, from quadruplicate survival analysis tanks. Each water sample was collected at the end of the static period just prior to flushing, such that virus had maximum and consistent time to accumulate in tanks. An 800 µL water sample was collected per tank and stored at -80°C prior to extraction and analysis. Extraction and qPCR procedures are detailed in Jones et al. 2020 (27) and outlined in chapter 3.

Statistical Analyses

All graphical and statistical analyses were completed in R Studio and significance was inferred with $\alpha = 0.05$. Mortality analyses were illustrated with Kaplan-Meier survival curves using package ‘survival’ (Fig.1). Statistically significant differences between treatments were determined with Cox proportional hazard models in R with the “coxph” function (package “survival”). All possible combinations of fixed and random effects were modeled. Possible fixed effects include treatment (combined microparticle and dose, see Table 1) and virus (IHNV+ or IHNV-), while tank was a possible random effect. The best fit model was determined, based on parsimony and Akaike Information Criterion (AIC). The best model included treatment and virus, but not their interaction, and tank as a random factor. This model was used to report the overall significance of virus exposure on mortality. However, because mortality levels in virus negative tanks were low, a second model using the same factors was generated among IHNV+ fish only, to determine how survival differed between particle treatments when fish were exposed to virus. These treatment results are denoted in Figure 1.

To determine the effect of weathering on mortality, survival analysis was also conducted comparing UV-weathered nylon microfiber treatments and the non-UV-weathered nylon microfiber treatments was also modeled separately (Fig. 2). Statistically significant differences between treatments were determined with Cox proportional hazard models in R with the “coxph” function (package “survival”). All possible combinations of fixed and random effects were modeled. Possible fixed effects include treatment (combined microparticle and dose for nylon fiber treatments and no particle, see Table 1) and virus (IHNV+ or IHNV-), while possible random effect was of tank. The best combination of factors was determined using AIC. The best model included treatment and virus, but not their interaction, and tank as a random factor. This model reports the significance of virus exposure in mortality. As the interactions failed to converge, another model using these same factors was generated among IHNV+ fish only, and these results are denoted in Figure 2.

Viral shedding among all IHNV+ tanks was modeled with a linear mixed effects model, considering all possible combinations of fixed explanatory variables (same as survival analysis with the addition of day as a continuous factor) and their interactions, as well as the random influence of tank. The best model was determined with AIC and included the collection day as a fixed effect and tank as a random variable. The microparticle treatment was not significant in any model (regardless of best fit) and dropped from the model.

Results and Discussion

Mortality

We monitored mortality among a population of fish exposed to combinations of IHNV and UV-weathered nylon microfibers, polystyrene microplastics, and spartina microparticles at low, medium and high concentrations (Fig. 1). Regardless of microparticle treatment, exposure to IHNV increased the hazard of death by 4.31 times ($X^2_{1,1554} = 234.21$, p-value < 0.001). Among all virus-exposed (IHNV+) treatments, compared to no particle controls, co-exposure to the medium concentration of UV-weathered nylon increased the hazard of death by 1.58 times ($X^2_{1,773} = 4.68$, p-value = 0.031), while high and low concentrations had no significant effect on mortality. Co-exposure to medium and low concentrations of UV-weathered polystyrene increased the hazard of death by 1.67 times ($X^2_{1,773} = 5.96$, p-value = 0.015) and 1.58 times ($X^2_{1,773} = 4.80$, p-value = 0.028), respectively, while highest concentration of UV-weathered polystyrene had no effect; co-exposure to high concentration of UV-weathered spartina increased the hazard of death by 1.51 times ($X^2_{1,773} = 3.89$, p-value = 0.048) while medium and low concentrations did not have a significant effect (Fig. 1). There was no significant influence of UV-weathered microparticles on mortality among fish not exposed to virus (IHNV-), compared to no particle controls.

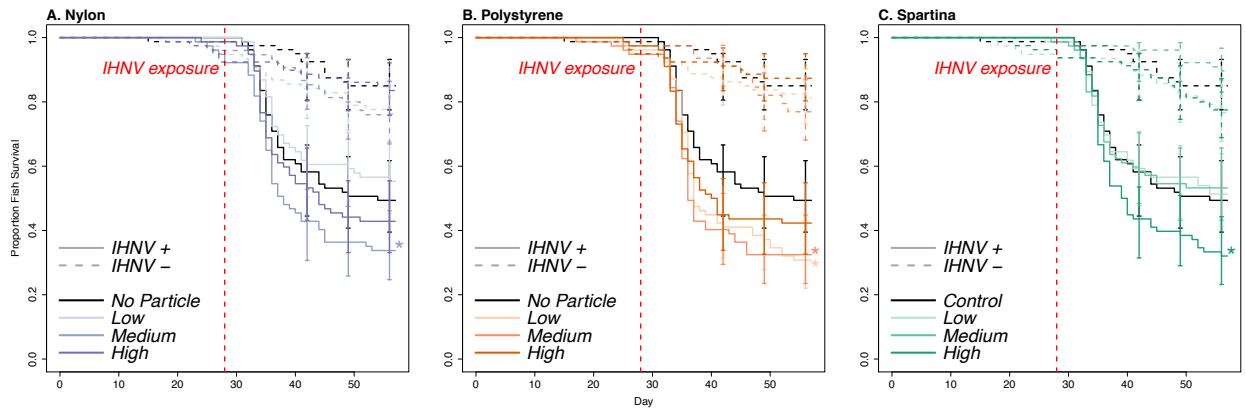


Fig. 1 Fish mortality is illustrated through time for different UV-weathered microparticle and IHNV treatments. Fish were monitored for eight weeks (56 days) and exposed to microparticles chronically. After four weeks, fish were exposed to IHNV once, indicated by the vertical red line on day 28. Virus unexposed treatments (IHNV-; dashed lines) elicited less mortality than virus exposed (IHNV+; solid lines). Fish not exposed to any microparticles are illustrated in black, while microparticle exposures are denoted in shades of blue (nylon, A), orange (polystyrene, B) and green (spartina, C). Color shade corresponds to low (0.1 mg L^{-1}), medium (1.0 mg L^{-1}) and high (10.0 mg L^{-1}) microparticle exposure concentrations. Mortality was found to be significantly affected by the microparticle treatment ($X^2_{9,773} = 20.68$, $p\text{-value} = 0.014$) and virus exposure ($X^2_{1,773} = 277.55$, $Df = 1$, $p\text{-value} < 0.001$) using Cox proportional hazard analysis. Significant differences in survival between IHNV+ no particle and particle treatments are noted (Cox proportional hazard analysis, $p\text{-values} \leq 0.05$: *).

These results were consistent with previous observations that specific microplastics at certain concentrations increase IHNV virulence (Chapter 2). Compared to that previous work, however, the magnitude of difference in particle-influenced virulence was lower. A difference in mortality of approximately 60% was observed between virus exposure in isolation and co-exposure with high concentrations of nylon microfibers previously, while the maximum virulence difference here between UV-weathered particles co-exposure and virus-only exposure was approximately 20%. This demonstrates that although UV-weathered microparticles still increased the virulence of IHNV in rainbow trout populations, possibly not moreso than unweathered particles.

Although a contaminant dose generally correlates with magnitude of effect, a clear dose response was not observed among any of the UV-weathered microplastics investigated here. In previous work, unweathered nylon fibers dosed from high to low concentrations had correspondingly decreasing effect on viral virulence (Chapter 2). Here, UV-weathered nylon microfibers had the greatest magnitude of effect at the medium concentration, while the high and low concentrations were not different from virus-only exposure. Likewise, the influence of UV-weathered polystyrene followed an inverse relationship with dose, whereby the lowest concentration had the highest magnitude of effect and the highest concentration had no effect on virulence. There are many potential mechanisms behind the observed lack of dose response, among them is changes in particle surface chemistry as a result of weathering. In chapter 2 we postulated that (unweathered) polystyrene microplastics aggregated at the highest concentration, effectively decreasing the number of particles and increasing the size of particles to which fish were exposed. This may alter the likelihood of a fish contacting microparticles, ingesting or respiring them, or may alter the mechanism of effect. Surface chemistry and particle concentration are two of many factors that can dictate particle aggregation, and surface chemistry of these particles was likely influenced by UV-weathering (15, 20, 34–36). For example, nylon fibers may have been more likely to aggregate than disperse in water following UV-weathering due to increased surface structure complexity, decreasing their likelihood of encountering sensitive epithelia when dosed at high concentrations. Based on the work here we can only speculate as to the role of microparticle aggregation on their effects and how that aggregation changes with UV-weathering. Indeed, the lack of dose response may simply be explained by stochasticity

in the exposure system. Nonetheless, future work should confirm the relationships between particle agglomeration and UV-exposure as it relates to organismal exposure, as this is an important question in assessing risk to natural organisms.

The only particle demonstrating a stereotypical dose response was UV-weathered spartina microparticles. In previous work, unweathered spartina microparticles were not found to increase virulence when co-exposed with IHNV (Chapter 2). Here, the highest concentration of spartina microparticles significantly increased virulence compared to fish exposed to IHNV only, suggesting natural microparticles may indeed act as a co-stressor in concert with disease. Again, the reason behind this change in effect may be attributable to changes in surface chemistry following UV-weathering. Unweathered spartina microparticles were likely to aggregate, given their organic and hydrophobic nature (similar to plastics). Following UV-weathering the surface charge may have been affected such that the particles became more hydrophilic, decreasing agglomeration and increasing encounters with fish. This is true of both natural and synthetic materials, which become oxidized under UV light, increasing the charge and polarity of the surface, decreasing hydrophobicity (15, 16, 37). Synthetic polymers, however, are often engineered with UV-stabilizers and antioxidants to be resistant to these surface changes, meaning that the same amount of UV-weathering could have had a dramatically larger influence on spartina than polystyrene or nylon (13). In addition, UV-weathering is likely to increase the amorphous regions of polymers, which could lead to cracking and embrittlement (7, 15, 16). The spartina particles may have become more irregular in surface shape, increasing the likelihood that they could damage tissues and potentially

increase host colonization. This supports the need for increased comparative studies between synthetic microplastics and natural polymeric microparticles (38–40).

It is important to note that there was greater background mortality in this study compared to the previous work (i.e., mortality was observed in populations of fish not exposed to virus). This mortality was not significantly different between microparticle treatments and the no particle control, which is consistent with previous work that these unweathered particles did not cause death in absence of virus. It underscores the differences in fish populations between this and the previous study, however. The fish in this study were smaller (approximately 2g compared to 5g) and may have been less robust to tank stresses over time, explaining the higher mortality without IHNV exposure. In fact, we anticipated these fish to be more susceptible to IHNV and lowered the dose by 20% compared to work with 5g fish in Chapter 2. However, lower cumulative mortality from IHNV infection was actually observed in this population than Chapter 2. Although the rainbow trout were procured from the same aquaculture source, the fish were of different strains with potentially different resistance to IHNV or even microplastics, which may explain these outcomes. As such, it is difficult to compare directly between this work and the previous study, which underscores that these effects are not just dependent upon the exposure toxicants, but also upon the organism and environment.

Although this study did not directly compare the weathered and unweathered versions of all microparticles in *in vivo*, a high concentration unweathered nylon microfibers was included for comparison. The effect of unweathered nylon was found to be similar to weathered nylon (Fig. 1 and 2). Among fish exposed to IHNV, co-exposure to the medium dose of UV-weathered microfibers significantly increased the hazard of

death by 1.58 times ($X_2 = 4.69$, $Df = 1$, $p\text{-value} = 3.0e-3$). Co-exposure with high concentration of unweathered nylon fibers elicited the second-highest increase in virulence, increasing the hazard of death by 1.34 times ($X_2 = 1.88$, $Df = 1$, $p\text{-value} = 1.7e-1$), but not significantly so. This suggests that the differences between populations of fish may indeed be important here, as the fish used in this study elicited a different response to the same co-exposure of unweathered nylon microfibers. Although their co-exposure with virus still increased virulence compared to IHNV alone, the magnitude of this change is far less than was observed previously (Chapter 2; total mortality difference of approximately 10%, compared to 40%). These changes may be a result of the fish size or line, as previously discussed.

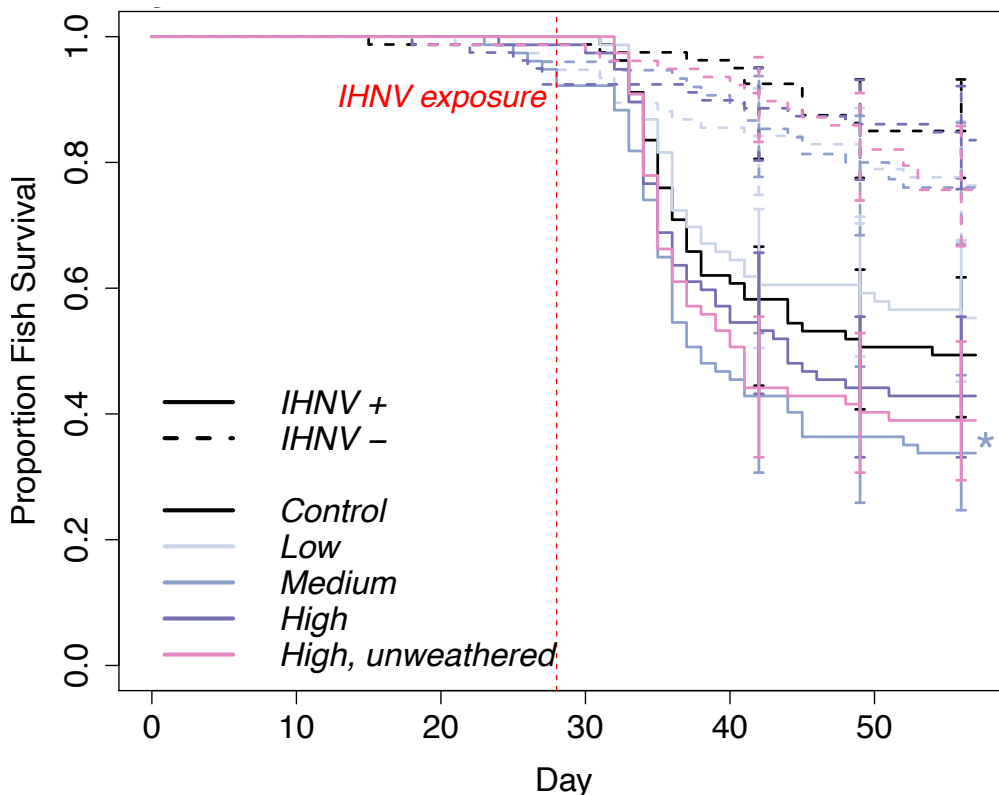


Fig. 2 Fish mortality over time modeled for different nylon microfiber and virus co-exposure scenarios. Mortality is illustrated as proportion of surviving fish over 56 days, with IHNV exposure on day 28 denoted with red vertical dashed line. Virus unexposed

treatments (IHNV-; dashed lines) elicited less mortality than virus exposed (IHNV+; solid lines). Treatments include UV-weathered nylon fibers in shades of purple for low (0.1 mg L^{-1}), medium (1.0 mg L^{-1}) and high (10.0 mg L^{-1}) exposure concentrations, as well as unweathered nylon microfibers in pink. In a Cox proportional hazards model, mortality was significantly affected by the presence of virus ($X_2 = 115.84$, $Df = 1$, $p < 00.1$). Significant differences in survival between IHNV+ control and other virus-exposed treatments is denoted on graph (p -value ≤ 0.1 : +, ≤ 0.05 : *).

Viral Shedding

Viral shedding from infected rainbow trout was monitored following IHNV exposure (Fig. 3). Neither the peak amount of shed (occurring on average on day 31) or the kinetics of shedding appeared to have been significantly different between microparticle treatments. Indeed, the best fit model did not include any aspect of microparticle exposure (type, concentration, or both). Although the amount of virus shed during the period of peak shedding or the total amount of virus shed over time may be informative, there were also no significant differences in either of these parameters as a result of UV-weathered particle co-exposure with virus (Fig. S4.1, Fig. S4.2).

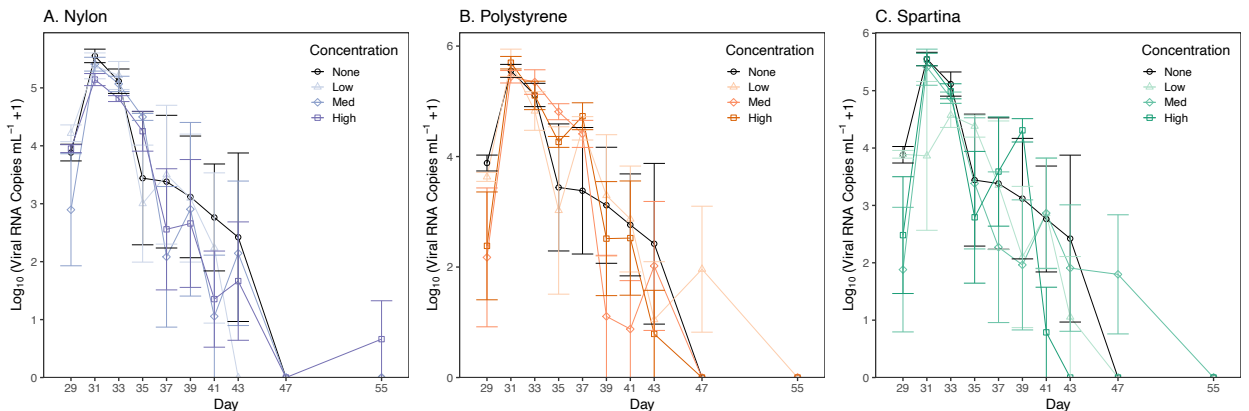


Fig. 3 Viral shedding over time is illustrated for all concentrations of UV-weathered nylon (A), polystyrene (B) and spartina (C). Virus exposure occurred on day 28. Viral shed was calculated for water samples collected on ten days and the mean virus shed (log-adjusted viral RNA copies mL^{-1} water) for each day among quadruplicate tanks is illustrated, ± 1 standard error of the mean (SEM). Only tanks exposed to IHNV are included. According to linear mixed effects model analysis, only the collection day had a significant influence on viral shed ($F_{1,385} = 329.36$, p -value < 0.001). Treatment type did not affect viral shedding and was not included in the model of best fit.

These viral shedding results illustrate the complications of assessing total viral shed by a population. Some *in vivo* models that found viral shed correlated with virulence using tanks with a single fish, so that shedding was from one individual and could be assumed to correlate with body burden (33, 41, 42). Here, we modeled the shedding for the entire population of a tank, adding considerable variability to the results. Although there was a significant association between population viral shedding and virulence in previous work (Chapter 2), the magnitude of difference in virulence between treatments in that experiment was more than twice what we observed here. While we did observe significant virulence changes as result of virus co-exposure with certain UV-weathered microparticles (Fig. 1), perhaps the magnitude of these differences was not dramatic enough to significantly influence total population shedding. Host body burden may be more informative, as that can assess load from an individual even when subsampled from a larger population. As such, these data neither confirmed nor denied the observed patterns in virulence for different UV-weathered microparticle treatments. Yet, it underscored that large differences in virulence for a population of rainbow trout, or other species for that matter, may be needed in order to detect corresponding changes in virus shed by those populations (i.e., tanks housing multiple fish).

Conclusions

In this work, we evaluated the effect of UV-weathering on capacities of different microplastics and a naturally derived microparticle (derived from a common marsh grass) to increase virulence of IHNV in rainbow trout populations. We originally hypothesized that UV-weathering would increase the hydrophilicity and surface complexity of

microparticles, which would increase their likelihood to interact with and disrupt sensitive gill and mucosal epithelia in fish, ultimately increasing virulence. Although we were unable to directly compare most UV-weathered and unweathered particles here (aside from high concentrations of nylon microfibers), we planned to compare the differences in virulence between microparticle co-exposures and IHNV-only exposures from each experiment. In general, the magnitude of virulence differences was lower for all UV-weathered particles than it had been for unweathered particles in previous work (Chapter 2). The type and concentrations of UV-weathered particles with the most notable effects, however, were different than those for the unweathered particles. Specifically, the highest concentration of UV-weathered spartina was more influential on virulence than expected. By including an unweathered nylon microfiber treatment, however, we saw that many of the observed differences in response may be attributable to the differences in the two different fish strains we used or an additional stressor that led to mortality among IHNV unexposed fish. The fish used in this experiment were a different line with different resistance to pathogen, and they were smaller in weight on average. As such, the ability to compare between our studies is somewhat confounded. Future work should address the effect of unweathered and UV-weathered microplastics in identical systems. Further, microplastics in the environment may be weathered for periods of time far longer than the exposure mimicked here. Comparing varying degrees of mild to advanced UV-weathering would be informative. Nonetheless, we conclude that UV-weathering influenced a microplastics ability to modulate disease virulence in this well-studied system. Future effects research should incorporate UV-weathering as this

naturally occurring phenomenon may be crucial in determining the environmental toxicity of microplastics.

References

1. R. Geyer, J. R. Jambeck, K. L. Law, Production, use, and fate of all plastics ever made. *Sci. Adv.* **3**, e1700782 (2017).
2. R. C. Hale, M. E. Seeley, M. J. La Guardia, L. Mai, E. Y. Zeng, A global perspective on microplastics. *J. Geophys. Res. Oceans.* **125** (2020), doi:10.1029/2018JC014719.
3. E. J. Carpenter, K. L. Smith, Plastics on the Sargasso Sea surface. *Science.* **175**, 1240–1241 (1972).
4. J. R. Jambeck, R. Geyer, C. Wilcox, T. R. Siegler, M. Perryman, A. Andrady, R. Narayan, K. L. Law, Plastic waste inputs from land into the ocean. *Science.* **347**, 768–771 (2015).
5. L. C. M. Lebreton, J. van der Zwet, J.-W. Damsteeg, B. Slat, A. Andrady, J. Reisser, River plastic emissions to the world's oceans. *Nat. Commun.* **8**, 15611 (2017).
6. E. van Sebille, C. Wilcox, L. Lebreton, N. Maximenko, B. D. Hardesty, J. A. van Franeker, M. Eriksen, D. Siegel, F. Galgani, K. L. Law, A global inventory of small floating plastic debris. *Environ. Res. Lett.* **10**, 124006 (2015).
7. A. ter Halle, L. Ladirat, M. Martignac, A. F. Mingotaud, O. Boyron, E. Perez, To what extent are microplastics from the open ocean weathered? *Environ. Pollut.* **227**, 167–174 (2017).
8. H. P. H. Arp, D. Kühnel, C. Rummel, M. MacLeod, A. Potthoff, S. Reichelt, E. Rojo-Nieto, M. Schmitt-Jansen, J. Sonnenberg, E. Toorman, A. Jahnke, Weathering plastics as a planetary boundary threat: exposure, fate, and hazards. *Environ. Sci. Technol.* **55**, 7246–7255 (2021).
9. L. W. McKeen, in *The effect of UV light and weather on plastics and elastomers* (Elsevier Inc., ed. 3, 2013), pp. 17–41.
10. E. Yousif, R. Haddad, Photodegradation and photostabilization of polymers, especially polystyrene: review. *SpringerPlus.* **2**, 398 (2013).
11. S. P. Garaba, H. M. Dierssen, Hyperspectral ultraviolet to shortwave infrared characteristics of marine-harvested, washed-ashore and virgin plastics. *Earth Syst. Sci. Data.* **12**, 77–86 (2020).
12. R. Kumar, S. A. Ali, A. K. Mahur, H. S. Virk, F. Singh, S. A. Khan, D. K. Avasthi, R. Prasad, Study of optical band gap and carbonaceous clusters in swift heavy ion irradiated polymers with UV-Vis spectroscopy. *Nucl. Instrum. Methods Phys. Res. Sect. B Beam Interact. Mater. At.* **266**, 1788–1792 (2008).

13. A. N. Walsh, C. M. Reddy, S. F. Niles, A. M. McKenna, C. M. Hansel, C. P. Ward, Plastic formulation is an emerging control of its photochemical fate in the ocean, *Environ. Sci. Technol.*, **55**, 12383–12392 (2021).
14. B. Gewert, M. M. Plassmann, M. MacLeod, Pathways for degradation of plastic polymers floating in the marine environment. *Environ. Sci. Process. Impacts*. **17**, 1513–1521 (2015).
15. L. W. McKeen, in *The Effect of UV Light and Weather on Plastics and Elastomers* (Elsevier, 2013; <https://linkinghub.elsevier.com/retrieve/pii/B9781455728510000025>), pp. 17–41.
16. A. L. Andrady, The plastic in microplastics: A review. *Mar. Pollut. Bull.* **119**, 12–22 (2017).
17. P. Gijsman, G. Meijers, G. Vitarelli, Comparison of the UV-degradation chemistry of polypropylene, polyethylene, polyamide 6 and polybutylene terephthalate. *Polym. Degrad. Stab.* **65**, 433–441 (1999).
18. R. Asmatulu, G. A. Mahmud, C. Hille, H. E. Misak, Effects of UV degradation on surface hydrophobicity, crack, and thickness of MWCNT-based nanocomposite coatings. *Prog. Org. Coat.* **72**, 553–561 (2011).
19. C. P. Ward, C. J. Armstrong, A. N. Walsh, J. H. Jackson, C. M. Reddy, Sunlight converts polystyrene to carbon dioxide and dissolved organic carbon. *Environ. Sci. Technol. Lett.* **6**, 669–674 (2019).
20. H. J. Shupe, K. M. Boenisch, B. J. Harper, S. M. Brander, S. L. Harper, Effect of nanoplastic type and surface chemistry on particle agglomeration over a salinity gradient. *Environ. Toxicol. Chem.* **40**, 1820–1826 (2021).
21. S. Bejgarn, M. MacLeod, C. Bogdal, M. Breitholtz, Toxicity of leachate from weathering plastics: An exploratory screening study with *Nitocra spinipes*. *Chemosphere*. **132**, 114–119 (2015).
22. C. M. Rochman, C. Brookson, J. Bikker, N. Djuric, A. Earn, K. Bucci, S. Athey, A. Huntington, H. McIlwraith, K. Munno, H. De Frond, A. Kolomijeca, L. Erdle, J. Grbic, M. Bayoumi, S. B. Borrelle, T. Wu, S. Santoro, L. M. Werbowski, X. Zhu, R. K. Giles, B. M. Hamilton, C. Thaysen, A. Kaura, N. Klasios, L. Ead, J. Kim, C. Sherlock, A. Ho, C. Hung, Rethinking microplastics as a diverse contaminant suite. *Environ. Toxicol. Chem.* **38**, 703–711 (2019).
23. M. D. Prokić, T. B. Radovanović, J. P. Gavrić, C. Faggio, Ecotoxicological effects of microplastics: Examination of biomarkers, current state and future perspectives. *TrAC Trends Anal. Chem.* **111**, 37–46 (2019).

24. I. V. Kirstein, S. Kirmizi, A. Wichels, A. Garin-Fernandez, R. Erler, M. Löder, G. Gerds, Dangerous hitchhikers? Evidence for potentially pathogenic *Vibrio spp.* on microplastic particles. *Mar. Environ. Res.* **120**, 1–8 (2016).
25. L. A. Amaral-Zettler, E. R. Zettler, T. J. Mincer, Ecology of the plastisphere. *Nat. Rev. Microbiol.* **18**, 139–151 (2020).
26. J. B. Lamb, B. L. Willis, E. A. Fiorenza, C. S. Couch, R. Howard, D. N. Rader, J. D. True, L. A. Kelly, A. Ahmad, J. Jompa, C. D. Harvell, Plastic waste associated with disease on coral reefs. *Science.* **359**, 460–462 (2018).
27. R. R. Leads, K. G. Burnett, J. E. Weinstein, The effect of microplastic ingestion on survival of the grass shrimp *Palaemonetes pugio* (Holthuis, 1949) challenged with *Vibrio campbellii*. *Environ. Toxicol. Chem.* **38**, 2233–2242 (2019).
28. L. Bootland, J.-A. Leong, in *Fish Diseases and Disorders* (2011), vol. 3, pp. 66–109.
29. P. Dixon, R. Paley, R. Alegria-Moran, B. Oidtmann, Epidemiological characteristics of infectious hematopoietic necrosis virus (IHNV): a review. *Vet. Res.* **47**, 63 (2016).
30. M. E. Seeley, B. Song, R. Passie, R. C. Hale, Microplastics affect sedimentary microbial communities and nitrogen cycling. *Nat. Commun.* **11**, 2372 (2020).
31. D. M. Grossman, Technical Bulletin “A discussion of the most frequently asked questions about accelerated weathering” Q-Lab LU-0833, 4.
32. J. L. Everson, D. R. Jones, A. K. Taylor, B. J. Rutan, T. D. Leeds, K. E. Langwig, A. R. Wargo, G. D. Wiens, Aquaculture reuse water, genetic line, and vaccination affect rainbow trout (*Oncorhynchus mykiss*) disease susceptibility and infection dynamics. *Front. Immunol.* **12**, 3894 (2021).
33. D. R. Jones, B. J. Rutan, A. R. Wargo, Impact of vaccination and pathogen exposure dosage on shedding kinetics of infectious hematopoietic necrosis virus (IHNV) in rainbow trout, 14.
34. W. P. de Haan, A. Sanchez-Vidal, M. Canals, Floating microplastics and aggregate formation in the Western Mediterranean Sea. *Mar. Pollut. Bull.* **140**, 523–535 (2019).
35. S. Summers, T. Henry, T. Gutierrez, Agglomeration of nano- and microplastic particles in seawater by autochthonous and de novo-produced sources of exopolymeric substances. *Mar. Pollut. Bull.* **130**, 258–267 (2018).
36. S. D. Burrows, S. Frustaci, K. V. Thomas, T. Galloway, Expanding exploration of dynamic microplastic surface characteristics and interactions. *TrAC Trends Anal. Chem.* **130**, 115993 (2020).

37. H. Luo, Y. Zhao, Y. Li, Y. Xiang, D. He, X. Pan, Aging of microplastics affects their surface properties, thermal decomposition, additives leaching and interactions in simulated fluids. *Sci. Total Environ.* **714**, 136862 (2020).
38. M. Ogonowski, Z. Gerdes, E. Gorokhova, What we know and what we think we know about microplastic effects – A critical perspective. *Curr. Opin. Environ. Sci. Health.* **1**, 41–46 (2018).
39. M. Ogonowski, C. Schür, Å. Jarsén, E. Gorokhova, The effects of natural and anthropogenic microparticles on individual fitness in *Daphnia magna*. *PLOS ONE.* **11**, e0155063 (2016).
40. L. Kim, S. A. Kim, T. H. Kim, J. Kim, Y.-J. An, Synthetic and natural microfibers induce gut damage in the brine shrimp *Artemia franciscana*. *Aquat. Toxicol.* **232**, 105748 (2021).
41. A. R. Wargo, G. Kurath, In vivo fitness associated with high virulence in a vertebrate virus is a complex trait regulated by host entry, replication, and shedding. *J. Virol.* **85**, 3959–3967 (2011).
42. A. R. Wargo, R. J. Scott, B. Kerr, G. Kurath, Replication and shedding kinetics of infectious hematopoietic necrosis virus in juvenile rainbow trout. *Virus Res.* **227**, 200–211 (2017).

Conclusions

The public, media, resource managers and policy makers have become increasingly aware of the breadth and persistence of microplastic pollution. Despite prevention and cleanup efforts to remove plastic debris from the aquatic environment, plastic pollution and thus, microplastic pollution, will continue to increase over the coming century unless dramatic (and largely unrealistic) changes are made to waste management infrastructure and global waste policy. As such, it is critical to understand the effects of microplastics on valuable aquatic resources and ecosystems, at current and projected pollution levels. The work presented here explored the complex nature of microplastics toxicity.

A theme across all chapters was that it is challenging to discern which aspect of a microplastic's characteristics creates an effect – size, shape, chemistry? Although tedious, future work may address these questions by re-probing the same systems with microplastics that vary across one (and not multiple) parameters. For example, the exploration of fiber size on effect as a viral co-stressor should be explored (e.g., nylon microfibers of discrete sizes, from 50 μm to 5000 μm long). Theoretically, this work could resolve an effect size range (e.g., only fibers 500-2000 μm in length are large enough to disrupt sensitive tissues but short enough to reach those tissues) and be practically applied to risk management/reduction applications. Likewise, expanded dose-response work could resolve an effect threshold at which, for example, there are enough microplastics present in a sediment to alter microbial community structure. Morphology, physiology, life history and ecology of exposed organisms will also affect toxicological outcomes following microplastic exposure.

Another key aspect of this work recognizes that microplastics do not exist in the absence of other microparticulate matter and, if microplastics effects are a product of their size or shape, natural particulate matter may be equally impactful. This is important to resolve considering that natural particulate organic matter in the coastal zones is in many cases higher than, microplastic pollution levels. Natural inorganic particles are also abundant. Future work should consider which microparticles best approximate natural particulate matter. Although the spartina marsh grass microparticles used in chapters 2-4 was chosen above non-polymeric particles (such as inert clays or silica), it also contained pigments and other compounds that may influence its effect. Additionally, in natural environments, spartina grass would be microbially-degraded into constituent compounds as well as reaching a detrital, particulate phase (i.e., its relevance is questionable). Our research illustrates that including a non-plastic particulate in comparison to plastics is paramount in distinguishing effects, and should be included in more studies. Further, although natural particulate matter may exceed microplastic levels when considering total carbon in a certain area, microplastic pollution is patchy and high concentrations often occur in discrete areas (e.g., a wastewater outfall). Like other pollutants (or even, pathogens) therefore, it is misleading to approximate an ‘environmentally relevant’ dose based on regional averages. This is particularly true considering the growing expanse and abundance of microplastic pollution, and our limited ability to detect and enumerate microplastics (particularly small microplastics).

In the research presented here, we strove to increase our understanding of complex system effects, such as those to microbial communities and the nutrient cycles that they mediate, or to host-pathogen dynamics. While many of the trends observed are

specific to the type of plastic used or the system probed, they underscore that microplastics are indeed capable of influencing valuable ecosystems and should not be disregarded as an over-emphasized pollutant.

Appendices

Chapter 1 Supplementary Information

Flame retardant and phthalate additives were determined in the polymers PE, PVC and PUF. Penta-BDE is a (poly)brominated diphenyl ether (BDE) mixture consisting of several major congeners: BDE47, 99, 100, 153 and 154¹. Penta-BDE was commonly used in PUF. Components of Firemaster® 550, a replacement flame retardant for Penta-BDE, were also determined (i.e. 2-ethylhexyl 2, 3, 4, 5-tetrabromobenzoate (TBB); 2-ethylhexyl 2, 3, 4, 5-tetrabromophthalate (TBPH)) and several phosphate FRs: tris (1,3-dichloro-2-propyl) phosphate (TDCPP) and triphenyl phosphate (TPP)). Tris (2-chloroethyl) phosphate (TCEP) and tris (1-chloro-2-propyl) phosphate (TCPP), additional phosphate-based flame retardants, were also analyzed. Three aliquots of finely milled PE, PVC and PUF (53-300 µm) were chemically analyzed. These were sequentially extracted with three 60 mL aliquots of dichloromethane (DCM). Extract aliquots were combined and reduced in volume (0.5 mL) under a stream of high purity nitrogen. All solvents used were high purity HPLC or residue grade from Burdick & Jackson. Residual solids in the extracts were removed by filtration (Whatman filter paper 11 µm, 7 cm diameter). The solvent extracts were purified to remove high molecular weight interferences by size exclusion liquid chromatography (Envirosep ABC column. 350 x 21.2 mm. Phenomenex Inc.) and then by elution through 2-g solid phase silica gel glass extraction columns (Isolute, International Sorbent Tech.; Hengoed Mid Glamorgan, U.K.)¹. Silica gel eluents were S1: 3.5ml (100% hexane-waste), S2: 6.5ml (60:40, hexane/methylene chloride-hydrophobic flame retardants) + 8mL (100% methylene chloride) and S3: 5ml (50:50, methylene chloride /acetone-polar compounds). The elution profiles of the additives were determined by processing standards of the target chemicals. Purified extracts were

diluted to produce chromatographic peak areas within the bounds of the LC/MS or GC/MS calibration curves.

Identification and quantitation of the target additives from PUF, PE, and PVC were accomplished by ultra-high performance liquid chromatography/mass spectrometry (UHPLC/MS). The UHPLC (Acquity UHPLC, Waters Corporation, Milford, MA, U.S.A.) was operated in the gradient mode and equipped with a C₁₈ UPLC analytical column (Acquity UPLC BEH C18, 1.7 μm particle diameter, 2.1 × 150 mm, Waters Corp. or equivalent). The UHPLC column temperature was maintained at 45°C and the mobile phase consisted of 100% water (A1) and 100% methanol (B1). The initial mobile phase composition was 95:5 A1/B1 at a flow rate of 250 μL/minute, held for 3 minutes. This was followed by a linear gradient to 30:70 A1/B1 over the next 12 minutes. The flow rate was then increased to 300 μL/minute, followed by a 5-minute linear solvent gradient to 100% methanol. The column was regenerated via a 3-minute linear gradient back to 95:5 A1/B1, followed by a 2 min hold at a flow rate of 250 μL/min. Analytes were subjected to atmospheric pressure photoionization (APPI), the dopant (acetone) was introduced at 150 μL/min by a liquid chromatography pump (LC-20AD, Shimadzu Corporation, Kyoto, Japan), and product ions detected on a triple quadrupole mass spectrometer (3200 QTrap, AB Sciex, Framingham, MA, U.S.A.) operated in the multiple reaction monitoring (MRM) mode. The following parameters were used: curtain gas 15 psi (N₂), probe temperature 300°C, nebulizer gas 55 psi (Zero air), auxiliary gas 40 psi (Zero air), interface heater on, collision gas medium (N₂), ion spray –850 V. TPP in the purified extracts was determined by UPLC-APPI-MS/MS, operated in the positive ion mode (ion spray 850 V). The analytical method has been validated previously for FRs

in complex environmental media (La Guardia et al., 2013). Phthalates in PVC were analyzed by GC/MS (Agilent 5975C MS coupled with a 7890A GC). Carrier gas was helium. The GC was equipped with a DB-5 column (Agilent Technologies: 60 m x 0.1 μm film thickness). Analytes were injected in the splitless mode and subjected to electron impact ionization mode at 70 eV. Ion mass-to-charges were obtained at unit resolution. Compound concentrations were calculated based on the area of selected ions (p-terphenyl m/z 230, DEHP m/z 149 and BDE166 m/z 484).

Of the polymers analyzed, as expected, PUF exhibited the most abundant and diverse additives. It contained both brominated and phosphate flame retardants (Table S1.15). These analytes were not detected in PE and PVC. Phthalate analysis was conducted only for PVC. One phthalate was found, di-ethylhexyl phthalate (DEHP), at a mean concentration of 8.61 mg g^{-1} . Neither phthalates nor flame retardant additives were detected in PE. As the analyses were highly targeted, the presence of other additives in the plastics cannot be excluded.

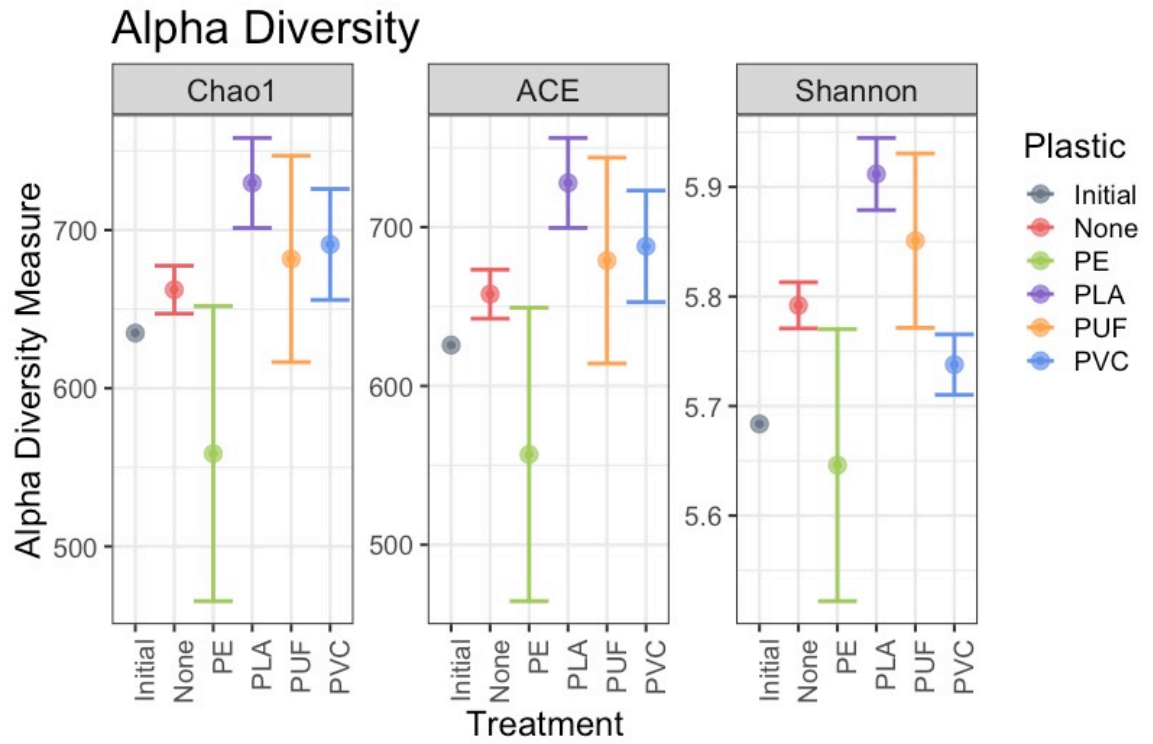


Fig. S1.1 Alpha diversity measures for three different diversity statistics, for the average of all 6 samples (3 replicates, 7 and 16 collection days) where error bars represent standard error, with the exception of the initial community, which is a single sample ($n = 1$).

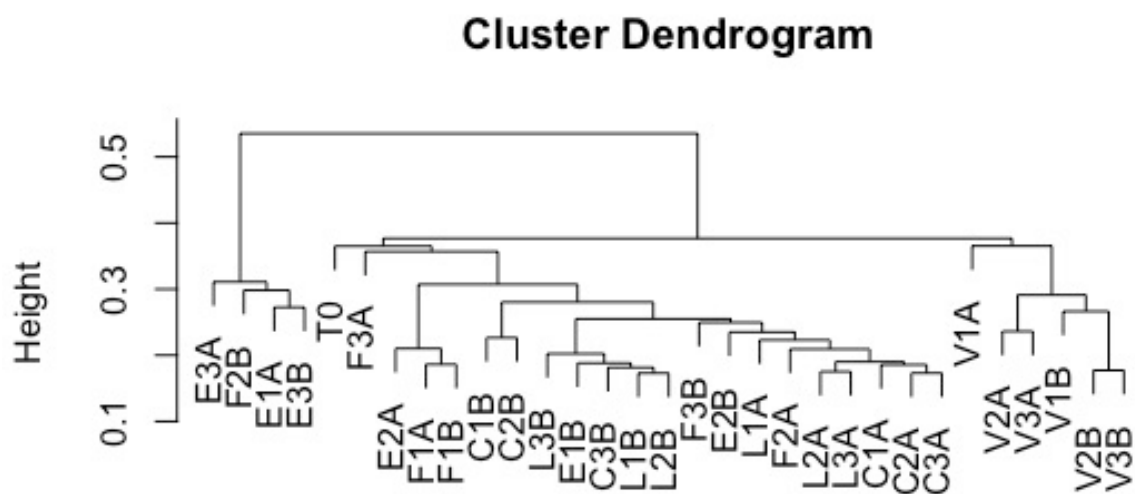


Fig. S1.2 Cluster dendrogram generated in phyloseq, illustrating the relatedness of different samples. Samples are named for polymer type (L = PLA, E = PE, F = PUF, V = PVC and C = Control), replicate (1, 2, or 3) and collection date (A = 7 and B = 16 days). T0 is the initial sample. All PVC samples are the most distinctly different lineage, on the right of the dendrogram.

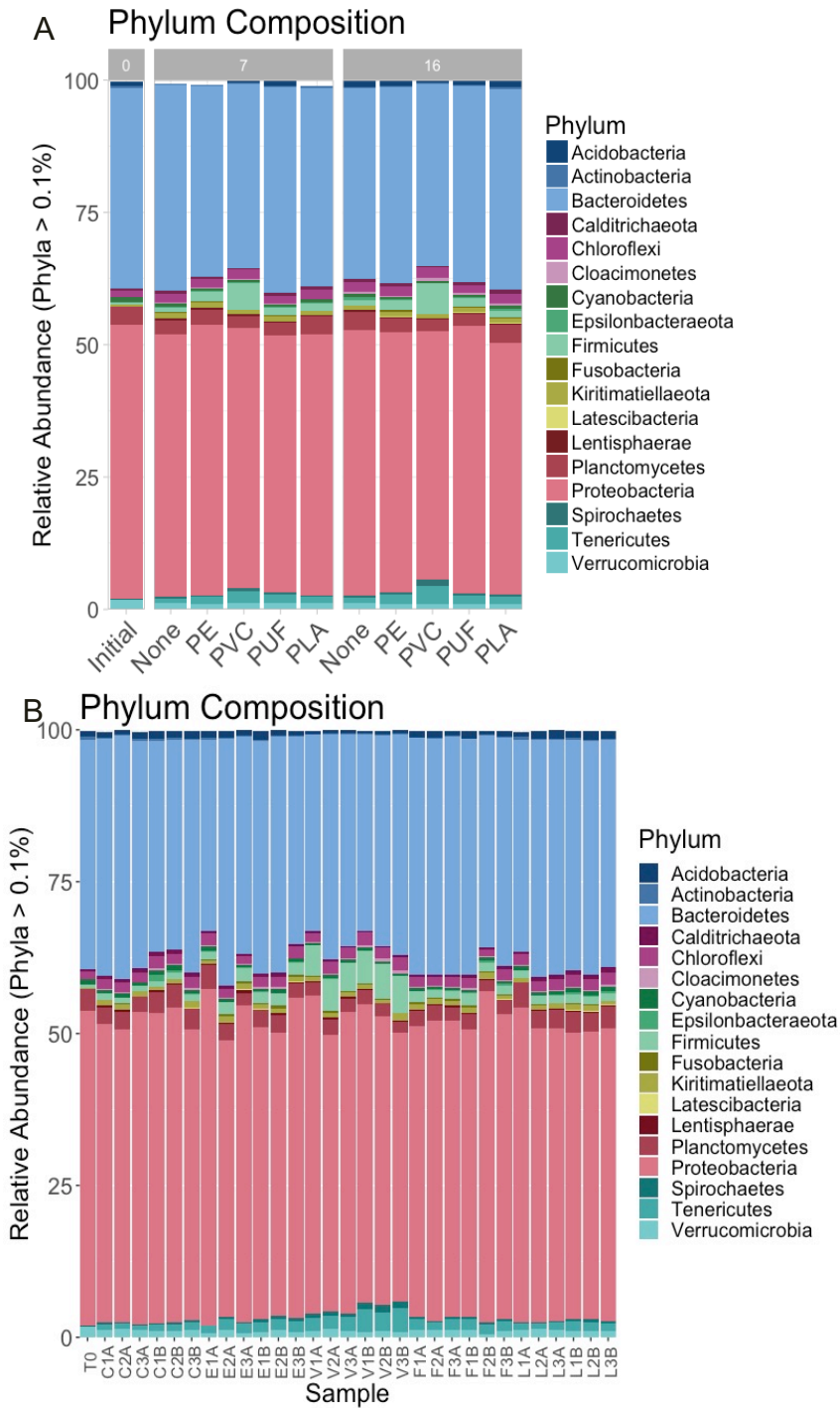


Fig. S1.3 Stacked bar plot showing relative abundance for all phyla present in samples at $>0.1\%$ relative abundance. In A, samples are averaged ($n = 3$) for each collection date, 7 days or 16 days, and the initial sample is on the left (0 days). For all individual samples (B), samples are named for polymer type (L = PLA, E = PE, F = PUF, V = PVC and C = Control), replicate (1, 2, or 3) and collection date (A = 7 and B = 16 days), and T0 is the initial sample.

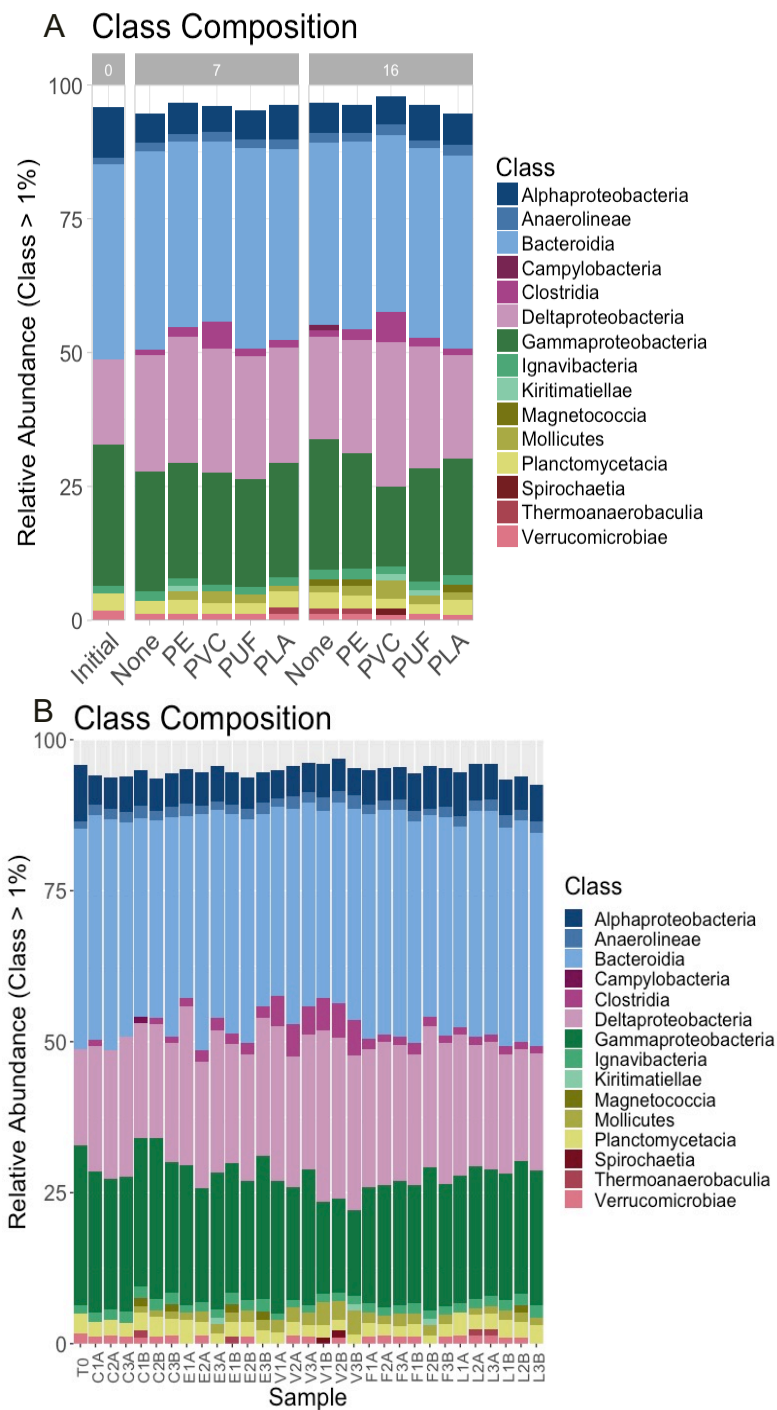


Fig. S1.4 Stacked bar plot showing relative abundance for all classes present in samples at >1% relative abundance. In A, samples are averaged ($n = 3$) for each collection date, 7 days or 16 days, and the initial sample is on the left (0 days). For all individual samples (B), samples are named for polymer type (L = PLA, E = PE, F = PUF, V = PVC and C = Control), replicate (1, 2, or 3) and collection date (A = 7 and B = 16 days), and T0 is the initial sample.

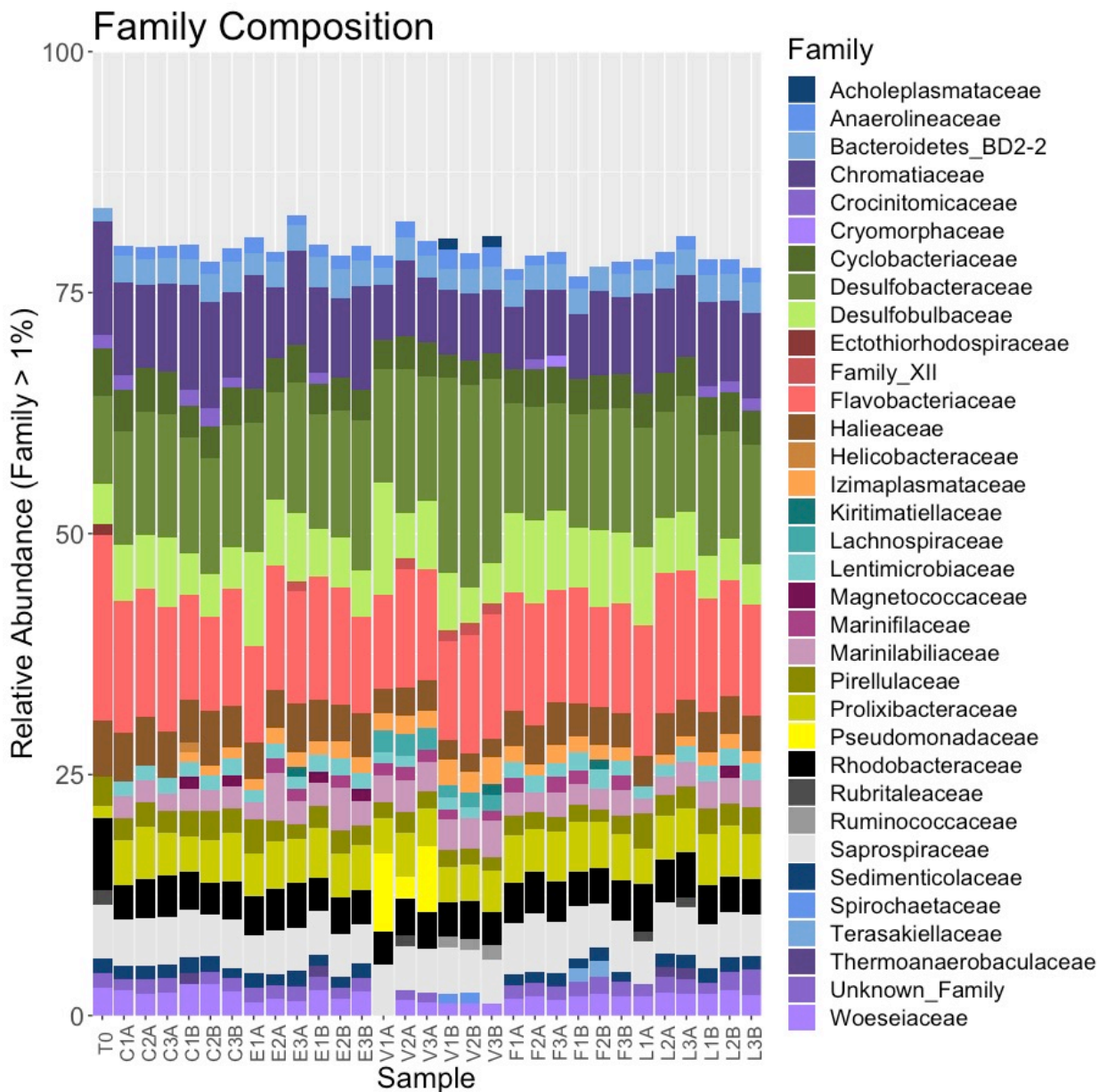


Fig. S1.5 Stacked bar plot showing relative abundance for all families present in samples at >1% relative abundance, corresponding to Fig. 3 in text. Samples are named for polymer type (L = PLA, E = PE, F = PUF, V = PVC and C = Control), replicate (1, 2, or 3) and collection date (A = 7 and B = 16 days), and T0 is the initial sample.

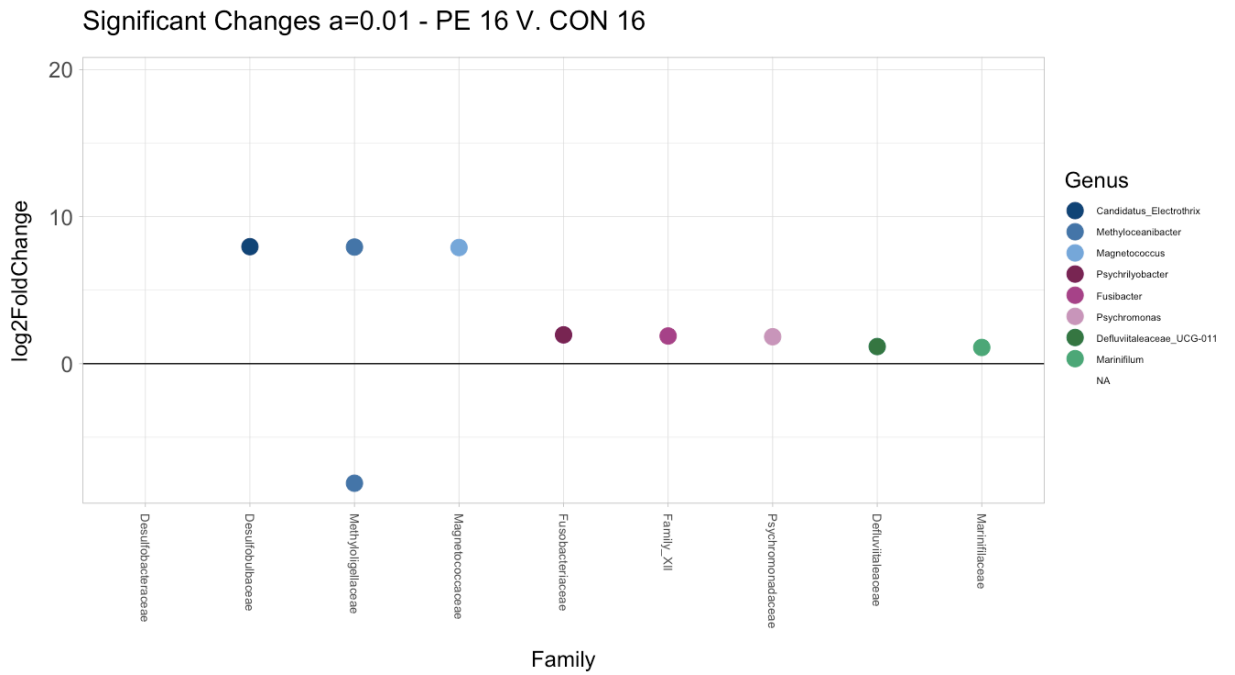


Fig. S1.6 DeSeq plot showing the log₂ fold change between PE and control treatment communities, organized by family with genus detailed by color. Points above the x-axis are higher in PE treatment, while those below are significantly higher in the control treatment ($\alpha = 0.01$).

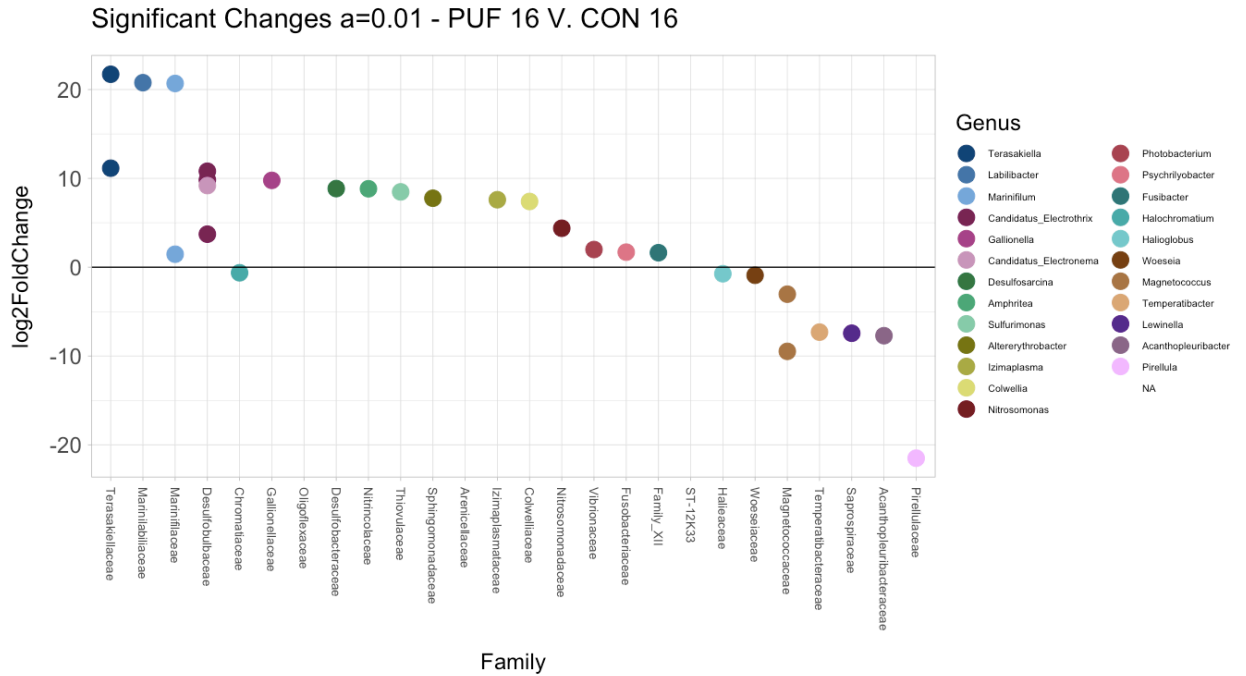


Fig. S1.7 DeSeq plot showing the log₂ fold change between PUF and control treatment communities, organized by family with genus detailed by color. Points above the x-axis are higher in PUF treatment, while those below are significantly higher in the control treatment ($\alpha = 0.01$).

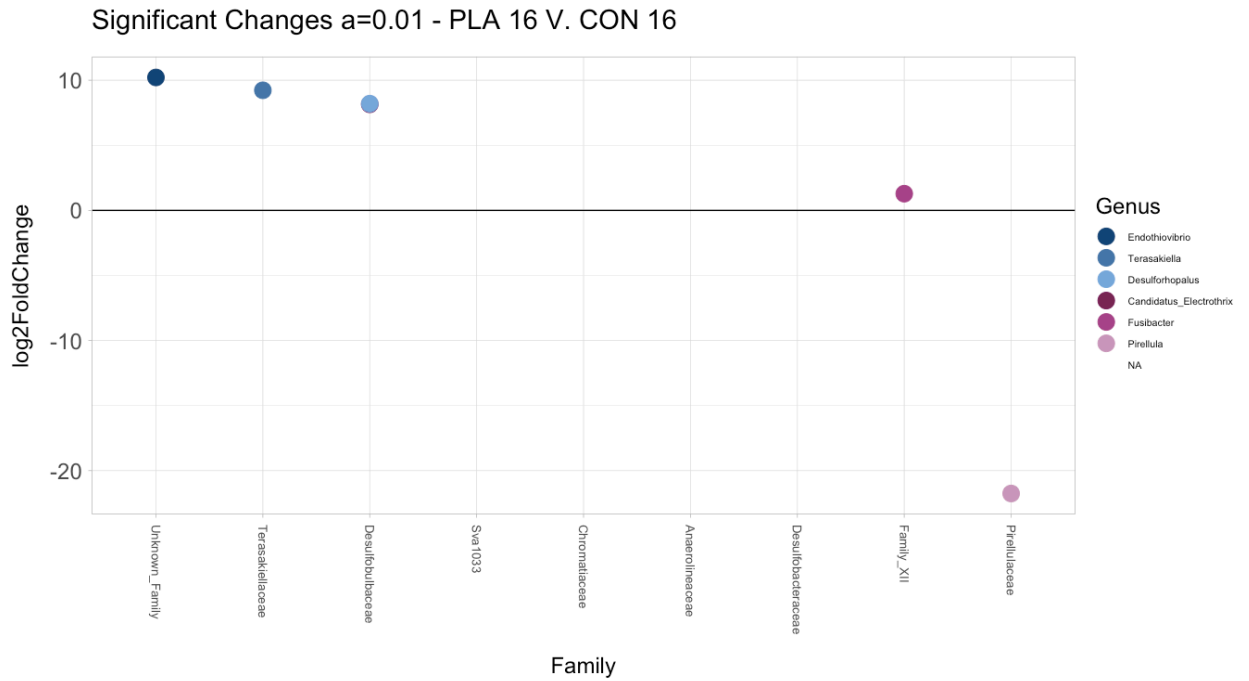


Fig. S1.8 DeSeq plot showing the log₂ fold change between PLA and control treatment communities, organized by family with genus detailed by color. Points above the x-axis are higher in PLA treatment, while those below are significantly higher in the control treatment ($\alpha = 0.01$).

Significant Changes $\alpha=0.01$ - PVC 16 V. CON 16

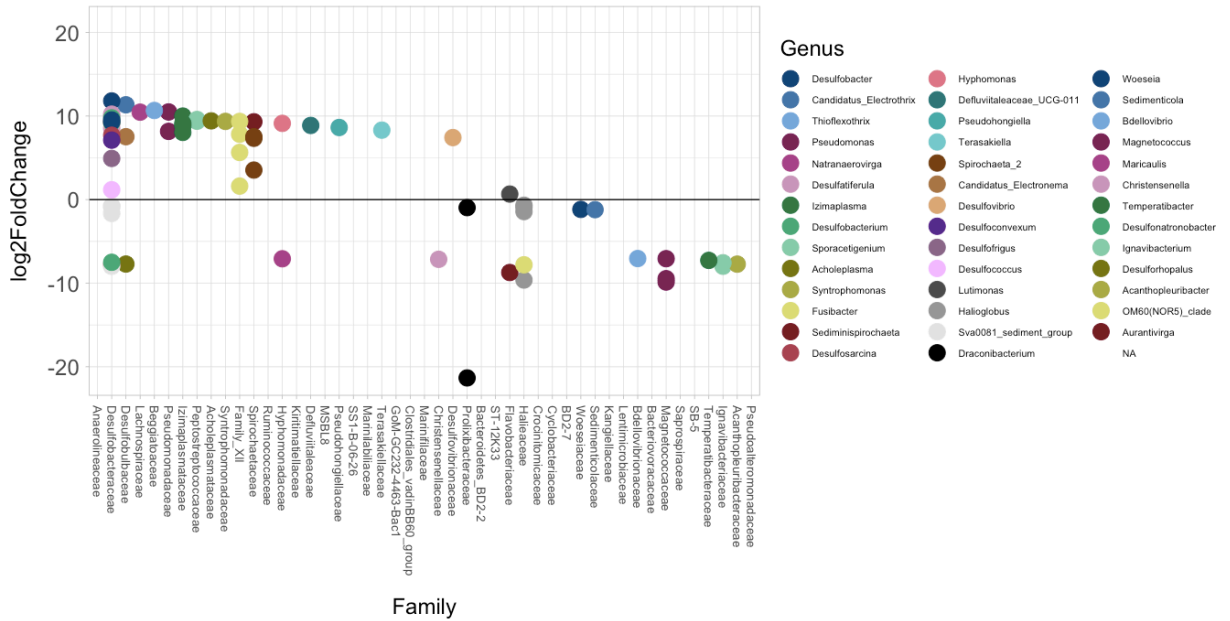


Fig. S1.9 DeSeq plot showing the log₂ fold change between PVC and control treatment communities, organized by family with genus detailed by color. Points above the x-axis are higher in PVC treatment, while those below are significantly higher in the control treatment ($\alpha = 0.01$).

Significant Changes $\alpha=0.01$ - PUF 16 V. PVC 16

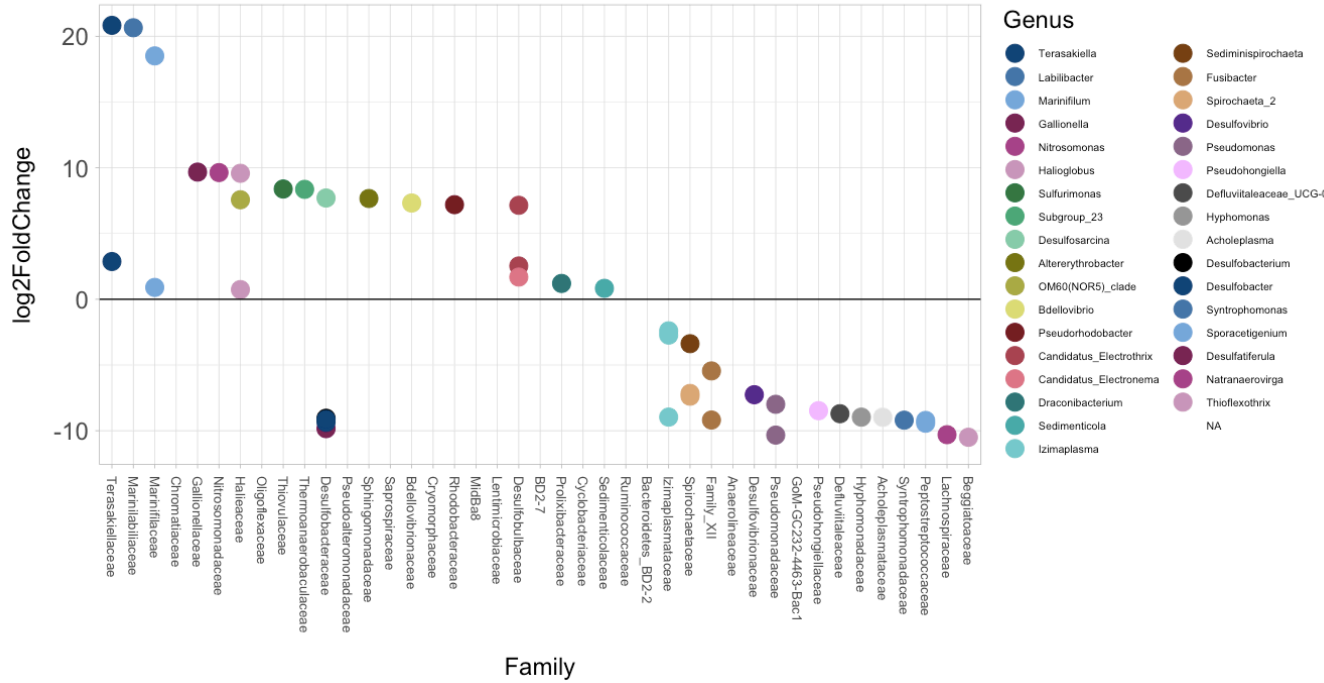


Fig. S1.11 DeSeq plot showing the log₂ fold change between PUF and PVC treatment communities, organized by family with genus detailed by color. Points above the x-axis are higher in PUF treatment, while those below are significantly higher in the PVC treatment ($\alpha = 0.01$).

Significant Changes $\alpha=0.01$ - PLA 16 V. PVC 16

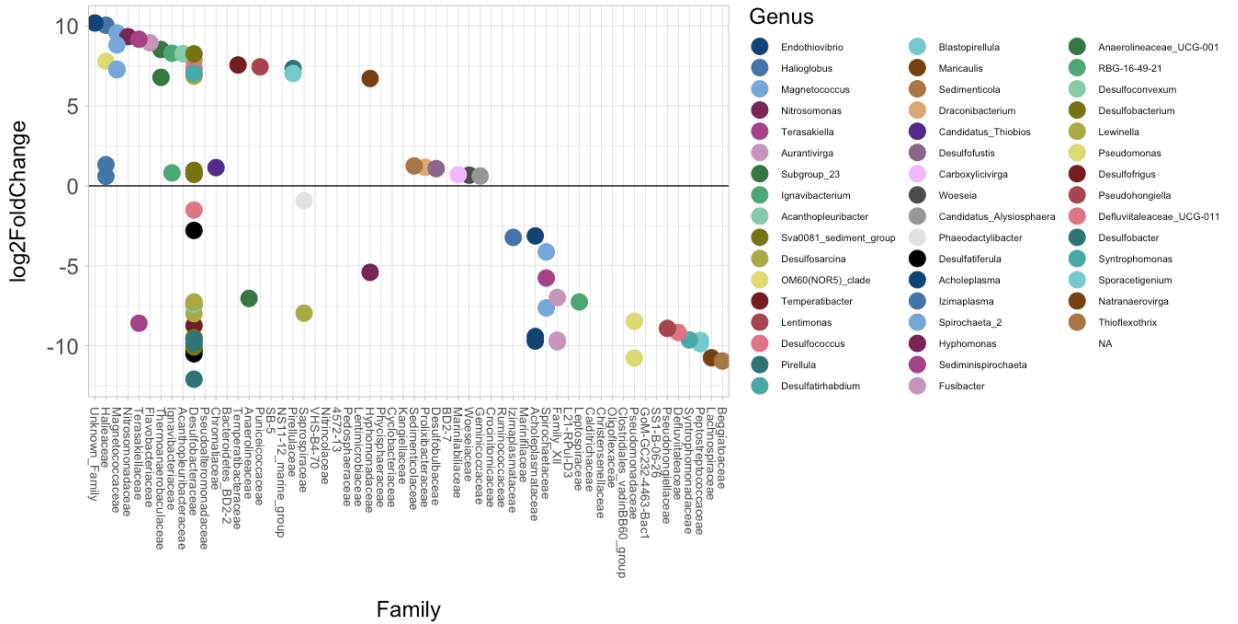


Fig. S1.12 DeSeq plot showing the log₂ fold change between PLA and PVC treatment communities, organized by family with genus detailed by color. Points above the x-axis are higher in PLA treatment, while those below are significantly higher in the PVC treatment ($\alpha = 0.01$).

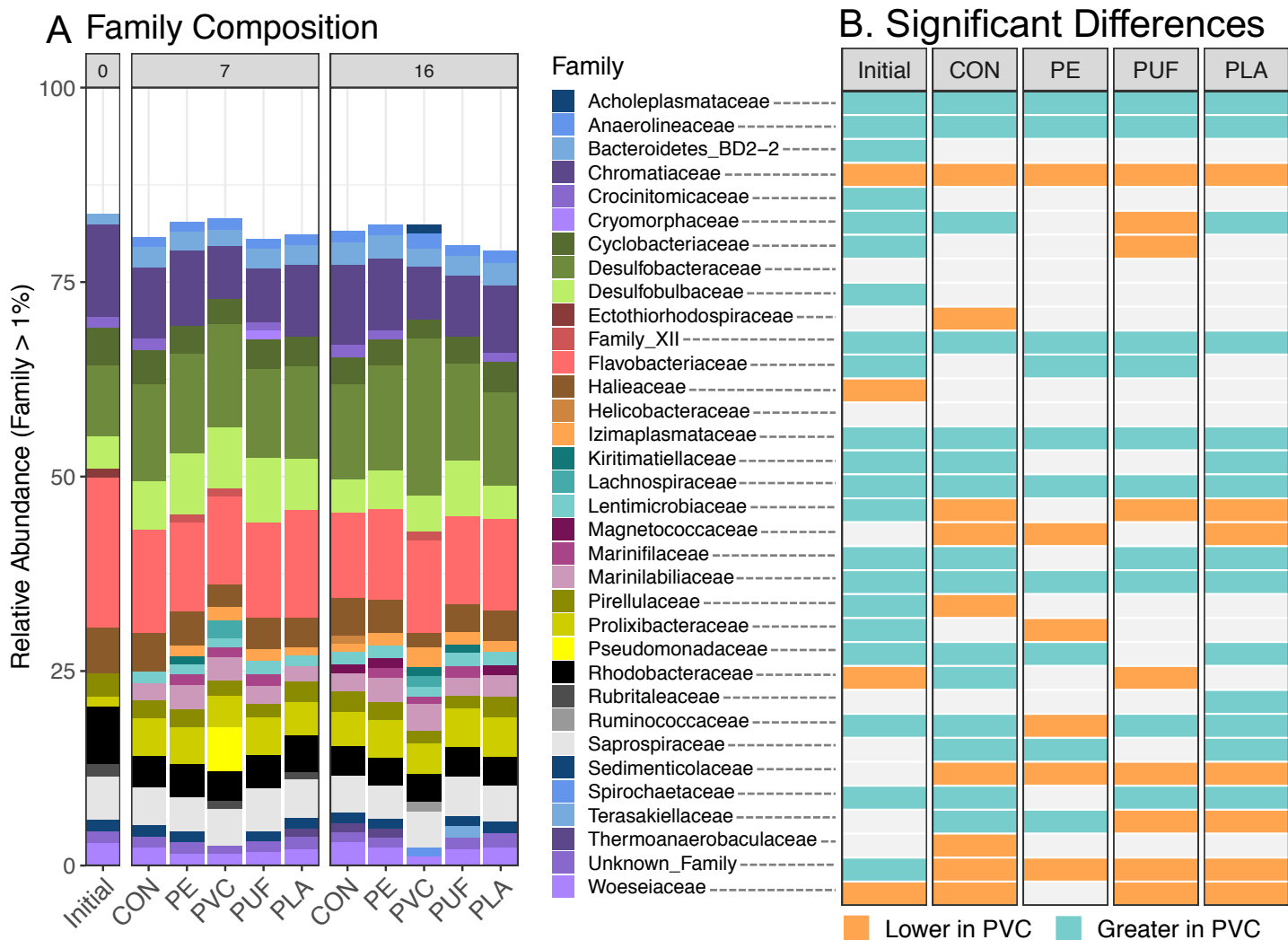


Fig. S1.13 A. Stacked bar plot of the relative abundance of families (greater than 1% abundance) for each plastic treatment (averaged for the three replicates) for each sediment collection date (0, 7 and 16 days). B. Families were determined to be significantly between PVC and other treatments (averaged across collection dates) using DeSeq ($\alpha = 0.01$). The left panel shows if each a family is significantly higher in PVC (blue) or the control (orange). In some cases there genera of one family were significantly higher in CON and some were significantly higher in the plastic treatment, in which case no color was assigned.

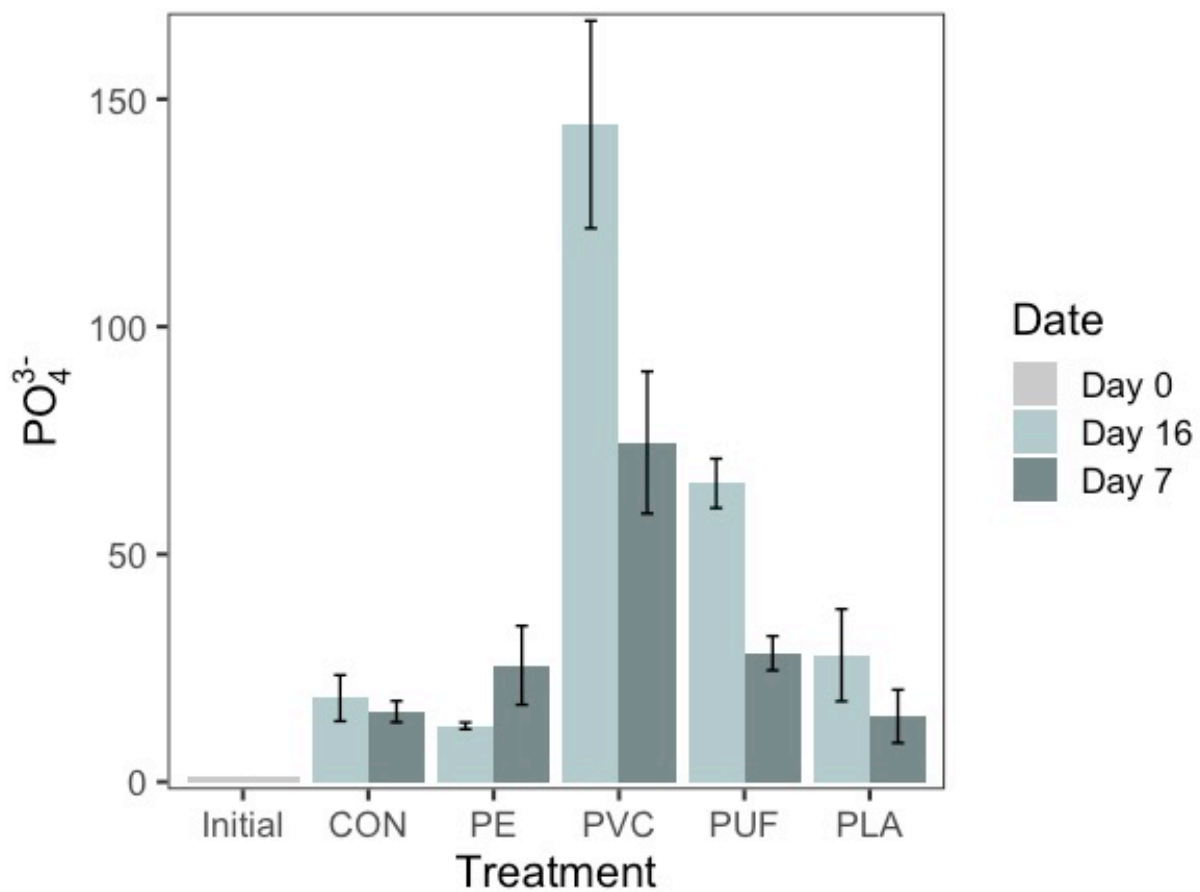


Fig. S1.14 Concentration (μM) of phosphate in the water initially and in all treatments after 7 and 16 days incubation ($n = 3$ per treatment). Error bars are standard error and CON is the control treatment.

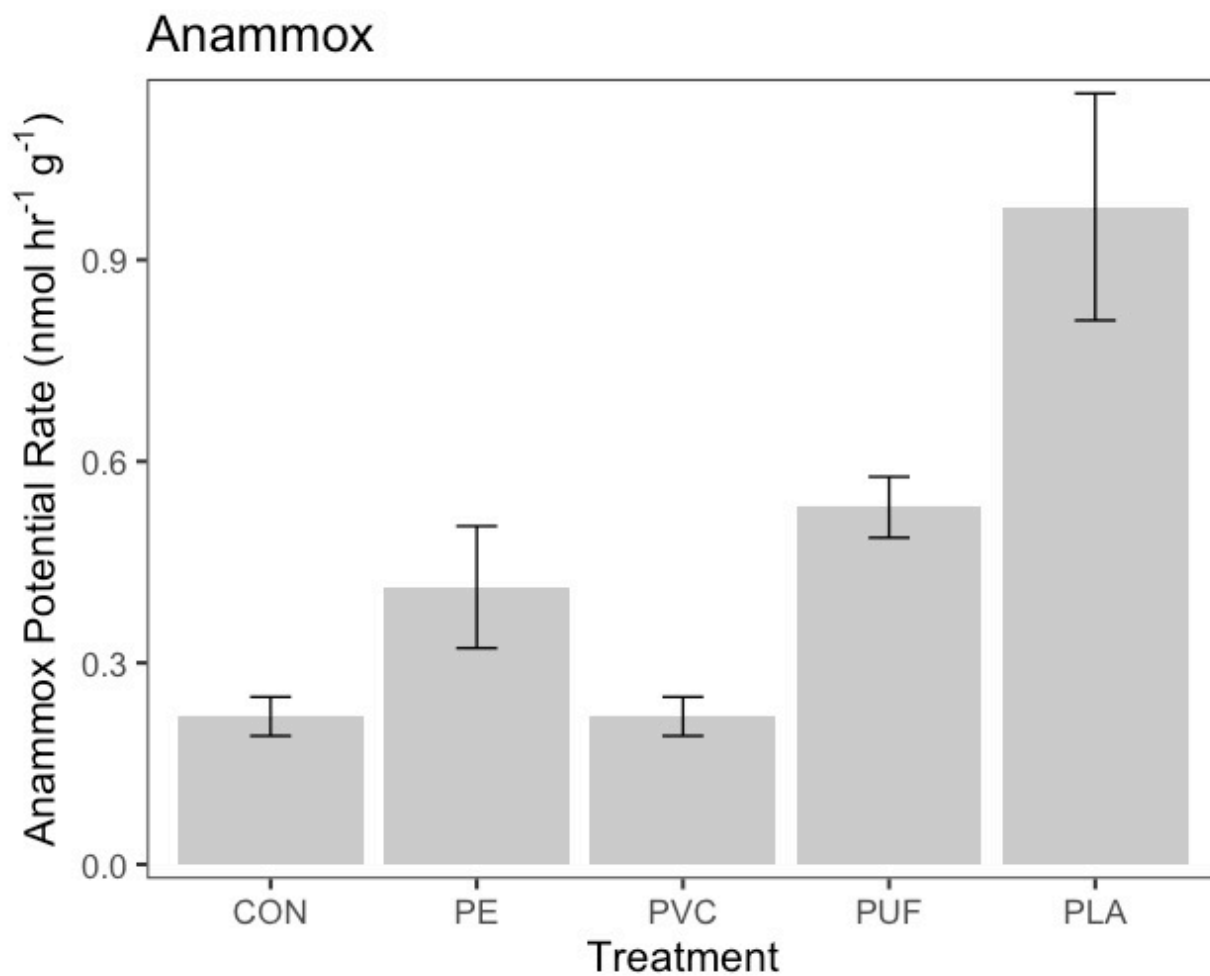


Fig. S1.15 Rates of anaerobic ammonium oxidation (Anammox), revealing highest anammox in the biopolymer, PLA and lowest anammox in PVC and the control (n=6 per treatment). Error bars are standard error and CON is the control treatment.

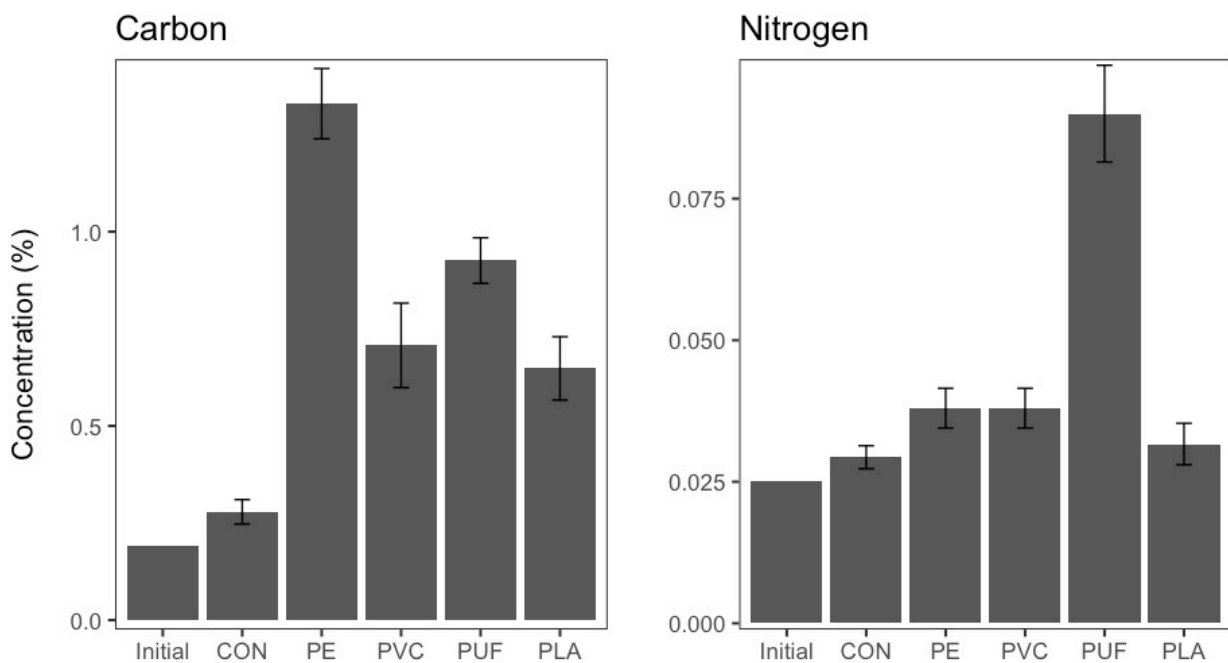


Fig. S1.16 The percent organic carbon and nitrogen present in the sediment at the end of the 16 day incubation (n = 3 for each treatment except initial, n = 1). Error bars are standard error and CON is the control treatment.

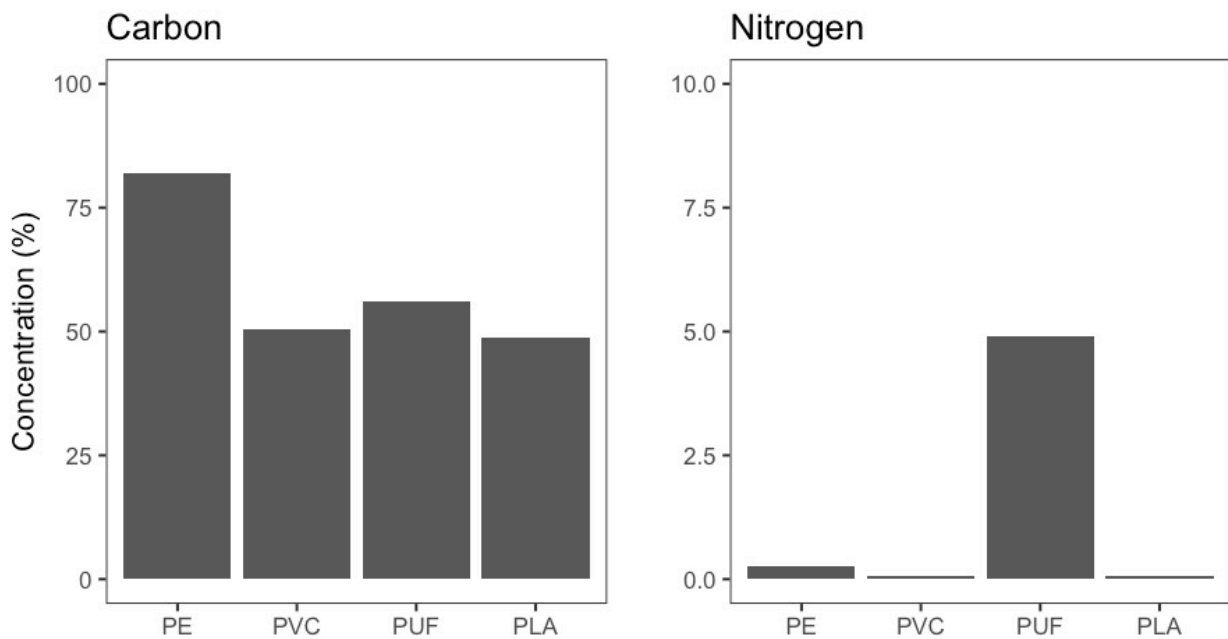


Fig. S1.17 The percent organic carbon and nitrogen present in the microplastics.

N Removal Efficiency

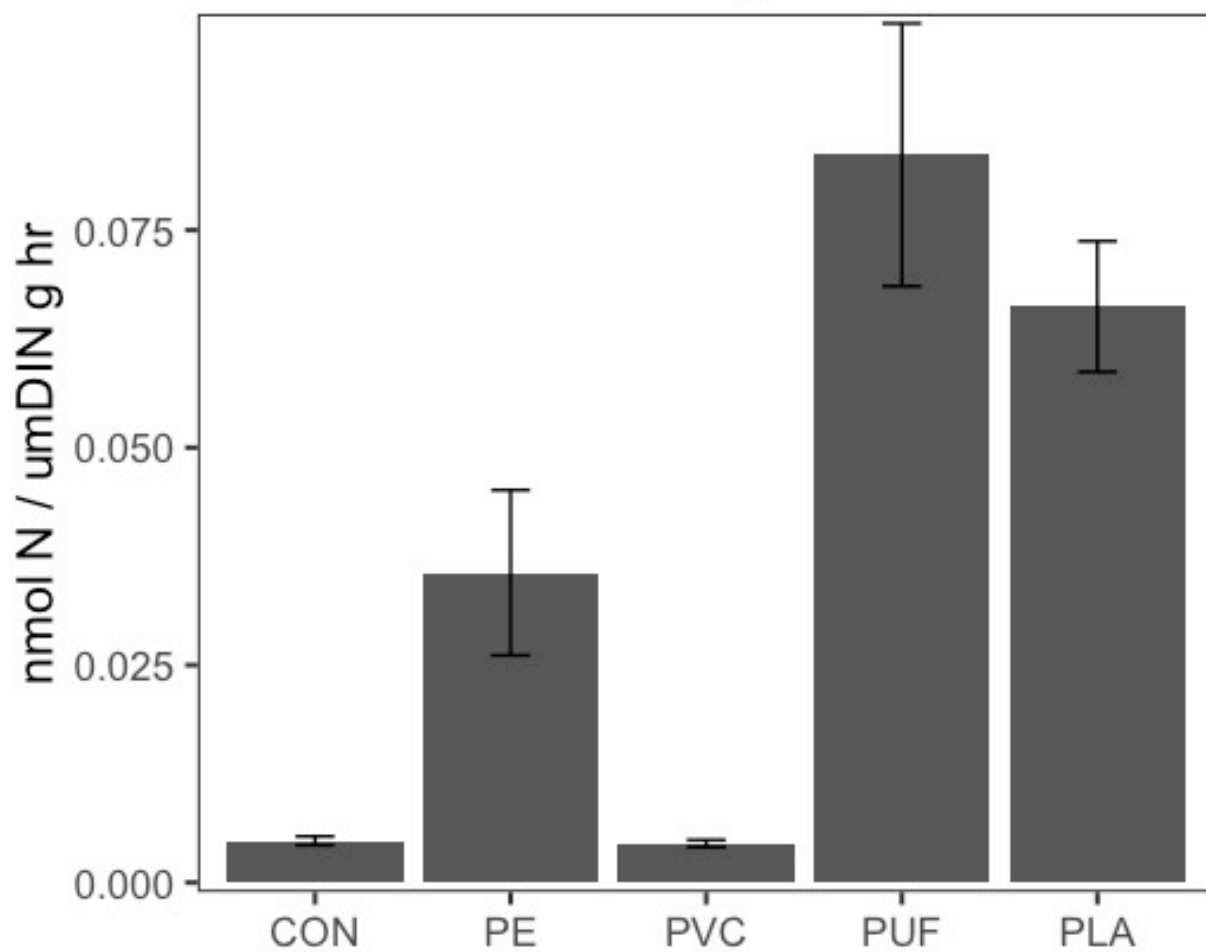


Fig. S1.18 The estimated N removal efficiency. Calculated as the sum of anammox and denitrification rates divided by the total DIN in the overlying water, following Semedo and Song (2020). Error bars represent standard error (n = 6 per treatment) and CON is the control treatment.

Supplementary tables

Table S1.1 Multivariate permutational ANOVA (PERMANOVA) evaluating community dissimilarity (Fig. 2).

TEST	Parameter	D.F.	Test Statistic	p-value
PERMANOVA	Plastic	5	4.034	0.001
	Day	1	3.323	0.001
	Plastic:Day	4	1.425	0.023
	Residuals	20		
	Total	30		

Table S1.2 NO₃⁻ in the overlying water column statistical analyses, including normality, homogeneity of variance, two-way ANOVA and post-hoc Tukey (Fig. 4).

TEST	Parameter	D.F.	Test Statistic	p-value
Normality (Shapiro -Wilks)			W = 0.68848	1.065E-06
Variance (Levene's)	Treatment	4	F = 2.976	3.869E-02
	Date	1	F = 17.099	2.922E-04
Two-way ANOVA	Treatment	4	F = 3.751	1.960E-02
	Date	1	F = 34.154	1.020E-05
	Treatment:Date	4	F = 3.733	2.000E-02
Post-hoc Tukey Test	PVC:Day 16-CON:Day 7			1.000E+00
	PUF:Day 7-CON:Day 7			1.000E+00
	PE:Day 7-CON:Day 7			1.000E+00
	PLA:Day 7-CON:Day 7			1.000E+00
	PVC:Day 7-CON:Day 7			1.000E+00
	CON:Day 16-CON:Day 7			8.917E-01
	PE:Day 16-CON:Day 7			9.520E-02
	PUF:Day 16-CON:Day 7			6.357E-02
	PLA:Day 16-CON:Day 7			2.025E-03
	PUF:Day 7-PVC:Day 16			1.000E+00
	PE:Day 7-PVC:Day 16			1.000E+00
	PLA:Day 7-PVC:Day 16			1.000E+00
	PVC:Day 7-PVC:Day 16			1.000E+00
	CON:Day 16-PVC:Day 16			8.961E-01
	PE:Day 16-PVC:Day 16			9.742E-02
	PUF:Day 16-PVC:Day 16			6.511E-02
	PLA:Day 16-PVC:Day 16			2.079E-03
	PE:Day 7-PUF:Day 7			1.000E+00
	PLA:Day 7-PUF:Day 7			1.000E+00
	PVC:Day 7-PUF:Day 7			1.000E+00
	CON:Day 16-PUF:Day 7			8.980E-01
	PE:Day 16-PUF:Day 7			9.842E-02
	PUF:Day 16-PUF:Day 7			6.581E-02
	PLA:Day 16-PUF:Day 7			2.103E-03
	PLA:Day 7-PE:Day 7			1.000E+00
	PVC:Day 7-PE:Day 7			1.000E+00
	CON:Day 16-PE:Day 7			8.988E-01
	PE:Day 16-PE:Day 7			9.882E-02
	PUF:Day 16-PE:Day 7			6.609E-02
	PLA:Day 16-PE:Day 7			2.113E-03
	PVC:Day 7-PLA:Day 7			1.000E+00
	CON:Day 16-PLA:Day 7			8.988E-01
	PE:Day 16-PLA:Day 7			9.883E-02
	PUF:Day 16-PLA:Day 7			6.610E-02
	PLA:Day 16-PLA:Day 7			2.113E-03
	CON:Day 16-PVC:Day 7			8.991E-01
	PE:Day 16-PVC:Day 7			9.899E-02
	PUF:Day 16-PVC:Day 7			6.621E-02
	PLA:Day 16-PVC:Day 7			2.117E-03
	PE:Day 16-CON:Day 16			7.550E-01
	PUF:Day 16-CON:Day 16			6.333E-01
	PLA:Day 16-CON:Day 16			4.693E-02
	PUF:Day 16-PE:Day 16			1.000E+00
	PLA:Day 16-PE:Day 16			7.166E-01
	PLA:Day 16-PUF:Day 16			8.273E-01

Table S1.3 NO₂⁻ in the overlying water column statistical analyses, including normality, homogeneity of variance, two-way ANOVA and post-hoc Tukey (Fig. 4).

TEST	Parameter	D.F.	Test Statistic	p-value
Normality (Shapiro -Wilks)			W = 0.70355	1.758E-06
Variance (Levene's)	Treatment	4	F = 10.707	3.394E-05
	Date	1	F = 30.118	7.320E-06
Two-way ANOVA	Treatment	4	F = 30.118	7.290E-06
	Date	1	F = 121.07	6.190E-10
	Treatment:Date	4	F = 15.05	7.900E-06
Post-hoc Tukey Test	PVC:Day 7-CON:Day 7			1
	PUF:Day 7-CON:Day 7			1
	PVC:Day 16-CON:Day 7			1
	PE:Day 7-CON:Day 7			1
	PLA:Day 7-CON:Day 7			1
	CON:Day 16-CON:Day 7			0.82954766
	PE:Day 16-CON:Day 7			3.12E-05
	PUF:Day 16-CON:Day 7			2.74E-05
	PLA:Day 16-CON:Day 7			7.08E-07
	PUF:Day 7-PVC:Day 7			1
	PVC:Day 16-PVC:Day 7			1
	PE:Day 7-PVC:Day 7			1
	PLA:Day 7-PVC:Day 7			1
	CON:Day 16-PVC:Day 7			0.82960955
	PE:Day 16-PVC:Day 7			3.12E-05
	PUF:Day 16-PVC:Day 7			2.74E-05
	PLA:Day 16-PVC:Day 7			7.09E-07
	PVC:Day 16-PUF:Day 7			1
	PE:Day 7-PUF:Day 7			1
	PLA:Day 7-PUF:Day 7			1
	CON:Day 16-PUF:Day 7			0.83045428
	PE:Day 16-PUF:Day 7			3.13E-05
	PUF:Day 16-PUF:Day 7			2.75E-05
	PLA:Day 16-PUF:Day 7			7.11E-07
	PE:Day 7-PVC:Day 16			1
	PLA:Day 7-PVC:Day 16			1
	CON:Day 16-PVC:Day 16			0.83083821
	PE:Day 16-PVC:Day 16			3.14E-05
	PUF:Day 16-PVC:Day 16			2.76E-05
	PLA:Day 16-PVC:Day 16			7.12E-07
	PLA:Day 7-PE:Day 7			1
	CON:Day 16-PE:Day 7			0.83496583
	PE:Day 16-PE:Day 7			3.19E-05
	PUF:Day 16-PE:Day 7			2.81E-05
	PLA:Day 16-PE:Day 7			7.23E-07
	CON:Day 16-PLA:Day 7			0.84556317
	PE:Day 16-PLA:Day 7			3.35E-05
	PUF:Day 16-PLA:Day 7			2.94E-05
	PLA:Day 16-PLA:Day 7			7.54E-07
	PE:Day 16-CON:Day 16			0.00093171
	PUF:Day 16-CON:Day 16			0.00081147
	PLA:Day 16-CON:Day 16			1.47E-05
	PUF:Day 16-PE:Day 16			1
	PLA:Day 16-PE:Day 16			0.61849747
	PLA:Day 16-PUF:Day 16			0.6571722

Table S1.4 NH₄⁺ in the overlying water column statistical analyses, including normality, homogeneity of variance, two-way ANOVA and post-hoc Tukey (Fig. 4).

TEST	Parameter	D.F.	Test Statistic	p-value
Normality (Shapiro -Wilks)			W = 0.89355	5.862E-03
Variance (Levene's)	Treatment	4	F = 7.0817	5.896E-04
	Date	1	F = 9.0058	5.604E-03
Two-way ANOVA	Treatment	4	F = 24.201	2.010E-07
	Date	1	F = 2.824	1.080E-01
	Treatment:Date	4	F = 45.382	9.270E-10
Post-hoc Tukey Test	PLA:Day 16-PUF:Day 16			1.000E+00
	PE:Day 16-PUF:Day 16			5.185E-01
	PVC:Day 7-PUF:Day 16			4.868E-01
	CON:Day 7-PUF:Day 16			1.267E-02
	PLA:Day 7-PUF:Day 16			9.757E-03
	PUF:Day 7-PUF:Day 16			2.671E-03
	PE:Day 7-PUF:Day 16			8.431E-04
	CON:Day 16-PUF:Day 16			4.356E-08
	PVC:Day 16-PUF:Day 16			7.452E-09
	PE:Day 16-PLA:Day 16			6.784E-01
	PVC:Day 7-PLA:Day 16			6.463E-01
	CON:Day 7-PLA:Day 16			2.221E-02
	PLA:Day 7-PLA:Day 16			1.718E-02
	PUF:Day 7-PLA:Day 16			4.748E-03
	PE:Day 7-PLA:Day 16			1.495E-03
	CON:Day 16-PLA:Day 16			6.657E-08
	PVC:Day 16-PLA:Day 16			1.106E-08
	PVC:Day 7-PE:Day 16			1.000E+00
	CON:Day 7-PE:Day 16			5.796E-01
	PLA:Day 7-PE:Day 16			5.063E-01
	PUF:Day 7-PE:Day 16			2.153E-01
	PE:Day 7-PE:Day 16			8.261E-02
	CON:Day 16-PE:Day 16			1.756E-06
	PVC:Day 16-PE:Day 16			2.299E-07
	CON:Day 7-PVC:Day 7			6.122E-01
	PLA:Day 7-PVC:Day 7			5.384E-01
	PUF:Day 7-PVC:Day 7			2.351E-01
	PE:Day 7-PVC:Day 7			9.155E-02
	CON:Day 16-PVC:Day 7			1.938E-06
	PVC:Day 16-PVC:Day 7			2.519E-07
	PLA:Day 7-CON:Day 7			1.000E+00
	PUF:Day 7-CON:Day 7			9.991E-01
	PE:Day 7-CON:Day 7			9.558E-01
	CON:Day 16-CON:Day 7			9.952E-05
	PVC:Day 16-CON:Day 7			9.821E-06
	PUF:Day 7-PLA:Day 7			9.998E-01
	PE:Day 7-PLA:Day 7			9.764E-01
	CON:Day 16-PLA:Day 7			1.282E-04
	PVC:Day 16-PLA:Day 7			1.245E-05
	PE:Day 7-PUF:Day 7			9.999E-01
	CON:Day 16-PUF:Day 7			4.539E-04
	PVC:Day 16-PUF:Day 7			4.100E-05
	CON:Day 16-PE:Day 7			1.428E-03
	PVC:Day 16-PE:Day 7			1.224E-04
	PVC:Day 16-CON:Day 16			9.733E-01

Table S1.5 PO₄²⁻ in the overlying water statistical analyses, including normality, homogeneity of variance, two-way ANOVA and post-hoc Tukey.

TEST	Parameter	D.F.	Test Statistic	p-value
Normality (Shapiro -Wilks)			W = 0.76875	1.434E-05
Variance (Levene's)	Treatment	5	F = 3.2391	2.168E-02
	Date	2	F = 1.7081	1.996E-01
Two-way ANOVA	Treatment	4	F = 3.2391	6.670E-08
	Date	1	F = 11.588	2.810E-03
	Treatment:Date	4	F = 5.006	5.830E-03
Post-hoc Tukey Test	PE:Day 16-Initial:Day 0			1.000E+00
	PLA:Day 7-Initial:Day 0			1.000E+00
	CON:Day 7-Initial:Day 0			1.000E+00
	CON:Day 16-Initial:Day 0			1.000E+00
	PE:Day 7-Initial:Day 0			9.979E-01
	PLA:Day 16-Initial:Day 0			9.947E-01
	PUF:Day 7-Initial:Day 0			9.938E-01
	PUF:Day 16-Initial:Day 0			2.243E-01
	PVC:Day 7-Initial:Day 0			1.039E-01
	PVC:Day 16-Initial:Day 0			9.138E-05
	PLA:Day 7-PE:Day 16			1.000E+00
	CON:Day 7-PE:Day 16			1.000E+00
	CON:Day 16-PE:Day 16			1.000E+00
	PE:Day 7-PE:Day 16			9.999E-01
	PLA:Day 16-PE:Day 16			9.994E-01
	PUF:Day 7-PE:Day 16			9.992E-01
	PUF:Day 16-PE:Day 16			8.802E-02
	PVC:Day 7-PE:Day 16			2.572E-02
	PVC:Day 16-PE:Day 16			1.685E-06
	CON:Day 7-PLA:Day 7			1.000E+00
	CON:Day 16-PLA:Day 7			1.000E+00
	PE:Day 7-PLA:Day 7			1.000E+00
	PLA:Day 16-PLA:Day 7			9.999E-01
	PUF:Day 7-PLA:Day 7			9.999E-01
	PUF:Day 16-PLA:Day 7			1.151E-01
	PVC:Day 7-PLA:Day 7			3.450E-02
	PVC:Day 16-PLA:Day 7			2.173E-06
	CON:Day 16-CON:Day 7			1.000E+00
	PE:Day 7-CON:Day 7			1.000E+00
	PLA:Day 16-CON:Day 7			1.000E+00
	PUF:Day 7-CON:Day 7			9.999E-01
	PUF:Day 16-CON:Day 7			1.309E-01
	PVC:Day 7-CON:Day 7			3.981E-02
	PVC:Day 16-CON:Day 7			2.464E-06
	PE:Day 7-CON:Day 16			1.000E+00
	PLA:Day 16-CON:Day 16			1.000E+00
	PUF:Day 7-CON:Day 16			1.000E+00
	PUF:Day 16-CON:Day 16			1.878E-01
	PVC:Day 7-CON:Day 16			5.993E-02
	PVC:Day 16-CON:Day 16			3.566E-06
	PLA:Day 16-PE:Day 7			1.000E+00
	PUF:Day 7-PE:Day 7			1.000E+00
	PUF:Day 16-PE:Day 7			4.025E-01
	PVC:Day 7-PE:Day 7			1.519E-01
	PVC:Day 16-PE:Day 7			8.884E-06
	PUF:Day 7-PLA:Day 16			1.000E+00
	PUF:Day 16-PLA:Day 16			4.898E-01
	PVC:Day 7-PLA:Day 16			1.980E-01
	PVC:Day 16-PLA:Day 16			1.185E-05
	PUF:Day 16-PUF:Day 7			5.079E-01
	PVC:Day 7-PUF:Day 7			2.083E-01
	PVC:Day 16-PUF:Day 7			1.255E-05
	PVC:Day 7-PUF:Day 16			1.000E+00
	PVC:Day 16-PUF:Day 16			2.304E-03
	PVC:Day 16-PVC:Day 7			8.568E-03

Table S1.6 *AmoA* gene ratio statistical analyses, including normality, homogeneity of variance, two-way ANOVA and post-hoc Tukey (Fig. 5).

TEST	Parameter	D.F.	Test Statistic	p-value
Normality (Shapiro -Wilks)			W = 0.73437	3.895E-06
Variance (Levene's)	Treatment	5	F = 4.51541	6.957E-03
	Date	2	F = 4.7398	1.687E-02
Two-way ANOVA	Treatment	5	F = 3.629	1.690E-02
	Date	1	F = 31.606	1.670E-05
	Treatment:Date	4	F = 6.554	5.140E-03
Post-hoc Tukey Test	CON:Day 16-Initial:Day 0			1
	PE:Day 16-Initial:Day 0			0.99997538
	PLA:Day 16-Initial:Day 0			0.62064767
	PUF:Day 16-Initial:Day 0			0.05606539
	PVC:Day 16-Initial:Day 0			1
	CON:Day 7-Initial:Day 0			1
	PE:Day 7-Initial:Day 0			1
	PLA:Day 7-Initial:Day 0			1
	PUF:Day 7-Initial:Day 0			0.9999994
	PVC:Day 7-Initial:Day 0			1
	PE:Day 16-CON:Day 16			0.999969
	PLA:Day 16-CON:Day 16			0.26392176
	PUF:Day 16-CON:Day 16			0.003866
	PVC:Day 16-CON:Day 16			1
	CON:Day 7-CON:Day 16			0.99999998
	PE:Day 7-CON:Day 16			0.9999994
	PLA:Day 7-CON:Day 16			0.99999933
	PUF:Day 7-CON:Day 16			0.99684812
	PVC:Day 7-CON:Day 16			0.99999675
	PLA:Day 16-PE:Day 16			0.73560763
	PUF:Day 16-PE:Day 16			0.02319693
	PVC:Day 16-PE:Day 16			0.9986454
	CON:Day 7-PE:Day 16			0.99176446
	PE:Day 7-PE:Day 16			0.98084004
	PLA:Day 7-PE:Day 16			0.98031038
	PUF:Day 7-PE:Day 16			0.79183531
	PVC:Day 7-PE:Day 16			0.9701644
	PUF:Day 16-PLA:Day 16			0.76362948
	PVC:Day 16-PLA:Day 16			0.15988391
	CON:Day 7-PLA:Day 16			0.10860366
	PE:Day 7-PLA:Day 16			0.08518213
	PLA:Day 7-PLA:Day 16			0.08443817
	PUF:Day 7-PLA:Day 16			0.02585948
	PVC:Day 7-PLA:Day 16			0.07322598
	PVC:Day 16-PUF:Day 16			0.00204044
	CON:Day 7-PUF:Day 16			0.00129624
	PE:Day 7-PUF:Day 16			0.00098689
	PLA:Day 7-PUF:Day 16			0.00097737
	PUF:Day 7-PUF:Day 16			0.00028324
	PVC:Day 7-PUF:Day 16			0.00083604
	CON:Day 7-PVC:Day 16			1

PE:Day 7-PVC:Day 16	1
PLA:Day 7-PVC:Day 16	1
PUF:Day 7-PVC:Day 16	0.99988027
PVC:Day 7-PVC:Day 16	1
PE:Day 7-CON:Day 7	1
PLA:Day 7-CON:Day 7	1
PUF:Day 7-CON:Day 7	0.99999643
PVC:Day 7-CON:Day 7	1
PLA:Day 7-PE:Day 7	1
PUF:Day 7-PE:Day 7	0.9999998
PVC:Day 7-PE:Day 7	1
PUF:Day 7-PLA:Day 7	0.99999982
PVC:Day 7-PLA:Day 7	1
PVC:Day 7-PUF:Day 7	0.99999998

Table S1.7 *NirS* gene ratio statistical analyses, including normality, homogeneity of variance, two-way ANOVA and post-hoc Tukey (Fig. 5).

TEST	Parameter	D.F.	Test Statistic	p-value
Normality (Shapiro -Wilks)			W = 0.97742	7.378E-01
Variance (Levene's)	Treatment	5	F = 0.3826	8.559E-01
	Date	2	F = 0.7885	4.644E-01
Two-way ANOVA	Treatment	5	F = 11.090	3.210E-05
	Date	1	F = 0.00	9.830E-01
	Treatment:Date	4	F = 0.221	9.240E-01
Post-hoc Tukey Test	CON:Day 16-Initial:Day 0			0.15978649
	PE:Day 16-Initial:Day 0			0.13621516
	PLA:Day 16-Initial:Day 0			0.60548759
	PUF:Day 16-Initial:Day 0			0.27450127
	PVC:Day 16-Initial:Day 0			0.00197416
	CON:Day 7-Initial:Day 0			0.19822851
	PE:Day 7-Initial:Day 0			0.17175571
	PLA:Day 7-Initial:Day 0			0.63960867
	PUF:Day 7-Initial:Day 0			0.09923979
	PVC:Day 7-Initial:Day 0			0.00329898
	PE:Day 16-CON:Day 16			1
	PLA:Day 16-CON:Day 16			0.99407658
	PUF:Day 16-CON:Day 16			1
	PVC:Day 16-CON:Day 16			0.25979486
	CON:Day 7-CON:Day 16			1
	PE:Day 7-CON:Day 16			1
	PLA:Day 7-CON:Day 16			0.98953241
	PUF:Day 7-CON:Day 16			1
	PVC:Day 7-CON:Day 16			0.42641165
	PLA:Day 16-PE:Day 16			0.98561727
	PUF:Day 16-PE:Day 16			0.99999984
	PVC:Day 16-PE:Day 16			0.31568153
	CON:Day 7-PE:Day 16			1
	PE:Day 7-PE:Day 16			1
	PLA:Day 7-PE:Day 16			0.97690569
	PUF:Day 7-PE:Day 16			1
	PVC:Day 7-PE:Day 16			0.49983989
	PUF:Day 16-PLA:Day 16			0.99996424
	PVC:Day 16-PLA:Day 16			0.02156645
	CON:Day 7-PLA:Day 16			0.99874386
	PE:Day 7-PLA:Day 16			0.99629147
	PLA:Day 7-PLA:Day 16			1
	PUF:Day 7-PLA:Day 16			0.94685847
	PVC:Day 7-PLA:Day 16			0.04335775
	PVC:Day 16-PUF:Day 16			0.11769376
	CON:Day 7-PUF:Day 16			1
	PE:Day 7-PUF:Day 16			1
	PLA:Day 7-PUF:Day 16			0.99988658
	PUF:Day 7-PUF:Day 16			0.99997677
	PVC:Day 7-PUF:Day 16			0.21411114
	CON:Day 7-PVC:Day 16			0.1943747
	PE:Day 7-PVC:Day 16			0.23655964
	PLA:Day 7-PVC:Day 16			0.01830798
	PUF:Day 7-PVC:Day 16			0.44275699

PVC:Day 7-PVC:Day 16	1
PE:Day 7-CON:Day 7	1
PLA:Day 7-CON:Day 7	0.99736714
PUF:Day 7-CON:Day 7	0.99999995
PVC:Day 7-CON:Day 7	0.33356447
PLA:Day 7-PE:Day 7	0.99310322
PUF:Day 7-PE:Day 7	1
PVC:Day 7-PE:Day 7	0.39431841
PUF:Day 7-PLA:Day 7	0.92580896
PVC:Day 7-PLA:Day 7	0.03698552
PVC:Day 7-PUF:Day 7	0.64828302

Table S1.8 *NirK* gene ratio statistical analyses, including normality, homogeneity of variance, two-way ANOVA and post-hoc Tukey (Fig. 5).

TEST	Parameter	D.F.	Test Statistic	p-value
Normality (Shapiro -Wilks)			W = 0.95951	2.832E-01
Variance (Levene's)	Treatment	5	F = 0.6653	6.532E-01
	Date	2	F = 0.5913	5.603E-01
Two-way ANOVA	Treatment	5	F = 1.145	3.700E-01
	Date	1	F = 2.220	1.520E-01
	Treatment:Date	4	F = 0.714	5.920E-01
Post-hoc Tukey Test	CON:Day 16-Initial:Day 0			0.99971571
	PE:Day 16-Initial:Day 0			1
	PLA:Day 16-Initial:Day 0			1
	PUF:Day 16-Initial:Day 0			1
	PVC:Day 16-Initial:Day 0			1
	CON:Day 7-Initial:Day 0			1
	PE:Day 7-Initial:Day 0			1
	PLA:Day 7-Initial:Day 0			1
	PUF:Day 7-Initial:Day 0			0.99997371
	PVC:Day 7-Initial:Day 0			0.99999834
	PE:Day 16-CON:Day 16			0.99920121
	PLA:Day 16-CON:Day 16			0.93859937
	PUF:Day 16-CON:Day 16			0.98786255
	PVC:Day 16-CON:Day 16			0.99997477
	CON:Day 7-CON:Day 16			0.9661984
	PE:Day 7-CON:Day 16			0.80388544
	PLA:Day 7-CON:Day 16			0.94963838
	PUF:Day 7-CON:Day 16			0.48347567
	PVC:Day 7-CON:Day 16			1
	PLA:Day 16-PE:Day 16			0.99999961
	PUF:Day 16-PE:Day 16			1
	PVC:Day 16-PE:Day 16			1
	CON:Day 7-PE:Day 16			0.99999999
	PE:Day 7-PE:Day 16			0.99982564
	PLA:Day 7-PE:Day 16			0.99999987
	PUF:Day 7-PE:Day 16			0.97834607
	PVC:Day 7-PE:Day 16			0.99999933
	PUF:Day 16-PLA:Day 16			1
	PVC:Day 16-PLA:Day 16			0.9999452
	CON:Day 7-PLA:Day 16			1
	PE:Day 7-PLA:Day 16			1
	PLA:Day 7-PLA:Day 16			1
	PUF:Day 7-PLA:Day 16			0.99994282
	PVC:Day 7-PLA:Day 16			0.99590878
	PVC:Day 16-PUF:Day 16			0.99999986
	CON:Day 7-PUF:Day 16			1
	PE:Day 7-PUF:Day 16			0.99999934
	PLA:Day 7-PUF:Day 16			1
	PUF:Day 7-PUF:Day 16			0.99797473
	PVC:Day 7-PUF:Day 16			0.99982422
	CON:Day 7-PVC:Day 16			0.99999342
	PE:Day 7-PVC:Day 16			0.99712222
	PLA:Day 7-PVC:Day 16			0.99997267
	PUF:Day 7-PVC:Day 16			0.92372424

PVC:Day 7-PVC:Day 16	1
PE:Day 7-CON:Day 7	0.99999999
PLA:Day 7-CON:Day 7	1
PUF:Day 7-CON:Day 7	0.99968455
PVC:Day 7-CON:Day 7	0.99870355
PLA:Day 7-PE:Day 7	1
PUF:Day 7-PE:Day 7	0.99999995
PVC:Day 7-PE:Day 7	0.96227042
PUF:Day 7-PLA:Day 7	0.99989127
PVC:Day 7-PLA:Day 7	0.99720391
PVC:Day 7-PUF:Day 7	0.7534891

Table S1.9 Potential denitrification rate statistical analyses, including normality, homogeneity of variance, one-way ANOVA and post-hoc Tukey (Fig. 6).

TEST	Parameter	D.F.	Test Statistic	p-value
Normality (Shapiro -Wilks)			W = 0.93972	8.940E-02
Variance (Levene's)	Treatment	4	F = 0.8949	4.817E-01
One-way ANOVA	Treatment	4	F = 16.35	1.060E-06
Post-hoc Tukey Test	PVC-CON			1.000E+00
	PE-CON			9.321E-02
	PUF-CON			2.779E-04
	PLA-CON			1.464E-05
	PE-PVC			9.321E-02
	PUF-PVC			2.779E-04
	PLA-PVC			1.464E-05
	PUF-PE			1.401E-01
	PLA-PE			1.091E-02
	PLA-PUF			7.676E-01

Table S1.10 Potential anammox rate statistical analyses, including normality, homogeneity of variance, one-way ANOVA and post-hoc Tukey.

TEST	Parameter	D.F.	Test Statistic	p-value
Normality (Shapiro -Wilks)			W = 0.81662	1.337E-04
Variance (Levene's)	Treatment	4	F = 1.5575	2.165E-01
One-way ANOVA	Treatment	4	F = 12.04	1.360E-05
Post-hoc Tukey Test	PVC-CON			1.000E+00
	PE-CON			5.653E-01
	PUF-CON			1.364E-01
	PLA-CON			2.968E-05
	PE-PVC			5.653E-01
	PUF-PVC			1.364E-01
	PLA-PVC			2.968E-05
	PUF-PE			8.810E-01
	PLA-PE			1.355E-03
	PLA-PUF			1.351E-02

Table S1.11 Carbon in the sediment statistical analyses, including normality, homogeneity of variance, one-way ANOVA and post-hoc Tukey.

TEST	Parameter	D.F.	Test Statistic	p-value
Normality (Shapiro -Wilks)			W = 0.95916	6.465E-01
Variance (Levene's)	Treatment	5	F = 0.3178	8.912E-01
One-way ANOVA	Treatment	5	F = 22.66	3.710E-05
Post-hoc Tukey Test	CON-Initial			9.927E-01
	PLA-Initial			1.212E-01
	PVC-Initial			6.893E-02
	PUF-Initial			8.622E-03
	PE-Initial			3.024E-04
	PLA-CON			6.384E-02
	PVC-CON			2.843E-02
	PUF-CON			1.729E-03
	PE-CON			2.934E-05
	PVC-PLA			9.934E-01
	PUF-PLA			2.140E-01
	PE-PLA			1.153E-03
	PUF-PVC			4.244E-01
	PE-PVC			2.323E-03
	PE-PUF			3.979E-02

Table S1.12 Nitrogen in the sediment statistical analyses, including normality, homogeneity of variance, one-way ANOVA and post-hoc Tukey.

TEST	Parameter	D.F.	Test Statistic	p-value
Normality (Shapiro -Wilks)			W = 0.72733	3.432E-04
Variance (Levene's)	Treatment	5	F = 0.3611	8.638E-01
One-way ANOVA	Treatment	5	F = 23.22	3.320E-05
Post-hoc Tukey Test	CON-Initial			9.969E-01
	PLA-Initial			9.785E-01
	PE-Initial			7.513E-01
	PVC-Initial			7.513E-01
	PUF-Initial			5.085E-04
	PLA-CON			9.992E-01
	PE-CON			7.909E-01
	PVC-CON			7.909E-01
	PUF-CON			4.728E-05
	PE-PLA			9.288E-01
	PVC-PLA			9.288E-01
	PUF-PLA			6.687E-05
	PVC-PE			1.000E+00
	PUF-PE			1.811E-04
	PUF-PVC			1.811E-04

Table S1.13 All species present in samples at great than 0.1% abundance (separate attachment). Available in online version of manuscript:
<https://www.nature.com/articles/s41467-020-16235-3>.

Table S1.14 Genera present in samples at greater than 1% abundance (separate attachment). Available in online version of manuscript:
<https://www.nature.com/articles/s41467-020-16235-3>.

Table S1.15 Mean concentrations and standard deviations of flame retardant additives in PUF. Available in online version of manuscript:
<https://www.nature.com/articles/s41467-020-16235-3>.

PUF: Concentration (mg/g)		
	mean	std dev
BDE-47	10.9	5.4
BDE-100	3.1	1.0
BDE-99	10.3	2.1
BDE-154	1.5	1.1
BDE-153	1.9	1.1
PentaBDE Total	27.8	
TBB	2.4	0.5
TBPH	0.8	0.3
TCEP	ND	
TCP	ND	
TDCPP	0.5	0.1
triphenyl phosphate (TPP)	3.1	2.0

Chapter 2 Supplementary Information

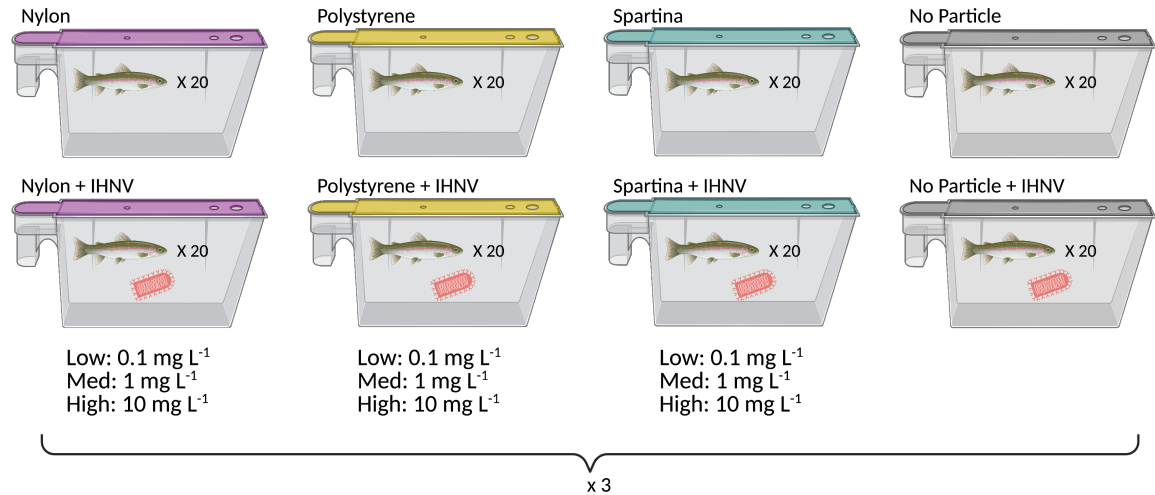
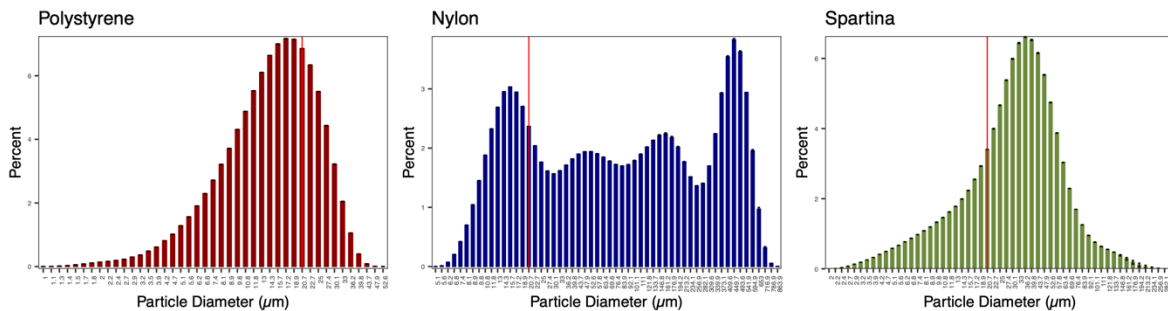


Fig. S2.1 Experimental design of tanks used to monitor mortality. Design consists of eight general treatments, with three concentrations for particle treatments. The high dose particle treatments and no particle treatments had a fourth replicate for destructive sampling, leading to 68 tanks total (see Table S2.1). Image created with biorender.com.

Particle Size Histograms:



Particle Images (10x):

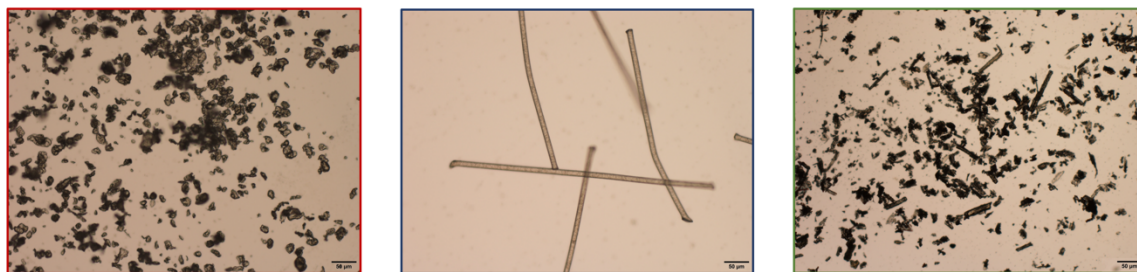


Fig. S2.2 Size characterization and microscopic images of polystyrene, nylon and spartina particles. Particle size histograms are illustrated in the first panel, with a red line at the 20 µm mark. Microscopic images of these particles at 4 and 10 times magnifications are shown below the histograms.

Table S2.1 Experimental tank treatments, including particle type, concentration, viral status (IHNV+: virus present; IHNV-: virus absent) and number of tanks. Treatments with 4* tanks include 3 tanks for mortality monitoring and one tank for destructive tissue sampling.

Particle	Concentration	IHNV +/-	Number of tanks
No particle	N/A	IHNV +	4*
No particle	N/A	IHNV -	4*
Polystyrene	10 mg L ⁻¹	IHNV +	4*
Polystyrene	10 mg L ⁻¹	IHNV -	4*
Polystyrene	1 mg L ⁻¹	IHNV +	3
Polystyrene	1 mg L ⁻¹	IHNV -	3
Polystyrene	0.1 mg L ⁻¹	IHNV +	3
Polystyrene	0.1 mg L ⁻¹	IHNV -	3
Nylon	10 mg L ⁻¹	IHNV +	4*
Nylon	10 mg L ⁻¹	IHNV -	4*
Nylon	1 mg L ⁻¹	IHNV +	3
Nylon	1 mg L ⁻¹	IHNV -	3
Nylon	0.1 mg L ⁻¹	IHNV +	3
Nylon	0.1 mg L ⁻¹	IHNV -	3
Spartina	10 mg L ⁻¹	IHNV +	4*
Spartina	10 mg L ⁻¹	IHNV -	4*
Spartina	1 mg L ⁻¹	IHNV +	3
Spartina	1 mg L ⁻¹	IHNV -	3
Spartina	0.1 mg L ⁻¹	IHNV +	3
Spartina	0.1 mg L ⁻¹	IHNV -	3
		<i>Total tanks</i>	68

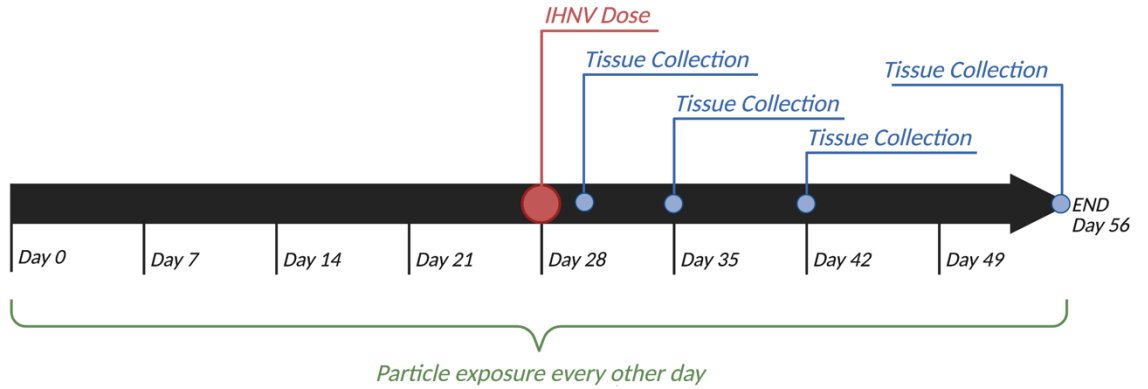


Fig. S2.3 Timeline of experimental activity. In total, the experiment lasted 56 days or 8 weeks. Fish were maintained with particles (except no particle controls) throughout all 8 weeks of the experiment. Fish were dosed with IHNV or a mock inoculate at the start of week 5 (day 28). Tissue samples from destructive sampling tanks were collected at days 31, 35, 42 and 56. Image created with biorender.com.

Table S2.2 Chemical composition of polystyrene microplastics and nylon microfibers.

Nylon Microfibers	
Compound	Concentration
Polymer: Nylon 6'6	N/A
Titanium Dioxide Delustrant	Unknown
<i>Method: communication with distributor, Claremont Flock Inc.</i>	
Polymer: Polystyrene	N/A
*Additives still under investigation	

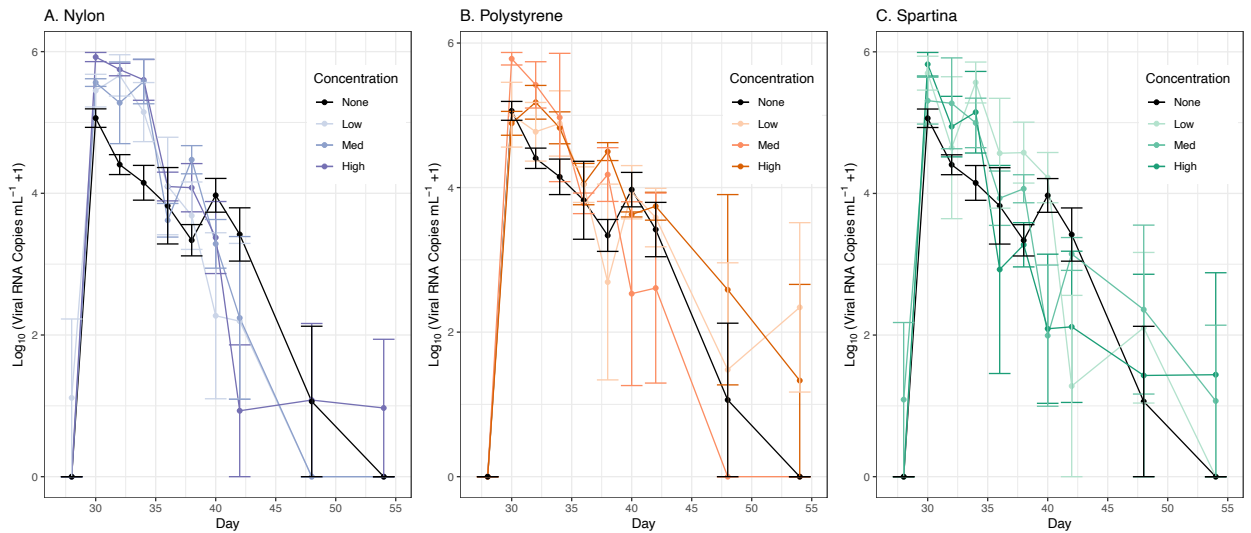


Fig. S2.4 Viral titer of RNA copies in water for all treatments (nylon, polystyrene and spartina) and microparticle concentrations (none/control, low, medium, and high) across day. Error bars are standard error across tanks (n=3). Significant differences between particle treatments were not observed, but days are significantly different from each other (linear model F-statistic = 6.844; p-value of Day = 1.71×10^{-14} , Nylon 0.1 = 0.938, Nylon 1 = 0.873, Nylon 10 = 0.612, Polystyrene 0.1 = 0.466, Polystyrene 1 = 0.993, Polystyrene 10 = 0.278, Spartina 0.1 = 0.499, Spartina 1 = 0.430, Spartina 10 = 0.994).

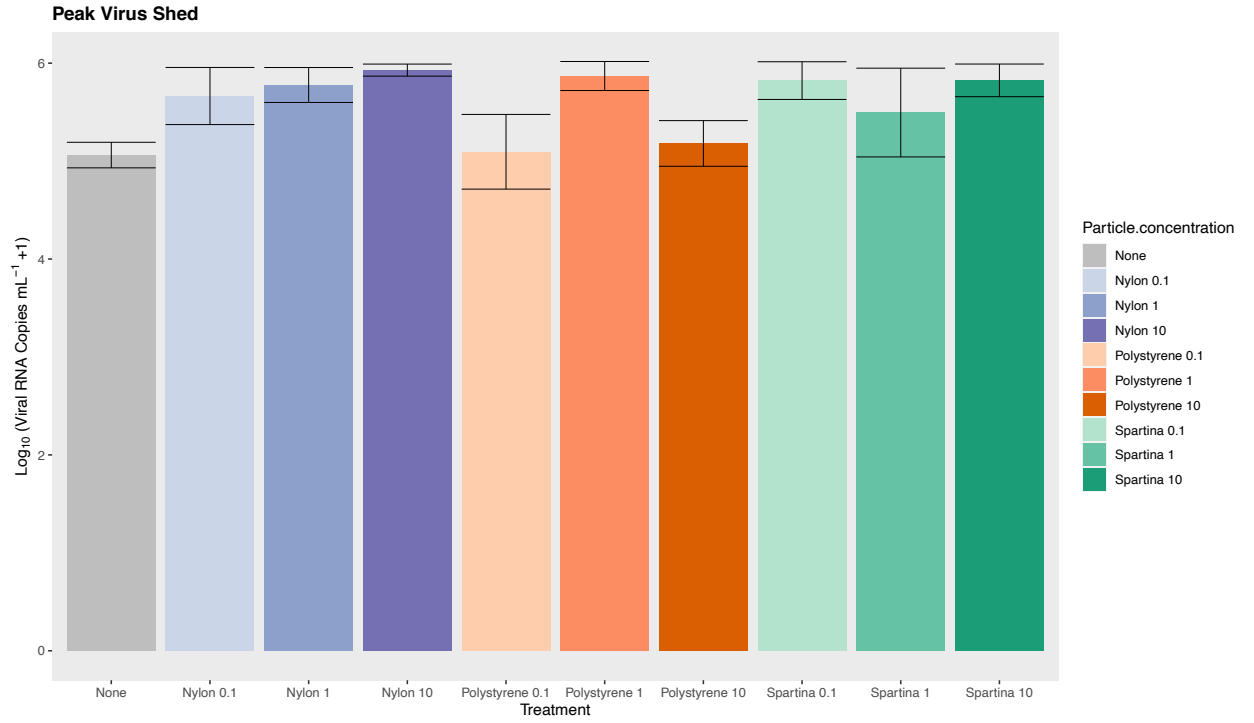


Fig. S2.5 Amount of virus shed at peak (highest) point of shed for each treatment with SEM (n = 3) for each treatment.

Tissue Viral Load, including virus negative fish

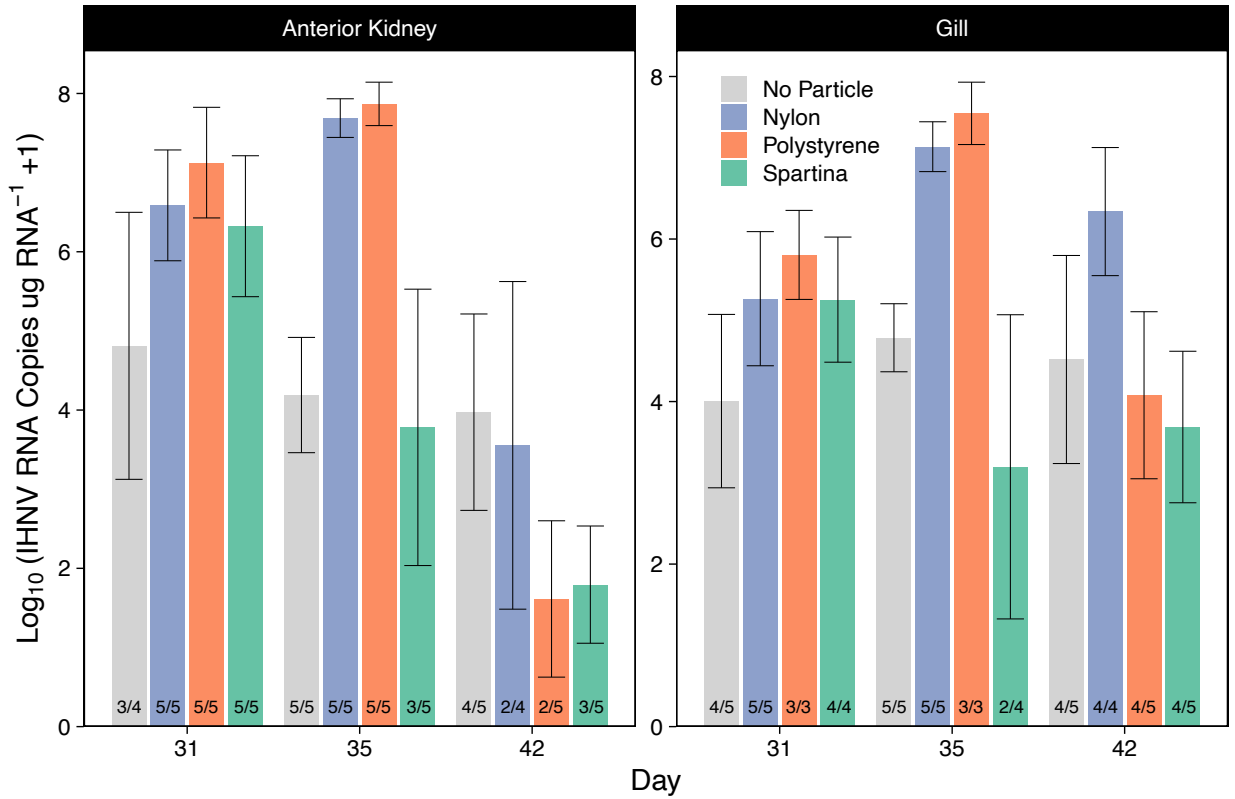


Fig. S2.6 IHNV loads in anterior kidney and gill tissues are presented for each collection day. Bars show mean viral RNA copies in one μg of RNA (± 1 SEM) for groups of fish terminally sampled on each day. Fish without virus detected are included in the means. The number of virus positive (numerator) out of total fish sampled (denominator) are shown as ratio at base of bars. In the anterior kidney, according to two-way ANOVA, viral load was significantly influenced by microparticle (F-stat = 2.07, Df = 3, $p = 5.08\text{e-}2$) and collection day (F-stat = 12.713, Df = 2, $p\text{-value} < 0.001$) but not their interaction (F-stat = 2.03, Df = 6, $p\text{-value} = 8.1\text{-}2$). In gill tissues, according to two-way ANOVA, viral load was significantly influenced by microparticle (F-stat = 13.82, Df = 3 and $p\text{-value} = 3.4\text{e-}2$) and day (F-stat = 2.35, Df = 2, $p\text{-value} = 4.7\text{e-}1$), but not their interaction (F-stat = 5.00, Df = 6, $p\text{-value} = 3.5\text{e-}1$).

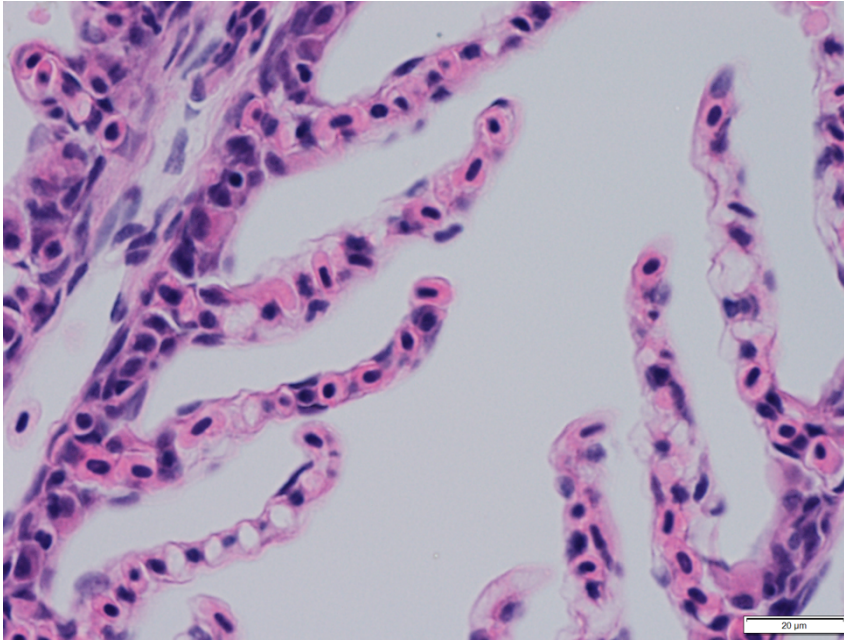


Fig. S2.7 Immune response in gill tissue of a fish exposed to only nylon (IHNV -). Appearance of mild damage to the respiratory epithelia and swelling of tissues is observed, alongside regions with healthy gill lamellae.

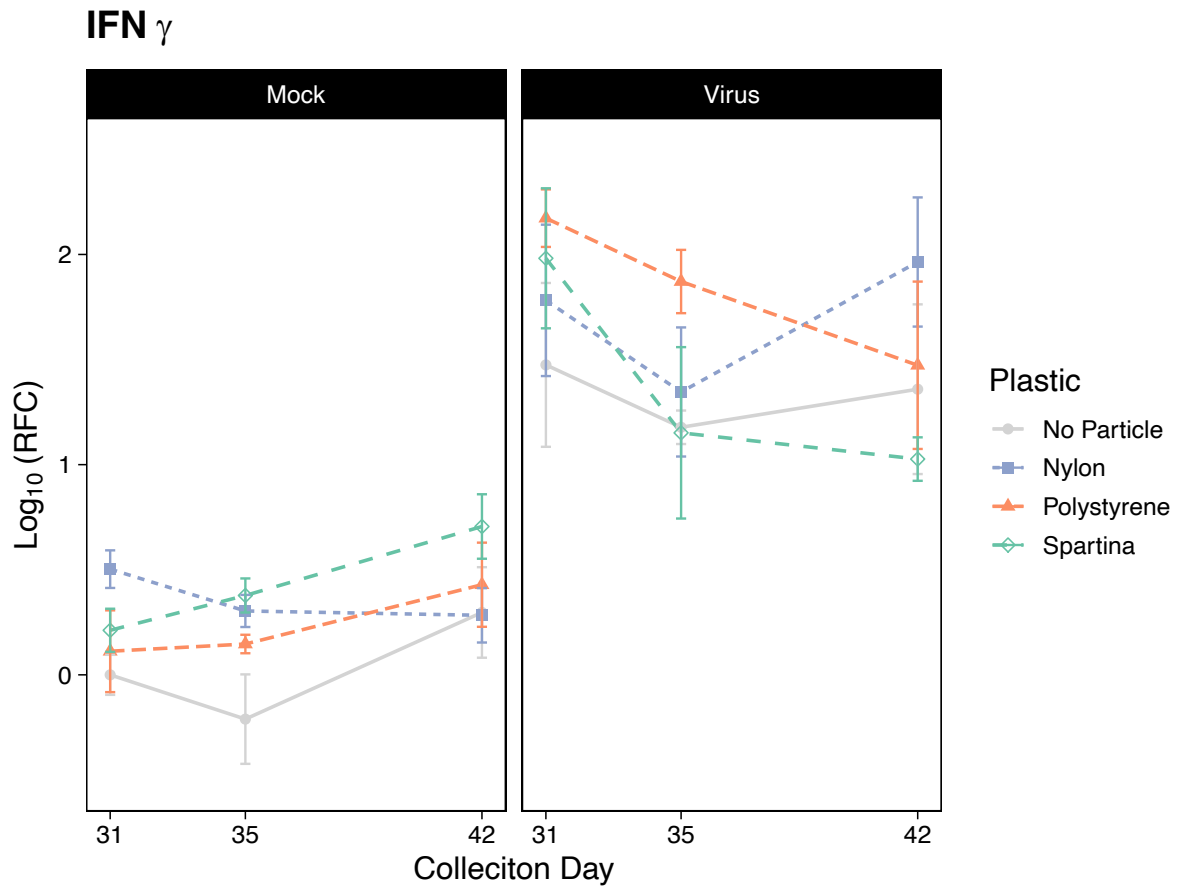


Fig. S2.8 Response of IFN γ to changes in microparticle exposure, among IHNV+ and – treatments, over time. The relative fold change (RFC; log₁₀-adjusted) compared to the control (no particle, IHNV-) on day 31 is plotted for each microparticle and virus treatment on each collection day, with +/- 1 SEM (n = 5, with exceptions: Table S2.3).

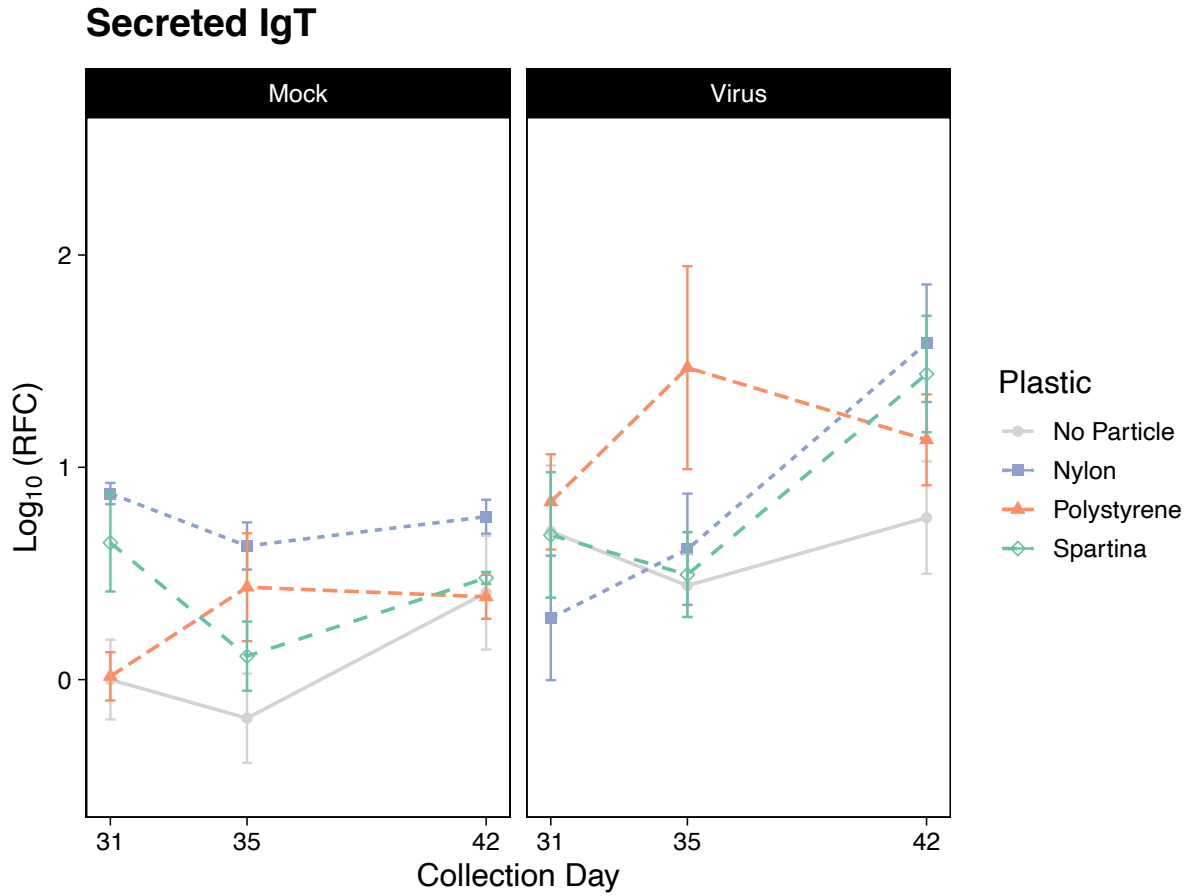


Fig. S2.9 Response of secreted IgT to changes in microparticle exposure, among IHNV+ and – treatments, over time. The relative fold change (RFC; log₁₀-adjusted) compared to the control (no particle, IHNV-) on day 31 is plotted for each microparticle and virus treatment on each collection day, with +/- 1 SEM (n = 5, with exceptions: Table S2.3).

Table S2.3 The RFC and standard error for all immune markers analyzed across all treatments. For all markers, the average

2 RFC (number of fish column n) standard error of the mean (se) are given.

Treatment	Tissue	Day	Days post IHNV	n	memHCmu (mem-bound IgM)	se	secHCmu (secreted IgM)	se	secHCtau (secreted IgT)	se	IFN γ	se	MCSFR	se
No Particle	AK	31	3	5	4.1803	1.3841	4.0239	1.2673	3.8972	1.6036	0.9912	0.4106	2.8832	1.0134
No Particle	AK	35	7	5	4.1013	1.0118	1.5502	1.3126	17.7937	4.7333	1.9368	0.8562	2.3861	0.9295
No Particle	AK	42	14	5	15.7781	5.5076	3.3576	0.4904	8.8590	2.2420	1.0859	0.2553	10.4340	1.3343
No Particle	Gill	31	3	5	2.4977	0.6290	1.7870	0.7938	1.3422	0.4054	0.9189	0.3812	2.0576	0.8369
No Particle	Gill	35	7	5	0.0518	0.0294	3.6708	1.2253	0.9541	0.3311	0.9920	0.4942	0.3241	0.1633
No Particle	Gill	42	14	4	10.9264	3.8569	1.0131	0.3117	4.0430	1.9432	2.6699	0.9963	3.2589	0.8613
No Particle, IHNV+	AK	31	3	4	22.8061	8.6079	7.5216	1.6713	15.8409	6.5367	1658.0365	1072.0334	5.1573	1.8509
No Particle, IHNV+	AK	35	7	5	8.4069	5.6271	3.9794	1.9563	41.7656	23.5829	51.5515	13.5830	0.5208	0.1865
No Particle, IHNV+	AK	42	14	5	37.8353	17.0899	10.5185	2.6883	65.6960	23.0419	297.1495	273.1470	6.1987	1.4210
No Particle, IHNV+	Gill	31	3	5	13.7566	7.9240	7.0946	6.1624	15.0253	11.2335	79.4350	32.0292	2.1702	0.7044
No Particle, IHNV+	Gill	35	7	5	0.2785	0.1284	1.1401	0.3625	3.3420	0.8573	16.0116	2.5538	0.6364	0.2107
No Particle, IHNV+	Gill	42	14	5	6.0647	3.3030	3.7504	1.0411	9.1040	2.8377	88.8754	63.1862	2.3854	0.5738
Nylon	AK	31	3	5	28.9071	11.7578	4.5087	1.4244	14.2737	5.1847	1.2598	0.6422	5.1095	1.3916
Nylon	AK	35	7	5	9.3878	8.5482	13.4179	2.9707	23.0531	8.9608	2.2854	0.7153	2.0370	0.5034
Nylon	AK	42	14	5	23.9586	9.5642	3.0146	0.7182	18.4365	8.7425	2.0105	0.8705	3.0430	0.7398
Nylon	Gill	31	3	3	9.7609	2.7594	6.4553	2.6215	7.6290	0.9235	3.3127	0.6227	3.1480	0.7888
Nylon	Gill	35	7	5	0.3553	0.2489	0.6546	0.3222	4.8125	1.1095	2.1359	0.3543	0.7451	0.2471

Nylon	Gill	42	14	4	4.9616	1.4961	1.0972	0.5519	6.1594	1.1419	2.2016	0.6879	2.0434	0.3640
Nylon, IHNV+	AK	31	3	5	12.3628	4.4870	11.4801	5.6156	28.6993	10.3579	974.9283	330.0734	4.2861	2.0535
Nylon, IHNV+	AK	35	7	5	1.6446	0.4879	5.5577	1.6425	15.2658	6.6387	68.5139	31.6237	0.7258	0.3927
Nylon, IHNV+	AK	42	14	4	56.4690	42.5908	15.4498	6.1866	39.3101	20.2907	215.9877	93.1869	9.5340	2.7480
Nylon, IHNV+	Gill	31	3	5	3.7198	1.3009	4.0381	1.8846	3.1176	0.7840	139.7193	60.7723	1.4780	0.4718
Nylon, IHNV+	Gill	35	7	5	0.4138	0.1276	3.7867	2.8937	8.9784	6.0415	38.6800	13.3263	0.6980	0.2717
Nylon, IHNV+	Gill	42	14	4	17.7083	2.3810	24.3570	10.7162	66.7836	36.9781	188.5881	123.5041	16.9825	6.3162
Polystyrene	AK	31	3	5	15.7553	7.8113	3.2697	1.6097	8.2543	3.8410	1.1739	0.2202	3.1652	0.4804
Polystyrene	AK	35	7	3	0.3243	0.1694	8.0984	4.2431	2.7069	2.0547	0.8385	0.4342	0.2194	0.1032
Polystyrene	AK	42	14	4	41.4338	23.1899	4.5832	1.9222	5.1313	2.0014	2.2573	0.6594	6.9023	1.6008
Polystyrene	Gill	31	3	3	1.7059	1.0436	0.7949	0.4075	1.1085	0.2854	1.5350	0.5315	1.2070	0.0397
Polystyrene	Gill	35	7	5	0.1943	0.0669	20.6487	7.9037	6.2207	4.4601	1.4290	0.1323	0.5202	0.1119
Polystyrene	Gill	42	14	4	6.7134	4.5999	0.2964	0.0989	2.6482	0.5314	3.5706	1.4655	4.1556	1.5941
Polystyrene, IHNV+	AK	31	3	5	38.0394	9.8535	7.7027	1.0500	210.9475	118.9283	5385.0550	2272.5362	7.2981	2.6820
Polystyrene, IHNV+	AK	35	7	5	1.4743	0.7460	6.5257	3.2812	8.5328	1.3538	41.4649	6.5806	0.9828	0.5138
Polystyrene, IHNV+	AK	42	14	5	85.0914	49.1345	9.7286	3.7289	34.9815	17.5683	26.9142	15.9649	7.1402	3.6993
Polystyrene, IHNV+	Gill	31	3	3	2.3563	0.4454	1.8806	0.4678	8.9281	4.4395	163.8028	49.0376	2.1848	0.9855
Polystyrene, IHNV+	Gill	35	7	3	0.4711	0.2396	0.5460	0.1504	93.8551	83.6723	84.1242	30.1613	0.8649	0.1527
Polystyrene, IHNV+	Gill	42	14	5	8.0410	3.0670	8.8733	3.9849	20.2352	8.0074	90.8492	60.5818	5.1646	1.4636
Spartina	AK	31	3	5	34.0733	6.1127	5.2443	0.7447	15.4110	10.9727	0.9403	0.2514	3.7185	1.2312
Spartina	AK	35	7	5	1.2510	0.4256	1.5736	0.8507	5.2336	2.0166	1.1427	0.5749	0.6516	0.1935
Spartina	AK	42	14	5	26.5637	12.3750	3.9258	1.2417	17.8756	13.1105	2.2812	0.6275	4.1331	0.7763

Spartina	Gill	31	3	4	10.8012	3.2025	2.2225	1.1351	7.0991	4.2910	1.7679	0.4009	1.2354	0.2546
Spartina	Gill	35	7	5	0.3569	0.1147	50.8603	19.2745	1.7738	0.8017	2.5442	0.4297	0.5513	0.0745
Spartina	Gill	42	14	4	21.4343	10.6669	1.4062	0.7950	3.0322	0.1930	6.2673	2.5828	6.5706	1.3484
Spartina, IHNV+	AK	31	3	5	12.7538	3.7978	5.4053	2.2555	31.2131	15.6312	2386.9987	1035.7297	4.4345	2.0987
Spartina, IHNV+	AK	35	7	5	3.3392	1.1926	7.4540	4.7567	30.1077	8.6692	100.4033	53.8142	1.7768	0.6870
Spartina, IHNV+	AK	42	14	5	49.1304	16.5945	17.3233	7.3820	151.7579	54.8616	64.6861	46.6550	8.0868	1.8900
Spartina, IHNV+	Gill	31	3	4	2.6654	0.7048	1.8276	1.0869	8.3078	4.3078	193.0899	97.1257	1.7459	0.5649
Spartina, IHNV+	Gill	35	7	4	0.1874	0.0927	1.4448	0.4593	4.3295	2.0963	42.0480	29.1215	0.5221	0.0097
Spartina, IHNV+	Gill	42	14	5	7.5855	2.1936	5.0819	2.4851	55.5914	27.5335	11.9012	2.8586	4.5314	1.1874

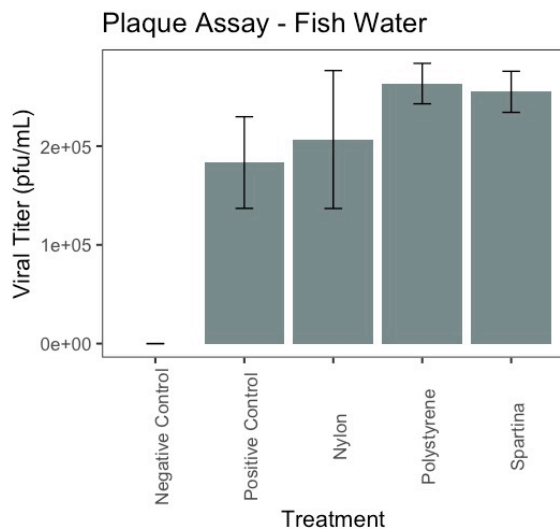


Fig. S2.10 Results of experiment investigating sorption of IHNV to microparticles. Particles were incubated with virus in fish water (i.e., water used for experiment) for 48 hours, then filtered (1 μ m) and remaining virus in the water measured via plaque assay (80). Negative control was untreated water (no virus or microparticle added), while positive control was water with virus but without microparticles. The statistically similar results between positive control and all microparticles treatments suggests that plastics did not sorb IHNV virions (if virions sorbed, a portion of the virions would remain with plastics during filtration and viral titer would be significantly lower). Error bars are standard error (n=3).

Table S2.4 Markers used for genetic analyses, including forward and reverse primers and references for methodology.

Marker name	Forward Primer Sequence	Reverse Primer Sequence	Method	Reference(s)
memHCmu (mem IgM)	5'-GCGCTGTAGAT CACATGGAA-3'	5'-TTTCACCTTGA TGGCAGTTG-3'	SYBR green	(81)
secHCmu (sec IgM)	5'-GCGCTGTAG ATCACATGGAA-3'	5'-GCAAGTCAG GGTCCACCGTAT-3'	SYBR green	(81)
secHCtau (sec IgT)	5'-CGGGTAACTCAT GTGAAGACAAGT-3'	5'-AGTCAATAAGAA GACACAACGACACA-3'	TaqMan	(82)
IFN γ	5'-CAAAGTAAAGTCC ACTATAAGATCTCCA-3'	5'-TTCTGAATTTTCCC CTTGACATATTT-3'	SYBR green	(70)
MCSFR	5'-GAACTTTGCCCTCC AGAGATATACAC-3'	5'-GATCACAATCCTCAG TAATCTTAGCTTGGC-3'	SYBR green	(71)
ARP	5'-GAAAATCATCCA ATTGCTGGATG-3'	5'-CTTCCCACGCAA GGACAGA-3'	SYBR green	(83)
IHNV N-gene	5'-AGAGCCAAGGCA CTGTGCG-3'	5'-TTCTTTGCGGCT TGGTTGA-3'	TaqMan	(44)

Statistics – Model Results

Mortality, model 1 including IHNV + and IHNV – fish (Fig. 1)

```
> summary(cox.ph.mod8) #Mortality Model 1
```

Call:

```
coxph(formula = Surv(day.died, censor) ~ particle.concentration +  
      virus + frailty(tank), data = data, control = coxph.control(iter.max = 1000))
```

n= 1166, number of events= 238

	coef	se(coef)	se2	Chisq	DF	p
particle.concentrationNyl	0.8473	0.5678	0.3415	2.23	1.00	1.4e-01
particle.concentrationNyl	1.0075	0.5633	0.3291	3.20	1.00	7.4e-02
particle.concentrationNyl	1.8297	0.5514	0.2992	11.01	1.00	9.1e-04
particle.concentrationPol	0.5630	0.5749	0.3559	0.96	1.00	3.3e-01
particle.concentrationPol	1.2728	0.5740	0.3172	4.92	1.00	2.7e-02
particle.concentrationPol	0.3935	0.5842	0.3768	0.45	1.00	5.0e-01
particle.concentrationSpa	0.8992	0.5652	0.3349	2.53	1.00	1.1e-01
particle.concentrationSpa	0.6098	0.5750	0.3558	1.12	1.00	2.9e-01
particle.concentrationSpa	0.7307	0.5772	0.3610	1.60	1.00	2.1e-01
virusVirus	5.8686	1.0105	1.0035	33.73	1.00	6.3e-09
frailty(tank)				34.33	13.93	1.8e-03

	exp(coef)	exp(-coef)	lower .95	upper .95
particle.concentrationNyl	2.333	0.428576	0.7668	7.100
particle.concentrationNyl	2.739	0.365120	0.9080	8.262
particle.concentrationNyl	6.232	0.160459	2.1148	18.366
particle.concentrationPol	1.756	0.569504	0.5691	5.418
particle.concentrationPol	3.571	0.280057	1.1593	10.998
particle.concentrationPol	1.482	0.674673	0.4717	4.658
particle.concentrationSpa	2.458	0.406882	0.8118	7.441
particle.concentrationSpa	1.840	0.543458	0.5962	5.679
particle.concentrationSpa	2.077	0.481551	0.6700	6.437
virusVirus	353.750	0.002827	48.8175	2563.404

Iterations: 7 outer, 110 Newton-Raphson

Variance of random effect= 0.2877886 I-likelihood = -1423.7

Degrees of freedom for terms= 2.2 1.0 13.9

Concordance= 0.876 (se = 0.008)

Likelihood ratio test= 515.4 on 17.16 df, p=<2e-16

Mortality model 2, including IHNV + fish only (Fig. 1)

```
> summary(cox.ph.mod8b) #Mortality Model 2
```

Call:

```
coxph(formula = Surv(day.died, censor) ~ particle.concentration +
      frailty(tank), data = data[data$virus == "Virus", ], control = coxph.control(iter.max = 1000))
```

n= 582, number of events= 237

	coef	se(coef)	se2	Chisq	DF	p
particle.concentrationNyl	0.8529	0.5690	0.3392	2.25	1.00	0.13000
particle.concentrationNyl	1.0138	0.5648	0.3264	3.22	1.00	0.07300
particle.concentrationNyl	1.8494	0.5550	0.2932	11.10	1.00	0.00086
particle.concentrationPol	0.5654	0.5756	0.3543	0.97	1.00	0.33000
particle.concentrationPol	1.1492	0.5673	0.3209	4.10	1.00	0.04300
particle.concentrationPol	0.3958	0.5848	0.3755	0.46	1.00	0.50000
particle.concentrationSpa	0.9049	0.5665	0.3325	2.55	1.00	0.11000
particle.concentrationSpa	0.6132	0.5759	0.3541	1.13	1.00	0.29000
particle.concentrationSpa	0.7348	0.5783	0.3592	1.61	1.00	0.20000
frailty(tank)				33.82	13.52	0.00170

	exp(coef)	exp(-coef)	lower .95	upper .95
particle.concentrationNyl	2.346	0.4262	0.7692	7.158
particle.concentrationNyl	2.756	0.3628	0.9111	8.337
particle.concentrationNyl	6.356	0.1573	2.1417	18.861
particle.concentrationPol	1.760	0.5681	0.5697	5.439
particle.concentrationPol	3.156	0.3169	1.0380	9.593
particle.concentrationPol	1.486	0.6732	0.4722	4.674
particle.concentrationSpa	2.472	0.4046	0.8144	7.502
particle.concentrationSpa	1.846	0.5416	0.5972	5.708
particle.concentrationSpa	2.085	0.4796	0.6712	6.478

Iterations: 7 outer, 127 Newton-Raphson

Variance of random effect= 0.2841262 I-likelihood = -1411.3

Degrees of freedom for terms= 2.2 13.5

Concordance= 0.718 (se = 0.016)

Likelihood ratio test= 135.1 on 15.71 df, p=<2e-16

IHNV shed (Fig. 2A)

```
> mod6 <- lme(LogQuant ~ Particle.concentration + Day + Particle.concentration:Day, random = ~1|Tank.Number, method
= "ML", weights=varPower(), data = virus)
> summary(mod6)
Linear mixed-effects model fit by maximum likelihood
Data: virus
      AIC      BIC    logLik
853.8559 936.5343 -403.9279

Random effects:
Formula: ~1 | Tank.Number
      (Intercept) Residual
StdDev: 8.810294e-05 1.786795

Variance function:
Structure: Power of variance covariate
Formula: ~fitted(.)
Parameter estimates:
      power
-0.454515
Fixed effects: LogQuant ~ Particle.concentration + Day + Particle.concentration:Day
              Value Std.Error  DF   t-value p-value
(Intercept)  10.493026 1.3791132 229   7.608532 0.0000
Particle.concentrationNylon 0.1  3.816595 1.9371717 20   1.970190 0.0628
Particle.concentrationNylon 1    3.531566 1.9687045 20   1.793853 0.0880
Particle.concentrationNylon 10   4.217360 1.9391478 20   2.174852 0.0418
Particle.concentrationPolystyrene 0.1 -1.292417 1.8488320 20  -0.699045 0.4926
Particle.concentrationPolystyrene 1    3.697145 1.9498708 20   1.896097 0.0725
Particle.concentrationPolystyrene 10  -0.793163 1.8029674 20  -0.439921 0.6647
Particle.concentrationSpartina 0.1    2.158794 1.9738854 20   1.093677 0.2871
Particle.concentrationSpartina 1     0.981502 1.9440707 20   0.504870 0.6192
Particle.concentrationSpartina 10    2.503715 1.9991961 20   1.252361 0.2249
Day -0.182650 0.0372789 229  -4.899545 0.0000
Particle.concentrationNylon 0.1:Day -0.100182 0.0527427 229  -1.899443 0.0588
Particle.concentrationNylon 1:Day  -0.088429 0.0536881 229  -1.647088 0.1009
Particle.concentrationNylon 10:Day  -0.103888 0.0528434 229  -1.965960 0.0505
Particle.concentrationPolystyrene 0.1:Day 0.041607 0.0495873 229   0.839057 0.4023
Particle.concentrationPolystyrene 1:Day  -0.095162 0.0531240 229  -1.791320 0.0746
Particle.concentrationPolystyrene 10:Day  0.034504 0.0482161 229   0.715620 0.4750
Particle.concentrationSpartina 0.1:Day  -0.046042 0.0537008 229  -0.857389 0.3921
Particle.concentrationSpartina 1:Day  -0.019797 0.0526567 229  -0.375969 0.7073
Particle.concentrationSpartina 10:Day  -0.069670 0.0545180 229  -1.277922 0.2026
```


IHNV load in gill (Fig. 2B)

```
> summary(mod1G0)
```

Call:

```
lm(formula = LogQuant ~ Plastic + Day, data = NgeneG0)
```

Residuals:

Min	1Q	Median	3Q	Max
-2.4475	-0.8530	-0.0513	0.9702	2.3031

Coefficients:

	Estimate	Std. Error	t value	Pr(> t)	
(Intercept)	4.6804	0.4380	10.686	2.02e-13	***
PlasticNylon	1.1528	0.4814	2.395	0.0213	*
PlasticPolystyrene	1.0008	0.5268	1.900	0.0645	.
PlasticSpartina	0.2837	0.5303	0.535	0.5955	
Day35	1.0329	0.4522	2.284	0.0276	*
Day42	0.1329	0.4427	0.300	0.7656	

Signif. codes: 0 '***' 0.001 '**' 0.01 '*' 0.05 '.' 0.1 ' ' 1

Residual standard error: 1.249 on 41 degrees of freedom

Multiple R-squared: 0.2505, Adjusted R-squared: 0.1591

F-statistic: 2.741 on 5 and 41 DF, p-value: 0.03163

IHNV load in anterior kidney (Fig. 2B)

```

> res.aov.Ngene.AK0 <- aov(LogQuant ~ Plastic*Day, data = NgeneAK0)
> summary(res.aov.Ngene.AK0) #plastic and day are significant, interaction is not (p = 0.0514...)

              Df Sum Sq Mean Sq F value Pr(>F)
Plastic       3  40.47  13.490    6.090 0.0019 **
Day           2   21.44   10.721    4.840 0.0139 *
Plastic:Day   6   36.40    6.067    2.739 0.0274 *
Residuals    35   77.53    2.215

---
Signif. codes:  0 '***' 0.001 '**' 0.01 '*' 0.05 '.' 0.1 ' ' 1

> res = TukeyHSD(res.aov.Ngene.AK0)
> res
Tukey multiple comparisons of means
 95% family-wise confidence level

Fit: aov(formula = LogQuant ~ Plastic * Day, data = NgeneAK0)

$Plastic
              diff          lwr          upr          p adj
Nylon-No Particle    2.1276481  0.4890244  3.76627191 0.0067153
Polystyrene-No Particle 1.9150110  0.2763873  3.55363480 0.0167017
Spartina-No Particle  0.4033542 -1.2720972  2.07800558 0.3150951
Polystyrene-Nylon    -0.2126371 -1.8512609  1.42598656 0.9850374
Spartina-Nylon       -1.7242939 -3.3997453 -0.04884256 0.0417080
Spartina-Polystyrene -1.5116568 -3.1871082  0.16379454 0.0892634

$Day
              diff          lwr          upr          p adj
35-31 -0.05418141 -1.268272  1.1599095 0.9934468
42-31 -1.59767132 -2.991595  -0.2037481 0.0216985
42-35 -1.54348992 -2.937413  -0.1495667 0.0272773

$`Plastic:Day`
              diff          lwr          upr          p adj
Nylon:31-No Particle:31  0.17117632 -3.6295262  3.9718789 1.0000000
Polystyrene:31-No Particle:31 0.71116001 -3.0895425  4.5118625 0.9993359
Spartina:31-No Particle:31 -0.09231844 -3.8930210  3.7083841 1.0000000
No Particle:35-No Particle:31 -2.22557628 -6.0262788  1.5751263 0.6599773
Nylon:35-No Particle:31  1.27370962 -2.5269929  5.0744122 0.9879245
Polystyrene:35-No Particle:31 1.45334695 -2.3473556  5.2540495 0.9678167
Spartina:35-No Particle:31 -0.11309525 -4.3624099  4.1362194 1.0000000
No Particle:42-No Particle:31 -1.44871278 -5.4235826  2.5261571 0.9772065
Nylon:42-No Particle:31  0.69230777 -4.0585704  5.4431859 0.9999949
Polystyrene:42-No Particle:31 -2.38256742 -7.1334456  2.3683107 0.8308519
Spartina:42-No Particle:31 -3.42491017 -7.6742248  0.8244044 0.2159549
Polystyrene:31-Nylon:31  0.5398369 -2.7515213  3.8314886 0.9999828
Spartina:31-Nylon:31  -0.26349476 -3.5549997  3.0280102 1.0000000
No Particle:35-Nylon:31 -2.39675260 -5.6882575  0.8947523 0.3464925
Nylon:35-Nylon:31  1.10253330 -2.1889716  4.3940382 0.9879698
Polystyrene:35-Nylon:31  1.28217063 -2.0093343  4.5736756 0.9633720
Spartina:35-Nylon:31  -0.28427157 -4.0849741  3.5164310 1.0000000
No Particle:42-Nylon:31 -1.61988910 -5.110573  1.8712791 0.8890329
Nylon:42-Nylon:31  0.52113145 -3.8331203  4.8753832 0.9999993
Polystyrene:42-Nylon:31 -2.55374374 -6.9079955  1.8005080 0.6578949
Spartina:42-Nylon:31 -3.59608649 -7.3967890  0.2046160 0.0776503
Spartina:31-Polystyrene:31 -0.80347845 -4.0949834  2.4880265 0.9991905
No Particle:35-Polystyrene:31 -2.93673629 -6.2282412  0.3547687 0.1177824
Nylon:35-Polystyrene:31  0.56254961 -2.7289553  3.8540546 0.9999740
Polystyrene:35-Polystyrene:31 0.74218694 -2.5493180  4.0336919 0.9996123
Spartina:35-Polystyrene:31 -0.82425526 -4.6249578  2.9764473 0.9997318
No Particle:42-Polystyrene:31 -2.15987279 -5.6510410  1.3312954 0.5843748
Nylon:42-Polystyrene:31 -0.01885224 -4.3731040  4.3353995 1.0000000
Polystyrene:42-Polystyrene:31 -3.09372743 -7.4479792  1.2605243 0.3814610
Spartina:42-Polystyrene:31 -4.13607018 -7.9367727  0.3353676 0.0232428
No Particle:35-Spartina:31 -2.13325784 -5.4247628  1.1582471 0.5168466
Nylon:35-Spartina:31  1.36602805 -1.9254769  4.6575330 0.9439354
Polystyrene:35-Spartina:31 1.54566539 -1.7458396  4.8371703 0.8812239
Spartina:35-Spartina:31 -0.02077681 -3.8214793  3.7799257 1.0000000
No Particle:42-Spartina:31 -1.35639434 -4.8475625  2.1347739 0.9640303
Nylon:42-Spartina:31  0.78462621 -3.5696256  5.1388780 0.9999559
Polystyrene:42-Spartina:31 -2.29074898 -6.6445007  2.0640028 0.7859850
Spartina:42-Spartina:31 -3.33259173 -7.1332943  0.4681108 0.1319810
Nylon:35-No Particle:35  3.49928590 0.2077809  6.7907908 0.0290513
Polystyrene:35-No Particle:35 3.67892323 0.3874183  6.9704282 0.0178083
Spartina:35-No Particle:35 2.11248103 -1.6882215  5.9131836 0.7252883
No Particle:42-No Particle:35 0.77686350 -2.7143047  4.2680317 0.9996578
Nylon:42-No Particle:35  2.91788405 -1.4363677  7.2721358 0.4674050
Polystyrene:42-No Particle:35 -0.15699114 -4.5112429  4.1972606 1.0000000
Spartina:42-No Particle:35 -1.19933389 -5.0000364  2.6013686 0.9925173
Polystyrene:35-Nylon:35  0.17963733 -3.1118676  3.4711423 1.0000000
Spartina:35-Nylon:35  -1.38680487 -5.1875074  2.4138977 0.9770164
No Particle:42-Nylon:35 -2.72242240 -6.2135906  0.7687458 0.2553612
Nylon:42-Nylon:35  -0.58140185 -4.9356536  3.7728499 0.9999979
Polystyrene:42-Nylon:35 -3.65627704 -8.0105288  0.6979747 0.1720085
Spartina:42-Nylon:35 -4.69861979 -8.4993223 -0.8979173 0.0058447
Spartina:35-Polystyrene:35 -1.56644220 -5.3671447  2.2342603 0.9464211
No Particle:42-Polystyrene:35 -2.90205973 -6.3932279  0.5891085 0.1823157
Nylon:42-Polystyrene:35 -0.76103918 -5.1152909  3.5932126 0.9996674
Polystyrene:42-Polystyrene:35 -3.83591437 -8.1901661  0.5183374 0.1280446
Spartina:42-Polystyrene:35 -4.87825712 -8.6789597 -1.0775546 0.0036904
No Particle:42-Spartina:35 -1.33561753 -5.3104874  2.6392523 0.9876722
Nylon:42-Spartina:35  0.80540302 -3.9454751  5.5562812 0.9999760
Polystyrene:42-Spartina:35 -2.26947217 -7.0203503  2.4814060 0.8693632
Spartina:42-Spartina:35 -3.31181492 -7.5611295  0.9374997 0.2560415
Nylon:42-No Particle:42  2.14102055 -2.3660582  6.6480993 0.8733287
Polystyrene:42-No Particle:42 -0.93385464 -5.4409334  3.5732241 0.9998267
Spartina:42-No Particle:42 -1.97619739 -5.9510672  1.9986725 0.8382469
Polystyrene:42-Nylon:42 -3.07487519 -8.2792015  2.1294511 0.6480966
Spartina:42-Nylon:42  -4.11721794 -8.8680961  0.6336602 0.1421576
Spartina:42-Polystyrene:42 -1.04234275 -5.7932209  3.7085354 0.9997006

```

Histopathology (Fig. 3)

> results

	Df	Sum Sq	Mean Sq	F value	Pr(>F)	
Plastic	3	8.436	2.812	13.158	1.63e-07	***
Virus	1	29.526	29.526	138.162	< 2e-16	***
Day	3	5.983	1.994	9.333	1.31e-05	***
Plastic:Virus	3	4.695	1.565	7.323	0.000147	***
Plastic:Day	9	8.198	0.911	4.262	7.79e-05	***
Virus:Day	3	4.389	1.463	6.846	0.000263	***
Plastic:Virus:Day	9	7.631	0.848	3.968	0.000181	***
Residuals	124	26.500	0.214			

Signif. codes: 0 '***' 0.001 '**' 0.01 '*' 0.05 '.' 0.1 ' ' 1

Histopathology post-hoc three-way interactions (significant interactions only)

Treatments	diff	lwr	upr	p adj
No Particle:Mock:42-Nylon:Virus:35	-2.6	-3.73230014	-1.46769986	3.23E-12
No Particle:Mock:42-Polystyrene:Virus:35	-2	-3.13230014	-0.86769986	1.56E-07
No Particle:Mock:56-Nylon:Virus:35	-2.4	-3.53230014	-1.26769986	1.21E-10
No Particle:Mock:56-Nylon:Virus:42	-1.6	-2.73230014	-0.46769986	0.000106184
No Particle:Mock:56-Polystyrene:Virus:35	-1.8	-2.93230014	-0.66769986	4.51E-06
No Particle:Virus:42-No Particle:Mock:31	1.2	0.06769986	2.33230014	0.023710218
No Particle:Virus:42-No Particle:Mock:35	1.2	0.06769986	2.33230014	0.023710218
No Particle:Virus:42-No Particle:Mock:42	1.2	0.06769986	2.33230014	0.023710218
No Particle:Virus:42-Nylon:Virus:35	-1.4	-2.53230014	-0.26769986	0.001906394
No Particle:Virus:42-Polystyrene:Mock:35	1.2	0.06769986	2.33230014	0.023710218
No Particle:Virus:42-Spartina:Mock:35	1.2	0.06769986	2.33230014	0.023710218
No Particle:Virus:56-No Particle:Mock:31	1.5	0.299014339	2.700985661	0.001569487
No Particle:Virus:56-No Particle:Mock:35	1.5	0.299014339	2.700985661	0.001569487
No Particle:Virus:56-No Particle:Mock:42	1.5	0.299014339	2.700985661	0.001569487
No Particle:Virus:56-No Particle:Mock:56	1.3	0.099014339	2.500985661	0.017594634
No Particle:Virus:56-Nylon:Mock:31	1.3	0.099014339	2.500985661	0.017594634
No Particle:Virus:56-Nylon:Mock:56	1.3	0.099014339	2.500985661	0.017594634
No Particle:Virus:56-Nylon:Virus:31	1.3	0.099014339	2.500985661	0.017594634
No Particle:Virus:56-Polystyrene:Mock:31	1.3	0.099014339	2.500985661	0.017594634
No Particle:Virus:56-Polystyrene:Mock:35	1.5	0.299014339	2.700985661	0.001569487
No Particle:Virus:56-Polystyrene:Mock:56	1.3	0.099014339	2.500985661	0.017594634
No Particle:Virus:56-Spartina:Mock:31	1.5	0.234049958	2.765950042	0.004153668
No Particle:Virus:56-Spartina:Mock:35	1.5	0.299014339	2.700985661	0.001569487
No Particle:Virus:56-Spartina:Mock:42	1.3	0.099014339	2.500985661	0.017594634
Nylon:Mock:42-Nylon:Virus:35	-2.35	3.550985661	-1.149014339	3.48E-09
Nylon:Mock:42-Polystyrene:Virus:35	-1.75	2.950985661	-0.549014339	4.94E-05
Nylon:Mock:56-Nylon:Virus:35	-2.4	-3.53230014	-1.26769986	1.21E-10
Nylon:Mock:56-Nylon:Virus:42	-1.6	-2.73230014	-0.46769986	0.000106184
Nylon:Mock:56-Polystyrene:Virus:35	-1.8	-2.93230014	-0.66769986	4.51E-06
Nylon:Virus:35-No Particle:Mock:31	2.6	1.46769986	3.73230014	3.23E-12
Nylon:Virus:35-No Particle:Mock:35	2.6	1.46769986	3.73230014	3.23E-12
Nylon:Virus:35-No Particle:Virus:31	2	0.86769986	3.13230014	1.56E-07
Nylon:Virus:35-No Particle:Virus:35	2.2	1.06769986	3.33230014	4.60E-09
Nylon:Virus:35-Nylon:Mock:31	2.4	1.26769986	3.53230014	1.21E-10
Nylon:Virus:35-Nylon:Mock:35	2.2	1.06769986	3.33230014	4.60E-09
Nylon:Virus:35-Nylon:Virus:31	2.4	1.26769986	3.53230014	1.21E-10

Nylon:Virus:35-Polystyrene:Mock:31	2.4	1.26769986	3.53230014	1.21E-10
Nylon:Virus:35-Polystyrene:Mock:35	2.6	1.46769986	3.73230014	3.23E-12
Nylon:Virus:35-Polystyrene:Virus:31	2	0.86769986	3.13230014	1.56E-07
Nylon:Virus:35-Spartina:Mock:31	2.6	1.399014339	3.800985661	4.72E-11
Nylon:Virus:35-Spartina:Mock:35	2.6	1.46769986	3.73230014	3.23E-12
Nylon:Virus:35-Spartina:Virus:31	2.2	1.06769986	3.33230014	4.60E-09
Nylon:Virus:42-No Particle:Mock:31	1.8	0.66769986	2.93230014	4.51E-06
Nylon:Virus:42-No Particle:Mock:35	1.8	0.66769986	2.93230014	4.51E-06
Nylon:Virus:42-No Particle:Mock:42	1.8	0.66769986	2.93230014	4.51E-06
Nylon:Virus:42-No Particle:Virus:31	1.2	0.06769986	2.33230014	0.023710218
Nylon:Virus:42-No Particle:Virus:35	1.4	0.26769986	2.53230014	0.001906394
Nylon:Virus:42-Nylon:Mock:31	1.6	0.46769986	2.73230014	0.000106184
Nylon:Virus:42-Nylon:Mock:35	1.4	0.26769986	2.53230014	0.001906394
Nylon:Virus:42-Nylon:Mock:42	1.55	0.349014339	2.750985661	0.000813161
Nylon:Virus:42-Nylon:Virus:31	1.6	0.46769986	2.73230014	0.000106184
Nylon:Virus:42-Polystyrene:Mock:31	1.6	0.46769986	2.73230014	0.000106184
Nylon:Virus:42-Polystyrene:Mock:35	1.8	0.66769986	2.93230014	4.51E-06
Nylon:Virus:42-Polystyrene:Mock:42	1.4	0.26769986	2.53230014	0.001906394
Nylon:Virus:42-Polystyrene:Virus:31	1.2	0.06769986	2.33230014	0.023710218
Nylon:Virus:42-Spartina:Mock:31	1.8	0.599014339	3.000985661	2.36E-05
Nylon:Virus:42-Spartina:Mock:35	1.8	0.66769986	2.93230014	4.51E-06
Nylon:Virus:42-Spartina:Mock:42	1.6	0.46769986	2.73230014	0.000106184
Nylon:Virus:42-Spartina:Virus:31	1.4	0.26769986	2.53230014	0.001906394
Nylon:Virus:42-Spartina:Virus:35	1.4	0.26769986	2.53230014	0.001906394
Nylon:Virus:56-No Particle:Mock:31	1.8	0.66769986	2.93230014	4.51E-06
Nylon:Virus:56-No Particle:Mock:35	1.8	0.66769986	2.93230014	4.51E-06
Nylon:Virus:56-No Particle:Mock:42	1.8	0.66769986	2.93230014	4.51E-06
Nylon:Virus:56-No Particle:Mock:56	1.6	0.46769986	2.73230014	0.000106184
Nylon:Virus:56-No Particle:Virus:31	1.2	0.06769986	2.33230014	0.023710218
Nylon:Virus:56-No Particle:Virus:35	1.4	0.26769986	2.53230014	0.001906394
Nylon:Virus:56-Nylon:Mock:31	1.6	0.46769986	2.73230014	0.000106184
Nylon:Virus:56-Nylon:Mock:35	1.4	0.26769986	2.53230014	0.001906394
Nylon:Virus:56-Nylon:Mock:42	1.55	0.349014339	2.750985661	0.000813161
Nylon:Virus:56-Nylon:Mock:56	1.6	0.46769986	2.73230014	0.000106184
Nylon:Virus:56-Nylon:Virus:31	1.6	0.46769986	2.73230014	0.000106184
Nylon:Virus:56-Polystyrene:Mock:31	1.6	0.46769986	2.73230014	0.000106184
Nylon:Virus:56-Polystyrene:Mock:35	1.8	0.66769986	2.93230014	4.51E-06
Nylon:Virus:56-Polystyrene:Mock:42	1.4	0.26769986	2.53230014	0.001906394
Nylon:Virus:56-Polystyrene:Mock:56	1.6	0.46769986	2.73230014	0.000106184

Nylon:Virus:56-Polystyrene:Virus:31	1.2	0.06769986	2.33230014	0.023710218
Nylon:Virus:56-Spartina:Mock:31	1.8	0.599014339	3.000985661	2.36E-05
Nylon:Virus:56-Spartina:Mock:35	1.8	0.66769986	2.93230014	4.51E-06
Nylon:Virus:56-Spartina:Mock:42	1.6	0.46769986	2.73230014	0.000106184
Nylon:Virus:56-Spartina:Mock:56	1.4	0.26769986	2.53230014	0.001906394
Nylon:Virus:56-Spartina:Virus:31	1.4	0.26769986	2.53230014	0.001906394
Nylon:Virus:56-Spartina:Virus:35	1.4	0.26769986	2.53230014	0.001906394
Nylon:Virus:56-Spartina:Virus:42	1.2	0.06769986	2.33230014	0.023710218
Polystyrene:Mock:42-Nylon:Virus:35	-2.2	-3.33230014	-1.06769986	4.60E-09
Polystyrene:Mock:42-Polystyrene:Virus:35	-1.6	-2.73230014	-0.46769986	0.000106184
Polystyrene:Mock:56-Nylon:Virus:35	-2.4	-3.53230014	-1.26769986	1.21E-10
Polystyrene:Mock:56-Nylon:Virus:42	-1.6	-2.73230014	-0.46769986	0.000106184
Polystyrene:Mock:56-Polystyrene:Virus:35	-1.8	-2.93230014	-0.66769986	4.51E-06
Polystyrene:Virus:35-No Particle:Mock:31	2	0.86769986	3.13230014	1.56E-07
Polystyrene:Virus:35-No Particle:Mock:35	2	0.86769986	3.13230014	1.56E-07
Polystyrene:Virus:35-No Particle:Virus:31	1.4	0.26769986	2.53230014	0.001906394
Polystyrene:Virus:35-No Particle:Virus:35	1.6	0.46769986	2.73230014	0.000106184
Polystyrene:Virus:35-Nylon:Mock:31	1.8	0.66769986	2.93230014	4.51E-06
Polystyrene:Virus:35-Nylon:Mock:35	1.6	0.46769986	2.73230014	0.000106184
Polystyrene:Virus:35-Nylon:Virus:31	1.8	0.66769986	2.93230014	4.51E-06
Polystyrene:Virus:35-Polystyrene:Mock:31	1.8	0.66769986	2.93230014	4.51E-06
Polystyrene:Virus:35-Polystyrene:Mock:35	2	0.86769986	3.13230014	1.56E-07
Polystyrene:Virus:35-Polystyrene:Virus:31	1.4	0.26769986	2.53230014	0.001906394
Polystyrene:Virus:35-Spartina:Mock:31	2	0.799014339	3.200985661	1.09E-06
Polystyrene:Virus:35-Spartina:Mock:35	2	0.86769986	3.13230014	1.56E-07
Polystyrene:Virus:35-Spartina:Virus:31	1.6	0.46769986	2.73230014	0.000106184
Polystyrene:Virus:42-No Particle:Mock:31	1.2	0.06769986	2.33230014	0.023710218
Polystyrene:Virus:42-No Particle:Mock:35	1.2	0.06769986	2.33230014	0.023710218
Polystyrene:Virus:42-No Particle:Mock:42	1.2	0.06769986	2.33230014	0.023710218
Polystyrene:Virus:42-Nylon:Virus:35	-1.4	-2.53230014	-0.26769986	0.001906394
Polystyrene:Virus:42-Polystyrene:Mock:35	1.2	0.06769986	2.33230014	0.023710218
Polystyrene:Virus:42-Spartina:Mock:35	1.2	0.06769986	2.33230014	0.023710218
Polystyrene:Virus:56-Nylon:Virus:35	-1.85	3.050985661	-0.649014339	1.11E-05
Polystyrene:Virus:56-Polystyrene:Virus:35	-1.25	2.450985661	-0.049014339	0.030246718
Spartina:Mock:42-Nylon:Virus:35	-2.4	-3.53230014	-1.26769986	1.21E-10
Spartina:Mock:42-Polystyrene:Virus:35	-1.8	-2.93230014	-0.66769986	4.51E-06
Spartina:Mock:56-Nylon:Virus:35	-2.2	-3.33230014	-1.06769986	4.60E-09
Spartina:Mock:56-Nylon:Virus:42	-1.4	-2.53230014	-0.26769986	0.001906394

Spartina:Mock:56-Polystyrene:Virus:35	-1.6	-2.73230014	-0.46769986	0.000106184
Spartina:Virus:35-Nylon:Virus:35	-2.2	-3.33230014	-1.06769986	4.60E-09
Spartina:Virus:35-Polystyrene:Virus:35	-1.6	-2.73230014	-0.46769986	0.000106184
Spartina:Virus:42-Nylon:Virus:35	-2	-3.13230014	-0.86769986	1.56E-07
Spartina:Virus:42-Nylon:Virus:42	-1.2	-2.33230014	-0.06769986	0.023710218
Spartina:Virus:42-Polystyrene:Virus:35	-1.4	-2.53230014	-0.26769986	0.001906394
Spartina:Virus:56-Nylon:Virus:35	-2	-3.13230014	-0.86769986	1.56E-07
Spartina:Virus:56-Nylon:Virus:42	-1.2	-2.33230014	-0.06769986	0.023710218
Spartina:Virus:56-Nylon:Virus:56	-1.2	-2.33230014	-0.06769986	0.023710218
Spartina:Virus:56-Polystyrene:Virus:35	-1.4	-2.53230014	-0.26769986	0.001906394

IFN γ response in gill (Fig. 4A)

```
> summary(mod1)
```

Call:

```
lm(formula = Log.IFN $\gamma$ .RFC3 ~ Plastic + Day + Virus, data = CT.Gill)
```

Residuals:

Min	1Q	Median	3Q	Max
-1.59303	-0.27161	0.01515	0.32434	1.20150

Coefficients:

	Estimate	Std. Error	t value	Pr(> t)
(Intercept)	0.1685	0.1372	1.228	0.2224
PlasticNylon	0.3510	0.1453	2.415	0.0176 *
PlasticPolystyrene	0.3310	0.1506	2.198	0.0303 *
PlasticSpartina	0.2228	0.1453	1.533	0.1284
Day35	-0.2682	0.1302	-2.061	0.0420 *
Day42	-0.1045	0.1319	-0.792	0.4301
VirusVirus	1.2617	0.1059	11.916	<2e-16 ***

Signif. codes: 0 '***' 0.001 '**' 0.01 '*' 0.05 '.' 0.1 ' ' 1

Residual standard error: 0.5377 on 97 degrees of freedom

Multiple R-squared: 0.6188, Adjusted R-squared: 0.5952

F-statistic: 26.24 on 6 and 97 DF, p-value: < 2.2e-16

Secreted IgT response in gill (Fig. 4B)

```
> summary(mod1)
```

Call:

```
lm(formula = Log.sechCtau.RFC3 ~ Plastic + Day + Virus, data = CT.Gill)
```

Residuals:

```
      Min       1Q   Median       3Q      Max
-1.7373 -0.2739 -0.0531  0.3019  1.6227
```

Coefficients:

	Estimate	Std. Error	t value	Pr(> t)	
(Intercept)	-0.003084	0.133093	-0.023	0.98156	
PlasticNylon	0.396346	0.140958	2.812	0.00596	**
PlasticPolystyrene	0.344486	0.146056	2.359	0.02035	*
PlasticSpartina	0.292717	0.140942	2.077	0.04046	*
Day35	-0.014991	0.126235	-0.119	0.90571	
Day42	0.385578	0.127925	3.014	0.00329	**
VirusVirus	0.467854	0.102695	4.556	1.52e-05	***

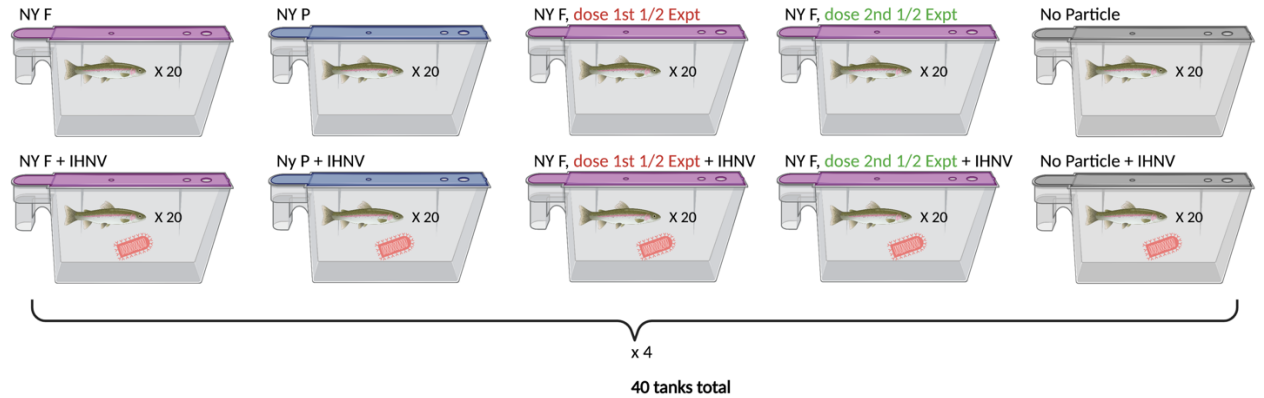
Signif. codes: 0 '***' 0.001 '**' 0.01 '*' 0.05 '.' 0.1 ' ' 1

Residual standard error: 0.5215 on 97 degrees of freedom

Multiple R-squared: 0.3214, Adjusted R-squared: 0.2794

F-statistic: 7.655 on 6 and 97 DF, p-value: 9.607e-07

Chapter 3 Supplementary Information



All treatments are at the high dose (10 mg L^{-1})

NY F = Nylon Fiber

NY P = Nylon Powder

dose 1st 1/2 Expt = Nylon is only dosed during first 4 weeks of experiment, not all 8 weeks

dose 2nd 1/2 Expt = Nylon is only dosed during second 4 weeks of experiment, not all 8 weeks

Fig. S3.1 Experimental design, including all treatments with quadruplicate tanks. Tanks with a red virion pictured signifies IHNV+ treatments (bottom row). Graphic created with biorender.com.

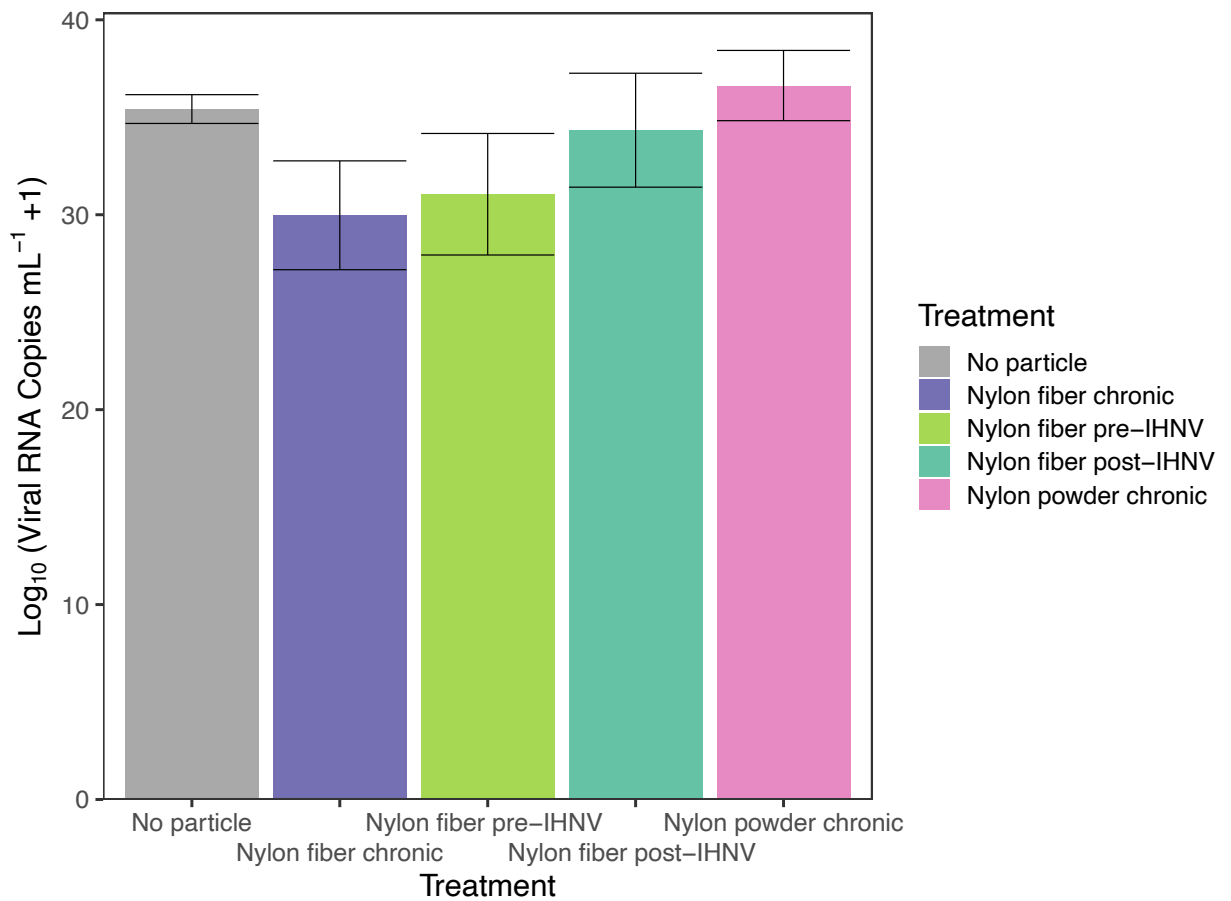


Fig. S3.2 Total amount of viral shed over time for each treatment. Mean of the total shed (Log-adjusted viral RNA copies mL⁻¹) is graphed +/- 1 SEM (n = 4 tanks). The treatment had no significant influence on total viral shed (one-way ANOVA analysis; F-stat = 1.37, Df = 4, p-value = 2.92e-1).

Statistical analysis results

Mortality model 1: IHNV- and IHNV+ treatments (Fig. 1)

Call:

```
coxph(formula = Surv(day.died, censor) ~ particle.concentration +
      virus, data = PartB, control = coxph.control(iter.max = 500))
```

n= 775, number of events= 255

	coef	exp(coef)	se(coef)	z	Pr(> z)
particle.concentrationNylon Fiber	0.55939	1.74961	0.19613	2.852	0.00434 **
particle.concentrationNylon Fiber, post-exposure	0.13896	1.14908	0.20800	0.668	0.50409
particle.concentrationNylon Fiber, pre-exposure	0.40390	1.49765	0.20367	1.983	0.04736 *
particle.concentrationNylon Powder	-0.08169	0.92156	0.21829	-0.374	0.70824
virusVirus	1.30520	3.68842	0.14231	9.171	< 2e-16 ***

Signif. codes: 0 '***' 0.001 '**' 0.01 '*' 0.05 '.' 0.1 ' ' 1

	exp(coef)	exp(-coef)	lower .95	upper .95
particle.concentrationNylon Fiber	1.7496	0.5716	1.1912	2.570
particle.concentrationNylon Fiber, post-exposure	1.1491	0.8703	0.7644	1.727
particle.concentrationNylon Fiber, pre-exposure	1.4977	0.6677	1.0047	2.232
particle.concentrationNylon Powder	0.9216	1.0851	0.6008	1.414
virusVirus	3.6884	0.2711	2.7906	4.875

Concordance= 0.687 (se = 0.016)

Likelihood ratio test= 108.8 on 5 df, p=<2e-16

Wald test = 96.45 on 5 df, p=<2e-16

Score (logrank) test = 108.1 on 5 df, p=<2e-16

Mortality model 2: IHNV+ treatments only (Fig. 1)

Call:

```
coxph(formula = Surv(day.died, censor) ~ particle.concentration,
      data = PartB[PartB$virus == "Virus", ], control = coxph.control(iter.max = 500))
```

n= 387, number of events= 187

	coef	exp(coef)	se(coef)	z	Pr(> z)
particle.concentrationNylon Fiber	0.48002	1.61611	0.22532	2.130	0.0331 *
particle.concentrationNylon Fiber, post-exposure	-0.07087	0.93158	0.24437	-0.290	0.7718
particle.concentrationNylon Fiber, pre-exposure	0.39098	1.47843	0.23201	1.685	0.0920 .
particle.concentrationNylon Powder	-0.10681	0.89870	0.24630	-0.434	0.6645

Signif. codes: 0 '***' 0.001 '**' 0.01 '*' 0.05 '.' 0.1 ' ' 1

	exp(coef)	exp(-coef)	lower .95	upper .95
particle.concentrationNylon Fiber	1.6161	0.6188	1.0391	2.513
particle.concentrationNylon Fiber, post-exposure	0.9316	1.0734	0.5770	1.504
particle.concentrationNylon Fiber, pre-exposure	1.4784	0.6764	0.9382	2.330
particle.concentrationNylon Powder	0.8987	1.1127	0.5546	1.456

Concordance= 0.568 (se = 0.021)

Likelihood ratio test= 11.61 on 4 df, p=0.02

Wald test = 11.83 on 4 df, p=0.02

Score (logrank) test = 12.09 on 4 df, p=0.02

Mortality model 3: IHNV- treatments only (Fig. 1)

```
> summary(cox.ph.mod3M)
```

```
Call:
```

```
coxph(formula = Surv(day.died, censor) ~ particle.concentration,
      data = PartB[PartB$virus == "Mock", ], control = coxph.control(iter.max = 500))
```

```
n= 388, number of events= 68
```

	coef	exp(coef)	se(coef)	z	Pr(> z)
particle.concentrationNylon Fiber	0.778359	2.177895	0.404688	1.923	0.0544 .
particle.concentrationNylon Fiber, post-exposure	0.713347	2.040809	0.412276	1.730	0.0836 .
particle.concentrationNylon Fiber, pre-exposure	0.452585	1.572372	0.427252	1.059	0.2895
particle.concentrationNylon Powder	-0.007302	0.992724	0.471409	-0.015	0.9876

```
---
```

```
Signif. codes:  0 '***' 0.001 '**' 0.01 '*' 0.05 '.' 0.1 ' ' 1
```

	exp(coef)	exp(-coef)	lower .95	upper .95
particle.concentrationNylon Fiber	2.1779	0.4592	0.9853	4.814
particle.concentrationNylon Fiber, post-exposure	2.0408	0.4900	0.9096	4.579
particle.concentrationNylon Fiber, pre-exposure	1.5724	0.6360	0.6806	3.633
particle.concentrationNylon Powder	0.9927	1.0073	0.3941	2.501

```
Concordance= 0.585 (se = 0.033 )
```

```
Likelihood ratio test= 7.24 on 4 df, p=0.1
```

```
Wald test = 6.83 on 4 df, p=0.1
```

```
Score (logrank) test = 7.11 on 4 df, p=0.1
```

Linear mixed effects model of viral shedding (Fig. 2)

```

> mod6 <- lme(LogQuant ~ Particle.concentration + Day, random = ~1|Tank.Number, method = "ML", data = B)
> summary(mod6)
Linear mixed-effects model fit by maximum likelihood
Data: B
      AIC      BIC    logLik
770.6302 797.0167 -377.3151

Random effects:
Formula: ~1 | Tank.Number
(Intercept) Residual
StdDev: 5.712496e-05 1.596218

Fixed effects: LogQuant ~ Particle.concentration + Day
              Value Std.Error DF   t-value p-value
(Intercept)  11.291462 0.6499114 179  17.373849 0.0000
Particle.concentrationNylon fiber chronic  -0.489396 0.3624026 15  -1.350421 0.1969
Particle.concentrationNylon fiber post-IHNV -0.080073 0.3624026 15  -0.220951 0.8281
Particle.concentrationNylon fiber pre-IHNV  -0.261119 0.3624026 15  -0.720522 0.4823
Particle.concentrationNylon powder chronic  0.157692 0.3624026 15   0.435130 0.6697
Day          -0.214068 0.0153143 179 -13.978324 0.0000

Correlation:
              (Intr) Pr.Nfc Prtcl.cncntrtnNfps-IHNV Prtcl.cncntrtnNfpr-IHNV Pr.Npc
Particle.concentrationNylon fiber chronic  -0.279
Particle.concentrationNylon fiber post-IHNV -0.279 0.500
Particle.concentrationNylon fiber pre-IHNV  -0.279 0.500 0.500
Particle.concentrationNylon powder chronic  -0.279 0.500 0.500          0.500
Day          -0.919 0.000 0.000          0.000          0.000

Standardized Within-Group Residuals:
      Min      Q1      Med      Q3      Max
-3.2834951 -0.7205648 0.3523129 0.7050803 2.2430202

Number of Observations: 200
Number of Groups: 20
> anova(mod6)
              numDF denDF F-value p-value
(Intercept)         1   179 600.4534 <.0001
Particle.concentration  4    15  0.9457 0.4648
Day                   1   179 195.3935 <.0001

```

Welch's ANOVA of peak viral shed (Fig. 3)

```
> WelchPeak <- oneway.test(Peak ~ Particle.concentration, data = BPT)
> WelchPeak
```

One-way analysis of means (not assuming equal variances)

data: Peak and Particle.concentration

F = 1.6218, num df = 4.0000, denom df = 7.1059, p-value = 0.269

Chapter 4 Supplementary Information

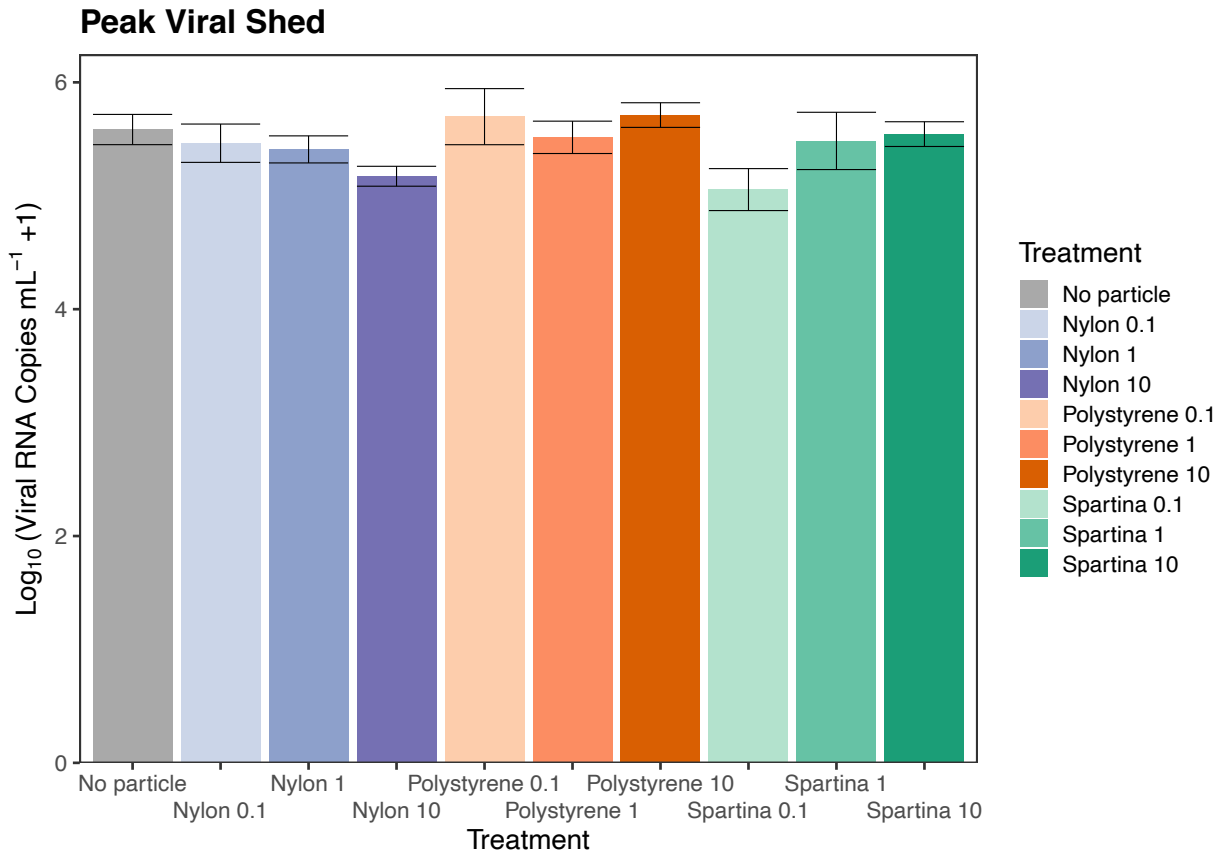


Fig. S4.1 Amount of virus shed during period of peak viral shedding for each treatment. The mean log-adjusted viral RNA copies mL⁻¹ water for each treatment is illustrated, +/- 1 SEM (n= 4 tanks). According to a one-way ANOVA, there are no significant differences in peak viral shed between treatments (F-stat = 1.813, Df = 9, p-value = 1.03e-1).

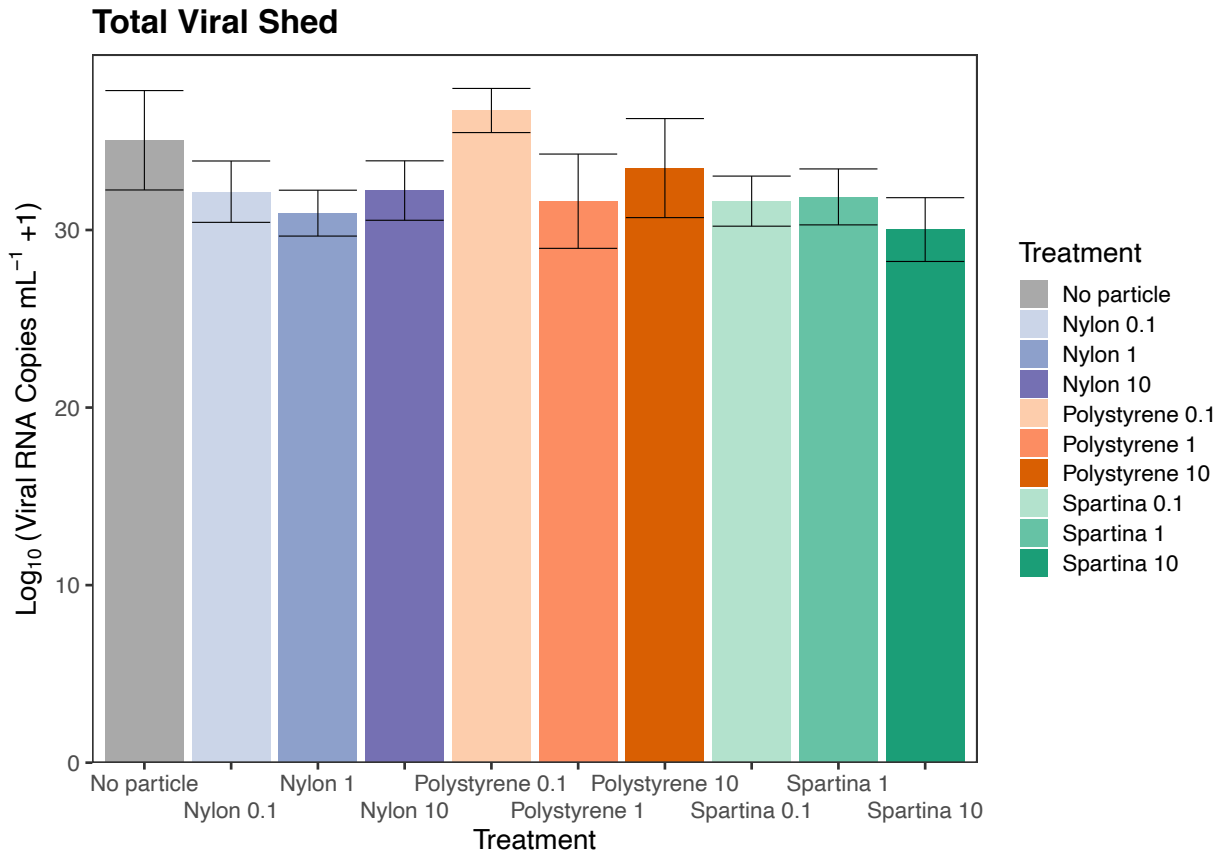


Fig. S4.2 Amount of virus shed during over all ten sampling days for each treatment. The mean log-adjusted viral RNA copies mL⁻¹ water for each treatment is illustrated, +/- 1 SEM (n= 4 tanks). According to a one-way ANOVA, there are no significant differences in total amount of viral shed between treatments (F-stat = 0.95, Df = 9, p-value = 4.95e-1).

Statistics Models

Cox proportional hazards model for all treatments, IHNV+ and IHNV- (Fig. 1)

```
> cox.ph.mod8<-coxph(Surv(day.died,censor)-particle.concentration + virus+ frailty(tank), data=data, control = coxph.control(iter.max = 1000))
> anova(cox.ph.mod8)
Analysis of Deviance Table
Cox model: response is Surv(day.died, censor)
Terms added sequentially (first to last)
```

	loglik	Chisq	Df	Pr(> Chi)
NULL	-4233.7			
particle.concentration	-4223.3	20.6835	9.000000	0.01413 *
virus	-4084.6	277.5484	1.000000	< 2e-16 ***
frailty(tank)	-4084.5	0.0602	0.020182	0.02946 *

```
---
Signif. codes:  0 '***' 0.001 '**' 0.01 '*' 0.05 '.' 0.1 ' ' 1
> summary(cox.ph.mod8)
Call:
coxph(formula = Surv(day.died, censor) ~ particle.concentration +
      virus + frailty(tank), data = data, control = coxph.control(iter.max = 1000))

n= 1554, number of events= 594
```

	coef	se(coef)	se2	Chisq	DF	p
particle.concentrationNyl	0.02039	0.19618	0.19614	0.01	1.00	9.2e-01
particle.concentrationNyl	0.47560	0.18373	0.18369	6.70	1.00	9.6e-03
particle.concentrationNyl	0.18258	0.19182	0.19177	0.91	1.00	3.4e-01
particle.concentrationPol	0.42325	0.18375	0.18370	5.31	1.00	2.1e-02
particle.concentrationPol	0.49864	0.18323	0.18319	7.41	1.00	6.5e-03
particle.concentrationPol	0.17439	0.19348	0.19344	0.81	1.00	3.7e-01
particle.concentrationSpa	0.10477	0.19347	0.19343	0.29	1.00	5.9e-01
particle.concentrationSpa	-0.13249	0.20488	0.20484	0.42	1.00	5.2e-01
particle.concentrationSpa	0.42895	0.18262	0.18257	5.52	1.00	1.9e-02
virusVirus	1.46189	0.09552	0.09551	234.21	1.00	7.2e-53
frailty(tank)				0.03	0.02	6.1e-01

	exp(coef)	exp(-coef)	lower .95	upper .95
particle.concentrationNyl	1.0206	0.9798	0.6948	1.499
particle.concentrationNyl	1.6090	0.6215	1.1224	2.306
particle.concentrationNyl	1.2003	0.8331	0.8242	1.748
particle.concentrationPol	1.5269	0.6549	1.0652	2.189
particle.concentrationPol	1.6465	0.6074	1.1497	2.358
particle.concentrationPol	1.1905	0.8400	0.8148	1.740
particle.concentrationSpa	1.1105	0.9005	0.7600	1.623
particle.concentrationSpa	0.8759	1.1417	0.5862	1.309
particle.concentrationSpa	1.5356	0.6512	1.0736	2.197
virusVirus	4.3141	0.2318	3.5775	5.202

```
Iterations: 5 outer, 20 Newton-Raphson
Variance of random effect= 5e-05 I-likelihood = -4084.6
Degrees of freedom for terms= 9 1 0
Concordance= 0.699 (se = 0.011 )
Likelihood ratio test= 298.3 on 10.02 df, p=<2e-16
```

Cox proportional hazards model for IHN⁺ treatments only (Fig. 1)

```

> cox.ph.mod8b<-coxph(Surv(day.died,censor)~particle.concentration + frailty(tank), data=data[data$virus=="Virus",], control = coxph.control(iter.max = 1000))
> anova(cox.ph.mod8b)
Analysis of Deviance Table
Cox model: response is Surv(day.died, censor)
Terms added sequentially (first to last)

              loglik   Chisq      Df Pr(>|Chi|)
NULL                -2801.8
particle.concentration -2789.3 24.9611 9.000000000 0.0030145 **
frailty(tank)         -2789.3  0.0004 0.00011586 0.0004592 ***
---
Signif. codes:  0 '***' 0.001 '**' 0.01 '*' 0.05 '.' 0.1 ' ' 1
> summary(cox.ph.mod8b)
Call:
coxph(formula = Surv(day.died, censor) ~ particle.concentration +
      frailty(tank), data = data[data$virus == "Virus", ], control = coxph.control(iter.max = 1000))

n= 773, number of events= 446

              coef      se(coef) se2   Chisq DF p
particle.concentrationNyl -0.17097 0.2333  0.2333 0.54  1 0.460
particle.concentrationNyl  0.45688 0.2113  0.2113 4.68  1 0.031
particle.concentrationNyl  0.19666 0.2185  0.2185 0.81  1 0.370
particle.concentrationPol  0.45722 0.2087  0.2087 4.80  1 0.028
particle.concentrationPol  0.51373 0.2104  0.2104 5.96  1 0.015
particle.concentrationPol  0.26495 0.2173  0.2173 1.49  1 0.220
particle.concentrationSpa -0.03063 0.2281  0.2281 0.02  1 0.890
particle.concentrationSpa -0.05532 0.2297  0.2297 0.06  1 0.810
particle.concentrationSpa  0.41337 0.2095  0.2095 3.89  1 0.048
frailty(tank)              0.00  0 0.890

              exp(coef) exp(-coef) lower .95 upper .95
particle.concentrationNyl  0.8429  1.1864  0.5336  1.331
particle.concentrationNyl  1.5791  0.6333  1.0438  2.389
particle.concentrationNyl  1.2173  0.8215  0.7933  1.868
particle.concentrationPol  1.5797  0.6330  1.0493  2.378
particle.concentrationPol  1.6715  0.5983  1.1066  2.525
particle.concentrationPol  1.3034  0.7672  0.8513  1.996
particle.concentrationSpa  0.9698  1.0311  0.6202  1.517
particle.concentrationSpa  0.9462  1.0569  0.6031  1.484
particle.concentrationSpa  1.5119  0.6614  1.0027  2.280

Iterations: 6 outer, 28 Newton-Raphson
Variance of random effect= 5e-07 I-likelihood = -2789.3
Degrees of freedom for terms= 9 0
Concordance= 0.573 (se = 0.014 )
Likelihood ratio test= 24.96 on 9 df, p=0.003

```

Cox proportional hazards model for IHNV- treatments only (Fig. 1)

```

> anova(cox.ph.mod8c) #effect of treatment is not significant
Analysis of Deviance Table
Cox model: response is Surv(day.died, censor)
Terms added sequentially (first to last)

              loglik   Chisq         Df Pr(>|Chi|)
NULL                -970.87
particle.concentration -964.84 12.0536 9.0000000  0.210304
frailty(tank)         -964.83  0.0146 0.0038733  0.008387 **
---
Signif. codes:  0 '***' 0.001 '**' 0.01 '*' 0.05 '.' 0.1 ' ' 1
> summary(cox.ph.mod8c) #no significant effects.
Call:
coxph(formula = Surv(day.died, censor) ~ particle.concentration +
      frailty(tank), data = data[data$virus == "Mock", ], control = coxph.control(iter.max = 1000))

n= 781, number of events= 148

              coef    se(coef) se2    Chisq DF  p
particle.concentrationNyl  0.5197 0.3727  0.3727 1.94  1.00 0.16
particle.concentrationNyl  0.5250 0.3727  0.3727 1.98  1.00 0.16
particle.concentrationNyl  0.1186 0.4004  0.4003 0.09  1.00 0.77
particle.concentrationPol  0.2627 0.3873  0.3873 0.46  1.00 0.50
particle.concentrationPol  0.4532 0.3727  0.3727 1.48  1.00 0.22
particle.concentrationPol -0.1634 0.4282  0.4282 0.15  1.00 0.70
particle.concentrationSpa  0.4821 0.3727  0.3727 1.67  1.00 0.20
particle.concentrationSpa -0.4096 0.4565  0.4564 0.81  1.00 0.37
particle.concentrationSpa  0.4403 0.3727  0.3727 1.40  1.00 0.24
frailty(tank)                                0.01  0.01 0.73

              exp(coef) exp(-coef) lower .95 upper .95
particle.concentrationNyl  1.6815  0.5947  0.8099  3.491
particle.concentrationNyl  1.6905  0.5915  0.8142  3.510
particle.concentrationNyl  1.1259  0.8882  0.5137  2.468
particle.concentrationPol  1.3004  0.7690  0.6087  2.778
particle.concentrationPol  1.5733  0.6356  0.7578  3.266
particle.concentrationPol  0.8493  1.1775  0.3669  1.966
particle.concentrationSpa  1.6194  0.6175  0.7800  3.362
particle.concentrationSpa  0.6639  1.5063  0.2714  1.624
particle.concentrationSpa  1.5532  0.6438  0.7481  3.225

Iterations: 5 outer, 19 Newton-Raphson
Variance of random effect= 5e-05 I-likelihood = -964.8
Degrees of freedom for terms= 9 0
Concordance= 0.589 (se = 0.023 )
Likelihood ratio test= 12.07 on 9 df, p=0.2

```

Cox proportional hazards model for all nylon treatments, IHNV+ and IHNV- (Fig. 2)

```
> anova(cox.ph.mod21) #virus and tank frailty are the only ones that are significant.
```

Analysis of Deviance Table

Cox model: response is Surv(day.died, censor)

Terms added sequentially (first to last)

	loglik	Chisq	Df	Pr(> Chi)
NULL	-1903.5			
particle.concentration	-1899.6	7.7511	4.00000000	0.1011341
virus	-1841.7	115.8354	1.00000000	< 2.2e-16 ***
frailty(tank)	-1841.7	0.0003	0.00010106	0.0004236 ***

Signif. codes: 0 '***' 0.001 '**' 0.01 '*' 0.05 '.' 0.1 ' ' 1

```
> summary(cox.ph.mod21) #nylon 1 is significant, but fiber is 0.057
```

Call:

```
coxph(formula = Surv(day.died, censor) ~ particle.concentration +
      virus + frailty(tank), data = NylonB, control = coxph.control(iter.max = 1000))
```

n= 774, number of events= 296

(20 observations deleted due to missingness)

	coef	se(coef)	se2	Chisq	DF	p
particle.concentrationNyl	0.02382	0.1962	0.1962	0.01	1	9.0e-01
particle.concentrationNyl	0.47420	0.1837	0.1837	6.66	1	9.9e-03
particle.concentrationNyl	0.18140	0.1918	0.1918	0.89	1	3.4e-01
particle.concentrationNyl	0.35335	0.1855	0.1855	3.63	1	5.7e-02
virusVirus	1.32197	0.1317	0.1317	100.81	1	1.0e-23
frailty(tank)				0.00	0	9.0e-01

	exp(coef)	exp(-coef)	lower .95	upper .95
particle.concentrationNyl	1.024	0.9765	0.6972	1.504
particle.concentrationNyl	1.607	0.6224	1.1209	2.303
particle.concentrationNyl	1.199	0.8341	0.8233	1.746
particle.concentrationNyl	1.424	0.7023	0.9899	2.048
virusVirus	3.751	0.2666	2.8977	4.855

Iterations: 6 outer, 23 Newton-Raphson

Variance of random effect= 5e-07 I-likelihood = -1841.7

Degrees of freedom for terms= 4 1 0

Concordance= 0.689 (se = 0.016)

Likelihood ratio test= 123.6 on 5 df, p=<2e-16

Cox proportional hazards model for all nylon treatments, IHNV+ only (Fig. 2)

```
> anova(cox.ph.mod21b) #treatment and tank frailty are significant
```

Analysis of Deviance Table

Cox model: response is Surv(day.died, censor)

Terms added sequentially (first to last)

	loglik	Chisq	Df	Pr(> Chi)
NULL	-1210.3			
particle.concentration	-1205.2	10.2243	4.000e+00	0.0368140 *
frailty(tank)	-1205.2	0.0002	5.874e-05	0.0002574 ***

Signif. codes: 0 '***' 0.001 '**' 0.01 '*' 0.05 '.' 0.1 ' ' 1

```
> summary(cox.ph.mod21b) #only nylon 10 weathered is significant
```

Call:

```
coxph(formula = Surv(day.died, censor) ~ particle.concentration +
      frailty(tank), data = NylonB[NylonB$virus == "Virus", ],
      control = coxph.control(iter.max = 1000))
```

n= 386, number of events= 216

	coef	se(coef)	se2	Chisq	DF	p
particle.concentrationNyl	-0.1717	0.2333	0.2333	0.54	1	0.46
particle.concentrationNyl	0.4575	0.2113	0.2113	4.69	1	0.03
particle.concentrationNyl	0.1961	0.2185	0.2185	0.81	1	0.37
particle.concentrationNyl	0.2950	0.2152	0.2152	1.88	1	0.17
frailty(tank)				0.00	0	0.91

	exp(coef)	exp(-coef)	lower .95	upper .95
particle.concentrationNyl	0.8422	1.1874	0.5332	1.330
particle.concentrationNyl	1.5801	0.6329	1.0443	2.391
particle.concentrationNyl	1.2167	0.8219	0.7929	1.867
particle.concentrationNyl	1.3432	0.7445	0.8810	2.048

Iterations: 6 outer, 63 Newton-Raphson

Variance of random effect= 5e-07 I-likelihood = -1205.2

Degrees of freedom for terms= 4 0

Concordance= 0.582 (se = 0.021)

Likelihood ratio test= 10.22 on 4 df, p=0.04

Cox proportional hazards model for all nylon treatments, IHNV- only (Fig. 2)

```

> anova(cox.ph.mod21c) #effect of treatment is not significant
Analysis of Deviance Table
Cox model: response is Surv(day.died, censor)
Terms added sequentially (first to last)

              loglik  Chisq      Df Pr(>|Chi|)
NULL                    -468.11
particle.concentration -466.17  3.8861  4.0000e+00  0.4216394
frailty(tank)          -466.17  0.0001  2.1912e-05  0.0001081 ***
---
Signif. codes:  0 '***' 0.001 '**' 0.01 '*' 0.05 '.' 0.1 ' ' 1
> summary(cox.ph.mod21c) #no significant effects.
Call:
coxph(formula = Surv(day.died, censor) ~ particle.concentration +
      frailty(tank), data = NylonB[NylonB$virus == "Mock", ], control = coxph.control(iter.max = 1000))

n= 388, number of events= 80

              coef  se(coef) se2    Chisq DF p
particle.concentrationNyl 0.5236 0.3727  0.3727  1.97  1 0.16
particle.concentrationNyl 0.5261 0.3727  0.3727  1.99  1 0.16
particle.concentrationNyl 0.1213 0.4003  0.4003  0.09  1 0.76
particle.concentrationNyl 0.5091 0.3687  0.3687  1.91  1 0.17
frailty(tank)              0.00  0  0.93

              exp(coef) exp(-coef) lower .95 upper .95
particle.concentrationNyl  1.688    0.5924  0.8131  3.504
particle.concentrationNyl  1.692    0.5909  0.8151  3.513
particle.concentrationNyl  1.129    0.8858  0.5151  2.474
particle.concentrationNyl  1.664    0.6011  0.8076  3.427

Iterations: 6 outer, 23 Newton-Raphson
Variance of random effect= 5e-07 I-likelihood = -466.2
Degrees of freedom for terms= 4 0
Concordance= 0.577 (se = 0.032 )
Likelihood ratio test= 3.89 on 4 df, p=0.4

```


Linear mixed effects model for viral shed (best model; Fig. 3)

```
> mod10 <- lme(LogQuant ~ Day, random = ~1|Tank.Number, method = "ML", data = A)
> summary(mod10)
```

Linear mixed-effects model fit by maximum likelihood

Data: A

	AIC	BIC	logLik
	1691.197	1707.443	-841.5987

Random effects:

Formula: ~1 | Tank.Number
(Intercept) Residual

StdDev: 8.225642e-05 1.72087

Fixed effects: LogQuant ~ Day

	Value	Std.Error	DF	t-value	p-value
(Intercept)	10.577005	0.4412092	385	23.97277	0
Day	-0.201645	0.0111110	385	-18.14819	0

Correlation:

(Intr)

Day -0.982

Standardized Within-Group Residuals:

	Min	Q1	Med	Q3	Max
	-2.7482017	-0.6390299	0.2983799	0.7238147	2.2775430

Number of Observations: 429

Number of Groups: 43

```
> anova(mod10)
```

	numDF	denDF	F-value	p-value
(Intercept)	1	385	1061.8996	<.0001
Day	1	385	329.3566	<.0001

Linear mixed effects model for viral shed, including particle effect (Fig. 3)

```
> #Shed Model 2: mod2  
> mod2 <- lme(LogQuant ~ Particle + Day, random = ~1|Tank.Number, method = "ML", data = A)  
> summary(mod2)
```

Linear mixed-effects model fit by maximum likelihood

Data: A

	AIC	BIC	logLik
	1694.349	1722.779	-840.1746

Random effects:

Formula: ~1 | Tank.Number
(Intercept) Residual
StdDev: 7.630559e-05 1.715167

Fixed effects: LogQuant ~ Particle + Day

	Value	Std.Error	DF	t-value	p-value
(Intercept)	10.831224	0.5121178	385	21.149868	0.0000
ParticleNylon	-0.306782	0.3122271	39	-0.982560	0.3319
ParticlePolystyrene	-0.123613	0.3119428	39	-0.396269	0.6941
ParticleSpartina	-0.412288	0.3119427	39	-1.321678	0.1940
Day	-0.201634	0.0111133	385	-18.143468	0.0000

Correlation:

	(Intr)	PrtclN	PrtclP	PrtclS
ParticleNylon	-0.465			
ParticlePolystyrene	-0.466	0.764		
ParticleSpartina	-0.466	0.764	0.765	
Day	-0.846	0.000	0.001	0.000

Standardized Within-Group Residuals:

	Min	Q1	Med	Q3	Max
	-2.8336718	-0.7176005	0.3582675	0.7217748	2.2612598

Number of Observations: 429

Number of Groups: 43

```
> anova(mod2)
```

	numDF	denDF	F-value	p-value
(Intercept)	1	385	1061.4632	<.0001
Particle	3	39	0.9534	0.4243
Day	1	385	329.1854	<.0001

One-way analysis of variance (ANOVA) for analysis of peak viral shed (Fig. S4.1)

```
> resPeak <- aov(Peak ~ Particle.concentration, data = APT)
> summary(resPeak)
```

	Df	Sum Sq	Mean Sq	F value	Pr(>F)
Particle.concentration	9	1.735	0.1927	1.813	0.103
Residuals	33	3.509	0.1063		

```
> TukeyHSD(resPeak)
```

Tukey multiple comparisons of means
95% family-wise confidence level

```
Fit: aov(formula = Peak ~ Particle.concentration, data = APT)
```

```
$Particle.concentration
```

	diff	lwr	upr	p adj
Nylon 0.1-No particle	-0.12056907	-0.9017595	0.66062136	0.9999387
Nylon 1-No particle	-0.17509095	-0.9562814	0.60609948	0.9987312
Nylon 10-No particle	-0.41183932	-1.1529416	0.32926300	0.6798367
Polystyrene 0.1-No particle	0.11345604	-0.6677344	0.89464648	0.9999633
Polystyrene 1-No particle	-0.06876246	-0.8499529	0.71242797	0.9999995
Polystyrene 10-No particle	0.12757216	-0.6135302	0.86867447	0.9998479
Spartina 0.1-No particle	-0.52947950	-1.3106699	0.25171093	0.4174457
Spartina 1-No particle	-0.10037260	-0.8815630	0.68081783	0.9999871
Spartina 10-No particle	-0.04034195	-0.7814443	0.70076037	1.0000000
Nylon 1-Nylon 0.1	-0.05452189	-0.8357123	0.72666854	0.9999999
Nylon 10-Nylon 0.1	-0.29127025	-1.0323726	0.44983206	0.9386360
Polystyrene 0.1-Nylon 0.1	0.23402511	-0.5471653	1.01521554	0.9891662
Polystyrene 1-Nylon 0.1	0.05180660	-0.7293838	0.83299703	1.0000000
Polystyrene 10-Nylon 0.1	0.24814123	-0.4929611	0.98924354	0.9770919
Spartina 0.1-Nylon 0.1	-0.40891043	-1.1901009	0.37228000	0.7461722
Spartina 1-Nylon 0.1	0.02019647	-0.7609940	0.80138690	1.0000000
Spartina 10-Nylon 0.1	0.08022712	-0.6608752	0.82132943	0.9999971
Nylon 10-Nylon 1	-0.23674836	-0.9778507	0.50435395	0.9832060
Polystyrene 0.1-Nylon 1	0.28854700	-0.4926434	1.06973743	0.9575023
Polystyrene 1-Nylon 1	0.10632849	-0.6748619	0.88751892	0.9999788
Polystyrene 10-Nylon 1	0.30266312	-0.4384392	1.04376543	0.9237417
Spartina 0.1-Nylon 1	-0.35438855	-1.1355790	0.42680188	0.8672935
Spartina 1-Nylon 1	0.07471835	-0.7064721	0.85590878	0.9999990
Spartina 10-Nylon 1	0.13474901	-0.6063533	0.87585132	0.9997615
Polystyrene 0.1-Nylon 10	0.52529536	-0.2158070	1.26639768	0.3570511
Polystyrene 1-Nylon 10	0.34307685	-0.3980255	1.08417917	0.8534252
Polystyrene 10-Nylon 10	0.53941148	-0.1593065	1.23812944	0.2503682
Spartina 0.1-Nylon 10	-0.11764018	-0.8587425	0.62346213	0.9999224
Spartina 1-Nylon 10	0.31146672	-0.4296356	1.05256903	0.9107539
Spartina 10-Nylon 10	0.37149737	-0.3272206	1.07021533	0.7296953
Polystyrene 1-Polystyrene 0.1	-0.18221851	-0.9634089	0.59897192	0.9982727
Polystyrene 10-Polystyrene 0.1	0.01411612	-0.7269862	0.75521843	1.0000000
Spartina 0.1-Polystyrene 0.1	-0.64293555	-1.4241260	0.13825488	0.1819481
Spartina 1-Polystyrene 0.1	-0.21382865	-0.9950191	0.56736179	0.9942900
Spartina 10-Polystyrene 0.1	-0.15379799	-0.8949003	0.58730432	0.9993073
Polystyrene 10-Polystyrene 1	0.19633463	-0.5447677	0.93743694	0.9955009
Spartina 0.1-Polystyrene 1	-0.46071704	-1.2419075	0.32047339	0.6061441
Spartina 1-Polystyrene 1	-0.03161014	-0.8128006	0.74958029	1.0000000
Spartina 10-Polystyrene 1	0.02842052	-0.7126818	0.76952283	1.0000000
Spartina 0.1-Polystyrene 10	-0.65705166	-1.3981540	0.08405065	0.1179053
Spartina 1-Polystyrene 10	-0.22794476	-0.9690471	0.51315755	0.9870078
Spartina 10-Polystyrene 10	-0.16791411	-0.8666321	0.53080385	0.9978302
Spartina 1-Spartina 0.1	0.42910690	-0.3520835	1.21029733	0.6933732
Spartina 10-Spartina 0.1	0.48913755	-0.2519648	1.23023987	0.4539740
Spartina 10-Spartina 1	0.06003065	-0.6810717	0.80113297	0.9999998

One-way analysis of variance (ANOVA) for analysis of total viral shed (Fig. S4.2)

```
> resTotal <- aov(Total ~ Particle.concentration, data = APT)
> summary(resTotal)
```

	Df	Sum Sq	Mean Sq	F value	Pr(>F)
Particle.concentration	9	151.4	16.82	0.952	0.495
Residuals	33	582.8	17.66		

```
> TukeyHSD(resTotal)
Tukey multiple comparisons of means
 95% family-wise confidence level
```

```
Fit: aov(formula = Total ~ Particle.concentration, data = APT)
```

\$Particle.concentration	diff	lwr	upr	p adj
Nylon 0.1-No particle	-2.894547025	-12.962068	7.172974	0.9918791
Nylon 1-No particle	-4.103315735	-14.170837	5.964205	0.9245865
Nylon 10-No particle	-2.831098322	-12.381987	6.719791	0.9899353
Polystyrene 0.1-No particle	1.676653547	-8.390868	11.744175	0.9998843
Polystyrene 1-No particle	-3.431151855	-13.498673	6.636369	0.9743079
Polystyrene 10-No particle	-1.566752736	-11.117642	7.984136	0.9998980
Spartina 0.1-No particle	-3.427516303	-13.495037	6.640005	0.9744826
Spartina 1-No particle	-3.189546370	-13.257067	6.877975	0.9841161
Spartina 10-No particle	-5.029278934	-14.580168	4.521610	0.7399518
Nylon 1-Nylon 0.1	-1.208768710	-11.276290	8.858752	0.9999928
Nylon 10-Nylon 0.1	0.063448704	-9.487440	9.614338	1.0000000
Polystyrene 0.1-Nylon 0.1	4.571200573	-5.496321	14.638722	0.8667078
Polystyrene 1-Nylon 0.1	-0.536604830	-10.604126	9.530916	1.0000000
Polystyrene 10-Nylon 0.1	1.327794290	-8.223095	10.878683	0.9999747
Spartina 0.1-Nylon 0.1	-0.532969277	-10.600490	9.534552	1.0000000
Spartina 1-Nylon 0.1	-0.294999345	-10.362520	9.772522	1.0000000
Spartina 10-Nylon 0.1	-2.134731908	-11.685621	7.416157	0.9987584
Nylon 10-Nylon 1	1.272217414	-8.278672	10.823107	0.9999824
Polystyrene 0.1-Nylon 1	5.779969283	-4.287552	15.847490	0.6402900
Polystyrene 1-Nylon 1	0.672163880	-9.395357	10.739685	1.0000000
Polystyrene 10-Nylon 1	2.536563000	-7.014326	12.087452	0.9954178
Spartina 0.1-Nylon 1	0.675799432	-9.391722	10.743321	1.0000000
Spartina 1-Nylon 1	0.913769365	-9.153752	10.981290	0.9999994
Spartina 10-Nylon 1	-0.925963198	-10.476852	8.624926	0.9999989
Polystyrene 0.1-Nylon 10	4.507751869	-5.043137	14.058641	0.8391861
Polystyrene 1-Nylon 10	-0.600053534	-10.150943	8.950836	1.0000000
Polystyrene 10-Nylon 10	1.264345586	-7.740319	10.269010	0.9999724
Spartina 0.1-Nylon 10	-0.596417981	-10.147307	8.954471	1.0000000
Spartina 1-Nylon 10	-0.358448049	-9.909337	9.192441	1.0000000
Spartina 10-Nylon 10	-2.198180612	-11.202845	6.806484	0.9975558
Polystyrene 1-Polystyrene 0.1	-5.107805402	-15.175327	4.959716	0.7772244
Polystyrene 10-Polystyrene 0.1	-3.243406283	-12.794295	6.307483	0.9748955
Spartina 0.1-Polystyrene 0.1	-5.104169850	-15.171691	4.963351	0.7779026
Spartina 1-Polystyrene 0.1	-4.866199917	-14.933721	5.201321	0.8202960
Spartina 10-Polystyrene 0.1	-6.705932481	-16.256822	2.844957	0.3696487
Polystyrene 10-Polystyrene 1	1.864399119	-7.686490	11.415288	0.9995755
Spartina 0.1-Polystyrene 1	0.003635552	-10.063886	10.071157	1.0000000
Spartina 1-Polystyrene 1	0.241605485	-9.825916	10.309127	1.0000000
Spartina 10-Polystyrene 1	-1.598127078	-11.149016	7.952762	0.9998797
Spartina 0.1-Polystyrene 10	-1.860763567	-11.411653	7.690126	0.9995821
Spartina 1-Polystyrene 10	-1.622793634	-11.173683	7.928095	0.9998634
Spartina 10-Polystyrene 10	-3.462526198	-12.467191	5.542138	0.9459643
Spartina 1-Spartina 0.1	0.237969933	-9.829551	10.305491	1.0000000
Spartina 10-Spartina 0.1	-1.601762631	-11.152652	7.949126	0.9998774
Spartina 10-Spartina 1	-1.839732564	-11.390622	7.711157	0.9996187